

ABSTRACT

Title of Thesis: GEOSTATISTICAL ESTIMATION OF BLUE CRAB *CALLINECTES SAPIDUS* ABUNDANCE IN CHESAPEAKE BAY AT LOCAL SCALES

Sarah Ann Jones, Master of Science, 2022

Thesis Directed By: Dr. Thomas J. Miller,
Marine Estuarine Environmental Science

Increases in the sizes of container ships due to the expansion of the Panama Canal has increased the need for dredging activities in the Chesapeake Bay. Placement of dredged material in the Bay is restricted to winter months owing to concerns for threatened and endangered species. Placement of dredged material in the lower Chesapeake Bay in Wolf Trap Alternate Open Water Placement Site (WTAPS) overlaps with overwintering locations for mature female blue crab. To estimate the potential magnitude of winter mortality in WTAPS and WTAPS Northern Extension (WTAPSNE) resulting from placement of dredged material, a range of geostatistical tools (e.g., inverse distance weighting and kriging) were used to map the distribution and estimate the abundance of blue crab in Chesapeake Bay, WTAPS, and WTAPSNE (i.e., small-scale estimation) from 1990–2020 using data from the winter dredge survey. These analyses indicated that a low proportion of the age-1+ female blue crab population occurs within WTAPS and WTAPSNE (<1.18% and <1.5% respectively). Variability of abundance estimates was high when female age-1+ abundance was less than 150 million in the

Chesapeake Bay. Therefore, we suggest the Port limit placement of dredged materials in WTAPS and WTAPSNE when female age-1+ abundance is less than 150 million; we recommend the Port not undertake placement activities when the stock is declared overfished (i.e., when female age-1+ abundance is less than 72.5 million).

GEOSTATISTICAL ESTIMATION OF BLUE CRAB *CALLINECTES SAPIDUS*
ABUNDANCE IN CHESAPEAKE BAY AT LOCAL SCALES

by

Sarah Ann Jones

Thesis submitted to the Faculty of the Graduate School of the
University of Maryland, College Park, in partial fulfillment
of the requirements for the degree of
Master of Science
2022

Advisory Committee:

Dr. Thomas J. Miller, Chair
Dr. Dong Liang
Dr. Geneviève Nessler

© Copyright by
Sarah Ann Jones
2022

Acknowledgements

I thank my advisor, Thomas J. Miller, for his patience, support, and optimism, especially in the months leading up to my master's defense. I thank my committee members, Dong Liang and Genny Nesslage, for their input and for providing winter dredge survey data. I thank Mike O'Brien for his expertise in R. I thank the Maryland Department of Natural Science and the Virginia Institute of Marine Science for conducting the annual winter dredge survey. I thank Glenn Davis for the time and effort he put in to analyzing the winter dredge survey data for use in these analyses. I also thank my University of Maryland Eastern Shore advisor, friend, and mentor, Maurice Crawford, who encouraged me to pursue a master's degree. This work was supported by the Maryland Port Administration and the Maryland Department of Transportation Port of Baltimore.

Table of Contents

Acknowledgements.....	ii
Table of Contents.....	iii
List of Tables.....	v
List of Figures.....	vii
List of Abbreviations.....	xx
Chapter 1: Introduction.....	1
The Port of Baltimore.....	2
The Blue Crab.....	7
Objectives.....	10
Figures for Chapter 1.....	12
Chapter 2: Impact of assumptions and data treatment on kriged estimates of blue crab abundance in Chesapeake Bay.....	16
Introduction.....	17
Objectives.....	21
Methods.....	21
Data.....	21
Design-Based Estimates.....	23
Inverse Distance Weighting (IDW).....	23
Kriging.....	24
Results and Discussion.....	26
Data.....	27
Inverse Distance Weighting.....	27
Kriging.....	28
Tables for Chapter 2.....	31
Figures for Chapter 2.....	37
Chapter 3: Small-scale estimation of adult female blue crab <i>Callinectes sapidus</i> abundance in Chesapeake Bay in dredged material placement sites.....	42
Abstract.....	43
Introduction.....	44
Methods.....	48
Design-Based Estimates.....	49
Kriging.....	50
Results.....	53
Winter Dredge Survey Data Summary.....	53
Bay-Wide Kriging.....	54
Small-Scale Kriging by Strata.....	56
Discussion.....	57
Tables for Chapter 3.....	63
Figures for Chapter 3.....	71
Chapter 4: Summary.....	131
Appendix A: R-Code for Kriging Analyses.....	136
Appendix B: Females.....	154
Tables for Appendix B.....	154
Figures for Appendix B.....	161
Appendix C: Total.....	192

Tables for Appendix C.....	192
Figures for Appendix C	194
Appendix D: Males	196
Tables for Appendix D.....	196
Figures for Appendix D	198
Appendix E: Juveniles	200
Tables for Appendix E.....	200
Figures for Appendix E.....	202
Bibliography	204

List of Tables

Table 2.1. Summary of Liang WDS data by strata location that was used in the IDW analysis. Number of stations is the number of WDS sampling locations used for analysis. The number of stations excluded is the number of stations that were removed during QA/QC procedures. 31

Table 2.2. Summary of Davis WDS data by strata used in the kriging analysis. Number of stations is the number of WDS sampling locations used for analysis. The number of stations excluded is the number of stations that were removed during QA/QC procedures..... 32

Table 2.3. Estimates of total blue crab (millions) (females and males of all ages) in Chesapeake Bay derived from IDW. Annual design-based abundance estimates are based on the stratified random design of the WDS. Percent difference (%) was calculated using the design-based estimates for the given year..... 33

Table 2.4. Effects of variogram model selection on blue crab abundance estimates (millions) (females and males of all ages) in Chesapeake Bay. Shown are kriged estimates of four different variogram models: i) Matérn, ii) exponential, iii) gaussian, and iv) spherical. The gaussian and spherical variogram model estimated fitted variograms with negative estimates of the sill, range, and nugget producing N/As... 34

Table 2.5. Effects of resolution of the predicted kriging grid on estimates of total blue crab abundance (millions) (females and males of all ages) in Chesapeake Bay. Shown are kriged estimates of four different resolutions: i) 100-m, ii) 250-m, iii) 500-m, and iv) 1,000-m..... 35

Table 2.6. Effects of normality assumption transformations on total blue crab abundance estimates (millions) (females and males of all ages) in Chesapeake Bay. Shown are kriged estimates of three different normality transformations: i) untransformed, ii) NScore, and iii) log. Annual design-based abundance estimates are based on the stratified random design of the WDS..... 36

Table 3.1. Summary of Davis WDS Strata by strata location used in the small-scale kriging analysis to estimate females age-1+. Number of stations is the number of WDS sampling locations used for analysis. The number of stations excluded is the number of stations that were removed during QA/QC procedures..... 63

Table 3.2. Estimates of female age-1+ abundance (millions) in Chesapeake Bay, WTAPS, and WTAPSNE, derived from Bay-wide kriging using Davis WDS Chesapeake Bay data. The proportion of females in WTAPS and WTAPSNE were calculated based on the Bay-wide female age-1+ kriging abundance estimate in Chesapeake Bay. 64

Table 3.3. Estimates of female age-1+ abundance (millions) in strata 2 and 3, WTAPS, and WTAPSNE, derived from kriging using Davis WDS Strata data only from strata 2 and 3. The proportion of females in WTAPS and WTAPSNE were calculated based on the Bay-wide female age-1+ kriging abundance estimate in Chesapeake Bay.....	66
Table 3.4. Estimates of female age-1+ abundance (millions) in strata 3 and WTAPS derived from kriging using Davis WDS Strata data only from strata 3. The proportion of females in WTAPS was calculated based on the Bay-wide female age-1+ kriging abundance estimate in Chesapeake Bay. WTAPSNE could not be estimated because the area extends into strata 2.....	68
Table 3.5. Estimates of female age-1+ abundance (millions) in WTAPS and WTAPSNE for Bay-wide, strata 2 and 3, and strata 3, derived from kriging by Davis WDS data. WTAPSNE for strata 3 could not be calculated because the area extends into strata 2.....	70
Table B.1. AIC values from multiple linear regression equations for female age-1+ abundance estimates derived from Bay-wide kriging using Davis WDS Chesapeake data. An * indicates the selected model used for fitting the variogram and kriging.	154
Table B.2. Estimated coefficients extracted from the best fitted multiple linear regression model derived from the Bay-wide female age-1+ kriging analysis. The coefficients were used to create trend maps and backtransform predicted kriged female abundance estimates.....	156
Table B.3. Selected fitted variogram models by year for female age-1+blue crab abundance estimates derived from Bay-wide kriging on the Davis WDS Chesapeake Bay data.	160
Table C.1. Estimates of total blue crab (females and males of all ages) abundance (millions) in Chesapeake Bay, WTAPS, and WTAPSNE, derived from Bay-wide kriging using Davis WDS Chesapeake Bay data.....	192
Table D.1. Estimates of male age-1+ abundance (millions) estimates in Chesapeake Bay, WTAPS, and WTAPSNE, derived from Bay-wide kriging in Chesapeake Bay using Davis WDS Chesapeake Bay data.	196
Table E.1. Estimates of juvenile age-0 abundance (millions) in Chesapeake Bay, WTAPS, and WTAPSNE, derived from Bay-wide kriging using Davis WDS data.	200

List of Figures

Figure 1.1. Location of WTAPSNE, WTAPS, York Split Channel, and York River Entrance Channel in the Chesapeake Bay. WTAPS and WTAPSNE are used as placement sites for material dredged from the York Split Channel.....	12
Figure 1.2. Life history of blue crab (<i>Callinectes sapidus</i>). Figure courtesy of C. Chenery.....	13
Figure 1.3. WDS total blue crab (males and females of all ages) abundance estimates (millions) in Chesapeake Bay (Chesapeake Bay Stock Assessment Committee (CBSAC) 2022).	14
Figure 1.4. Upper Bay and tributaries (white), Middle Bay (polka dots), and Lower Bay (diagnol lines), according to the stratified design of the WDS in the Chesapeake Bay.	15
Figure 2.1. 2018 IDW results for: a) Chesapeake Bay total blue crab abundance estimates (females and males of all ages), b) WTAPSNE total blue crab abundance estimates, and c) WTAPS total blue crab abundance estimates.	37
Figure 2.2. Estimates of total blue crab abundance (millions) (females and males of all ages) in Chesapeake Bay. Shown are IDW estimates (open circles; solid, grey line) and design-based abundance estimates (solid squares; dashed, black line) for 1990–2018.....	38
Figure 2.3. Effects of variogram model selection on total blue crab abundance estimates (millions) (females and males of all ages) in Chesapeake Bay from 1990–2020. Shown are kriged estimates of four different variogram models: i) Matérn (open diamond; solid, grey line), ii) exponential (solid triangles; dashed, black line), iii) gaussian (open squares; dashed, grey line), and iv) spherical (solid circles; solid, black line).....	39
Figure 2.4. Effects of resolution of the predicted kriging grid on total blue crab abundance estimates (millions) (females and males of all ages) in Chesapeake Bay from 1990–2020. Shown are kriged estimates of four different resolutions: i) 100-m (open diamond; solid, grey line), ii) 250-m (solid triangles; dashed, black line), iii) 500-m (open squares; dashed, grey line), and iv) 1,000-m (solid circles; solid, black line).	40
Figure 2.5. Effects of normality assumption transformations on total blue crab abundance estimates (millions) (females and males of all ages) in Chesapeake Bay from 1990–2020. Shown are kriged estimates of three different normality transformations: i) untransformed (open diamond; solid, grey line), ii) NScore (solid diamond; dashed, black line), and iii) log (solid circles; solid, black line).	41

Figure 3.1. Various 1990 female age-1+ blue crab maps in the Chesapeake Bay: a) map of female age-1+ blue crab density in 1990, b) selected trend map based on the best fitting multiple linear regression model in 1990, c) map of female age-1+ blue crab abundance estimates in 1990, and d) standard error map of female age-1+ blue crab abundance estimates in 1990..... 71

Figure 3.2. Various 1991 female age-1+ blue crab maps in the Chesapeake Bay: a) map of female age-1+ blue crab density in 1991, b) selected trend map based on the best fitting multiple linear regression model in 1991, c) map of female age-1+ blue crab abundance estimates in 1991, and d) standard error map of female age-1+ blue crab abundance estimates in 1991..... 72

Figure 3.3. Various 1992 female age-1+ blue crab maps in the Chesapeake Bay: a) map of female age-1+ blue crab density in 1992, b) selected trend map based on the best fitting multiple linear regression model in 1992, c) map of female age-1+ blue crab abundance estimates in 1992, and d) standard error map of female age-1+ blue crab abundance estimates in 1992..... 73

Figure 3.4. Various 1993 female age-1+ blue crab maps in the Chesapeake Bay: a) map of female age-1+ blue crab density in 1993, b) selected trend map based on the best fitting multiple linear regression model in 1993, c) map of female age-1+ blue crab abundance estimates in 1993, and d) standard error map of female age-1+ blue crab abundance estimates in 1993..... 74

Figure 3.5. Various 1994 female age-1+ blue crab maps in the Chesapeake Bay: a) map of female age-1+ blue crab density in 1994, b) selected trend map based on the best fitting multiple linear regression model in 1994, c) map of female age-1+ blue crab abundance estimates in 1994, and d) standard error map of female age-1+ blue crab abundance estimates in 1994..... 75

Figure 3.6. Various 1995 female age-1+ blue crab maps in the Chesapeake Bay: a) map of female age-1+ blue crab density in 1995, b) selected trend map based on the best fitting multiple linear regression model in 1995, c) map of female age-1+ blue crab abundance estimates in 1995, and d) standard error map of female age-1+ blue crab abundance estimates in 1995..... 76

Figure 3.7. Various 1996 female age-1+ blue crab maps in the Chesapeake Bay: a) map of female age-1+ blue crab density in 1996, b) selected trend map based on the best fitting multiple linear regression model in 1996, c) map of female age-1+ blue crab abundance estimates in 1996, and d) standard error map of female age-1+ blue crab abundance estimates in 1996..... 77

Figure 3.8. Various 1997 female age-1+ blue crab maps in the Chesapeake Bay: a) map of female age-1+ blue crab density in 1997, b) selected trend map based on the best fitting multiple linear regression model in 1997, c) map of female age-1+ blue crab abundance estimates in 1997, and d) standard error map of female age-1+ blue crab abundance estimates in 1997..... 78

Figure 3.9. Various 1998 female age-1+ blue crab maps in the Chesapeake Bay: a) map of female age-1+ blue crab density in 1998, b) selected trend map based on the best fitting multiple linear regression model in 1998, c) map of female age-1+ blue crab abundance estimates in 1998, and d) standard error map of female age-1+ blue crab abundance estimates in 1998..... 79

Figure 3.10. Various 1999 female age-1+ blue crab maps in the Chesapeake Bay: a) map of female age-1+ blue crab density in 1999, b) selected trend map based on the best fitting multiple linear regression model in 1999, c) map of female age-1+ blue crab abundance estimates in 1999, and d) standard error map of female age-1+ blue crab abundance estimates in 1999..... 80

Figure 3.11. Various 2000 female age-1+ blue crab maps in the Chesapeake Bay: a) map of female age-1+ blue crab density in 2000, b) selected trend map based on the best fitting multiple linear regression model in 2000, c) map of female age-1+ blue crab abundance estimates in 2000, and d) standard error map of female age-1+ blue crab abundance estimates in 2000..... 81

Figure 3.12. Various 2001 female age-1+ blue crab maps in the Chesapeake Bay: a) map of female age-1+ blue crab density in 2001, b) selected trend map based on the best fitting multiple linear regression model in 2001, c) map of female age-1+ blue crab abundance estimates in 2001, and d) standard error map of female age-1+ blue crab abundance estimates in 2001..... 82

Figure 3.13. Various 2002 female age-1+ blue crab maps in the Chesapeake Bay: a) map of female age-1+ blue crab density in 2002, b) selected trend map based on the best fitting multiple linear regression model in 2002, c) map of female age-1+ blue crab abundance estimates in 2002, and d) standard error map of female age-1+ blue crab abundance estimates in 2002..... 83

Figure 3.14. Various 2003 female age-1+ blue crab maps in the Chesapeake Bay: a) map of female age-1+ blue crab density in 2003, b) selected trend map based on the best fitting multiple linear regression model in 2003, c) map of female age-1+ blue crab abundance estimates in 2003, and d) standard error map of female age-1+ blue crab abundance estimates in 2003..... 84

Figure 3.15. Various 2004 female age-1+ blue crab maps in the Chesapeake Bay: a) map of female age-1+ blue crab density in 2004, b) selected trend map based on the best fitting multiple linear regression model in 2004, c) map of female age-1+ blue crab abundance estimates in 2004, and d) standard error map of female age-1+ blue crab abundance estimates in 2004..... 85

Figure 3.16. Various 2005 female age-1+ blue crab maps in the Chesapeake Bay: a) map of female age-1+ blue crab density in 2005, b) selected trend map based on the best fitting multiple linear regression model in 2005, c) map of female age-1+ blue crab abundance estimates in 2005, and d) standard error map of female age-1+ blue crab abundance estimates in 2005..... 86

Figure 3.17. Various 2006 female age-1+ blue crab maps in the Chesapeake Bay: a) map of female age-1+ blue crab density in 2006, b) selected trend map based on the best fitting multiple linear regression model in 2006, c) map of female age-1+ blue crab abundance estimates in 2006, and d) standard error map of female age-1+ blue crab abundance estimates in 2006..... 87

Figure 3.18. Various 2007 female age-1+ blue crab maps in the Chesapeake Bay: a) map of female age-1+ blue crab density in 2007, b) selected trend map based on the best fitting multiple linear regression model in 2007, c) map of female age-1+ blue crab abundance estimates in 2007, and d) standard error map of female age-1+ blue crab abundance estimates in 2007..... 88

Figure 3.19. Various 2008 female age-1+ blue crab maps in the Chesapeake Bay: a) map of female age-1+ blue crab density in 2008, b) selected trend map based on the best fitting multiple linear regression model in 2008, c) map of female age-1+ blue crab abundance estimates in 2008, and d) standard error map of female age-1+ blue crab abundance estimates in 2008..... 89

Figure 3.20. Various 2009 female age-1+ blue crab maps in the Chesapeake Bay: a) map of female age-1+ blue crab density in 2009, b) selected trend map based on the best fitting multiple linear regression model in 2009, c) map of female age-1+ blue crab abundance estimates in 2009, and d) standard error map of female age-1+ blue crab abundance estimates in 2009..... 90

Figure 3.21. Various 2010 female age-1+ blue crab maps in the Chesapeake Bay: a) map of female age-1+ blue crab density in 2010, b) selected trend map based on the best fitting multiple linear regression model in 2010, c) map of female age-1+ blue crab abundance estimates in 2010, and d) standard error map of female age-1+ blue crab abundance estimates in 2010..... 91

Figure 3.22. Various 2011 female age-1+ blue crab maps in the Chesapeake Bay: a) map of female age-1+ blue crab density in 2011, b) selected trend map based on the best fitting multiple linear regression model in 2011, c) map of female age-1+ blue crab abundance estimates in 2011, and d) standard error map of female age-1+ blue crab abundance estimates in 2011..... 92

Figure 3.23. Various 2012 female age-1+ blue crab maps in the Chesapeake Bay: a) map of female age-1+ blue crab density in 2012, b) selected trend map based on the best fitting multiple linear regression model in 2012, c) map of female age-1+ blue crab abundance estimates in 2012, and d) standard error map of female age-1+ blue crab abundance estimates in 2012..... 93

Figure 3.24. Various 2013 female age-1+ blue crab maps in the Chesapeake Bay: a) map of female age-1+ blue crab density in 2013, b) selected trend map based on the best fitting multiple linear regression model in 2013, c) map of female age-1+ blue crab abundance estimates in 2013, and d) standard error map of female age-1+ blue crab abundance estimates in 2013..... 94

Figure 3.25. Various 2014 female age-1+ blue crab maps in the Chesapeake Bay: a) map of female age-1+ blue crab density in 2014, b) selected trend map based on the best fitting multiple linear regression model in 2014, c) map of female age-1+ blue crab abundance estimates in 2014, and d) standard error map of female age-1+ blue crab abundance estimates in 2014..... 95

Figure 3.26. Various 2015 female age-1+ blue crab maps in the Chesapeake Bay: a) map of female age-1+ blue crab density in 2015, b) selected trend map based on the best fitting multiple linear regression model in 2015, c) map of female age-1+ blue crab abundance estimates in 2015, and d) standard error map of female age-1+ blue crab abundance estimates in 2015..... 96

Figure 3.27. Various 2016 female age-1+ blue crab maps in the Chesapeake Bay: a) map of female age-1+ blue crab density in 2016, b) selected trend map based on the best fitting multiple linear regression model in 2016, c) map of female age-1+ blue crab abundance estimates in 2016, and d) standard error map of female age-1+ blue crab abundance estimates in 2016..... 97

Figure 3.28. Various 2017 female age-1+ blue crab maps in the Chesapeake Bay: a) map of female age-1+ blue crab density in 2017, b) selected trend map based on the best fitting multiple linear regression model in 2017, c) map of female age-1+ blue crab abundance estimates in 2017, and d) standard error map of female age-1+ blue crab abundance estimates in 2017..... 98

Figure 3.29. Various 2018 female age-1+ blue crab maps in the Chesapeake Bay: a) map of female age-1+ blue crab density in 2018, b) selected trend map based on the best fitting multiple linear regression model in 2018, c) map of female age-1+ blue crab abundance estimates in 2018, and d) standard error map of female age-1+ blue crab abundance estimates in 2018..... 99

Figure 3.30. Various 2019 female age-1+ blue crab maps in the Chesapeake Bay: a) map of female age-1+ blue crab density in 2019, b) selected trend map based on the best fitting multiple linear regression model in 2019, c) map of female age-1+ blue crab abundance estimates in 2019, and d) standard error map of female age-1+ blue crab abundance estimates in 2019..... 100

Figure 3.31. Various 2020 female age-1+ blue crab maps in the Chesapeake Bay: a) map of female age-1+ blue crab density in 2020, b) selected trend map based on the best fitting multiple linear regression model in 2020, c) map of female age-1+ blue crab abundance estimates in 2020, and d) standard error map of female age-1+ blue crab abundance estimates in 2020..... 101

Figure 3.32. Estimates of female age-1+ blue crab abundance (millions) in Chesapeake Bay. Shown are female age-1+ kriged abundance estimates (open circles; solid, grey line) and design-based female age-1+ abundance estimates (solid squares; dashed, black line) for 1990–2020..... 102

Figure 3.33. Female age 1+ blue crab abundance maps in WTAPSNE (top) and WTAPS (bottom) derived from kriging in the Chesapeake Bay for 1990–1993: a) WTAPSNE female age-1+ abundance in 1990, b) WTAPS female age-1+ abundance in 1990, c) WTAPSNE female age-1+ abundance in 1991, d) WTAPS female age-1+ abundance in 1991, e) WTAPSNE female age-1+ abundance in 1992, f) WTAPS female age-1+ abundance in 1992, g) WTAPSNE female age-1+abundance in 1993, and h) WTAPS age-1+ abundance in 1993. 103

Figure 3.34. Female age 1+ blue crab abundance maps in WTAPSNE (top) and WTAPS (bottom) derived from kriging in the Chesapeake Bay for 1994–1997: a) WTAPSNE female age-1+ abundance in 1994, b) WTAPS female age-1+ abundance in 1994, c) WTAPSNE female age-1+ abundance in 1995, d) WTAPS female age-1+ abundance in 1995, e) WTAPSNE female age-1+ abundance in 1996, f) WTAPS female age-1+ abundance in 1996, g) WTAPSNE female age-1+abundance in 1997, and h) WTAPS age-1+ abundance in 1997. 104

Figure 3.35. Female age 1+ blue crab abundance maps in WTAPSNE (top) and WTAPS (bottom) derived from kriging in the Chesapeake Bay for 1998–2001: a) WTAPSNE female age-1+ abundance in 1998, b) WTAPS female age-1+ abundance in 1998, c) WTAPSNE female age-1+ abundance in 1999, d) WTAPS female age-1+ abundance in 1999, e) WTAPSNE female age-1+ abundance in 2000, f) WTAPS female age-1+ abundance in 2000, g) WTAPSNE female age-1+abundance in 2001, and h) WTAPS age-1+ abundance in 2001. 105

Figure 3.36. Female age 1+ blue crab abundance maps in WTAPSNE (top) and WTAPS (bottom) derived from kriging in the Chesapeake Bay for 2002–2005: a) WTAPSNE female age-1+ abundance in 2002, b) WTAPS female age-1+ abundance in 2002, c) WTAPSNE female age-1+ abundance in 2003, d) WTAPS female age-1+ abundance in 2003, e) WTAPSNE female age-1+ abundance in 2004, f) WTAPS female age-1+ abundance in 2004, g) WTAPSNE female age-1+abundance in 2005, and h) WTAPS age-1+ abundance in 2005. 106

Figure 3.37. Female age 1+ blue crab abundance maps in WTAPSNE (top) and WTAPS (bottom) derived from kriging in the Chesapeake Bay for 2006–2009: a) WTAPSNE female age-1+ abundance in 2006, b) WTAPS female age-1+ abundance in 2006, c) WTAPSNE female age-1+ abundance in 2007, d) WTAPS female age-1+ abundance in 2007, e) WTAPSNE female age-1+ abundance in 2008, f) WTAPS female age-1+ abundance in 2008, g) WTAPSNE female age-1+abundance in 2009, and h) WTAPS age-1+ abundance in 2009. 107

Figure 3.38. Female age 1+ blue crab abundance maps in WTAPSNE (top) and WTAPS (bottom) derived from kriging in the Chesapeake Bay for 2010–2013: a) WTAPSNE female age-1+ abundance in 2010, b) WTAPS female age-1+ abundance in 2010, c) WTAPSNE female age-1+ abundance in 2011, d) WTAPS female age-1+ abundance in 2011, e) WTAPSNE female age-1+ abundance in 2012, f) WTAPS female age-1+ abundance in 2012, g) WTAPSNE female age-1+abundance in 2013, and h) WTAPS age-1+ abundance in 2013. 108

Figure 3.39. Female age 1+ blue crab abundance maps in WTAPSNE (top) and WTAPS (bottom) derived from kriging in the Chesapeake Bay for 2014–2017: a) WTAPSNE female age-1+ abundance in 2014, b) WTAPS female age-1+ abundance in 2014, c) WTAPSNE female age-1+ abundance in 2015, d) WTAPS female age-1+ abundance in 2015, e) WTAPSNE female age-1+ abundance in 2016, f) WTAPS female age-1+ abundance in 2016, g) WTAPSNE female age-1+ abundance in 2017, and h) WTAPS age-1+ abundance in 2017. 109

Figure 3.40. Female age 1+ blue crab abundance maps in WTAPSNE (top) and WTAPS (bottom) derived from kriging in the Chesapeake Bay for 2018–2020: a) WTAPSNE female age-1+ abundance in 2018, b) WTAPS female age-1+ abundance in 2018, c) WTAPSNE female age-1+ abundance in 2019, d) WTAPS female age-1+ abundance in 2019, e) WTAPSNE female age-1+ abundance in 2020, and f) WTAPS female age-1+ abundance in 2020. 110

Figure 3.41. Proportion of female age-1+ blue crab abundance in WTAPS and WTAPSNE (%) out of the Bay-wide kriging abundance estimates in Chesapeake Bay. Shown are kriged estimates of the proportion of females age-1+ (%) in WTAPS (closed triangles; solid, black line) and WTAPSNE (solid circle; dashed, grey line) for 1990–2020. 111

Figure 3.42. The proportion of females age-1+ in WTAPS (%) out of the Bay-wide female age-1+ kriging abundance estimate versus the Bay-wide female age-1+ abundance in Chesapeake Bay (millions) from 1990–2020. $y = -0.0002x + 0.6140$. 112

Figure 3.43. Female age-1+ blue crab abundance maps in WTAPSNE (top) and WTAPS (bottom) derived from kriging using data only from Strata 2 and 3 in the Davis WDS Strata for 1990–1993: a) WTAPSNE female age-1+ abundance in 1990, b) WTAPS female age-1+ abundance in 1990, c) WTAPSNE female age-1+ abundance in 1991, d) WTAPS female age-1+ abundance in 1991, e) WTAPSNE female age-1+ abundance in 1992, f) WTAPS female age-1+ abundance in 1992, g) WTAPSNE female age-1+ abundance in 1993, and h) WTAPS female age-1+ abundance in 1993. 113

Figure 3.44. Female age-1+ blue crab abundance maps in WTAPSNE (top) and WTAPS (bottom) derived from kriging using data only from Strata 2 and 3 in the Davis WDS Strata for 1994–1997: a) WTAPSNE female age-1+ abundance in 1994, b) WTAPS female age-1+ abundance in 1994, c) WTAPSNE female age-1+ abundance in 1995, d) WTAPS female age-1+ abundance in 1995, e) WTAPSNE female age-1+ abundance in 1996, f) WTAPS female age-1+ abundance in 1996, g) WTAPSNE female age-1+ abundance in 1997, and h) WTAPS female age-1+ abundance in 1997. 114

Figure 3.45. Female age-1+ blue crab abundance maps in WTAPSNE (top) and WTAPS (bottom) derived from kriging using data only from Strata 2 and 3 in the Davis Strata WDS for 1998–2001: a) WTAPSNE female age-1+ abundance in 1998, b) WTAPS female age-1+ abundance in 1998, c) WTAPSNE female age-1+

abundance in 1999, d) WTAPS female age-1+ abundance in 1999, e) WTAPSNE female age-1+ abundance in 2000, f) WTAPS female age-1+ abundance in 2000, g) WTAPSNE female age-1+ abundance in 2001, and h) WTAPS female age-1+ abundance in 2001. 115

Figure 3.46. Female age-1+ blue crab abundance maps in WTAPSNE (top) and WTAPS (bottom) derived from kriging using data only from Strata 2 and 3 in the Davis WDS Strata for 2002–2005: a) WTAPSNE female age-1+ abundance in 2002, b) WTAPS female age-1+ abundance in 2002, c) WTAPSNE female age-1+ abundance in 2003, d) WTAPS female age-1+ abundance in 2003, e) WTAPSNE female age-1+ abundance in 2004, f) WTAPS female age-1+ abundance in 2004, g) WTAPSNE female age-1+ abundance in 2005, and h) WTAPS female age-1+ abundance in 2005. 116

Figure 3.47. Female age-1+ blue crab abundance maps in WTAPSNE (top) and WTAPS (bottom) derived from kriging using data only from Strata 2 and 3 in the Davis WDS Strata for 2006–2009: a) WTAPSNE female age-1+ abundance in 2006, b) WTAPS female age-1+ abundance in 2006, c) WTAPSNE female age-1+ abundance in 2007, d) WTAPS female age-1+ abundance in 2007, e) WTAPSNE female age-1+ abundance in 2008, f) WTAPS female age-1+ abundance in 2008, g) WTAPSNE female age-1+ abundance in 2009, and h) WTAPS female age-1+ abundance in 2009. 117

Figure 3.48. Female age-1+ blue crab abundance maps in WTAPSNE (top) and WTAPS (bottom) derived from kriging using data only from Strata 2 and 3 in the Davis WDS Strata for 2010–2013: a) WTAPSNE female age-1+ abundance in 2010, b) WTAPS female age-1+ abundance in 2010, c) WTAPSNE female age-1+ abundance in 2011, d) WTAPS female age-1+ abundance in 2011, e) WTAPSNE female age-1+ abundance in 2012, f) WTAPS female age-1+ abundance in 2012, g) WTAPSNE female age-1+ abundance in 2013, and h) WTAPS female age-1+ abundance in 2013. 118

Figure 3.49. Female age-1+ blue crab abundance maps in WTAPSNE (top) and WTAPS (bottom) derived from kriging using data only from Strata 2 and 3 in the Davis WDS Strata for 2014–2017: a) WTAPSNE female age-1+ abundance in 2014, b) WTAPS female age-1+ abundance in 2014, c) WTAPSNE female age-1+ abundance in 2015, d) WTAPS female age-1+ abundance in 2015, e) WTAPSNE female age-1+ abundance in 2016, f) WTAPS female age-1+ abundance in 2016, g) WTAPSNE female age-1+ abundance in 2017, and h) WTAPS female age-1+ abundance in 2017. 119

Figure 3.50. Female age-1+ blue crab abundance maps in WTAPSNE (top) and WTAPS (bottom) derived from kriging using data only from Strata 2 and 3 in the Davis WDS Strata for 2018–2020: a) WTAPSNE female age-1+ abundance in 2018, b) WTAPS female age-1+ abundance in 2018, c) WTAPSNE female age-1+ abundance in 2019, d) WTAPS female age-1+ abundance in 2019, e) WTAPSNE

female age-1+ abundance in 2020, and f) WTAPS female age-1+ abundance in 2020. 120

Figure 3.51. Female age-1+ blue crab abundance maps in WTAPS derived from kriging using Davis WDS Strata data only from Strata 3 for 1990–1993: a) WTAPS age-1+ abundance in 1990, b) WTAPS age-1+ abundance in 1991, c) WTAPS age-1+ abundance in 1992, and d) WTAPS age-1+ abundance in 1993. 121

Figure 3.52. Female age-1+ blue crab abundance maps in WTAPS derived from kriging using Davis WDS Strata data only from Strata 3 for 1994–1997: a) WTAPS age-1+ abundance in 1994, b) WTAPS age-1+ abundance in 1995, c) WTAPS age-1+ abundance in 1996, and d) WTAPS age-1+ abundance in 1997. 122

Figure 3.53. Female age-1+ blue crab abundance maps in WTAPS derived from kriging using Davis WDS Strata data only from Strata 3 for 1998–2001: a) WTAPS age-1+ abundance in 1998, b) WTAPS age-1+ abundance in 1999, c) WTAPS age-1+ abundance in 2000, and d) WTAPS age-1+ abundance in 2001. 123

Figure 3.54. Female age-1+ blue crab abundance maps in WTAPS derived from kriging using Davis WDS Strata data only from Strata 3 for 2002–2005: a) WTAPS age-1+ abundance in 2002, b) WTAPS age-1+ abundance in 2003, c) WTAPS age-1+ abundance in 2004, and d) WTAPS age-1+ abundance in 2005. 124

Figure 3.55. Female age-1+ blue crab abundance maps in WTAPS derived from kriging using Davis WDS Strata data only from Strata 3 for 2006–2009: a) WTAPS age-1+ abundance in 2006, b) WTAPS age-1+ abundance in 2007, c) WTAPS age-1+ abundance in 2008, and d) WTAPS age-1+ abundance in 2009. 125

Figure 3.56. Female age-1+ blue crab abundance maps in WTAPS derived from kriging using Davis WDS Strata data only from Strata 3 for 2010–2013: a) WTAPS age-1+ abundance in 2010, b) WTAPS age-1+ abundance in 2011, c) WTAPS age-1+ abundance in 2012, and d) WTAPS age-1+ abundance in 2013. 126

Figure 3.57. Female age-1+ blue crab abundance maps in WTAPS derived from kriging using Davis WDS data only from Strata 3 for 2014–2017: a) WTAPS age-1+ abundance in 2014, b) WTAPS age-1+ abundance in 2015, c) WTAPS age-1+ abundance in 2016, and d) WTAPS age-1+ abundance in 2017. 127

Figure 3.58. Female age-1+ blue crab abundance maps in WTAPS derived from kriging using Davis WDS Strata data only from Strata 3 for 2018–2020: a) WTAPS age-1+ abundance in 2018, b) WTAPS age-1+ abundance in 2019, and c) WTAPS age-1+ abundance in 2020. 128

Figure 3.59. Comparison of female age-1+ blue crab abundance estimates in WTAPSNE (millions) based on Davis WDS data either for Bay-wide or Strata 2 and 3 from 1990–2020. Shown are kriged estimates of female age-1+ Bay-wide abundance estimates in WTAPSNE (closed triangles; solid, black line) and Strata 2

and 3 abundance estimates in WTAPSNE (solid circle; dashed, black line) for 1990–2020..... 129

Figure 3.60. Comparison of female age-1+ blue crab abundance estimates in WTAPS (millions) based on either Davis WDS Chesapeake Bay (Bay-wide) or Davis WDS Strata data either for Bay-wide, strata 2 and 3, or strata 3 only from 1990–2020. Shown are kriged estimates of female age-1+ Bay-wide abundance estimates in WTAPS (closed triangles; solid, black line), Strata 2 and 3 abundance estimates in WTAPS (solid circle; dashed, black line), and strata 3 abundance estimates in WTAPS (solid square; solid, grey line) for 1990–2020. 130

Figure B.1. 1990 female age-1+ blue crab fitted variogram derived from Bay-wide kriging using Davis WDS Chesapeake Bay data. Model parameters are provided in Table B.3..... 161

Figure B.2. 1991 female age-1+ blue crab fitted variogram derived from Bay-wide kriging using Davis WDS Chesapeake Bay data. Model parameters are provided in Table B.3..... 162

Figure B.3. 1992 female age-1+ blue crab fitted variogram derived from Bay-wide kriging using Davis WDS Chesapeake Bay data. Model parameters are provided in Table B.3..... 163

Figure B.4. 1993 female age-1+ blue crab fitted variogram derived from Bay-wide kriging using Davis WDS Chesapeake Bay data. Model parameters are provided in Table B.3..... 164

Figure B.5. 1994 female age-1+ blue crab fitted variogram derived from Bay-wide kriging using Davis WDS Chesapeake Bay data. Model parameters are provided in Table B.3..... 165

Figure B.6. 1995 female age-1+ blue crab fitted variogram derived from Bay-wide kriging using Davis WDS Chesapeake Bay data. Model parameters are provided in Table B.3..... 166

Figure B.7. 1996 female age-1+ blue crab fitted variogram derived from Bay-wide kriging using Davis WDS Chesapeake Bay data. Model parameters are provided in Table B.3..... 167

Figure B.8. 1997 female age-1+ blue crab fitted variogram derived from Bay-wide kriging using Davis WDS Chesapeake Bay data. Model parameters are provided in Table B.3..... 168

Figure B.9. 1998 female age-1+ blue crab fitted variogram derived from Bay-wide kriging using Davis WDS Chesapeake Bay data. Model parameters are provided in Table B.3..... 169

Figure B.10. 1999 female age-1+ blue crab fitted variogram derived from Bay-wide kriging using Davis WDS Chesapeake Bay data. Model parameters are provided in Table B.3.....	170
Figure B.11. 2000 female age-1+ blue crab fitted variogram derived from Bay-wide kriging using Davis WDS Chesapeake Bay data. Model parameters are provided in Table B.3.....	171
Figure B.12. 2001 female age-1+ blue crab fitted variogram derived from Bay-wide kriging using Davis WDS Chesapeake Bay data. Model parameters are provided in Table B.3.....	172
Figure B.13. 2002 female age-1+ blue crab fitted variogram derived from Bay-wide kriging using Davis WDS Chesapeake Bay data. Model parameters are provided in Table B.3.....	173
Figure B.14. 2003 female age-1+ blue crab fitted variogram derived from Bay-wide kriging using Davis WDS Chesapeake Bay data. Model parameters are provided in Table B.3.....	174
Figure B.15. 2004 female age-1+ blue crab fitted variogram derived from Bay-wide kriging using Davis WDS Chesapeake Bay data. Model parameters are provided in Table B.3.....	175
Figure B.16. 2005 female age-1+ blue crab fitted variogram derived from Bay-wide kriging using Davis WDS Chesapeake Bay data. Model parameters are provided in Table B.3.....	176
Figure B.17. 2006 female age-1+ blue crab fitted variogram derived from Bay-wide kriging using Davis WDS Chesapeake Bay data. Model parameters are provided in Table B.3.....	177
Figure B.18. 2007 female age-1+ blue crab fitted variogram derived from Bay-wide kriging using Davis WDS Chesapeake Bay data. Model parameters are provided in Table B.3.....	178
Figure B.19. 2008 female age-1+ blue crab fitted variogram derived from Bay-wide kriging using Davis WDS Chesapeake Bay data. Model parameters are provided in Table B.3.....	179
Figure B.20. 2009 female age-1+ blue crab fitted variogram derived from Bay-wide kriging using Davis WDS Chesapeake Bay data. Model parameters are provided in Table B.3.....	180
Figure B.21. 2010 female age-1+ blue crab fitted variogram derived from Bay-wide kriging using Davis WDS Chesapeake Bay data. Model parameters are provided in Table B.3.....	181

Figure B.22. 2011 female age-1+ blue crab fitted variogram derived from Bay-wide kriging using Davis WDS Chesapeake Bay data. Model parameters are provided in Table B.3.....	182
Figure B.23. 2012 female age-1+ blue crab fitted variogram derived from Bay-wide kriging using Davis WDS Chesapeake Bay data. Model parameters are provided in Table B.3.....	183
Figure B.24. 2013 female age-1+ blue crab fitted variogram derived from Bay-wide kriging using Davis WDS Chesapeake Bay data. Model parameters are provided in Table B.3.....	184
Figure B.25. 2014 female age-1+ blue crab fitted variogram derived from Bay-wide kriging using Davis WDS Chesapeake Bay data. Model parameters are provided in Table B.3.....	185
Figure B.26. 2015 female age-1+ blue crab fitted variogram derived from Bay-wide kriging using Davis WDS Chesapeake Bay data. Model parameters are provided in Table B.3.....	186
Figure B.27. 2016 female age-1+ blue crab fitted variogram derived from Bay-wide kriging using Davis WDS Chesapeake Bay data. Model parameters are provided in Table B.3.....	187
Figure B.28. 2017 female age-1+ blue crab fitted variogram derived from Bay-wide kriging using Davis WDS Chesapeake Bay data. Model parameters are provided in Table B.3.....	188
Figure B.29. 2018 female age-1+ blue crab fitted variogram derived from Bay-wide kriging using Davis WDS Chesapeake Bay data. Model parameters are provided in Table B.3.....	189
Figure B.30. 2019 female age-1+ blue crab fitted variogram derived from Bay-wide kriging using Davis WDS Chesapeake Bay data. Model parameters are provided in Table B.3.....	190
Figure B.31. 2020 female age-1+ blue crab fitted variogram derived from Bay-wide kriging using Davis WDS Chesapeake Bay data. Model parameters are provided in Table B.3.....	191
Figure C.1. Estimates of total blue crab (females and males of all ages) abundance (millions) in Chesapeake Bay. Shown are total blue crab kriged abundance estimates (open circles; solid, grey line) and design-based blue crab abundance estimates (solid squares; dashed, black line) for 1990–2020.....	194
Figure C.2. Proportion of total blue crab (females and males of all ages) abundance in WTAPS and WTAPSNE (%) out of the Bay-wide kriging abundance in Chesapeake Bay. Shown are kriged estimates of the proportion of blue crab (%) in WTAPS	

(closed triangles; solid, black line) and WTAPSNE (solid circle; dashed, grey line) for 1990–2020. 195

Figure D.1. Estimates of male age-1+ blue crab abundance (millions) in Chesapeake Bay. Shown are male age-1+ blue crab kriged estimates (open circles; solid, grey line) and design-based male age-1+ abundance estimates (solid squares; dashed, black line) for 1990–2020. 198

Figure D.2. Proportion of male age-1+ blue crab abundance in WTAPS and WTAPSNE (%) out of the Bay-wide abundance. Shown are kriged estimates of the proportion of males age-1+ (%) in WTAPS (closed triangles; solid, black line) and WTAPSNE (solid circle; dashed, grey line) for 1990–2020. 199

Figure E.1. Estimates of juvenile age-0 blue crab abundance (millions) in Chesapeake Bay. Shown are juvenile age-0 blue crab kriged estimates (open circles; solid, grey line) and design-based juvenile age-0 abundance estimates (solid squares; dashed, black line) for 1990–2020. 202

Figure E.2. Proportion of juvenile age-0 blue crab abundance in WTAPS and WTAPSNE (%) out of the Bay-wide kriging abundance in Chesapeake Bay. Shown are kriged estimates of the proportion of juveniles age-0 (%) in WTAPS (closed triangles; solid, black line) and WTAPSNE (solid circle; dashed, grey line) for 1990–2020. 203

List of Abbreviations

IDW	Inverse distance weighting is a method within geostatistics that uses a deterministic approach to derive point estimates based on a weighted sum of sampled locations in which the weights are proportional to the distances between stations.
MDOT MPA	Maryland Department of Transportation Maryland Port Administration works to maintain operations in the Port of Baltimore, including working collaboratively to dredge shipping channels in the Chesapeake Bay and identifying solutions for the placement of dredged material in the Chesapeake Bay.
USACE	The United States Army Corps of Engineers works collaboratively with MDOT MPA to maintain the shipping channels of the Chesapeake Bay through dredging and placement of dredged material.
WDS	The winter dredge survey is an extensive survey of the Chesapeake Bay blue crab population that uses a stratified design to produce design-based abundance estimates of blue crab in the Chesapeake Bay for management purposes.
WTAPS	Wolf Trap Alternate Open Water Placement Site is located in the lower portion of the Chesapeake Bay between the Piankatank River, VA, and Mobjack Bay, VA. WTAPS is an authorized placement site for material dredged from the York Spit Channel.
WTAPSNE	Wolf Trap Alternate Open Water Placement Site Northern Extension extends the WTAPS site to the north and is an alternative placement site to the WTAPS site.
MDNR	Maryland Department of Natural Resources
VIMS	Virginia Institute of Marine Science

Chapter 1: Introduction

The Port of Baltimore

The Port of Baltimore is located on the Patapsco River, a tributary of the Chesapeake Bay (Lynch 2001). The 72-kilometer (45-mile) shoreline of the Port of Baltimore provides terminals for commercial trade and public and private cargo terminals (Lynch 2001). The Port is a major economic engine in Maryland's economy. The Port of Baltimore imported approximately 43.6 billion tons of international cargo in 2021, worth approximately \$61.3 billion (Doyle and Ports 2022). The Port of Baltimore also stimulates the economy through the provision of approximately 140,000 jobs in Maryland (Doyle and Ports 2022; Maryland Department of Transportation Maryland Port Administration (MDOT MPA) 2021). In 2021, the Port of Baltimore generated \$3.3 billion in personal wages and salary income and \$395 million in state and local tax revenues in 2021 (Doyle and Ports 2022; MDOT MPA 2021). Consequently, maintaining and even expanding port operations in Baltimore is a high priority in Maryland (Doyle and Ports 2022).

In 2016, the Panama Canal Authority completed expansion of the Panama Canal (Wang, Talley, and Brooks 2016). The expansion permits the canal to accommodate larger containerhips, called post-Panamax vessels, with drafts of 15-m (50-feet) compared to 13-m (42-feet) prior to the expansion (Rodrigue and Notteboom 2015; Sabonge 2014). Baltimore was one of only four Eastern United States (U.S.) ports with a 15-m shipping channel and a 15-m container berth to allow passage and processing of post-Panamax ships (Lynch 2001; State of Maryland 2022). The larger size of post-Panamax vessels emphasizes the necessity to maintain shipping channels leading to the Port of Baltimore (MDOT MPA 2021).

The Maryland Department of Transportation Maryland Port Administration (MDOT MPA) and the U.S. Army Corps of Engineers (USACE) work collaboratively to maintain shipping channels in the Chesapeake Bay that lead to the Port of Baltimore (Doyle and Ports 2022; Fischer-Huettner et al. 2015; The Independent Technical Review Team 2009; MDOT MPA 2021). Approximately 3.9 million cubic meters (5.1 million cubic yards) of material are dredged from the channels leading to the Port of Baltimore every year (The Independent Technical Review Team 2009). The identification and maintenance of locations for dredged material placement including long-range capacity planning, site engineering, optimization of operations at dredged material placement sites, permit acquisition, and compliance are key factors in maintaining operations in Baltimore (Fischer-Huettner et al. 2015; MDOT MPA 2021).

The USACE has permitting authority to regulate discharges of dredged or fill material into waters of the United States and structures or work in navigable waters of the United States under Section 404 of the Clean Water Act and Section 10 of the Rivers and Harbors Act of 1899 (Maryland Department of the Environment 2019). Section 404 of the Clean Water Act provides that permits will be denied if the placement site has adverse effects on municipal water supplies, shellfish beds and fishery areas (including spawning and breeding areas), wildlife, or recreational areas (United States Environmental Protection Agency 2021). Section 10 of the Rivers and Harbors Act of 1899 states that work such as dredging or disposal of dredged material, or excavation, filling, or other modifications to navigable waters of the United States construction of any structure in or over any navigable water of the U.S.

is unlawful unless the work has been recommended by the Chief of Engineers and authorized by the Secretary of the Army (USACE 2012).

The Maryland Department of the Environment (2019) has determined that dredged material in Maryland is a valuable resource since the material consists of naturally occurring particulates derived from the natural erosion of rocks and soil. Usage of the dredged material in the Chesapeake Bay is split into three categories: beneficial use, innovative reuse and open water placement. Beneficial use of dredged material from the Chesapeake Bay and its tributary waters includes: i) the restoration of underwater grasses, ii) the restoration of islands, iii) the stabilization of eroding shorelines, iv) the creation or restoration of wetlands, and v) the creation, restoration, or enhancement of fish or shellfish habitats (Maryland Department of the Environment 2019). The successful restoration and habitat creation of Poplar Island is a high-profile example of beneficial use of dredged material in the Chesapeake Bay (Derrick et al. 2007). Innovative reuse is the use of dredged material in the development or manufacturing of commercial, industrial, horticultural, agricultural, or other products. Some innovative reuse projects to date include landfill cover and topsoil for landscaping and agriculture usage (Maryland Department of the Environment 2019). Open water placement involves placing dredged material in an approved site in open waters (i.e., the mainstem of the Chesapeake Bay).

The 15-m (50-foot) shipping channel in the mainstem of the Chesapeake Bay is an important access route for post-Panamax ships using the Port of Baltimore. Dredging material from this channel to maintain its depth is important to maintaining port operations. Wolf Trap Alternate Open Water Placement Site (WTAPS), located

between the Piankatank River, VA, and Mobjack Bay, VA, is an authorized placement site for material dredged from the York Spit Channel in the lower portion of the Chesapeake Bay (Figure 1.1) (USACE Baltimore District 2019). Placement of dredged material has occurred in the area since the late 1980s with the most recent placement in 2017 (USACE Baltimore District 2019). WTAPS is an 1,810-hectare (4,474-acre) site characterized by depths between 13–16-m (Lipcius and Knick 2016) with very fine to fine sand and silts throughout the site (USACE Baltimore District 2019). Placement of up to 1.1 million cubic meters (1.4 million cubic yards) of dredged material in WTAPS occurs every three to five years (MDOT MPA 2021; USACE Baltimore District 2019). There is an additional site called WTAPS Northern Extension (WTAPSNE) which extends the WTAPS site to the north (Figure 1.1) (USACE Baltimore District 2019). The cost for this placement site exceeds the cost in WTAPS by approximately \$21.9 million (in FY 19 dollars) over a 20-year planning period due to the increased travel distance and fuel consumption between the dredging site and placement site (USACE Baltimore District 2019).

An important decision in the permitting of placement activities is the potential risk to threatened and endangered species. The federal Endangered Species Act of 1973 (16 U.S.C. ch. 35 § 1531 et seq) directs federal agencies, such as the USACE, to avoid impacts on species listed as either threatened or endangered. Where impacts to threatened or endangered species are unavoidable, dredging activities are required to obtain a “take” permit that specifies the estimated number of individuals that may be killed within the area prior to the activities. The Act establishes a process under which individual species are evaluated to determine their population status and

whether they merit protection under the Act because of low levels of abundance.

Relative to dredging operations in the lower Bay, there are six federally listed threatened and endangered species: i) loggerhead sea turtle (*Caretta caretta*), ii) green sea turtle (*Chelonia mydas*), iii) leatherback sea turtle (*Dermochelys coriacea*), iv) Kemp's ridley sea turtle (*Lepidochelys kempii*), v) Atlantic sturgeon (*Acipenser oxyrinchus*), and vi) shortnose sturgeon (*Acipenser brevirostrum*).

The Chesapeake Bay is toward the northern end of the range of the three turtle species, and, as a result, these species are occasional visitors to the Bay during summer months. In contrast, Atlantic and shortnose sturgeon are more common members of the Chesapeake Bay ecosystem. During the colonial period, both species supported important fisheries (Balazik 2017; Hilton et al. 2016). Due to the targeted fisheries and by-catch in offshore gill net fisheries, the abundance of both sturgeon species declined precipitously. More recently, restoration and conservation measures have resulted in abundance increases of both sturgeon species. There are two important spawning areas for Atlantic sturgeon in the Chesapeake Bay: i) James River, VA, and ii) Marshyhope Creek, VA - Nanticoke River, MD (Secor et al. 2022). Shortnose sturgeon are less common than their larger conspecific, the Atlantic sturgeon, but this species also occurs regularly in the Chesapeake Bay (Welsh et al. 2002).

The USACE must consider ways to mitigate or avoid negative impacts on these threatened and endangered species when dredging and selecting areas for placement activities in the Chesapeake Bay. Since endangered sea turtles are only present during summer months, and both Atlantic and shortnose sturgeon reproduce

from late spring to autumn, the USACE has limited placement of dredged material overboard to winter in the Chesapeake Bay (USACE Baltimore District 2019).

The Blue Crab

The blue crab (*Callinectes sapidus*) is an important component of estuarine and coastal ecosystems from Texas to New Hampshire (Williams 1974). Throughout this range, blue crab exhibits a complex life history spanning both marine (larvae) and estuarine habitats (juvenile – adult stages – Figure 1.2). In the Chesapeake region, females release their zoea at the mouth of the Bay, and the larvae are advected out into the coastal ocean (Roman and Boicourt 1999). In the coastal ocean, these larvae feed and molt 7 or 8 times to form the last larval stage, the megalopae, which reinvade the Bay (Epifanio 2007). The megalopae begin settling into structurally complex environments and eventually transform into the first juvenile crab stage (Lipcius et al. 2007). Growth occurs from spring to autumn when water temperatures are above ~11°C (Brylawski and Miller 2006). In winter months when the Chesapeake Bay temperature drops below ~11°C, blue crab exhibit torpor and are associated with sediments (Bauer and Miller 2010a; Bauer and Miller 2010b).

Blue crab distribution patterns while overwintering in the Chesapeake Bay is sex and life stage specific. Immature females migrate throughout the Bay, including to lower salinity waters which coincides with overwintering habitat of mature males in the upper portion of the Chesapeake Bay (Millikin and Williams 1984). Mature male blue crabs also frequent the deeper channels of the Chesapeake Bay. Immature juvenile blue crabs predominate in the lower salinity waters of the upper Chesapeake Bay and tributaries (Millikin and Williams 1984). Inseminated, mature females

migrate to the saltier, deeper waters of the lower Chesapeake Bay to overwinter in preparation to release broods close to the mouth of the Bay in the late spring and early summer to promote larval dispersal (Jivoff, Hines, and Quackenbush 2007; van Engel 1958). Agencies of the Commonwealth of Virginia have expressed concerns over the placement of dredged material in WTAPS due to the possibility of high abundances of overwintering mature female blue crab who migrate to lower Bay waters during the late autumn to prepare for spawning in the spring (USACE Baltimore District 2019).

Blue crab supports important commercial and recreational fisheries in Chesapeake Bay (Miller et al. 2011). The fisheries are managed cooperatively by the Commonwealth of Virginia, the State of Maryland, and the Potomac River Fisheries Commission. Owing to the importance of these fisheries, there have been substantial investments in surveying the abundance of blue crab in the Chesapeake Bay (Miller et al. 2011). Currently, four principal fishery independent surveys for blue crab are conducted. The Commonwealth of Virginia and the State of Maryland conduct trawl surveys for blue crab, principally during summer months. These surveys have been conducted since 1955 and 1968, respectively. A Bay-wide trawl survey, the Chesapeake Bay Multispecies Monitoring and Assessment Program (ChesMMAP) has been conducted since 2002. All three of these surveys provide indices of abundance (Miller et al. 2011). However, the most comprehensive survey for blue crab in Chesapeake Bay takes advantage of the period of winter quiescence to estimate crab abundance. Conducted from December to March since 1990, the winter dredge survey (WDS) is a stratified random survey that uses a commercial 1.8-m (6-

foot) Virginia dredge to sample waters of the Chesapeake Bay deeper than 1.5 m (5-foot) (Sharov et al. 2003). The dredge is towed for approximately one minute. The primary objectives of the annual WDS are to: i) describe the size and sex composition of the Bay-wide population, ii) develop accurate estimates of Bay-wide blue crab abundance (Figure 1.3), and iii) estimate exploitation and fishing mortality and evaluate the status of the stock annually.

Typically, data from the WDS are analyzed using standard design-based methods to yield estimates of blue crab abundance (Sharov et al. 2003). Since 1992, three fixed geographic strata have been employed: i) the upper Bay and principal tributaries, ii) the middle Bay, and iii) the lower Bay (Figure 1.4). More recently, Liang et al. (2017) have combined Bayesian approaches with the traditional design-based estimates to more fully estimate variability associated with the abundance estimates. Jensen and Miller (2005) and Jensen, Christman, and Miller (2006) applied geostatistical techniques to WDS data to estimate abundance, thereby assessing potential uncertainties in the design-based estimates. Jensen, Christman, and Miller (2006) indicated that design-based estimates and geostatistical estimates were broadly similar, but geostatistical approaches had the advantage that they could also estimate distributional changes across the time series. These analyses indicated that the center of distribution of mature females demonstrated a density-dependent response.

For this application, geostatistical approaches offer one advantage over the traditional design-based approach in that geostatistical approaches can be applied to any smaller region within the survey area. Specifically, because the design-based approach employs a probability-based allocation of sampling effort, estimates can

only be developed for individual strata or aggregates of individual strata. In contrast, the geostatistical approach can be applied to any shape within the sampled region.

Objectives

The primary objective of my thesis is to estimate the potential magnitude of winter mortality in WTAPS and WTAPSNE resulting from placement of dredged material. To achieve this goal, I apply a range of geostatistical tools to estimate the abundance of blue crab in Chesapeake Bay and in both placement areas. Specifically, I build from deterministic interpolation approaches (i.e., inverse distance weighting (IDW)) to statistical approaches (i.e., kriging) to map the distribution and abundance of blue crab in Chesapeake Bay using data from the WDS.

My analyses set forth to answer four specific objectives: i) to provide baseline estimates of blue crab in the Chesapeake Bay, WTAPS, and WTAPSNE using IDW maps, ii) to examine the importance of statistical assumptions required for kriging, iii) assess the possible impacts of placement of dredged material on overwintering age-1+ females in WTAPS and WTAPSNE, and iv) analyze the effects of small-scale female blue crab abundance estimates in WTAPS and WTAPSNE.

Chapter 2 explores the effects of alternative modeling approaches and assumptions on resulting estimates. I developed IDW maps for 1990–2018 using WDS data to obtain blue crab abundance estimates in Chesapeake Bay, WTAPS, and WTAPSNE (Objective i). These abundance estimates provide baseline blue crab estimates within the Chesapeake Bay and in the two placement sites. The normality assumption of kriging was analyzed to determine the importance of the assumption prior to obtaining abundance estimates of female age-1+, male age-1+, and juvenile

age-0 blue crab (Objective ii). The effects of resolution and variogram model selection were also analyzed.

In Chapter 3, based on the results from Chapter 2, I assessed the possible impacts of dredged material placement on overwintering, mature age-1+ female blue crab by estimating abundance annually from 1990–2020 through ordinary kriging. Female age-1+ blue crab abundance estimates in WTAPS and WTAPSNE were calculated using predicted kriged values for each year of WDS data. The proportion of females in WTAPS and WTAPSNE was calculated using kriging Bay-wide female abundance estimates. I analyzed the female blue crab abundance estimates as worst-case scenario estimates where I assumed 100% mortality within the two placement sites (Objective iii). In Chapter 3, I also assessed the effects of small-scale estimation on female blue crab estimates in WTAPS and WTAPSNE (Objective iv). The effects of scale on female blue crab abundance were analyzed using three different WDS datasets: Bay-wide, WDS data in strata two and three, and WDS data in strata three only.

Figures for Chapter 1

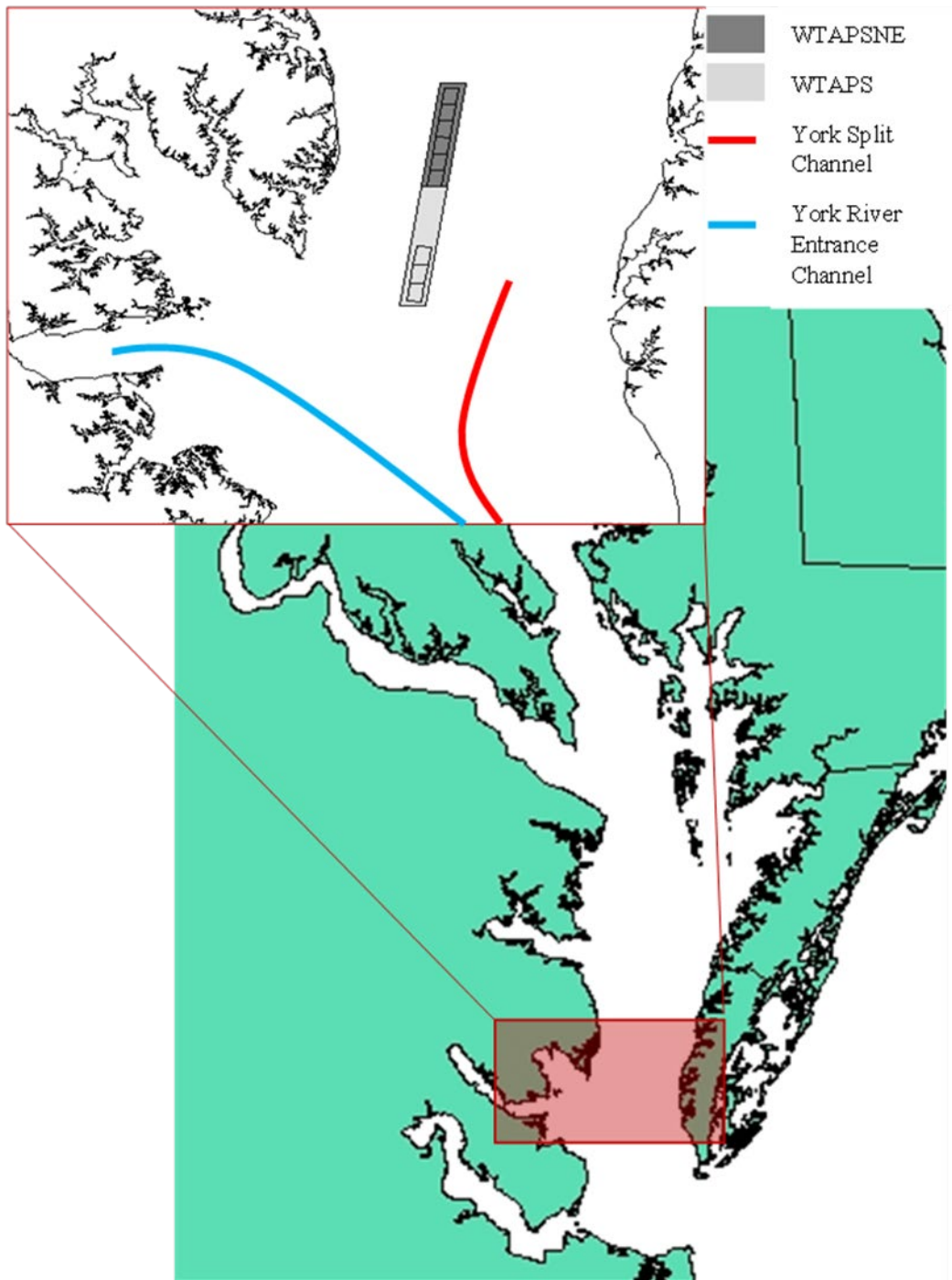


Figure 1.1. Location of WTAPSNE, WTAPS, York Split Channel, and York River Entrance Channel in the Chesapeake Bay. WTAPS and WTAPSNE are used as placement sites for material dredged from the York Split Channel.

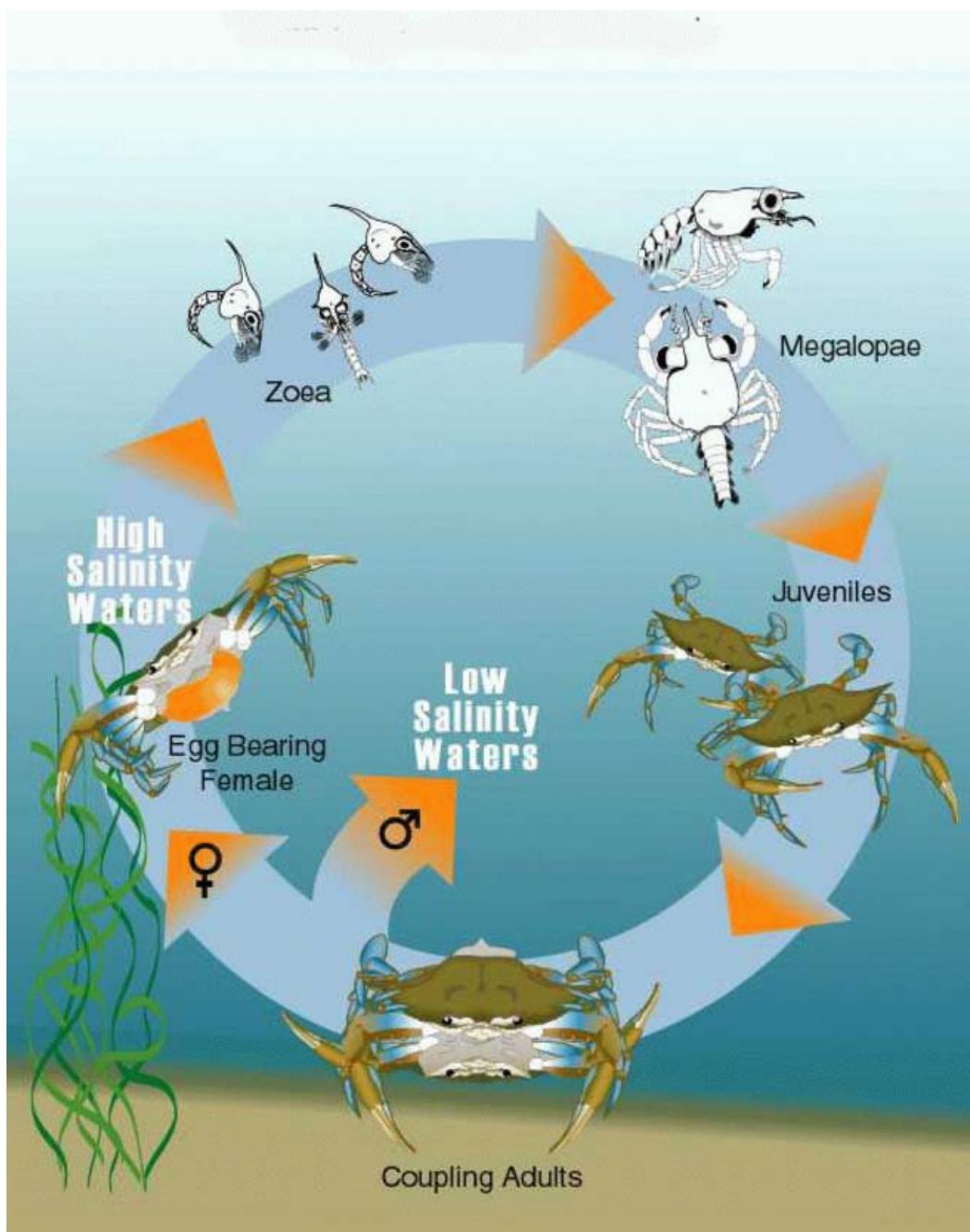


Figure 1.2. Life history of blue crab (*Callinectes sapidus*). Figure courtesy of C. Cheney.

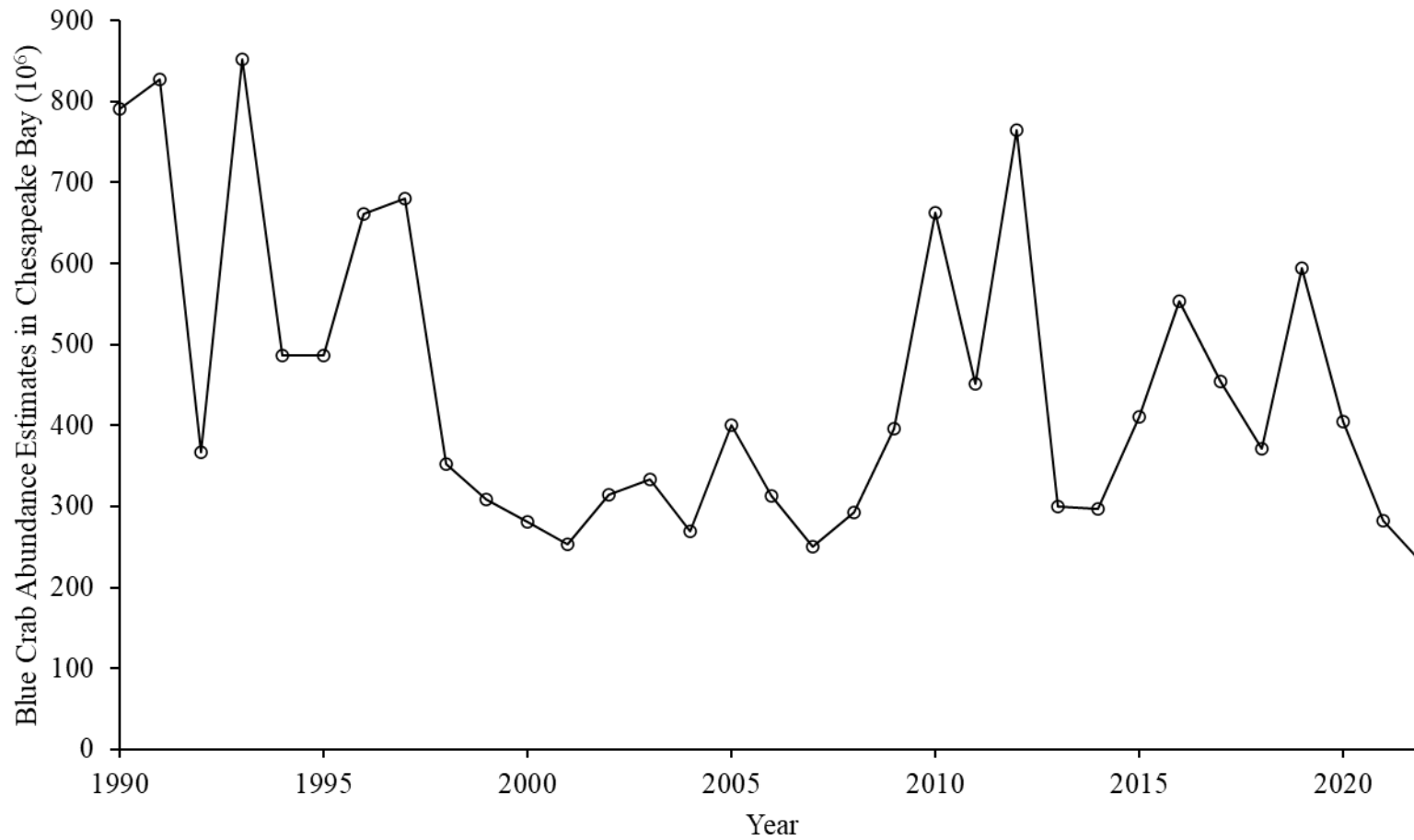


Figure 1.3. WDS total blue crab (males and females of all ages) abundance estimates (millions) in Chesapeake Bay (Chesapeake Bay Stock Assessment Committee (CBSAC) 2022).

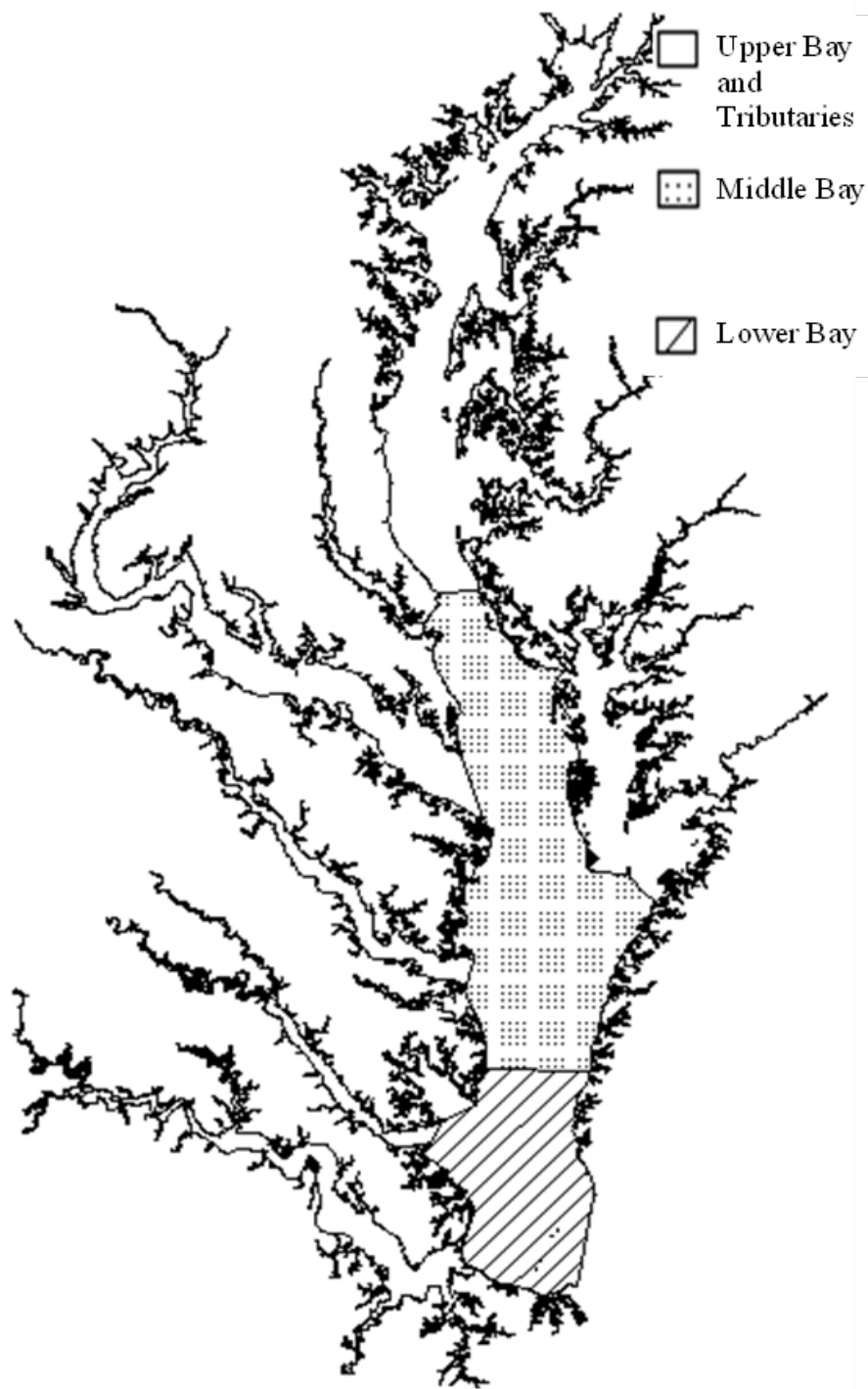


Figure 1.4. Upper Bay and tributaries (white), Middle Bay (polka dots), and Lower Bay (diagonal lines), according to the stratified design of the WDS in the Chesapeake Bay.

Chapter 2: Impact of assumptions and data treatment on kriged estimates of blue crab abundance in Chesapeake Bay

Introduction

The winter dredge survey (WDS) has been conducted annually since the winter of 1989/1990, indexed as 1990 (Sharov et al. 2003). Approximately 1,500 stations are sampled each year between late December and mid-March when blue crab are quiescent in the sediments. The WDS is a stratified random survey with three fixed geographic strata: i) the upper Bay and principal tributaries, ii) the middle Bay, and iii) the lower Bay (Figure 1.4) (Sharov et al. 2003). The stratified design of the WDS allows for Bay-wide estimates of total (males and females of all ages), female age-1+, male age-1+, and juvenile age-0 blue crab but lacks the ability to estimate blue crab at small scales (Sharov et al. 2003; Vølstad, Rothschild, and Maurer 1994). The smallest scale at which the design-based approach can produce estimates is that of the three individual strata in the upper Bay and tributaries, the middle Bay, and the lower Bay. As a result of the large number of sample sites visited during the survey, it may be feasible to reallocate stations to new, smaller strata. However, the smaller the strata area, the fewer stations (re)allocated to each stratum and the lower the precision of the estimates. The inability to create distributional maps of abundance is another shortcoming of design-based stratified random surveys.

Fisheries management often needs smaller scale estimates that the design-based approach lacks. For example, small-scale estimates and areas of high species abundances can aid management in determining valuable species habitat or spawning sites that need protection (Hirzel et al. 2006; Morris and Ball 2006). Small-scale estimates would also enable managers to determine areas to avoid when discussing plausible disturbances to species with high ecological and economic values.

Disturbances to valuable species includes development of offshore energy resources and infrastructure (Bailey, Brookes, and Thompson 2014) and dredging and dredged material placement (Nichols, Diaz, and Schaffner 1990).

The Maryland Department of Transportation Maryland Port Administration (MDOT MPA) operates the Port of Baltimore. The Port is a major economic engine within the state, supporting jobs directly associated with shipping but also related to economic activity that relies on imports and exports of key resources and materials. Following the widening of the Panama Canal, the size of container ships has increased substantially. Shipping channels within Chesapeake Bay must be dredged to maintain a 15-m (50-foot) channel to ensure passage of post-Panamax ships to the Port of Baltimore.

Dredging requires the Port to develop a placement plan for the material removed from the shipping channels. Some of this material is used to restore and rebuild islands in the Chesapeake Bay, but much of the material is relocated to nearby open water, licensed placement areas in the Bay. Within the context of my research, this requires that the Port be able to estimate the abundance of blue crab within placement areas; However, these placement regions are much smaller than the predefined strata of the WDS. The Port of Baltimore is interested in developing blue crab abundance estimates in two regions that have been licensed for placement of dredged material: i) Wolf Trap Alternate Open Water Placement Site (WTAPS) which is in the lower Bay and ii) the northern extension of this region – WTAPSNE which is in both the middle Bay and lower Bay (Figures 1.1 and 1.4).

There are three approaches to small-scale estimation: i) uniformity assumption, ii) deterministic estimation, and iii) statistical estimation. The uniformity principle relies on an assumption of uniformity in the value of a property of interest within the strata. The uniformity assumption uses the following equation to estimate a given property in a region of interest:

(1)

$$B = A * D$$

where B is the aggregate value of the property in the region of interest, D is the average density of the property within the strata, and A is the area of the region of interest. If this assumption is not justified, the second two approaches use values of a property (e.g., abundance) at a predetermined number of sampled locations to evaluate the value of the property at unsampled locations.

In deterministic approaches, such as inverse distance weighting (IDW), the value of the unsampled location is calculated analytically. Liu et al. (2021) provide an equation for the classic IDW mathematical expression, given by:

(2)

$$\hat{z} = \frac{\sum_{i=1}^n \frac{z_i}{d_i^p}}{\sum_{i=1}^n \frac{1}{d_i^p}}$$

where \hat{z} is the value of the property at an unsampled location to be estimated, Z_i is the value of a property at a sampled location, d_i is the Euclidean distance between the point to be estimated and the value of the sampled location, n is the number of stations, and p is the exponential power exponent. The power exponent determines how fast the weights tend to zero as the distance from the unsampled location

increases (Roberts, Sheley, and Lawrence 2004). Commonly, p is set to 1, so that IDW becomes a simple linear weighted averaging process.

IDW has a low computational cost (Chen and Liu 2012), and it is rather straightforward to obtain spatial patterns in an area of interest. However, IDW does not provide estimates of uncertainty and is constrained by the number of sampled locations in an area. A further limitation of this deterministic approach is that it is constrained to produce estimates for an outer convex hull, and thus estimates are limited to the absolute range of the available data.

Kriging is a statistical or probabilistic approach to small-scale estimation that provides standard errors for the kriged values thereby quantifying the uncertainty associated with the kriged estimates (Krivoruchko 2012). Kriging uses similarities between pairs of values of the property at sampled locations separated by a measured distance to calculate the value at an unsampled location using the following equation:

(3)

$$Z(x_0) = \sum_{i=1}^{N(x_0)} \lambda_i Z(x_i)$$

where $Z(x_0)$ is the point to be estimated at a given location, $N(x_0)$ is the number of samples from the neighborhood considered for the point to be estimated, λ_i is the ordinary kriging weights, and $Z(x_i)$ is the measured values at multiple locations (Salvelieva 2005). In contrast to deterministic approaches, kriging uses a semivariogram to quantify the spatial dependence (kriging weights) or similarity in terms of the distance and direction separating two points (Krivoruchko 2012). The semi-variance will continue to increase until a distance is reached where the

population semi-variance equals the sample semi-variance (Fischer and Getis 2010). The strongest assumption of kriging is stationarity or spatial homogeneity where the data mean and the semivariogram are the same at all locations within the data (Krivoruchko 2012). Compared to IDW, kriging is less sensitive to sample size concerns but is more complex and computationally demanding than IDW.

I used data from the WDS to estimate the distribution of abundance of blue crab during winter in Chesapeake Bay. Small-scale estimates of these properties are then used to estimate the abundance of blue crab within regions licensed to serve as placement regions for material dredged from the Chesapeake Bay to maintain shipping channels. These placement areas are smaller than the size of the strata in the design-based survey. Prior to undertaking the final analysis (Chapter 3), work presented in this chapter explores the characteristics of small-scale estimates derived from different methods.

Objectives

There are two primary objectives for this chapter: i) to provide baseline estimates of blue crab in the Chesapeake Bay, WTAPS, and WTAPSNE and ii) to examine the importance of statistical assumptions for kriging. Due to the exploratory nature of the analyses in this chapter, the results and discussion are combined into a single section.

Methods

Data

All analyses were accomplished using data from the WDS. The methods of the WDS are briefly described here, but detailed descriptions of the methods of the

survey can be found in Sharov et al. (2003). The WDS is a stratified random survey that uses one-minute tows of a commercial 1.8-m (6-foot) Virginia dredge to sample waters of the Chesapeake Bay deeper than 1.5-m (5-foot) (Sharov et al. 2003). The WDS has been conducted since 1990 by the Maryland Department of Natural Resources (MDNR) and the Virginia Institute of Marine Science (VIMS) from December to March to take advantage of overwintering blue crab in the Chesapeake Bay. Since 1992, three fixed geographic strata have been employed: i) the upper Bay and principal tributaries, ii) the middle Bay, and iii) the lower Bay (Figure 1.4). Since 1993, the number of sites sampled in the different strata are proportional to the area totaling approximately 900–1,500 stations (Sharov et al. 2003).

WDS data were explored for quality assurance by identifying outliers. This process involved removing stations whose coordinates were in error (e.g., appeared to be on land) and duplicate locations identified by stations with the same latitude and longitude. Based on the 1.8-m length of the Virginia dredge and variable tow length at each station, sampled stations with tow areas less than 50-m² or larger than 500-m² were removed based on a presumption of unreliability of resulting estimates.

The total catch of remaining stations was standardized by dividing the number of crabs caught at a station by an estimated annual and vessel-specific catchability coefficient provided by Glenn Davis (MDNR). Catchability coefficients were estimated by defined studies in which the catch of sequential tows over the same narrow path was recorded, and the rate of decline in catch with successive tows provided an estimate of catchability (Sharov et al. 2003; Vølstad et al. 2000). Catchability-corrected total catch was then standardized by the tow area to obtain the

catchability-corrected number of crabs per m². Coordinates of the stations were transformed to Easting (m) and Northing (m) and projected to Universal Transverse Mercator zone 18N.

Design-Based Estimates

For comparative purposes, I assembled estimates of total Bay-wide abundance of blue crab during winter months using the design-based approach outlined by Sharov et al. (2003). These estimates are routinely developed each year by the Chesapeake Bay Stock Assessment Committee (CBSAC) (CBSAC 2022; Miller et al. 2011).

Inverse Distance Weighting (IDW)

IDW maps were created using the Geostatistical Wizard tool in ArcMap 10.5 (ESRI Corporation, Redlands, CA). Preliminary analyses of the effects of different resolutions of the predicted cell size (50-m², 100-m², and 250-m²) indicated only slight differences in blue crab abundance estimates. Thus, IDW maps were predicted based on a cell size of 100-m² and a power of 2 to emphasize the importance of nearby stations. IDW surfaces were created annually for 1990–2018 using WDS data that had undergone QA/QC processes in separate analysis to estimate sample variances for design-based surveys (Liang et al. 2017). This will be termed the Liang WDS dataset. After the interpolated surfaces were created, the IDW maps were clipped to the Chesapeake Bay, WTAPS, and WTAPSNE, based on shapefiles to generate blue crab density estimates within the selected area. Total blue crab

abundance (females and males of all ages) in Chesapeake Bay, WTAPS, and WTAPSNE were calculated as follows:

(4)

$$Z = rows * columns * \bar{X} * res^2$$

where Z is blue crab abundance in either Chesapeake Bay, WTAPS, or WTAPSNE, $rows$ is the number of rows within the IDW interpolated surface after clipping to a shapefile, $columns$ is the number of columns within the IDW interpolated surface after clipping to the desired area, \bar{X} is the average cell value, and res^2 is the resolution of the prediction grid cell size. Percent differences between the IDW and design-based estimates were calculated annually from 1990–2018 in Chesapeake Bay given by:

(5)

$$Percent\ difference\ (\%) = \frac{IDW - Design}{Design} * 100.$$

Kriging

WDS data provided by Glenn Davis (MDNR) was used for the kriging analysis as this dataset provided WDS results for 2019 and 2020. The Glenn Davis WDS dataset was provided after the completion of the IDW analysis. Total catch was adjusted for the catchability coefficients according to the year, vessel, and tow area. Stations with tow areas less than 50-m² or greater than 500-m² were removed from the analysis. The annual fitted variograms were selected based on the *autofitVariogram* function in the *automap* package (Hiemstra 2022) within the R statistics language (R Core Team 2013). The *autofitVariogram* function selects the

best fitting model based on the smallest residual sum of squares. I allowed the *autofitVariogram* to select the best fitting model among spherical, exponential, Matérn, and gaussian variogram functions. A grid of cells was used to predict blue crab abundance within the *krige* function. The *krige* function in the *gstat* package in R (Pebesma and Graeler 2022) was used to predict blue crab abundance using ordinary kriging which assumes that the mean is unknown (Oliver 2010). A maximum neighborhood of 25 sampled locations was used to predict unsampled locations with a maximum distance of 40-km. The maximum neighborhood and distance were selected to avoid estimating an unsampled point using a sampled location that logically did not make sense (e.g., using a sampled point in the Potomac River to estimate an unsampled location in the Patuxent River). Also, the maximum neighborhood and distance had to be large enough to predict abundance in the entirety of the Chesapeake Bay. The predicted kriged surface was then clipped to the desired shapefile of either Chesapeake Bay, WTAPS, or WTAPSNE, using the *raster* package in R (Hijmans et al. 2022). The blue crab estimates in each cell were then summed to obtain annual blue crab abundance estimates in either the Chesapeake Bay, WTAPS, or WTAPSNE. Ordinary kriging maps were created using the *ggplot2* package in R (Wickham et al. 2022) for 1990–2020 and associated standard errors of the point estimates were also created for each year.

Four different variogram models were analyzed to determine the effects of model selection on blue crab abundance estimates: Matérn, exponential, gaussian, and spherical. The effects of cell size were also analyzed to determine the importance of cell resolution on blue crab abundance estimates. Four different resolutions were

analyzed: 100-m, 250-m, 500-m, and 1,000-m, and the resulting blue crab abundance estimates compared.

One criteria of kriging is that the data follow a normal distribution. Catch data in the WDS are strongly zero-inflated. I tested the effects of three different normality transformations to address this breach of assumption: i) no transformation, ii) a parametric log transformation, and iii) a *NScore* transformation, a non-parametric approach. A log of base 10 was used for the log transformation. A small constant (i.e., 0.00000001) was added to the catch prior to log transforming due to the high number of zeros in the blue crab catch data. The *NScore* transformation was developed by Ashton Shortridge in 2008 and was used to transform the WDS data to a normal distribution.

Results and Discussion

IDW-based blue crab abundance estimates were smaller relative to design-based estimates; however, unlike the design-based estimates, the IDW analysis produced annual visualizations of high and low blue crab abundance areas in the Chesapeake Bay. The effects of the variogram selection and resolution size of cells indicated minor deviations among Chesapeake Bay blue crab abundance estimates. Transforming the WDS to meet the assumptions of normality resulted in larger deviations of blue crab abundance estimates when compared to the *NScore* transformed data. Following the results of these analyses, I selected 250-m cell resolutions and used the untransformed, skewed, and zero-inflated WDS data for subsequent analyses in Chapter 3. I also chose to select the best variogram model

between Matérn, exponential, gaussian, and spherical using the *autofitVariogram* function.

Data

A total of 4,699 stations (9.6%) were excluded from the Liang WDS dataset following QA/QC procedures (Table 2.1). A total of 2,333 stations (4.8%) were excluded from the Davis WDS dataset following QA/QC procedures (Table 2.2). Approximately 2,500 more sampled locations were excluded from the Liang WDS data than the Davis WDS data. Because of the lack of a database for the WDS, there are many forms of the WDS data. The Liang WDS data was readily available at the start of the analysis which is why the Liang WDS dataset was used instead of the Davis WDS dataset. Regardless, the excluded points from the Liang WDS dataset only represent 10% of the extensive WDS data.

Inverse Distance Weighting

IDW maps of blue crab abundance were created using cell resolutions of 100-m². Blue crab density maps generated by IDW estimation for 2018 in Chesapeake Bay, WTAPS, and WTAPSNE are provided as an example (Figure 2.1). Figure 2.1 shows areas of high and low blue crab abundance during winter months in the Chesapeake Bay, WTAPS, and WTAPSNE. Such maps provide management with visualizations of plausible areas that are important to blue crab in the Chesapeake Bay. IDW-based blue crab abundance estimates in the Chesapeake Bay were calculated for 1990–2018 and are provided in Table 2.3. The percent difference ranged from -59%–25% (Table 2.3).

IDW-based blue crab abundance estimates were smaller relative to design-based estimates (Figure 2.2). The underestimation by the IDW approach could be attributed to the limitations of IDW. IDW can estimate unsampled locations only if there are sampled locations within the given neighborhood. In Figure 2.1, IDW was not able to estimate blue crab abundance in the upper Bay and in portions of the Potomac River because of the lack of sampling locations in these portions resulting from the restriction of WDS only sampling waters deeper than 1.5-m (5-foot).

Kriging

Analysis of deviations of blue crab abundance estimates based on four different variogram models indicated minor differences (Figure 2.3). Models with reasonable parameter values could not be derived for all variogram models in all years. The gaussian variogram model estimated fitted variograms with negative estimates of the sill, range, and nugget for 1992, 1998, 2010, 2015, 2017, and 2019 (Table 2.4). The spherical model also failed in 1999, producing negative estimated parameter values (Table 2.4).

Overall estimates of the average blue crab abundance in Chesapeake Bay based on the WDS data from 1990–2020 varied among variogram models: Matérn (587.24 ± 276.86 (mean \pm SD), exponential (585.50 ± 277.10), gaussian (582.75 ± 299.70), and spherical (591.96 ± 267.42) (Table 2.4). The larger standard deviation for the gaussian model can be attributed to the years that could not be estimated due to null variogram models. Due to the minor deviations in the blue crab abundance estimates, I used the *autofitVariogram* function to select the best variogram model between Matérn, exponential, gaussian, and spherical in Chapter 3.

The effects of the resolution size of cells also indicated minor deviations among Chesapeake Bay blue crab abundance estimates (Figure 2.4). Estimates of average Bay-wide abundance based on the Davis WDS dataset from 1990–2020 were: 583.22 ± 267.08 (mean \pm SD) at 100-m resolution, 583.09 ± 267.25 at 250-m resolution, 584.25 ± 267.65 at 500-m resolution, and 585.75 ± 268.57 at 1,000-m resolution (Table 2.5). I selected the 250-m cell resolutions for subsequent analyses due to the decrease in computational time in R for the 250-m resolution analyses compared to 100-m resolution.

Transforming the skewed, zero inflated catch data to meet the assumptions of kriging resulted in larger deviations of kriged estimates of blue crab in Chesapeake Bay compared to design-based estimates (Figure 2.5): design-based abundance 457.68 ± 183.17 (mean \pm SD), untransformed 583.09 ± 267.25 , log transformed estimates 585.44 ± 324.51 , and *NScore* transformation 236.40 ± 139.91 (Table 2.6). This difference between kriged estimates of *NScore* transformed data compared to design-based estimates may be attributed to overfitting the original data to produce a perfect Gaussian curve. The untransformed blue crab abundance estimates in the Chesapeake Bay performed similar to the log transformation. Given the small deviations between the untransformed and log transformation methods, I continued explorations of the WDS data using the untransformed, skewed, and zero-inflated data for simplicity when estimating blue crab abundance.

Decisions regarding geostatistical analyses, like the ones explored in this chapter, are largely at the hands of the investigator. The investigator chooses how to handle the data that are being analyzed. The open-endedness of geostatistics makes

the methodology specific to the investigator, study area, and species, as to which criteria to prioritize in the analyses. The different criteria (i.e., maximum neighborhood, maximum distance, normality assumption, variogram selection, or resolution size), even if the deviations are considered minor, change the final estimates. Due to the complexity of geostatistics, a more streamlined approach should be developed for researchers to ensure that they are setting the correct criteria to obtain precise estimates.

Tables for Chapter 2

Table 2.1. Summary of Liang WDS data by strata location that was used in the IDW analysis. Number of stations is the number of WDS sampling locations used for analysis. The number of stations excluded is the number of stations that were removed during QA/QC procedures.

Year	Number of Stations			Number of Stations Excluded		
	Strata 1	Strata 2	Strata 3	Strata 1	Strata 2	Strata 3
1990	596	219	76	647	0	33
1991	515	175	211	866	11	135
1992	781	301	210	1,011	313	138
1993	673	327	244	183	40	145
1994	850	294	265	2	36	185
1995	918	375	281	15	18	193
1996	917	440	272	0	0	150
1997	824	479	297	0	0	171
1998	860	448	282	0	1	147
1999	850	443	304	31	16	0
2000	786	456	315	0	0	0
2001	790	479	321	0	2	0
2002	803	499	276	0	0	0
2003	851	434	225	0	0	0
2004	829	463	231	0	17	0
2005	857	465	221	0	12	0
2006	992	310	227	0	171	0
2007	790	500	228	0	0	0
2008	806	395	231	0	0	0
2009	800	507	228	0	0	0
2010	782	511	228	0	2	0
2011	818	494	243	0	0	0
2012	828	502	228	0	0	0
2013	818	495	228	0	0	0
2014	830	486	228	0	0	3
2015	831	489	228	0	0	0
2016	840	493	228	0	0	2
2017	853	498	228	0	0	3
2018	834	493	232	0	0	0
Total	23,522	12,470	7,016	2,755	639	1,305

Table 2.2. Summary of Davis WDS data by strata used in the kriging analysis. Number of stations is the number of WDS sampling locations used for analysis. The number of stations excluded is the number of stations that were removed during QA/QC procedures.

Year	Number of Stations			Number of Stations Excluded		
	Strata 1	Strata 2	Strata 3	Strata 1	Strata 2	Strata 3
1990	1,047	113	104	196	1	5
1991	1,247	182	340	134	4	6
1992	1,666	592	344	126	22	4
1993	764	353	377	92	14	12
1994	800	321	436	52	9	14
1995	853	381	442	80	12	32
1996	814	430	398	74	6	24
1997	724	451	444	43	23	24
1998	752	444	419	62	5	10
1999	814	450	237	67	9	7
2000	711	447	234	35	8	5
2001	708	473	242	42	8	3
2002	732	493	190	56	2	2
2003	762	420	174	47	6	2
2004	725	477	178	72	3	4
2005	737	471	180	55	6	4
2006	737	470	211	47	11	3
2007	712	476	185	52	4	2
2008	727	378	182	54	7	2
2009	713	493	182	45	1	0
2010	728	511	171	32	2	0
2011	720	483	182	53	3	2
2012	732	491	169	51	8	2
2013	752	479	173	39	2	0
2014	738	479	230	49	3	1
2015	735	480	172	41	3	1
2016	737	476	229	50	7	1
2017	739	483	230	42	5	1
2018	783	489	232	51	4	0
2019	785	486	230	54	6	2
2020	780	489	232	57	3	1
Total	24,974	13,661	7,749	1,950	207	176

Table 2.3. Estimates of total blue crab (millions) (females and males of all ages) in Chesapeake Bay derived from IDW. Annual design-based abundance estimates are based on the stratified random design of the WDS. Percent difference (%) was calculated using the design-based estimates for the given year.

Year	IDW Abundance Estimates (*10 ⁶)	Design-Based Abundance Estimates (*10 ⁶)	Percent Difference (%)
1990	746.20	791.04	-5.67
1991	1,034.58	827.69	25.00
1992	432.24	366.84	17.83
1993	384.20	852.09	-54.91
1994	407.34	487.20	-16.39
1995	199.19	486.53	-59.06
1996	532.66	661.47	-19.47
1997	452.52	679.60	-33.41
1998	250.47	352.76	-29.00
1999	182.05	308.05	-40.90
2000	191.94	281.29	-31.77
2001	160.00	253.62	-36.91
2002	161.65	314.96	-48.68
2003	243.66	334.37	-27.13
2004	214.01	270.04	-20.75
2005	361.00	399.74	-9.69
2006	317.78	313.17	1.47
2007	238.51	251.42	-5.14
2008	250.51	293.15	-14.54
2009	316.13	396.01	-20.17
2010	491.71	663.08	-25.84
2011	445.95	452.45	-1.44
2012	680.33	764.92	-11.06
2013	257.46	299.62	-14.07
2014	261.63	297.16	-11.96
2015	392.83	410.64	-4.34
2016	483.65	553.25	-12.58
2017	352.35	454.79	-22.52
2018	329.27	371.76	-11.43
		Average:	-0.19

Table 2.4. Effects of variogram model selection on blue crab abundance estimates (millions) (females and males of all ages) in Chesapeake Bay. Shown are kriged estimates of four different variogram models: i) Matérn, ii) exponential, iii) gaussian, and iv) spherical. The gaussian and spherical variogram model estimated fitted variograms with negative estimates of the sill, range, and nugget producing N/As.

Year	Matérn Abundance Estimates (*10 ⁶)	Exponential Abundance Estimates (*10 ⁶)	Guassian Abundance Estimates (*10 ⁶)	Spherical Abundance Estimates (*10 ⁶)
1990	1,555.20	1,555.20	1,555.20	1,469.34
1991	1,191.07	1,185.16	1,191.37	1,184.34
1992	456.40	448.48	N/A	455.58
1993	671.94	708.32	695.61	681.54
1994	745.87	745.20	740.84	746.93
1995	422.35	430.09	423.48	428.94
1996	925.25	923.62	925.05	923.43
1997	768.52	775.07	765.39	773.90
1998	428.79	399.03	N/A	430.77
1999	354.86	354.82	354.17	N/A
2000	338.22	341.65	332.47	342.38
2001	337.25	339.93	334.49	340.53
2002	369.33	369.52	368.84	367.72
2003	459.28	460.59	453.77	462.66
2004	375.35	373.65	382.32	368.95
2005	492.44	492.61	490.42	491.98
2006	455.09	454.57	450.46	455.23
2007	322.22	325.22	319.75	324.46
2008	352.29	353.86	350.35	353.46
2009	482.19	489.20	481.76	477.13
2010	873.22	874.20	N/A	875.15
2011	604.14	606.97	604.11	605.24
2012	869.82	866.72	873.91	863.67
2013	370.68	370.06	370.90	370.29
2014	386.85	386.31	392.59	384.39
2015	611.33	540.14	N/A	596.06
2016	689.10	688.50	681.40	686.45
2017	524.36	522.00	N/A	523.23
2018	482.90	485.01	481.32	485.13
2019	738.27	732.60	N/A	738.00
2020	549.80	552.25	548.77	552.01
Mean	587.24	585.50	582.75	591.96
Standard Deviation	276.86	277.10	299.70	267.42

Table 2.5. Effects of resolution of the predicted kriging grid on estimates of total blue crab abundance (millions) (females and males of all ages) in Chesapeake Bay. Shown are kriged estimates of four different resolutions: i) 100-m, ii) 250-m, iii) 500-m, and iv) 1,000-m.

Year	100-m Abundance Estimates (*10 ⁶)	250-m Abundance Estimates (*10 ⁶)	500-m Abundance Estimates (*10 ⁶)	1,000-m Abundance Estimates (*10 ⁶)
1990	1,469.23	1,469.34	1,471.65	1,476.81
1991	1,191.17	1,191.07	1,193.87	1,198.57
1992	455.47	455.58	456.68	459.01
1993	671.70	671.94	673.35	674.19
1994	741.08	740.84	743.11	747.87
1995	422.38	422.35	424.39	425.41
1996	923.59	923.43	925.59	928.04
1997	765.09	765.39	766.16	767.73
1998	428.63	428.79	429.67	430.73
1999	355.06	354.86	355.44	356.42
2000	336.57	332.47	333.07	333.63
2001	337.04	337.25	338.46	339.48
2002	369.15	369.33	369.82	369.98
2003	454.18	453.77	455.55	457.38
2004	376.76	375.35	375.25	374.62
2005	492.26	492.44	493.60	494.73
2006	450.44	450.46	451.28	452.59
2007	319.65	319.75	320.03	321.24
2008	350.29	350.35	351.08	351.39
2009	477.31	477.13	477.89	476.85
2010	872.66	873.22	873.73	874.98
2011	604.34	604.14	605.19	606.50
2012	863.73	863.67	864.91	865.64
2013	370.75	370.68	371.88	373.17
2014	383.88	384.39	385.53	387.69
2015	611.09	611.33	613.37	616.04
2016	689.18	689.10	689.91	691.13
2017	524.33	524.36	525.02	526.07
2018	482.82	482.90	483.91	485.25
2019	737.77	738.00	738.59	739.42
2020	552.29	552.01	553.64	555.72
Mean	583.22	583.09	584.25	585.75
Standard Deviation	267.08	267.25	267.65	268.57

Table 2.6. Effects of normality assumption transformations on total blue crab abundance estimates (millions) (females and males of all ages) in Chesapeake Bay. Shown are kriged estimates of three different normality transformations: i) untransformed, ii) *NScore*, and iii) log. Annual design-based abundance estimates are based on the stratified random design of the WDS.

Year	Design-Based Abundance Estimates (*10 ⁶)	Untransformed Abundance Estimates (*10 ⁶)	<i>NScore</i> Abundance Estimates (*10 ⁶)	Log Abundance Estimates (*10 ⁶)
1990	791.04	1,469.34	510.16	1,761.30
1991	827.69	1,191.07	623.68	1,344.86
1992	366.84	455.58	172.79	438.60
1993	852.09	671.94	281.64	1,010.97
1994	487.20	740.84	312.44	743.05
1995	486.53	422.35	144.43	473.93
1996	661.47	923.43	388.16	822.60
1997	679.60	765.39	371.03	763.29
1998	352.76	428.79	123.33	392.78
1999	308.05	354.86	102.35	367.67
2000	281.29	332.47	109.09	319.07
2001	253.62	337.25	98.30	293.95
2002	314.96	369.33	103.32	343.23
2003	334.37	453.77	191.04	422.03
2004	270.04	375.35	85.08	329.41
2005	399.74	492.44	233.61	475.73
2006	313.17	450.46	219.39	411.51
2007	251.42	319.75	96.25	284.83
2008	293.15	350.35	130.67	348.90
2009	396.01	477.13	186.70	458.36
2010	663.08	873.22	418.41	796.70
2011	452.45	604.14	300.90	572.45
2012	764.92	863.67	485.06	864.67
2013	299.62	370.68	85.23	358.55
2014	297.16	384.39	112.33	346.23
2015	410.64	611.33	269.58	543.04
2016	553.25	689.10	337.35	652.50
2017	454.79	524.36	200.67	528.35
2018	371.76	482.90	163.13	484.89
2019	594.47	738.00	276.44	708.42
2020	404.75	552.01	195.86	486.88
Mean	457.68	583.09	236.40	585.44
Standard Deviation	183.17	267.25	139.91	324.51

Figures for Chapter 2

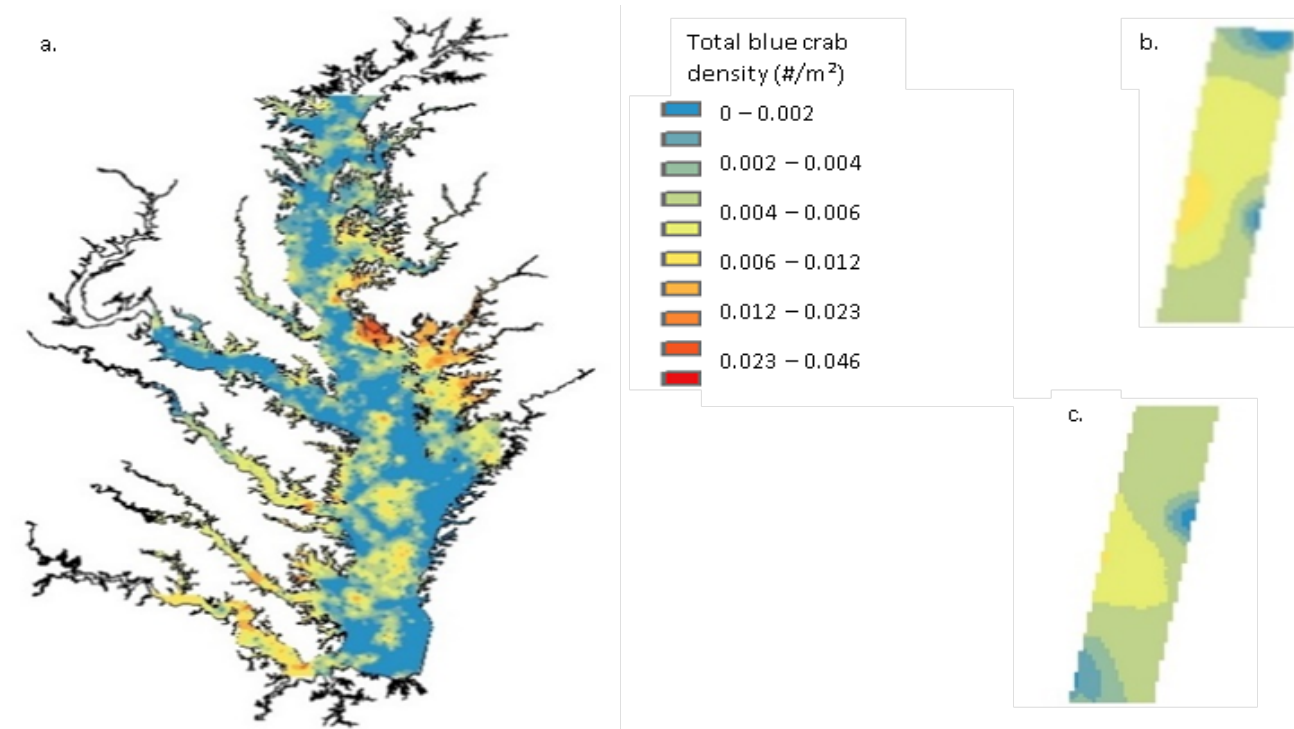


Figure 2.1. 2018 IDW results for: a) Chesapeake Bay total blue crab abundance estimates (females and males of all ages), b) WTAPSNE total blue crab abundance estimates, and c) WTAPS total blue crab abundance estimates.

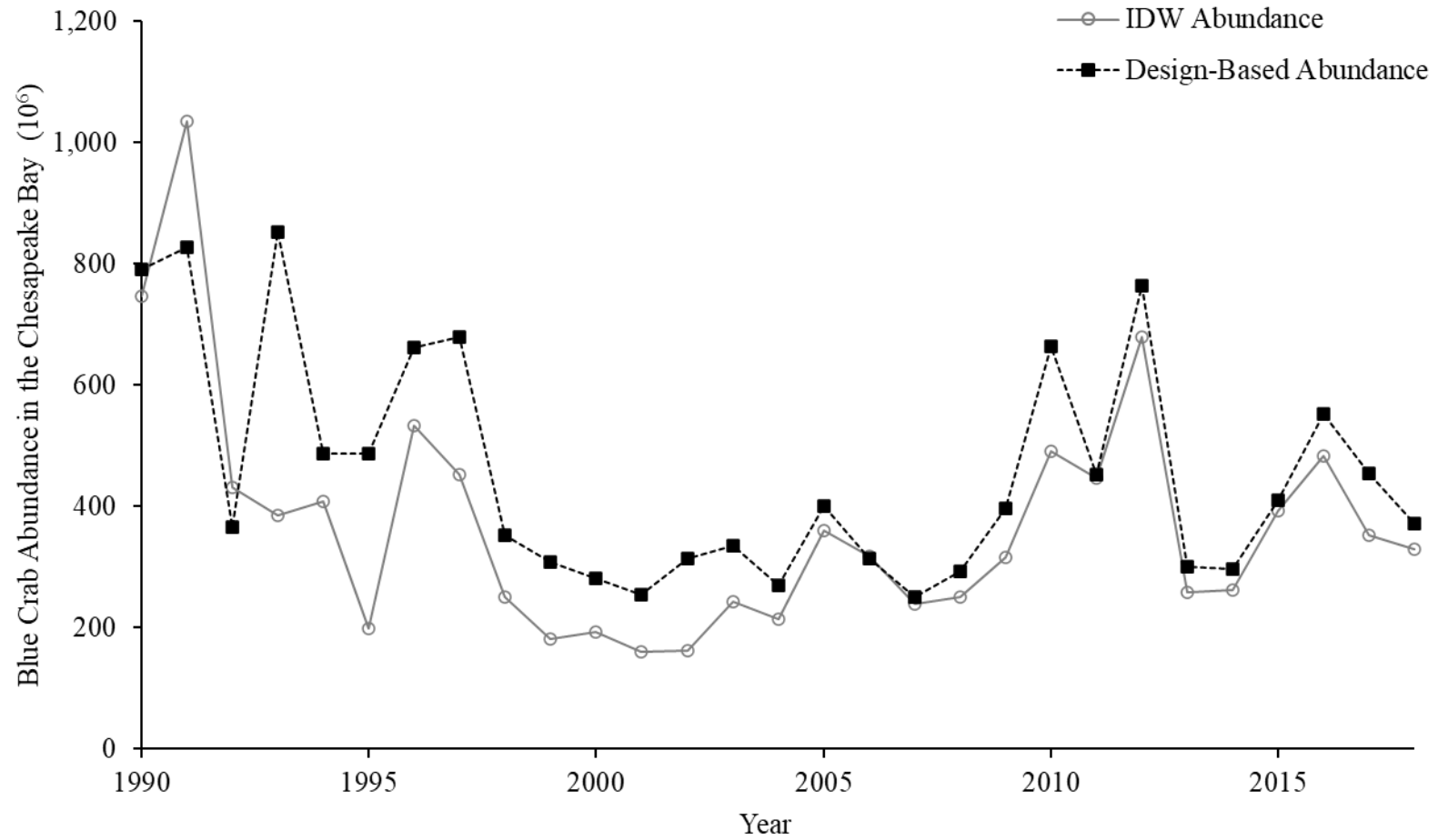


Figure 2.2. Estimates of total blue crab abundance (millions) (females and males of all ages) in Chesapeake Bay. Shown are IDW estimates (open circles; solid, grey line) and design-based abundance estimates (solid squares; dashed, black line) for 1990–2018.

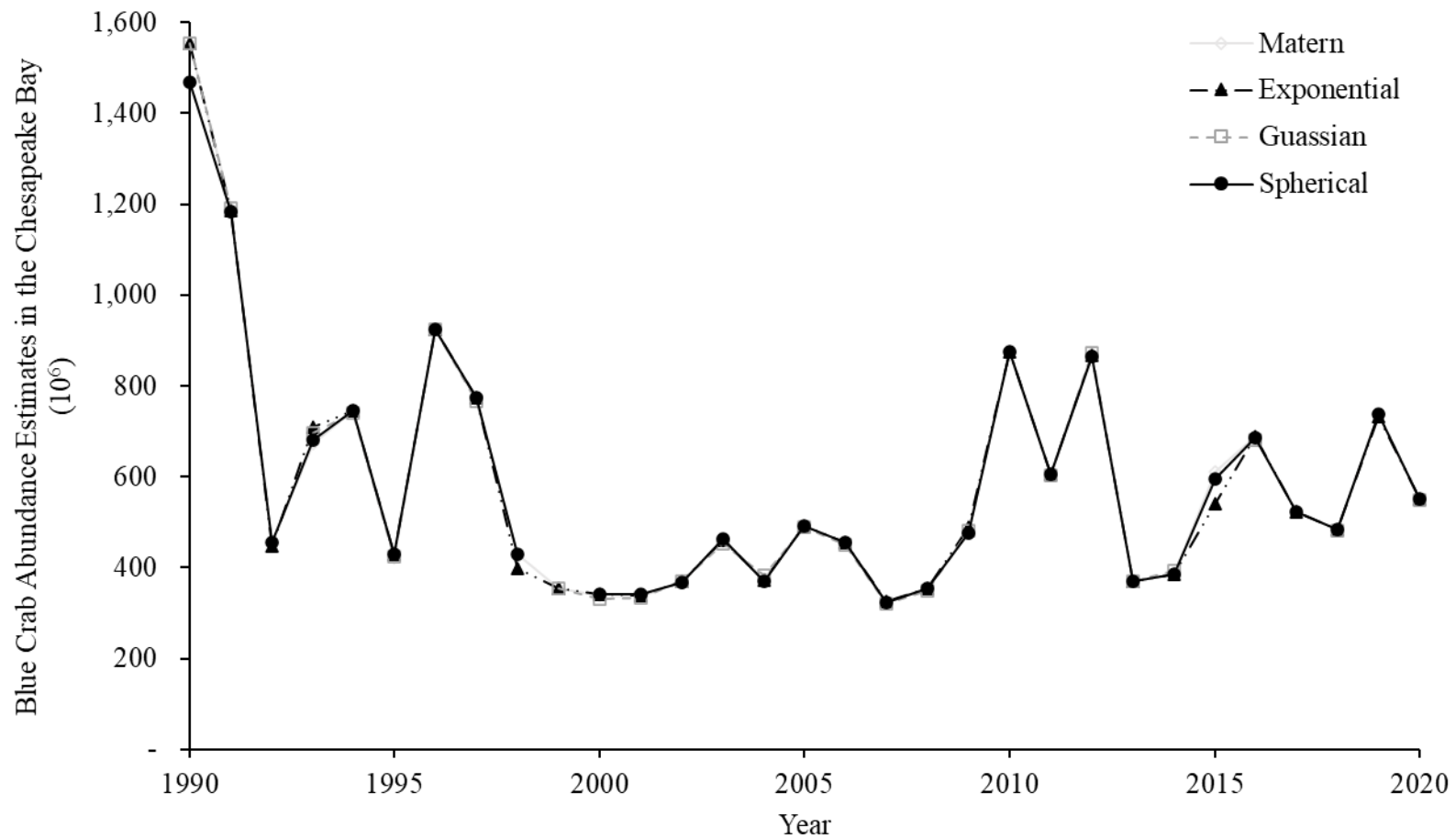


Figure 2.3. Effects of variogram model selection on total blue crab abundance estimates (millions) (females and males of all ages) in Chesapeake Bay from 1990–2020. Shown are kriged estimates of four different variogram models: i) Matérn (open diamond; solid, grey line), ii) exponential (solid triangles; dashed, black line), iii) gaussian (open squares; dashed, grey line), and iv) spherical (solid circles; solid, black line).

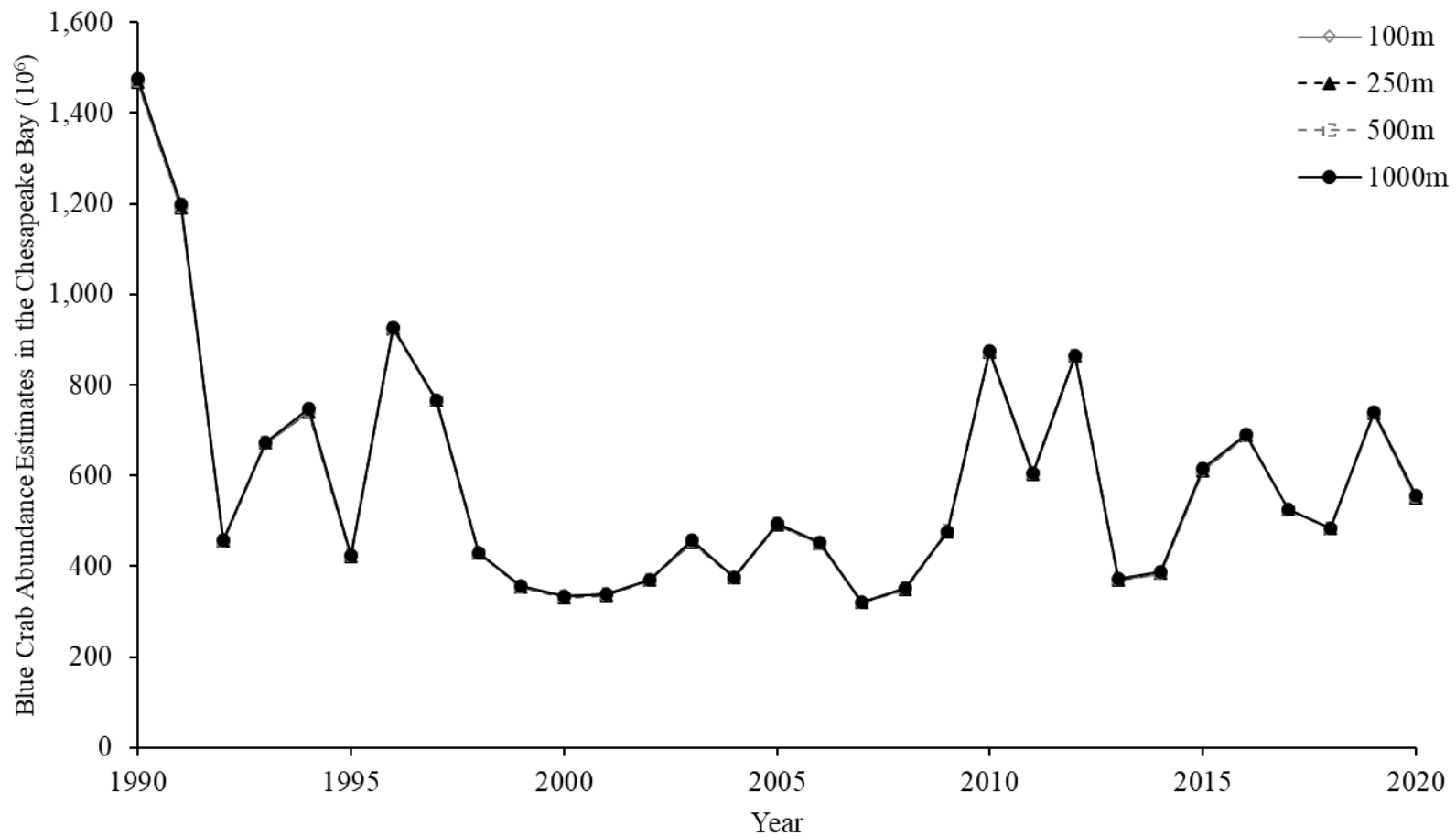


Figure 2.4. Effects of resolution of the predicted kriging grid on total blue crab abundance estimates (millions) (females and males of all ages) in Chesapeake Bay from 1990–2020. Shown are kriged estimates of four different resolutions: i) 100-m (open diamond; solid, grey line), ii) 250-m (solid triangles; dashed, black line), iii) 500-m (open squares; dashed, grey line), and iv) 1,000-m (solid circles; solid, black line).

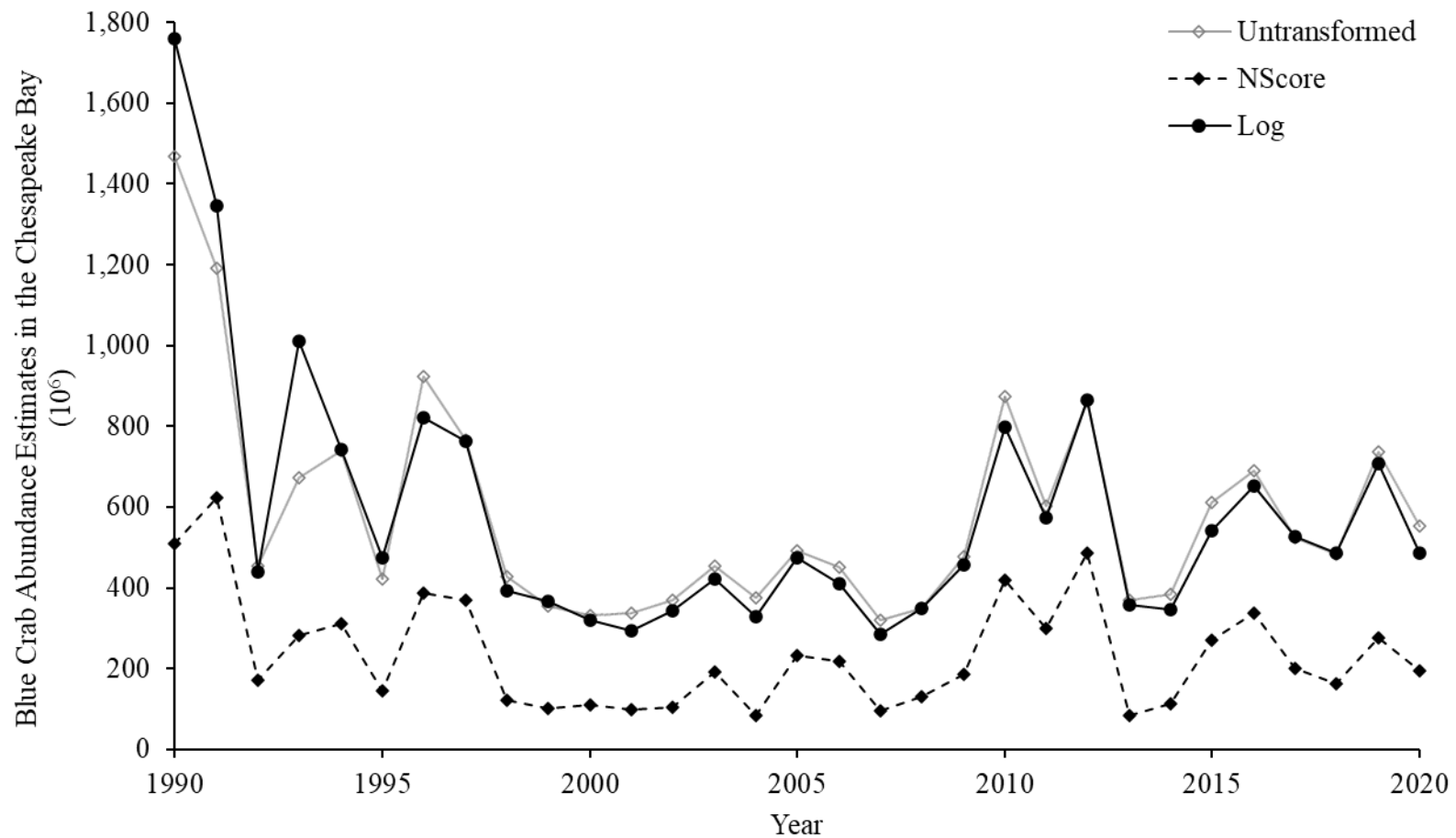


Figure 2.5. Effects of normality assumption transformations on total blue crab abundance estimates (millions) (females and males of all ages) in Chesapeake Bay from 1990–2020. Shown are kriged estimates of three different normality transformations: i) untransformed (open diamond; solid, grey line), ii) *NScore* (solid diamond; dashed, black line), and iii) log (solid circles; solid, black line).

Chapter 3: Small-scale estimation of adult female blue crab *Callinectes
sapidus* abundance in Chesapeake Bay in dredged material placement
sites

Abstract

Increases in the sizes of container ships due to the expansion of the Panama Canal has increased the need for dredging activities in the Chesapeake Bay. Placement of dredged material in the Bay is restricted to winter months to limit potential interactions with threatened and endangered species. Placement of dredged material in the lower Chesapeake Bay (York Split Channel) in Wolf Trap Alternate Open Water Placement Site (WTAPS) overlaps with overwintering locations for mature female blue crab. The Port of Baltimore is interested in developing age-1+ female blue crab abundance estimates in WTAPS and WTAPSNE (northern extension to WTAPS) to help assess the impact of dredge deposit activities on the blue crab population. Winter dredge survey data was used to visualize the distribution of overwintering female blue crab and estimate abundance in Chesapeake Bay through ordinary kriging each year from 1990–2020. Estimates can also be derived for age-1+ females in WTAPS and WTAPSNE to develop worst-case scenario estimates of mature, overwintering females in the two placement areas. The effects of small-scale estimation on characterization of the female blue crab population in the two placement sites were also evaluated by calculating abundance in the different strata of the WDS. Our results indicated that when Bay-wide female abundance estimates was less than 150 million, the proportion of females estimated to be in WTAPS was highly variable. I suggest that the Port, if able, limit placement activities in WTAPS and WTAPSNE to years when Bay-wide female age-1+ abundance estimates is >150 million. I suggest postponing placement when female age-1+ abundance estimates in the Chesapeake Bay is below the overfished threshold for females (72.5 million).

Introduction

The Maryland Department of Transportation Maryland Port Administration (MDOT MPA) operates the Port of Baltimore. The Port is a major economic engine within the state, supporting jobs directly associated with shipping but also related to economic activity that relies on imports and exports of key resources and material. Following the widening of the Panama Canal, the size of container ships, called post-Panamax ships, has increased substantially. Shipping channels within Chesapeake Bay must be dredged to maintain a 15-m (50-foot) channel to ensure passage of post-Panamax ships to the Port of Baltimore.

Dredging requires the Port to develop a placement plan for the material removed from the shipping channels. Some of this material is used to restore and rebuild islands in the Chesapeake Bay, but much of the material is relocated to nearby open water, licensed placement areas in the Bay. There are two licensed open water placement sites for dredged material removed from the York Split Channel in the lower Chesapeake Bay: i) Wolf Trap Alternate Open Water Placement Site (WTAPS), located between the Piankatank River, VA, and Mobjack Bay, VA, and ii) WTAPS northern extension (WTAPSNE) which extends the WTAPS site to the north (USACE Baltimore District 2019).

Placement of dredged material has occurred in WTAPS since the late 1980s with the most recent placement in 2017 (USACE Baltimore District 2019). WTAPS is an 1,810-hectare (4,474-acre) site characterized by depths between 13–16-m (Lipcius and Knick 2016) with very fine to fine sand and silts throughout the site (USACE Baltimore District 2019). WTAPSNE was identified as an alternative to

WTAPS, but the cost for this placement site exceeds the cost in WTAPS by approximately \$21.9 million (in FY 19 dollars) over a 20-year planning period due to the increased travel distance and fuel consumption between the dredging site and placement site (USACE Baltimore District 2019).

The USACE must consider ways to mitigate or avoid negative impacts on threatened and endangered species in licensed placement locations. Relative to dredging operations in WTAPS, WTAPSNE, and York Split Channel, there are six federally listed threatened and endangered species: i) loggerhead sea turtle (*Caretta caretta*), ii) green sea turtle (*Chelonia mydas*), iii) leatherback sea turtle (*Dermochelys coriacea*), iv) Kemp's ridley sea turtle (*Lepidochelys kempii*), v) Atlantic sturgeon (*Acipenser oxyrinchus*), and vi) shortnose sturgeon (*Acipenser brevirostrum*). Since endangered sea turtles are only present during summer months, and both Atlantic and shortnose sturgeon reproduce only from late spring to autumn, the USACE has limited placement of dredged material overboard in the Chesapeake Bay to winter (USACE 2019); however, winter placement of dredged material in the Chesapeake Bay overlaps with overwintering blue crab, an ecologically and economically important species in the region.

The blue crab (*Callinectes sapidus*) is an important component of estuarine and coastal ecosystems from Texas to New Hampshire (Williams 1974). Throughout this range, blue crab exhibits a complex life history spanning both marine (larvae) and estuarine habitats (juvenile – adult stages – Figure 1.2). In the Chesapeake region, females release their zoea at the mouth of the Bay, and the larvae are advected out into the coastal ocean (Roman and Boicourt 1999). In the coastal ocean, these larvae

feed and molt 7 or 8 times to form the last larval stage, the megalopae, which reinvade the Bay (Epifanio 2007). The megalopae begin settling into structurally complex environments and eventually transform into the first juvenile crab stage (Lipcius et al. 2007). Growth occurs from spring to autumn when water temperatures are above $\sim 11^{\circ}\text{C}$ (Brylawski and Miller 2006). In winter months when the Chesapeake Bay temperature drops below $\sim 11^{\circ}\text{C}$, blue crab exhibit torpor and are associated with sediments (Bauer and Miller 2010a; Bauer and Miller 2010b).

Blue crab distribution patterns while overwintering in the Chesapeake Bay is sex and life stage specific (Jensen and Miller 2005; Jensen, Christman, and Miller 2006). Immature females migrate throughout the Bay, including to lower salinity waters which coincides with overwintering habitat of mature males in the upper portion of the Chesapeake Bay (Millikin and Williams 1984). Mature male blue crabs also frequent the deeper channels of the Chesapeake Bay. Immature juvenile blue crabs predominate in the lower salinity waters of the upper Chesapeake Bay and tributaries (Millikin and Williams 1984). Inseminated, mature females migrate to the saltier, deeper waters of the lower Chesapeake Bay to overwinter in preparation to release broods into the mouth of the Bay for larval dispersal in the late spring and early summer (Jivoff, Hines, and Quackenbush 2007; van Engel 1958).

Blue crab is a valuable resource in the Chesapeake Bay due to its ecologic and economic importance. Blue crab in the Chesapeake Bay supports an iconic commercial and recreational fishery that is important for the livelihood of individuals who surround the Chesapeake Bay region. Owing to the importance of the fishery, substantial investments are inputted into surveying the population and assessing the

stock status. The blue crab stock status in the Chesapeake Bay is assessed based on female-based reference points (CBSAC 2022). The female-based reference points are currently based on the maximum sustainable yield for female blue crabs only (Miller et al. 2011). Management uses these reference points to ensure that the number of females in the population remains above the overfished threshold (CBSAC 2022). The female-based management strategies within the Chesapeake Bay infer of the importance of females to the blue crab population. Female blue crabs are responsible for bearing the next generation and adding to the population. If the females are depleted, the next generation of juvenile blue crab who make it to adulthood are also depleted; Therefore, without egg-bearing females, the blue crab population eventually dies out.

Agencies of the Commonwealth of Virginia have expressed concerns over the placement of dredged material in WTAPS due to the possibility of higher abundances of overwintering, mature female blue crab who migrate to lower Bay waters during the late autumn to prepare for spawning in the spring (USACE Baltimore District 2019). Because of these concerns, the Port of Baltimore is interested in developing mature female blue crab abundance estimates in WTAPS and WTAPSNE (i.e., small-scale estimates). Small-scale female abundance estimates in WTAPS and WTAPSNE can be accomplished through a geostatistical approach (e.g., kriging).

The goal of this analysis was to determine the possible impacts to mature, overwintering female blue crab in two licensed placement sites for dredged material from the York Split Channel in the Chesapeake Bay: i) WTAPS and ii) WTAPSNE. This analysis was accomplished by using the WDS data to visualize the annual

distribution of overwintering female blue crab and estimate female abundance in Chesapeake Bay through ordinary kriging from 1990–2020. Estimates can also be derived for age-1+ females in WTAPS and WTAPSNE to develop worst-case scenario estimates of mortality within the two placement areas. The effects of small-scale estimation on female blue crab in the two placement sites were also evaluated by calculating abundance in the different strata of the WDS.

Methods

All analyzes were accomplished using data from the WDS. The methods of the WDS are briefly described here, but detailed descriptions of the methods of the survey can be found in Sharov et al. (2003). The WDS conducts one-minute tows of a commercial 1.8-m (6-foot) Virginia dredge to sample waters of the Chesapeake Bay deeper than 1.5-m (5-foot) (Sharov et al. 2003). The WDS has been conducted annually by the Maryland Department of Natural Resources (MDNR) and the Virginia Institute of Marine Science (VIMS) since the winter of 1989/1990, indexed as 1990 (Sharov et al. 2003). The WDS is conducted from December to March to take advantage of overwintering blue crab in the Chesapeake Bay. Since 1992, three fixed geographic strata have been employed to represent the stratified random design of the WDS: i) the upper Bay and tributaries, ii) the middle Bay, and iii) the lower Bay (Figure 1.4). Since 1993, the number of sites sampled in the different strata are proportional to the area totaling approximately 900–1500 stations in the Chesapeake Bay where juveniles age-0, males age-1+, females age-1+, and total blue crab (females and males of all ages) caught are recorded at each station (Sharov et al. 2003).

WDS data were explored for quality assurance by identifying outliers. This process involved removing stations whose coordinates were in error (e.g., appeared to be on land) and duplicate locations identified by stations with the same latitude and longitude. Based on the 1.8-m length of the Virginia dredge and variable tow length at each station, sampled stations with tow areas less than 50-m² or larger than 500-m² were removed based on a presumption of unreliability of resulting estimates.

The total catch of remaining stations was standardized by dividing the number of crabs caught at a station by an estimated annual and vessel-specific catchability coefficient provided by Glenn Davis (MDNR). Catchability coefficients were estimated by defined studies in which the catch of sequential tows over the same narrow path was recorded, and the rate of decline in catch with successive tows provided an estimate of catchability (Sharov et al. 2003; Vølstad et al. 2000). Catchability-corrected total catch was then standardized by the tow area to obtain the catchability-corrected number of crabs per m². Coordinates of the stations were transformed to Easting (m) and Northing (m) and projected to Universal Transverse Mercator zone 18N.

Design-Based Estimates

For comparative purposes, I assembled estimates of total Bay-wide abundance of blue crab during winter months using the design-based approach outlined by Sharov et al. (2003). These estimates are routinely developed each year by the Chesapeake Bay Stock Assessment Committee (CBSAC). The stratified design allows for Bay-wide estimates of blue crab but lacks the ability to estimate blue crab at small scales (Sharov et al. 2003; Vølstad, Rothschild, and Maurer 1994) and

visualize blue crab distribution. Because of these disadvantages, the design-based approach lacked the ability to answer the main objectives of these analyses.

Kriging

Kriging is a statistical or probabilistic approach to small-scale estimation that provides standard errors for the kriged values thereby quantifying the uncertainty associated with the kriged estimates (Krivoruchko 2012). Kriging uses similarities between pairs of values of the property at sampled locations separated by a measured distance by the following equation:

(6)

$$Z(x_0) = \sum_{i=1}^{N(x_0)} \lambda_i Z(x_i)$$

where $Z(x_0)$ is a point to be estimated at a given location, $N(x_0)$ is the number of samples from the neighborhood considered for the point to be estimated, λ_i is the ordinary kriging weights, and $Z(x_i)$ is the measured values at multiple locations (Salvelieva 2005). Kriging relies on a variogram that defines how the semi-variance between pairs of sampled points varies as the distance between sampled points increases. A common property of the variogram is that the semi-variance will continue to increase until a distance is reached where the population semi-variance equals the sample semi-variance (Fischer and Getis 2010). The increasing distance and variance are represented in a semivariogram (Fischer and Getis 2010). The semivariogram is used in kriging to produce kriged predictions based on the distance between sampled locations. Ordinary kriging was used for these analyses.

I used data from the Davis WDS dataset that retained sampled locations that fell within the Chesapeake Bay for the Bay-wide kriging analysis (Table 2.2). This dataset will be referred to as Davis WDS Chesapeake Bay. Total catch was adjusted for the catchability coefficients according to the year and vessel, tow area, and cell resolution (250-m²). Stations with tow areas less than 50-m² or greater than 500-m² were excluded from the dataset. No transformation method was used based on the results of the normality analysis presented in Chapter 2.

The strongest assumption of kriging is stationarity or spatial homogeneity where the data mean and the semivariogram are the same at all locations within the data (Krivoruchko 2012). Trend removal to meet the assumption of stationarity was accomplished using multiple linear regression for each year from 1990–2020. Numerous multiple linear regressions, up to the order with all interactions, were fitted, and the Akaike’s Information Criterion (AIC) values for each model was used to select the best fitting model for each year. The residuals of the best fitting model for that given year were then used to estimate the fitted variogram and for kriging. The kriged estimates were backtransformed using the following equation:

(7)

$$\hat{Y}_b = \hat{Y}_k + b_0 + b_1x_1 + b_2x_2 + \dots + b_n * x_n$$

where \hat{Y}_b is the backtransformed kriging estimate, Y_k is the kriged prediction, b_0 is the intercept, b_1 through b_n are the regression coefficients corresponding to the selected multiple linear regression, and x_1 through x_n are predictor variables corresponding to b_1 through b_n .

Based on the analysis from Chapter 2, the annual fitted variogram was selected based on the *autofitVariogram* function in the *automap* package (Hiemstra 2022) within the R statistics language (R Core Team 2013). The *autofitVariogram* function selects the best fitting model based on the smallest residual sum of squares. I allowed the *autofitVariogram* to select the best fitting model among spherical, exponential, Matérn, and gaussian variogram functions. A grid of 250-m² cells was used to predict blue crab abundance for total crabs (females and males of all ages), juveniles age-0, females age-1+, and males age-1+ within the *krige* function. The *krige* function is found in the *gstat* package in R (Pebesma and Graeler 2022) and was used to predict blue crab abundance using ordinary kriging which assumes that the mean is unknown (Oliver 2010). A maximum neighborhood of 25 sampled locations was used to predict unsampled locations with a maximum distance of 40-km. The maximum neighborhood and distance were selected to avoid estimating an unsampled point using a sampled location that logically did not make sense (i.e., using a sampled point in the Potomac River to estimate an unsampled location in the Patuxent River). Also, the maximum neighborhood and distance had to be large enough to predict the entirety of the Chesapeake Bay. The predicted kriged surface was then clipped to the desired shapefile of either Chesapeake Bay, WTAPS, or WTAPSNE, using the *raster* package in R (Hijmans et al. 2022). The blue crab abundance estimates in each 250-m² cell were then summed to obtain annual blue crab abundance estimates in either the Chesapeake Bay, WTAPS, or WTAPSNE. The proportion of blue crabs by life stage and sex in WTAPS and WTAPSNE out of the Bay-wide kriging abundance estimates for the given life stage and sex were then calculated. Kriged abundance

maps, associated standard errors of the kriged abundance estimates, trend maps of the best fitting multiple linear regression model, and density plots were created using the *ggplot2* package in R (Wickham et al. 2022) for each year from 1990–2020 (Figures 3.1–3.31). The standard errors were adjusted by taking the square root for uniformity to the kriged estimates in meters.

To assess the impact of small-scale estimations, I conducted additional kriging analyses by strata following similar methods to Bay-wide kriging. I retained only sampled locations that fell within the Chesapeake Bay and the correct strata designation according to the three geographic strata of the WDS. This dataset will be referred to as the Davis WDS Strata. Female age-1+ abundance was estimated at smaller scales through kriging using two different criteria to analyze the effect of small-scale estimation on female blue crab abundance in WTAPS and WTAPSNE: i) Davis WDS Strata for Strata 2 and 3 only and ii) Davis WDS Strata for strata 3 only. The predicted kriged surface was then clipped to the shapefile of either WTAPS or WTAPSNE to obtain female age-1+ abundance in the specified area of interest.

The Bay-wide kriging analysis was accomplished in R statistical language. The full R script can be found in Appendix A.

Results

Winter Dredge Survey Data Summary

A WDS dataset provided by Glenn Davis at MDNR was used for these analyses. Two datasets were created based on different QA/QC criteria: i) Davis WDS Chesapeake Bay and ii) Davis WDS Strata. Davis WDS Chesapeake Bay

retained sampled locations that fell within the Chesapeake Bay. Davis WDS Chesapeake Bay was used for the Bay-wide kriging analysis. A total of 2,333 stations (4.8%) were excluded from Davis WDS Chesapeake Bay data following QA/QC procedures (Table 2.2). Davis WDS Strata retained sampled locations that fell within the Chesapeake Bay and the correct strata designation according to the three geographic strata of the WDS. Davis WDS Strata was used for small-scale kriging by strata. A total of 3,072 stations (6.3%) were excluded from Davis WDS Strata following QA/QC procedures (Table 3.1). The number of stations per year ranged from 1,179–2,567 for both WDS data files provided by Glenn Davis.

Bay-Wide Kriging

The Bay-wide kriging estimates in Chesapeake Bay, WTAPS, and WTAPSNE, were derived for females age-1+, males age-1+, juveniles age-0, and total blue crabs (females and males of all ages). Due to the importance of mature females who carry the next generation, I focused on results for females-age-1+ (Tables 3.1–3.5; Figures 3.1–3.60; and Appendix B). Results and estimates for total blue crab abundance, males age-1+ abundance, and juveniles age-0 abundance are provided in Appendix C–E.

The residuals of the best fitting multiple regression according to the smallest AIC (Table B.1) was used to estimate the fitted variogram for each year from 1990–2020 (Figures B.1–B.31). Following kriging, the predictions were backtransformed based on the coefficients of the best fitting model for each year from 1990–2020 (Table B.2). Either Matérn, spherical, exponential, or gaussian was selected each year using *autofitVariogram* in R from 1990–2020 (Table B.3). The exponential model

was selected for 1993, 1994, 1996, 2001, and 2015, and the spherical model was selected for 1995 and 2019 (Table B.3).

Female distributional maps derived from the Bay-wide kriging analysis used to estimate female abundance in Chesapeake Bay show interannual variations; however, females age-1+ occurred in higher densities in the lower Bay in each year from 1990–2020 (Figures 3.1–3.31). The years 2009, 2010, and 2019 (Figures 3.20c, 3.21c and 3.30c), are the only ones demonstrating areas of female abundance on the highest range (red and burgundy). Female distributional maps for Chesapeake Bay also show low abundance of females in the Bay from 1998–2007 (Figures 3.9–3.18c).

Kriging abundance estimates of female blue crab age-1+ derived in the Chesapeake Bay from 1990–2020 varied annually (Figure 3.32). When comparing our estimates to the design-based approach, the Bay-wide kriging abundance estimates were higher compared to design-based estimates of females age-1+ in the Chesapeake Bay; however, our estimates exhibited similar interannual patterns to the design-based estimates (Figure 3.32).

Female blue crab distributional abundance maps were created based on Bay-wide kriging estimation for each year from 1990–2020 for WTAPS and WTAPSNE (Figures 3.33–3.40). Female abundance estimates in WTAPS ranged from 0.13–2.52 million while abundance estimates in WTAPSNE ranged from 0.10–2.57 million (Table 3.2). Female abundance in WTAPS from 1990–2020 were slightly higher than in WTAPSNE (WTAPS= 0.99 ± 0.61 (mean \pm SD), WTAPSNE= 0.73 ± 0.54) (Table 3.2).

The proportion of females age-1+ in WTAPS out of the total Bay-wide female age-1+ kriging abundance during winter ranged from 0.12%–1.50% (Table 3.2). The proportion of the total female age 1+ abundance occurring in WTAPSNE out of the total Bay-wide female age-1+ kriging abundance during winter months ranged from 0.07% –1.11% (Table 3.2). The proportion of females in WTAPS versus WTAPSNE were highly variable with no clear pattern (Figure 3.41). There was a negative ($y = -0.0002x + 0.6145$), but non-significant ($t\text{-stat} = -0.29$, $p=0.77$), relationship between the proportion of age-1+ females that occurred in WTAPS and the Bay-wide kriging abundance of age-1+ females in Chesapeake Bay (Figure 3.42). However, a clear pattern is evident in the variance around this non-significant relationship (Figure 3.42), such that when Bay-wide female abundance is less than 150 million, the proportion of females in WTAPS is highly variable, and can be 2-3 times higher than predicted.

Small-Scale Kriging by Strata

To determine the effects of small-scale estimation, female age 1+ blue crab abundance and distributional plots in WTAPS and WTAPSNE were calculated based on the three geographic strata of the WDS two different ways: i) using WDS data in strata 2 and 3 only (Table 3.3; Figures 3.43–3.50) and ii) using WDS data in strata 3 only (Table 3.4; Figures 3.51–3.58). Estimates of the abundance of age-1+ females in WTAPSNE were not feasible for strata 3 alone as WTAPSNE spans both strata 2 and 3. Strata 2 and 3 estimates of age-1+ female blue crab in WTAPSNE were higher than Chesapeake Bay abundance estimates (Chesapeake Bay= 0.73 ± 0.54 and Strata 2 and 3= 1.34 ± 0.99) (Table 3.4; Figure 3.59). The proportion of females in WTAPSNE for

strata 2 and 3 out of the Bay-wide kriging abundance estimates were also higher compared to the proportion of females in WTAPSNE calculated for Bay-wide abundance (Chesapeake Bay= $0.45\% \pm 0.25\%$, Strata 2 and 3= $0.81\% \pm 0.47\%$) (Tables 3.2–3.3).

Strata 2 and 3 age-1+ female kriging abundance estimates for 1990–2020 in WTAPS ranged from 0.40–4.60 million compared to 0.40–6.38 million for kriging estimates of age-1+ female abundance in WTAPS based on strata 3 only (Table 3.5; Figure 3.60). Strata 3 estimates of females age-1+ in WTAPS were higher than Chesapeake Bay and strata 2 and 3 abundance estimates (Chesapeake Bay= 0.99 ± 0.61 (mean \pm SD), Strata 2 and 3= 1.67 ± 0.93 , Strata 3= 1.94 ± 1.25) (Table 3.5). The proportion of age-1+ females in WTAPS for strata 3 out of the Bay-wide kriging abundance estimates in Chesapeake Bay were also higher compared to the proportion of females in WTAPS calculated in the Bay-wide kriging analysis and for the strata 2 and 3 kriging analysis (Chesapeake Bay= $0.59\% \pm 0.26\%$, Strata 2 and 3= $1.02\% \pm 0.40\%$, Strata 3= $1.17\% \pm 0.54\%$) (Tables 3.2–3.4). The largest proportion of age-1+ females in WTAPS from the three estimation techniques was 3.14% in 2008 calculated through the strata 3 kriging analysis.

Discussion

Our results show that geostatistical approaches can be used to estimate the abundance of age-1+ female blue crab both at the Bay-wide level and also at smaller scales, such as those relevant to the evaluation of the possible impacts of the placement of dredged material. At the Bay-wide scale, geostatistical estimates of age-1+ female abundance were broadly similar to those generated from the traditional

design-based estimates. This finding supports the earlier conclusions of Jensen and Miller (2005). For all but one year out of the 31 years of available data in the WDS, geostatistical estimates of age-1+ female abundance were higher than comparable estimates from design-based approaches. The mean percent difference between the two approaches over the entire 31-year period of record was 32.96%.

The ability to produce distributional maps of age-1+ female abundance is a specific advantage of geostatistical approaches. These maps indicate that age-1+ female abundance is concentrated in the lower Bay between the mouths of the Rappahannock and York Rivers. Years of higher age-1+ female abundance are characterized by higher densities of crabs in these lower Bay regions rather than any dramatic shifts in distributions. Additional exploration of the spatial pattern in the distribution of age-1+ females is warranted based on the patterns evident in maps produced here. For example, quantification of how the moments of each annual distribution could be usefully explored as a function of overall abundance. To date this has only been done for the average latitude (Jensen and Miller 2005).

Our analyses indicate that a low proportion of the age-1+ female blue crab population occurs within the WTAPS and WTAPSNE placement areas. I compared estimates of abundance of age-1+ female blue crab derived from three different spatial resolutions: Bay-wide, strata 2 and 3 combined, and strata 3. The highest proportion of females in WTAPS and WTAPSNE from the three different kriging analyses was 3.14%. Estimated abundances of age-1+ female blue crab were highest for analyses that were based on the smallest spatial resolution (i.e., strata 3).

Estimates of the impacts of placement of dredged material on overwintering blue crab are not available. However, as a worst-case scenario, I assume that all crabs in WTAPS or WTAPSNE are killed in any year that placement activities occur. In this case, our data indicate that placement activities will result in the deaths of an average of 0.59% of all age-1+ female blue crab in WTAPS when estimates are based on the Bay-wide distribution and up to 1.18% of all age-1+ females in WTAPS when estimates are based solely on strata 3. The central question becomes whether this level of mortality is likely to have a significant impact on the dynamics of the blue crab population in Chesapeake Bay.

Since 2008, the blue crab population and the fisheries it supports in the Chesapeake Bay have been managed based on the abundance and exploitation fraction of age-1+ female blue crab (Miller et al. 2011). Both threshold and target exploitation rates of age-1+ female blue crab have been established. If female age-1+ exploitation rates exceed the threshold ($U=0.37$), the population is described as experiencing overfishing. A population experiencing overfishing is not capable of supporting the long-term sustainable yield of the population. The target exploitation rate ($U=0.28$) is the level of exploitation that is expected to generate maximum sustainable levels of yield. Compared to these levels, the maximum feasible impact of the placement of dredged material in WTAPS is 30-60 times lower than the threshold exploitation level. This suggests that the average maximum impact of placement of dredged material is unlikely to have a substantial impact on the dynamics of the population of blue crab in Chesapeake Bay.

Threshold and target abundances have also been established for age-1+ female blue crab in Chesapeake Bay. When abundances drop below the threshold abundance, currently estimated to be 72.5 million age-1+ females, the population is termed overfished or depleted. A healthy blue crab population would support 196 million age-1+ females as is indicated by the target abundance. Our results indicate a relationship between the variance in the percentage of age-1+ female crabs in WTAPS and their Bay-wide abundance (Figure 3.42). The Bay-wide abundance of age-1+ female blue crab is a reliable predictor of the percentage of age-1+ female blue crab in WTAPS when the Bay-wide abundance exceeds 150 million age-1+ females. When abundance of age-1+ females falls below 150 million female crabs, the variability in the percentage of these crabs in WTAPS increases. These two lines of evidence suggest the need for consideration of placement activities when there are fewer than 150 million age-1+ females in Chesapeake Bay. When female blue crabs are more abundant than this level, it is unlikely that placement activities would substantially and negatively impact future population levels even if all crabs were to be killed by placement activities. However, when female age-1+ crab abundance are below 150 million, the impact of potential mortality resulting from placement activities becomes more difficult to predict and may have a larger relative impact on future levels of crab populations.

The analysis of the annual WDS survey is completed by late spring in the year in which the survey is completed and the estimate of female age-1+ abundance produced can serve as a tool for determining whether or not placement activities might negatively impact the stock. I would suggest that placements are not advisable

if there are fewer than 72.5 million age-1+ female blue crab in Chesapeake Bay because the stock will be overfished and significant reductions in human-caused mortality will be necessary to rebuild the stock. At this level, it is likely that crab fisheries would be severely restricted or even temporarily closed. As a result, arguments against placement activities on an overfished blue crab population become strong. In years when female age-1+ abundance is between 72.5–150 million age-1+ female blue crab, caution is warranted within this range for the placement of dredged material. In years when the population abundance of age-1+ females exceeds 150 million, I suggest it would be safe for dredging placement activities to occur without consideration of its impact on blue crab populations.

I recognize that these scenarios assume that there is 100% mortality of blue crabs in WTAPS or WTAPSNE when placement of dredged materials occurs. It is unlikely that there is complete mortality. Several lines of evidence suggest this may be the case. First, although it is commonly believed that overwintering crabs are “buried” in the sediments, knowledge from local watermen suggest that crabs still move during winter months – and are likely only loosely associated with the sediments. This is particularly the case when water temperature is above 5°C (Bauer and Miller 2010b). Secondly, researchers at Virginia Commonwealth University conducted preliminary mesocosm experiments in which they report mortality levels substantial lower than 100% (Pers. Comm.). Thus, the recommendations I provide above are strongly conservative and likely overestimate the risk to blue crab from the placement of dredge material in Chesapeake Bay.

A second conservative aspect of our analyses is that placement activities do not occur every year. Over the last 20 years, placement activities have occurred only in 2002, 2003/2004, 2004, 2007, 2009, 2015 and 2017. I suggest that fuller analysis of the impact of placement activities on blue crab populations requires a stochastic model of blue crab populations that can quantify the impact of episodic placement events under conditions of variable proportions of the population in the placement areas and a variable level of mortality resulting from such placements. I suggest a stage-based projection model, such as that developed by Miller (2003) for future explorations.

Tables for Chapter 3

Table 3.1. Summary of Davis WDS Strata by strata location used in the small-scale kriging analysis to estimate females age-1+. Number of stations is the number of WDS sampling locations used for analysis. The number of stations excluded is the number of stations that were removed during QA/QC procedures.

Year	Number of Stations			Number of Stations Excluded		
	Strata 1	Strata 2	Strata 3	Strata 1	Strata 2	Strata 3
1990	977	113	89	266	1	20
1991	1,165	180	333	216	6	13
1992	1,645	585	337	147	29	11
1993	745	347	361	111	20	28
1994	769	320	419	83	10	31
1995	838	380	423	95	13	51
1996	796	428	381	92	8	41
1997	721	445	425	46	29	43
1998	745	438	412	69	11	17
1999	809	441	223	72	18	21
2000	707	444	228	39	11	11
2001	703	472	236	47	9	9
2002	729	490	184	59	5	8
2003	749	419	172	60	7	4
2004	717	472	170	80	8	12
2005	732	467	173	60	10	11
2006	730	463	205	54	18	9
2007	708	465	180	56	15	7
2008	725	376	175	56	9	9
2009	705	479	177	53	15	5
2010	722	506	169	38	7	2
2011	716	480	174	57	6	10
2012	732	480	167	51	19	4
2013	747	476	170	44	5	3
2014	737	478	225	50	4	6
2015	732	477	168	44	6	5
2016	737	473	223	50	10	7
2017	736	480	223	45	8	8
2018	780	489	228	54	4	4
2019	782	481	229	57	11	3
2020	777	483	226	60	9	7
Total	24,613	13,527	7,505	2,311	341	420

Table 3.2. Estimates of female age-1+ abundance (millions) in Chesapeake Bay, WTAPS, and WTAPSNE, derived from Bay-wide kriging using Davis WDS Chesapeake Bay data. The proportion of females in WTAPS and WTAPSNE were calculated based on the Bay-wide female age-1+ kriging abundance estimate in Chesapeake Bay.

Year	Female Bay-wide Abundance Estimates (*10 ⁶)	# of 250 m ² Cells	Area (m ²)	WTAPS Female Abundance Estimates (*10 ⁶)	Proportion of Females in WTAPS (%)	WTAPSNE Female Abundance Estimates (*10 ⁶)	Proportion of Females in WTAPSNE (%)
1990	238.89	182,218	11,389	1.08	0.45	0.88	0.37
1991	255.44	178,956	11,185	1.56	0.61	0.56	0.22
1992	227.58	182,971	11,436	1.18	0.52	0.73	0.32
1993	163.30	184,205	11,513	0.93	0.57	0.83	0.51
1994	136.50	184,174	11,511	1.21	0.89	0.74	0.55
1995	92.02	182,962	11,435	0.31	0.34	0.44	0.47
1996	124.90	183,167	11,448	1.17	0.94	0.46	0.37
1997	110.55	182,896	11,431	0.13	0.12	0.14	0.13
1998	129.38	182,142	11,384	0.99	0.76	0.10	0.07
1999	57.30	183,303	11,456	0.57	0.99	0.29	0.51
2000	134.91	182,990	11,437	0.42	0.31	0.70	0.52
2001	67.79	182,702	11,419	0.36	0.53	0.18	0.26
2002	62.59	182,879	11,430	0.26	0.42	0.40	0.64
2003	100.18	182,855	11,428	0.60	0.60	0.25	0.25
2004	129.66	183,087	11,443	0.39	0.30	1.20	0.92
2005	120.15	182,909	11,432	0.43	0.35	0.39	0.32
2006	104.49	182,519	11,407	0.71	0.68	0.33	0.32
2007	106.49	182,669	11,417	0.82	0.77	0.46	0.43
2008	92.94	182,692	11,418	1.39	1.50	1.03	1.11
2009	253.58	182,637	11,415	1.24	0.49	1.74	0.68
2010	420.85	181,500	11,344	2.52	0.60	0.53	0.13

Table 3.2 (continued).

2011	325.73	182,564	11,410	2.27	0.70	2.57	0.79
2012	117.85	182,680	11,418	0.38	0.32	0.45	0.38
2013	167.43	182,600	11,413	0.88	0.53	0.89	0.53
2014	113.40	182,775	11,423	0.66	0.58	0.49	0.43
2015	198.51	182,377	11,399	1.15	0.58	0.61	0.30
2016	243.51	182,748	11,422	1.44	0.59	0.86	0.35
2017	347.77	182,661	11,416	2.35	0.67	1.11	0.32
2018	214.49	182,893	11,431	1.19	0.56	1.36	0.64
2019	253.80	182,779	11,424	1.43	0.56	0.37	0.15
2020	175.34	183,032	11,440	0.67	0.38	1.67	0.95
Mean	170.56	182,695	11,419	0.99	0.59	0.73	0.45
Standard Deviation	88.68	854	53	0.61	0.26	0.54	0.25

Table 3.3. Estimates of female age-1+ abundance (millions) in strata 2 and 3, WTAPS, and WTAPSNE, derived from kriging using Davis WDS Strata data only from strata 2 and 3. The proportion of females in WTAPS and WTAPSNE were calculated based on the Bay-wide female age-1+ kriging abundance estimate in Chesapeake Bay.

Year	Female Abundance Estimates in Strata 2 & 3 (*10 ⁶)	# of 250 m ² Cells	Area (m ²)	WTAPS Female Abundance Estimates (*10 ⁶)	Proportion of Females in WTAPS (%)	WTAPSNE Female Abundance Estimates (*10 ⁶)	Proportion of Females in WTAPSNE (%)
1990	122.03	52,538	3,284	1.55	0.65	1.36	0.57
1991	232.04	56,923	3,558	2.53	0.99	0.85	0.33
1992	205.87	66,172	4,136	2.10	0.92	1.75	0.77
1993	159.89	67,697	4,231	1.95	1.19	2.86	1.75
1994	128.19	67,000	4,188	2.00	1.46	1.13	0.83
1995	58.26	66,092	4,131	0.60	0.66	0.77	0.84
1996	151.32	68,000	4,250	1.82	1.46	0.99	0.79
1997	107.22	68,346	4,272	0.40	0.36	0.41	0.37
1998	112.10	68,960	4,310	2.15	1.66	0.59	0.45
1999	65.65	68,997	4,312	0.93	1.62	0.56	0.98
2000	143.91	68,841	4,303	0.92	0.68	1.58	1.17
2001	70.94	69,522	4,345	0.69	1.01	0.34	0.5
2002	75.80	69,404	4,338	0.51	0.82	0.88	1.41
2003	90.69	66,848	4,178	0.93	0.93	0.35	0.35
2004	147.49	68,403	4,275	0.82	0.63	0.43	0.34
2005	148.24	68,768	4,298	1.09	0.91	0.65	0.54
2006	96.15	69,011	4,313	1.06	1.01	0.54	0.52
2007	106.31	68,219	4,264	1.31	1.23	0.99	0.92
2008	122.43	62,859	3,929	2.15	2.31	1.40	1.50
2009	287.13	68,919	4,307	2.50	0.99	2.17	0.85
2010	385.90	68,133	4,258	4.60	1.09	2.56	0.61

Table 3.3 (continued).

2011	304.12	69,265	4,329	3.67	1.13	3.84	1.18
2012	132.84	68,956	4,310	0.77	0.65	0.53	0.45
2013	197.48	69,027	4,314	1.28	0.76	1.13	0.68
2014	106.91	69,392	4,337	1.48	1.30	1.03	0.91
2015	189.45	69,238	4,327	2.46	1.24	0.96	0.48
2016	303.93	69,269	4,329	2.34	0.96	1.26	0.52
2017	313.69	69,032	4,315	2.13	0.61	2.41	0.69
2018	196.58	69,478	4,342	1.98	0.92	2.07	0.97
2019	273.97	69,343	4,334	1.80	0.71	0.82	0.32
2020	135.84	69,391	4,337	1.12	0.64	4.22	2.41
Mean	166.85	67,485	4,218	1.67	1.02	1.34	0.81
Standard Deviation	84.56	3,718	232	0.93	0.40	0.99	0.47

Table 3.4. Estimates of female age-1+ abundance (millions) in strata 3 and WTAPS derived from kriging using Davis WDS Strata data only from strata 3. The proportion of females in WTAPS was calculated based on the Bay-wide female age-1+ kriging abundance estimate in Chesapeake Bay. WTAPSNE could not be estimated because the area extends into strata 2.

Year	Female Abundance Estimates in Strata 3 (*10 ⁶)	# of 250 m ² Cells	Area (m ²)	WTAPS Female Abundance Estimates (*10 ⁶)	Proportion of Females in WTAPS (%)
1990	61.18	18,428	1,152	1.92	0.80
1991	122.80	21,443	1,340	2.89	1.13
1992	105.48	20,988	1,312	2.20	0.97
1993	95.11	22,339	1,396	2.18	1.34
1994	71.75	22,433	1,402	2.24	1.64
1995	31.55	22,346	1,397	0.63	0.68
1996	76.13	21,890	1,368	2.17	1.73
1997	74.88	21,948	1,372	0.40	0.36
1998	75.33	22,329	1,396	2.39	1.84
1999	49.75	22,565	1,410	1.13	1.96
2000	82.63	22,434	1,402	0.84	0.62
2001	45.84	22,531	1,408	0.79	1.16
2002	47.10	22,333	1,396	0.48	0.77
2003	49.03	22,388	1,399	1.10	1.10
2004	119.51	21,901	1,369	1.09	0.84
2005	120.24	22,092	1,381	1.05	0.87
2006	70.34	22,427	1,402	1.17	1.12
2007	75.76	22,064	1,379	1.74	1.64
2008	88.79	22,363	1,398	2.91	3.14
2009	159.96	22,394	1,400	2.36	0.93
2010	289.68	22,243	1,390	6.38	1.52

Table 3.4 (continued).

2011	169.48	22,363	1,398	5.08	1.56
2012	101.58	21,969	1,373	0.99	0.84
2013	101.72	22,361	1,398	1.64	0.98
2014	55.78	22,388	1,399	1.54	1.35
2015	107.71	22,395	1,400	2.22	1.12
2016	201.54	22,385	1,399	2.41	0.99
2017	150.67	22,300	1,394	2.92	0.84
2018	81.73	22,354	1,397	2.10	0.98
2019	112.15	22,473	1,405	1.74	0.69
2020	39.41	22,519	1,407	1.29	0.73
Mean	97.89	22,109	1,382	1.94	1.17
Standard Deviation	53.61	759	47	1.25	0.54

Table 3.5. Estimates of female age-1+ abundance (millions) in WTAPS and WTAPSNE for Bay-wide, strata 2 and 3, and strata 3, derived from kriging by Davis WDS data. WTAPSNE for strata 3 could not be calculated because the area extends into strata 2.

WTAPS Female Abundance Estimates (*10 ⁶)				WTAPSNE Female Abundance Estimates (*10 ⁶)	
Year	Bay- wide	Strata 2 & 3	Strata 3	Bay-wide	Strata 2 & 3
1990	1.08	1.55	1.92	0.88	1.36
1991	1.56	2.53	2.89	0.56	0.85
1992	1.18	2.10	2.20	0.73	1.75
1993	0.93	1.95	2.18	0.83	2.86
1994	1.21	2.00	2.24	0.74	1.13
1995	0.31	0.60	0.63	0.44	0.77
1996	1.17	1.82	2.17	0.46	0.99
1997	0.13	0.40	0.40	0.14	0.41
1998	0.99	2.15	2.39	0.10	0.59
1999	0.57	0.93	1.13	0.29	0.56
2000	0.42	0.92	0.84	0.70	1.58
2001	0.36	0.69	0.79	0.18	0.34
2002	0.26	0.51	0.48	0.40	0.88
2003	0.60	0.93	1.10	0.25	0.35
2004	0.39	0.82	1.09	1.20	0.43
2005	0.43	1.09	1.05	0.39	0.65
2006	0.71	1.06	1.17	0.33	0.54
2007	0.82	1.31	1.74	0.46	0.99
2008	1.39	2.15	2.91	1.03	1.40
2009	1.24	2.50	2.36	1.74	2.17
2010	2.52	4.60	6.38	0.53	2.56
2011	2.27	3.67	5.08	2.57	3.84
2012	0.38	0.77	0.99	0.45	0.53
2013	0.88	1.28	1.64	0.89	1.13
2014	0.66	1.48	1.54	0.49	1.03
2015	1.15	2.46	2.22	0.61	0.96
2016	1.44	2.34	2.41	0.86	1.26
2017	2.35	2.13	2.92	1.11	2.41
2018	1.19	1.98	2.10	1.36	2.07
2019	1.43	1.80	1.74	0.37	0.82
2020	0.67	1.12	1.29	1.67	4.22
Mean	0.99	1.67	1.94	0.73	1.34
Standard Deviation	0.61	0.93	1.25	0.54	0.99

Figures for Chapter 3

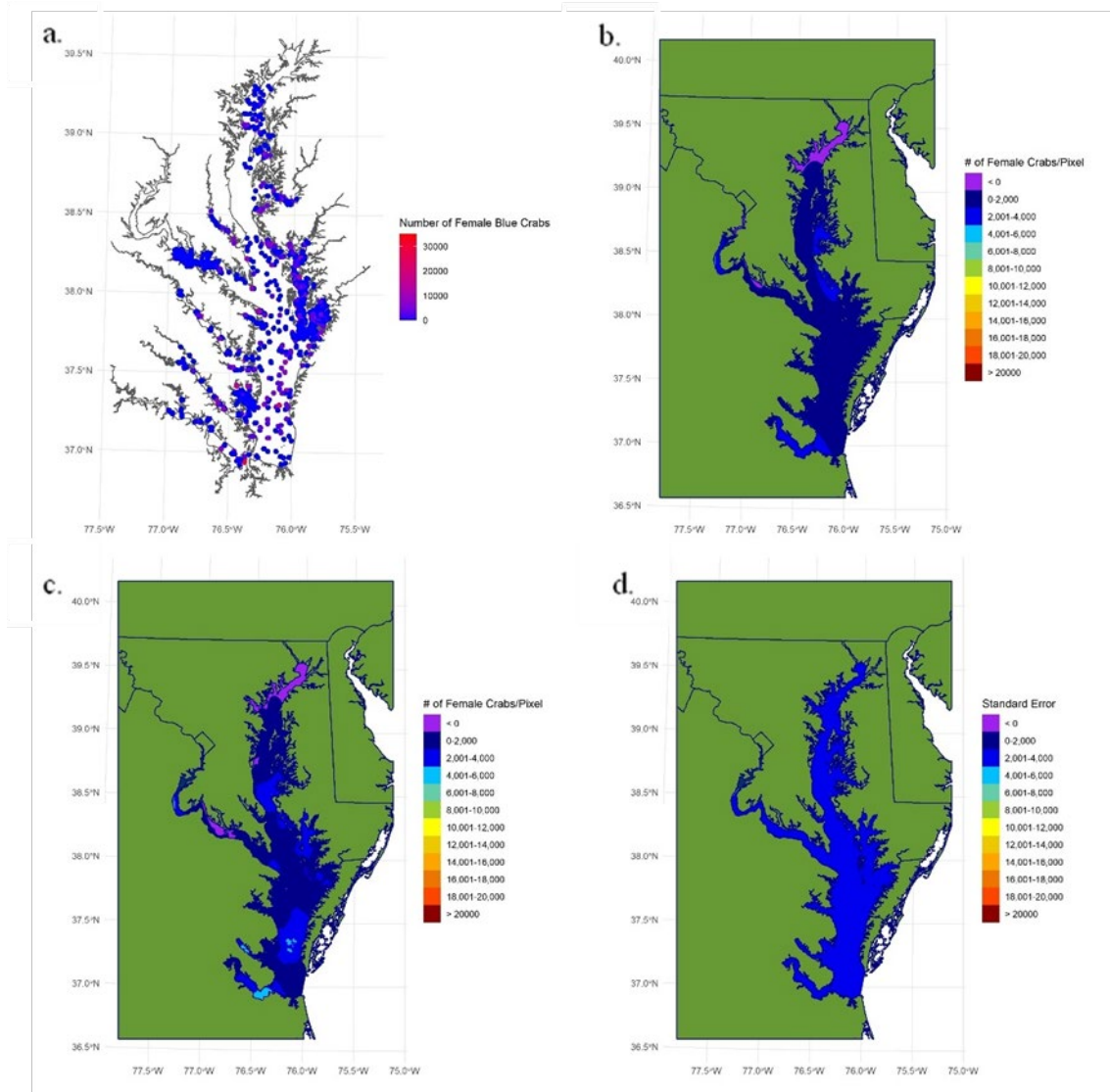


Figure 3.1. Various 1990 female age-1+ blue crab maps in the Chesapeake Bay: a) map of female age-1+ blue crab density in 1990, b) selected trend map based on the best fitting multiple linear regression model in 1990, c) map of female age-1+ blue crab abundance estimates in 1990, and d) standard error map of female age-1+ blue crab abundance estimates in 1990.

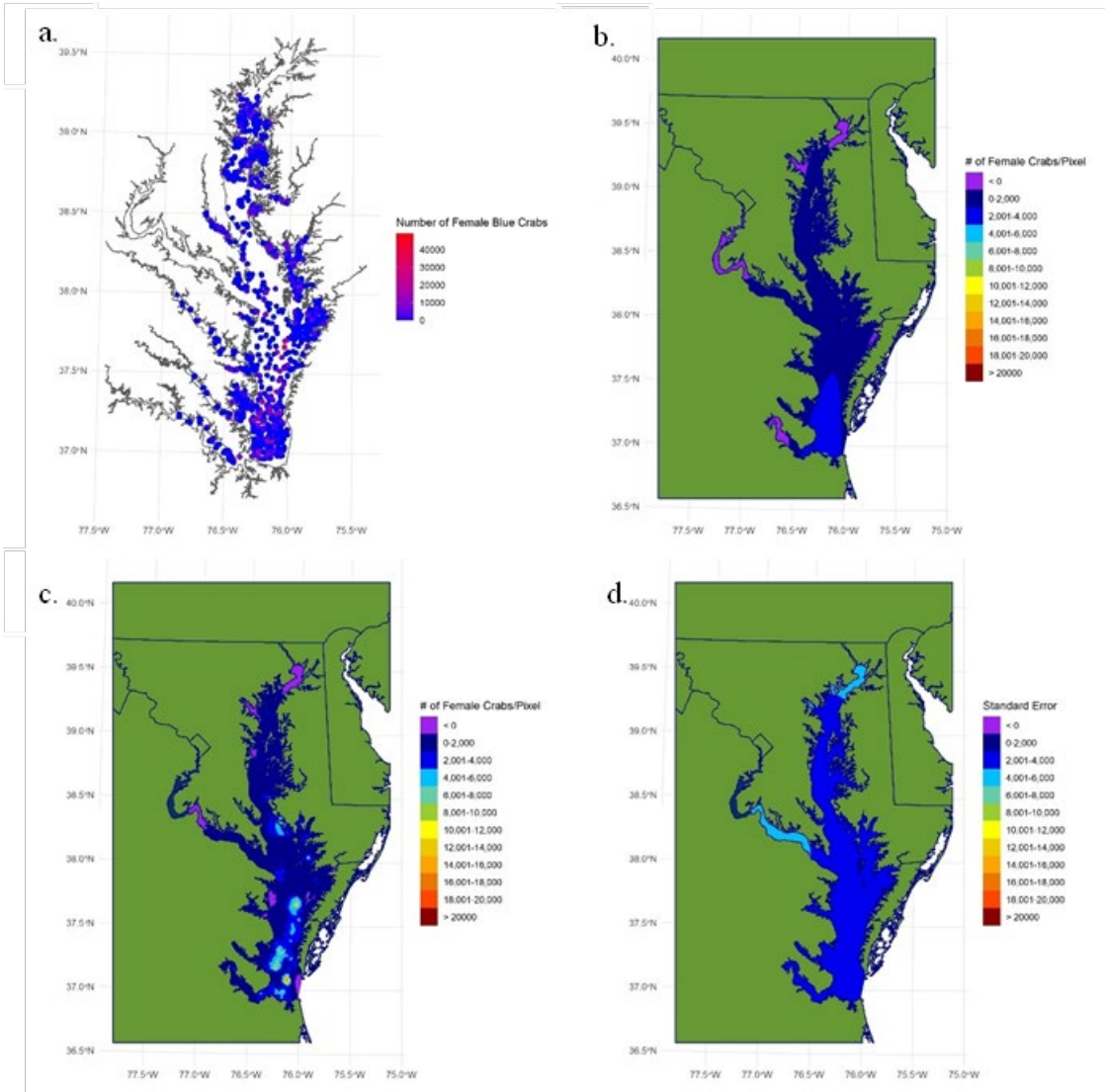


Figure 3.2. Various 1991 female age-1+ blue crab maps in the Chesapeake Bay: a) map of female age-1+ blue crab density in 1991, b) selected trend map based on the best fitting multiple linear regression model in 1991, c) map of female age-1+ blue crab abundance estimates in 1991, and d) standard error map of female age-1+ blue crab abundance estimates in 1991.

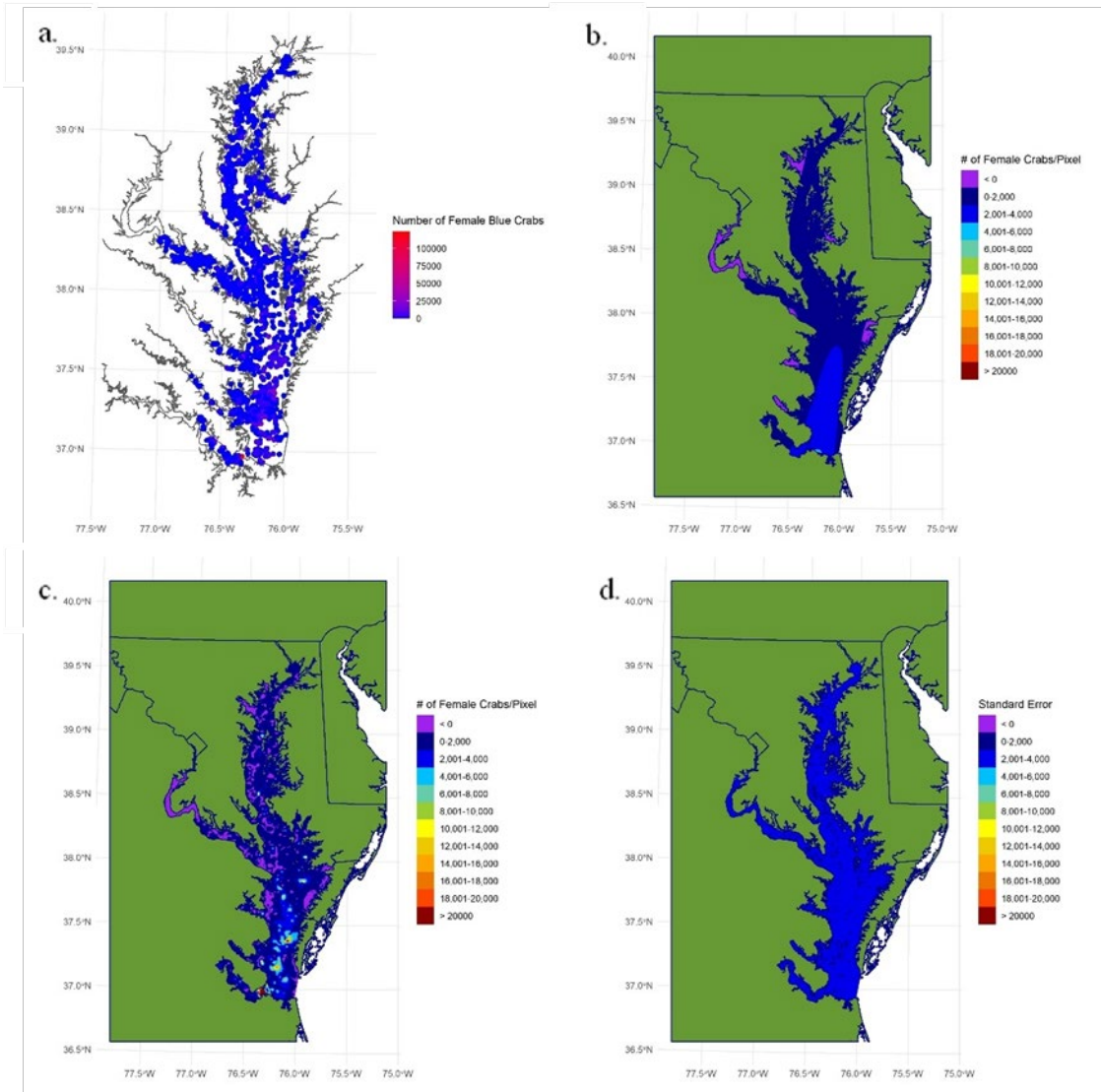


Figure 3.3. Various 1992 female age-1+ blue crab maps in the Chesapeake Bay: a) map of female age-1+ blue crab density in 1992, b) selected trend map based on the best fitting multiple linear regression model in 1992, c) map of female age-1+ blue crab abundance estimates in 1992, and d) standard error map of female age-1+ blue crab abundance estimates in 1992.

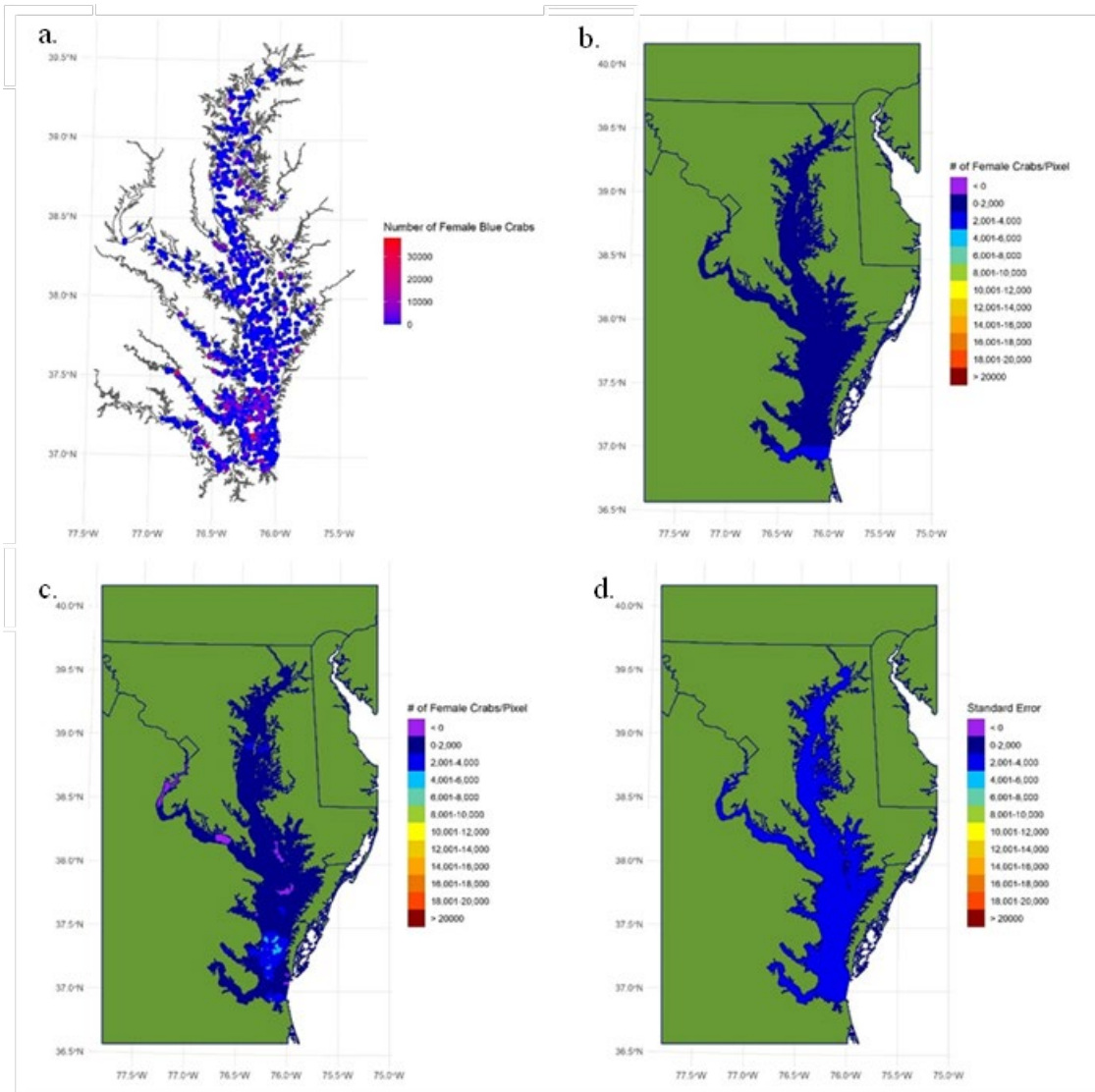


Figure 3.4. Various 1993 female age-1+ blue crab maps in the Chesapeake Bay: a) map of female age-1+ blue crab density in 1993, b) selected trend map based on the best fitting multiple linear regression model in 1993, c) map of female age-1+ blue crab abundance estimates in 1993, and d) standard error map of female age-1+ blue crab abundance estimates in 1993.

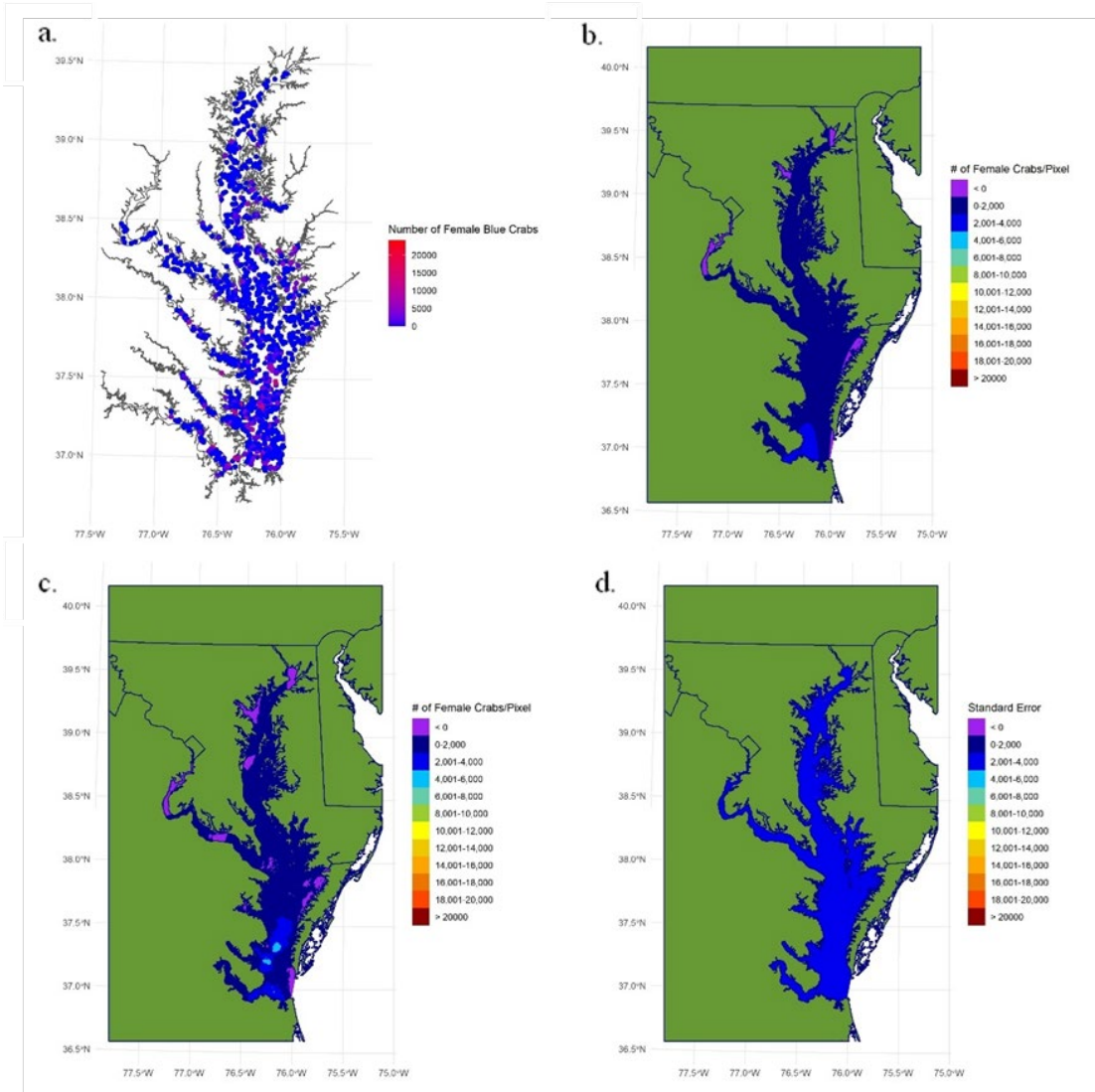


Figure 3.5. Various 1994 female age-1+ blue crab maps in the Chesapeake Bay: a) map of female age-1+ blue crab density in 1994, b) selected trend map based on the best fitting multiple linear regression model in 1994, c) map of female age-1+ blue crab abundance estimates in 1994, and d) standard error map of female age-1+ blue crab abundance estimates in 1994.

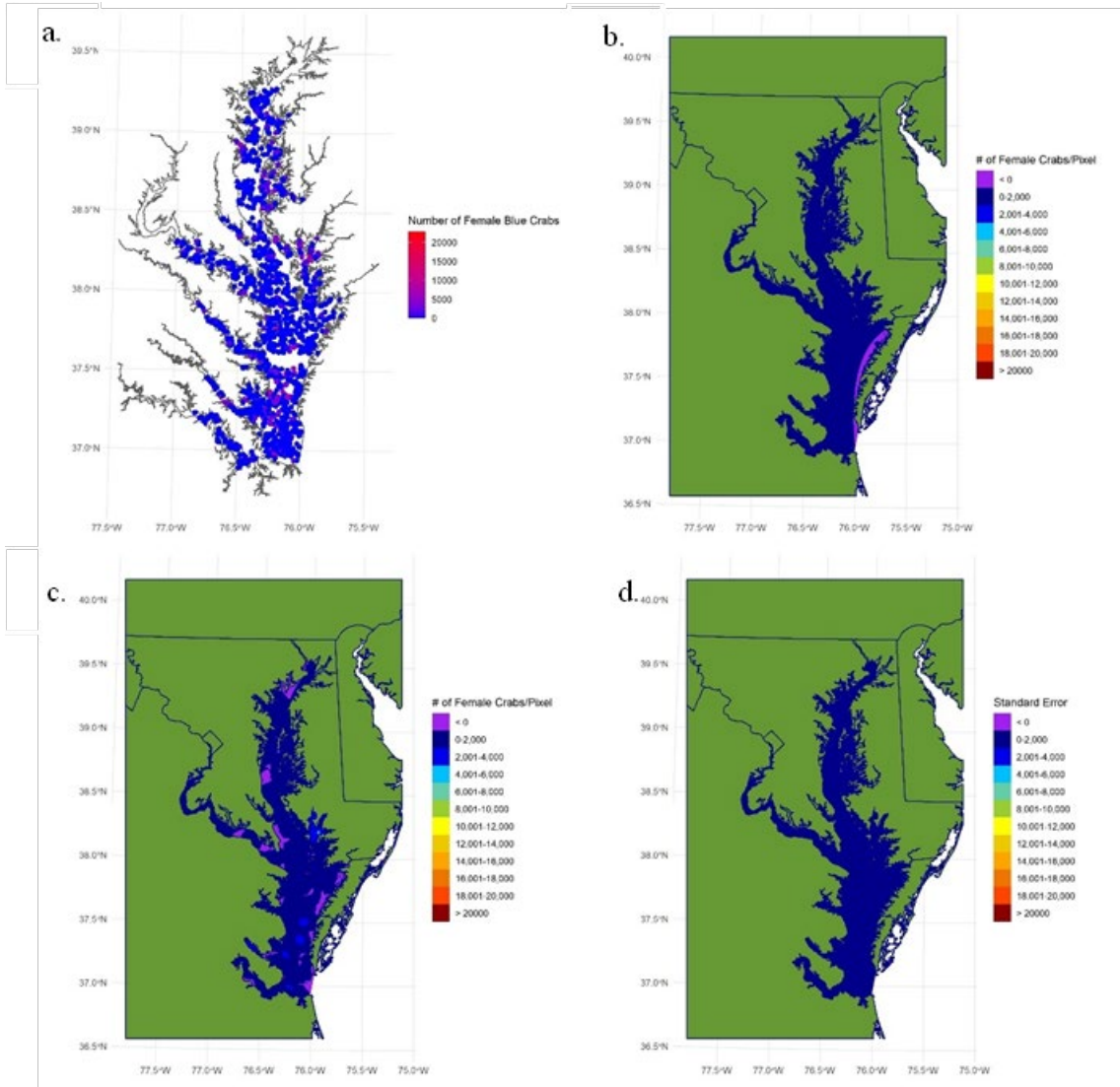


Figure 3.6. Various 1995 female age-1+ blue crab maps in the Chesapeake Bay: a) map of female age-1+ blue crab density in 1995, b) selected trend map based on the best fitting multiple linear regression model in 1995, c) map of female age-1+ blue crab abundance estimates in 1995, and d) standard error map of female age-1+ blue crab abundance estimates in 1995.

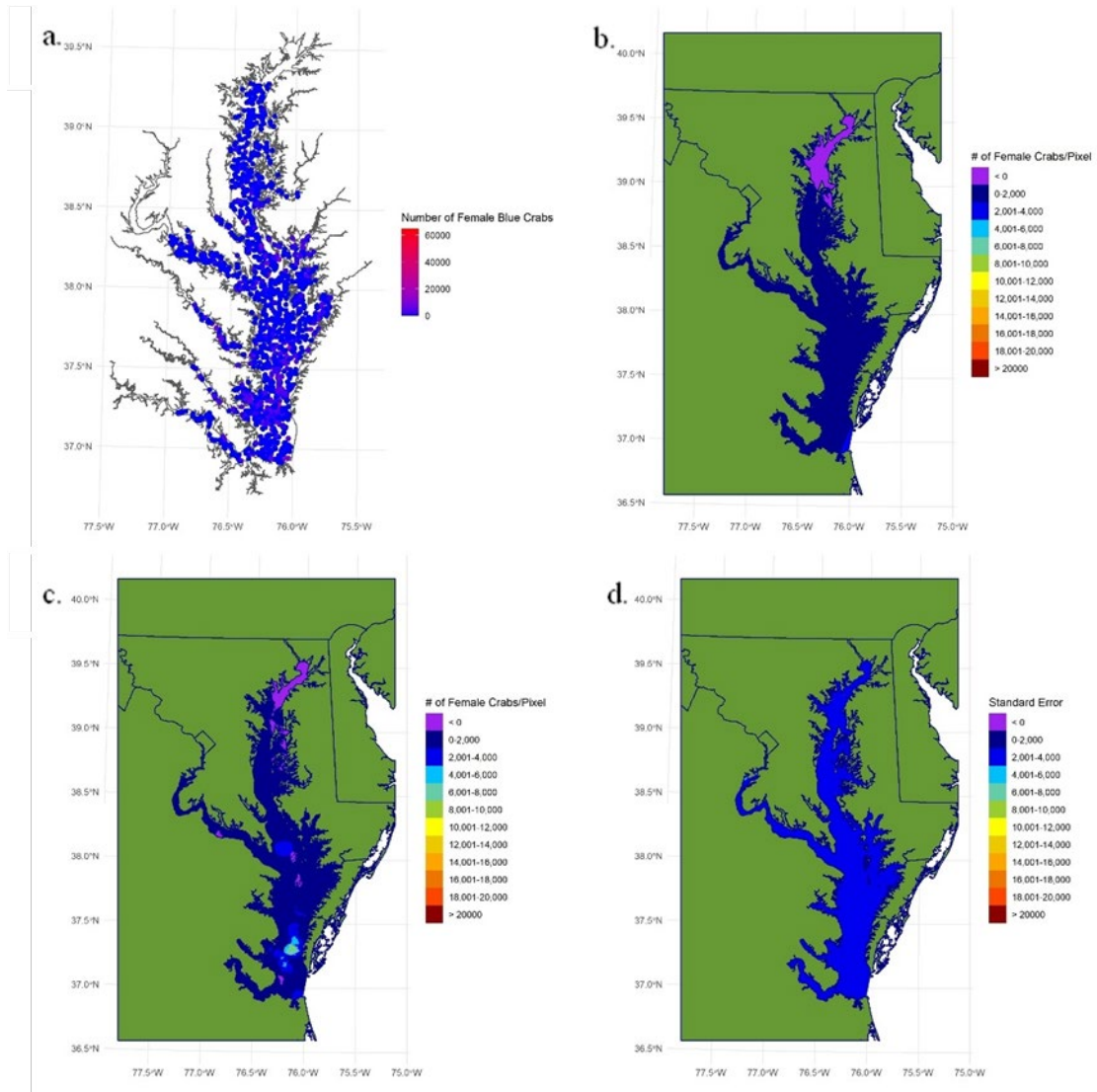


Figure 3.7. Various 1996 female age-1+ blue crab maps in the Chesapeake Bay: a) map of female age-1+ blue crab density in 1996, b) selected trend map based on the best fitting multiple linear regression model in 1996, c) map of female age-1+ blue crab abundance estimates in 1996, and d) standard error map of female age-1+ blue crab abundance estimates in 1996.

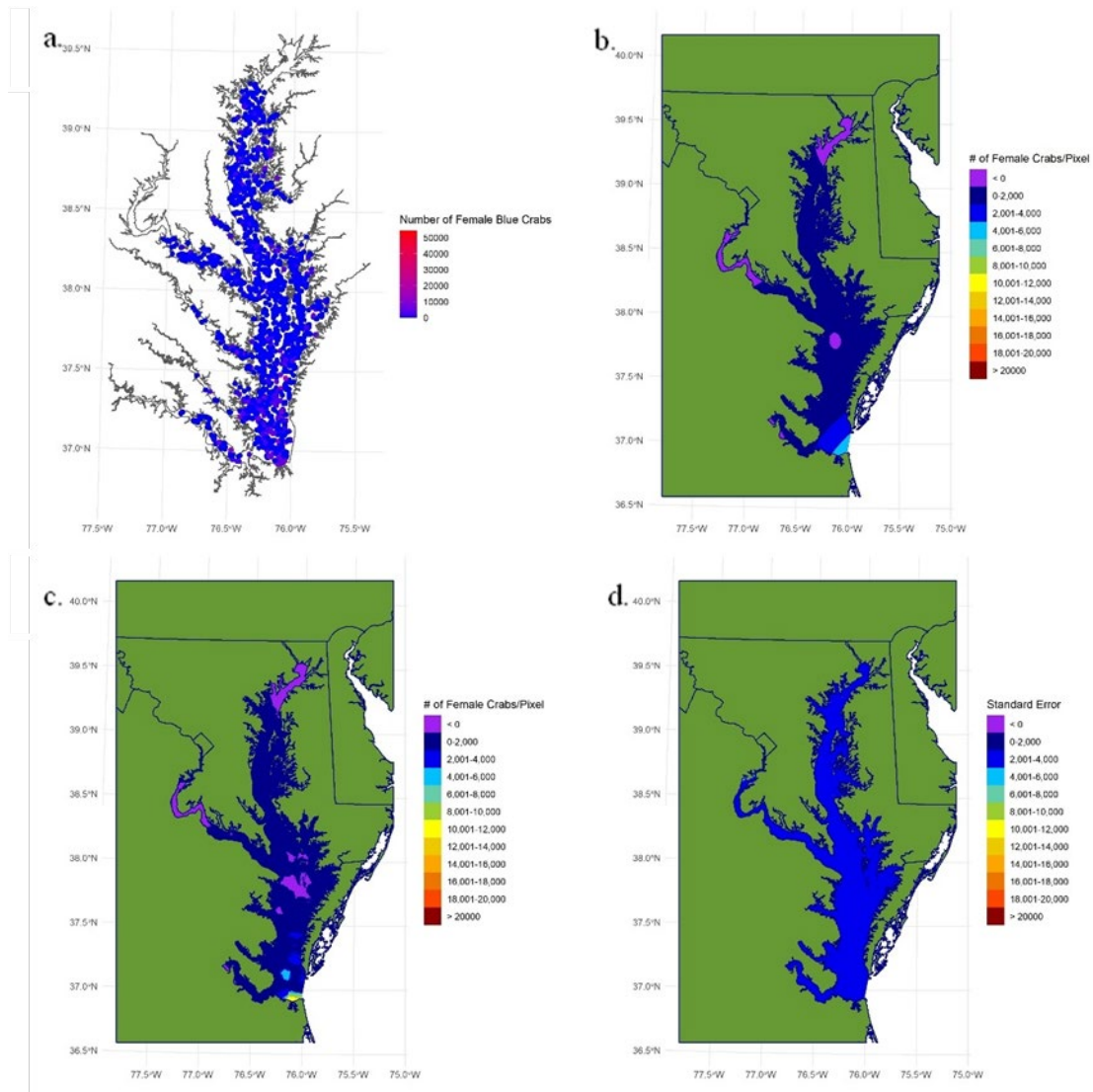


Figure 3.8. Various 1997 female age-1+ blue crab maps in the Chesapeake Bay: a) map of female age-1+ blue crab density in 1997, b) selected trend map based on the best fitting multiple linear regression model in 1997, c) map of female age-1+ blue crab abundance estimates in 1997, and d) standard error map of female age-1+ blue crab abundance estimates in 1997.

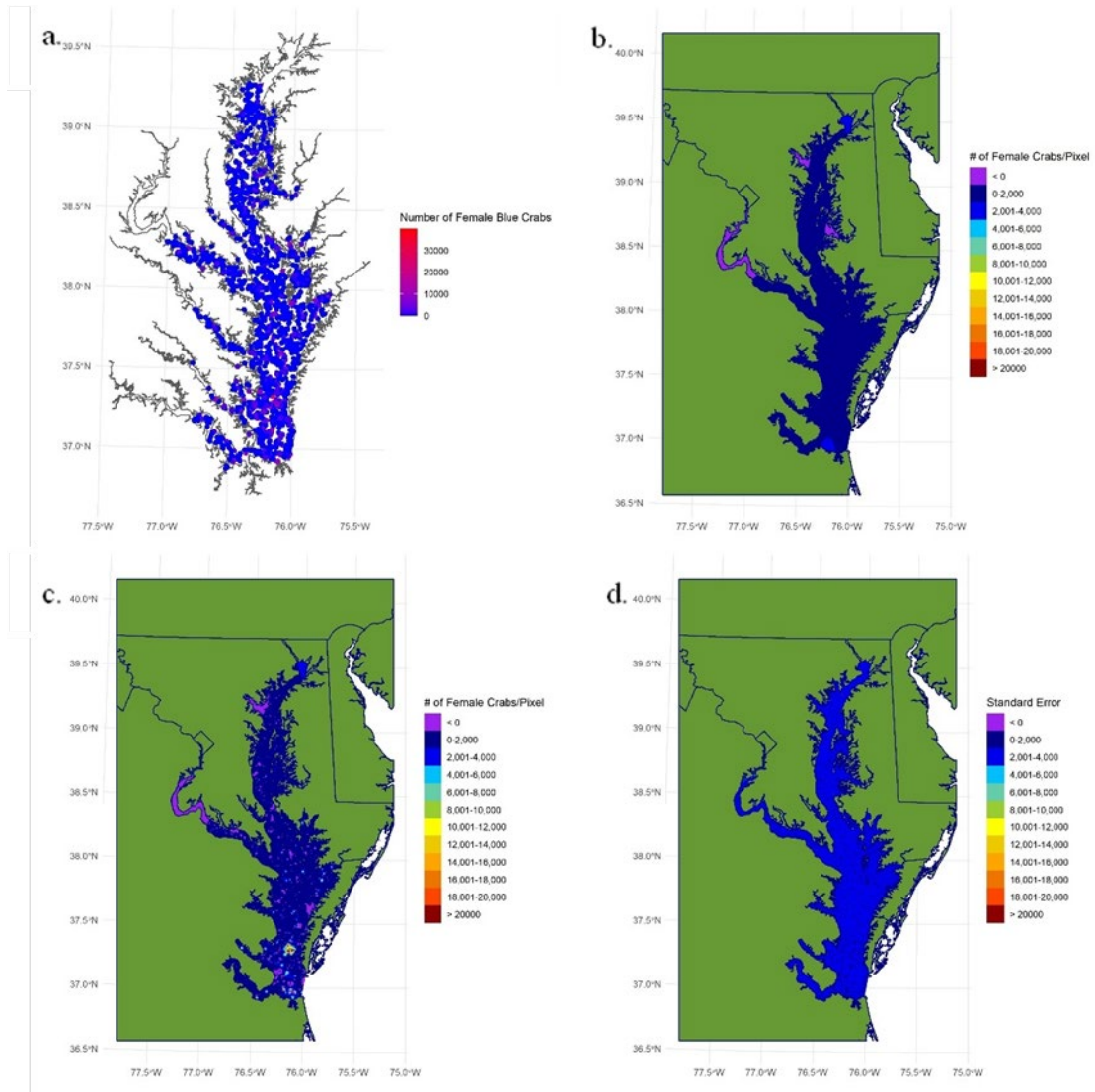


Figure 3.9. Various 1998 female age-1+ blue crab maps in the Chesapeake Bay: a) map of female age-1+ blue crab density in 1998, b) selected trend map based on the best fitting multiple linear regression model in 1998, c) map of female age-1+ blue crab abundance estimates in 1998, and d) standard error map of female age-1+ blue crab abundance estimates in 1998.

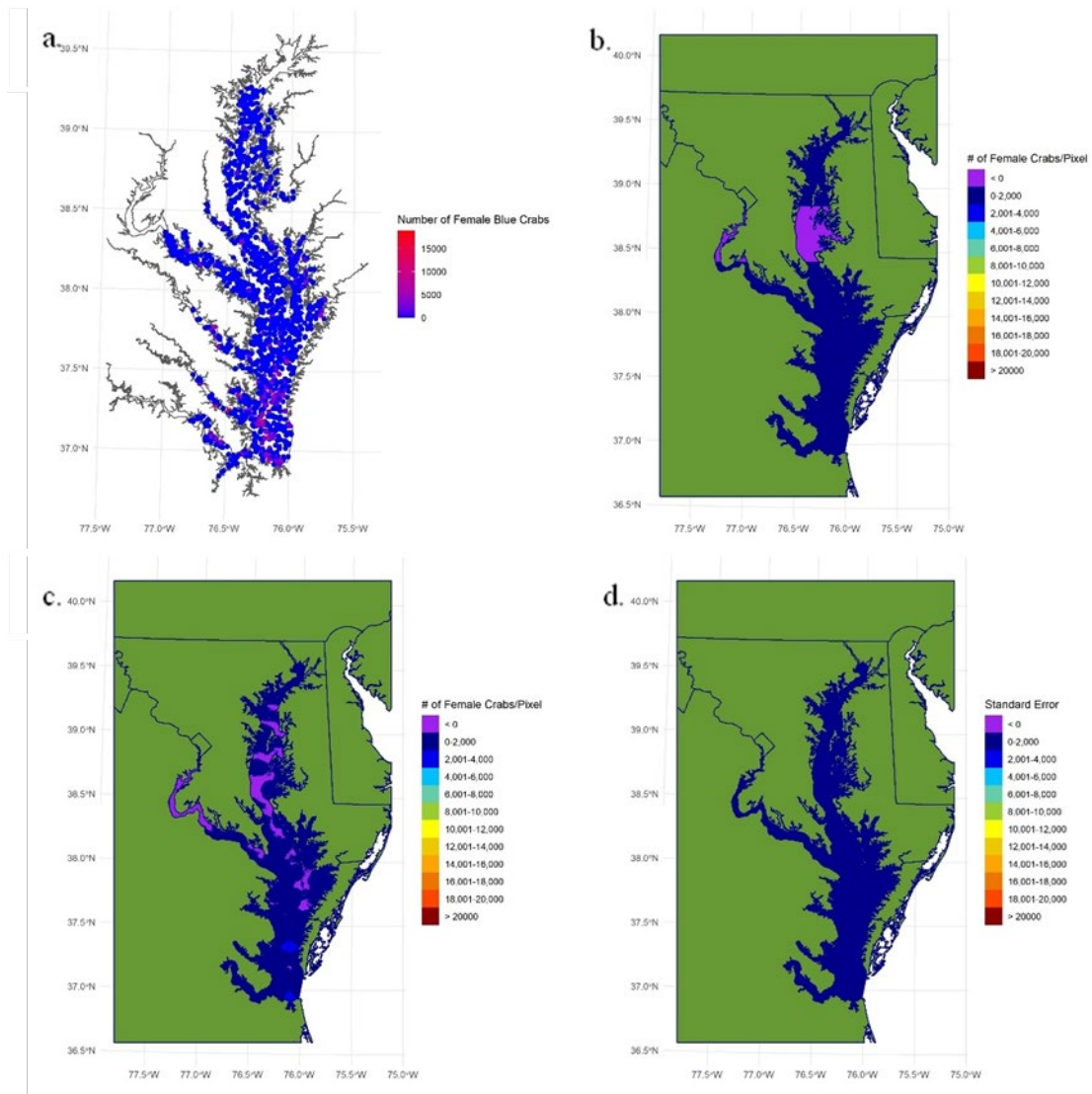


Figure 3.10. Various 1999 female age-1+ blue crab maps in the Chesapeake Bay: a) map of female age-1+ blue crab density in 1999, b) selected trend map based on the best fitting multiple linear regression model in 1999, c) map of female age-1+ blue crab abundance estimates in 1999, and d) standard error map of female age-1+ blue crab abundance estimates in 1999.

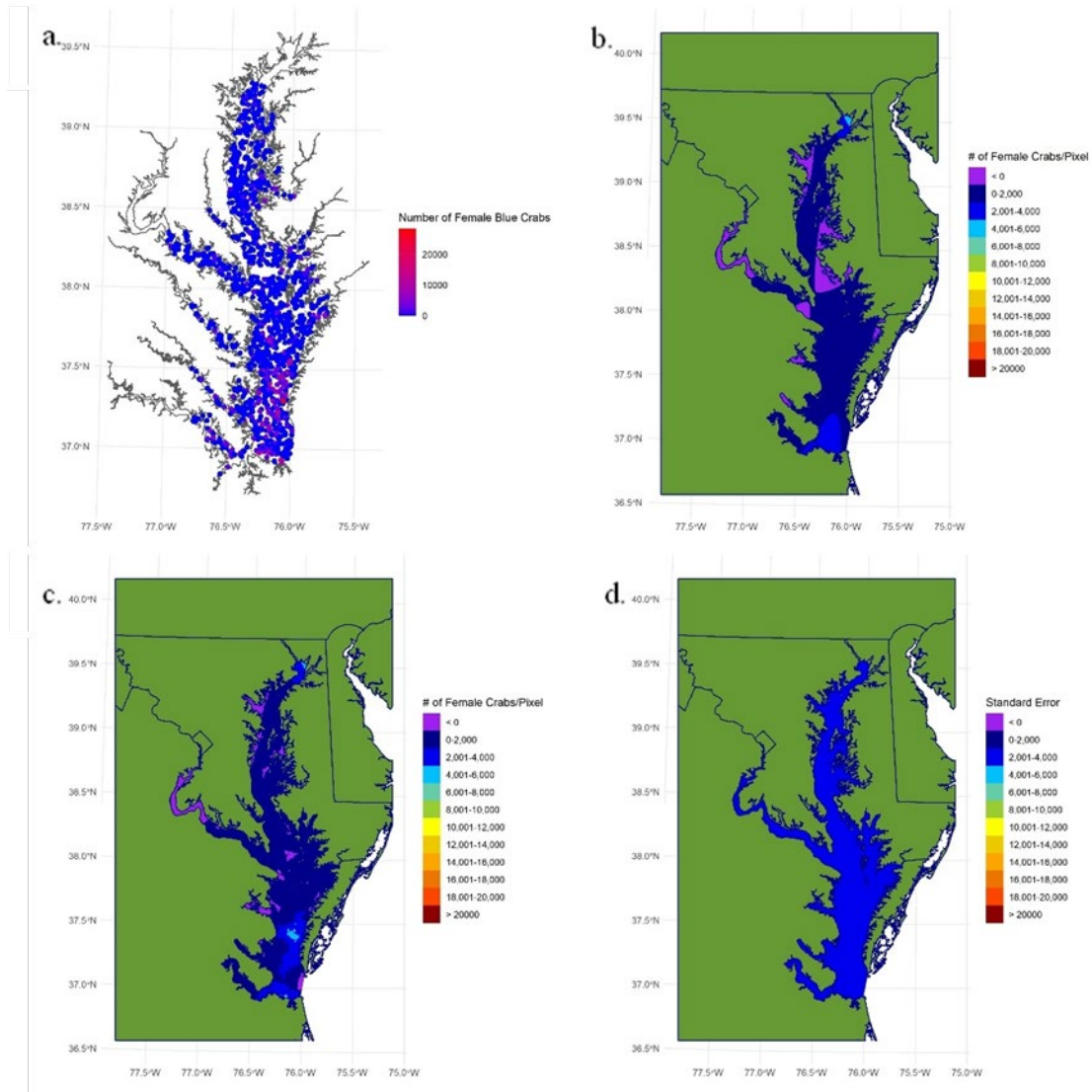


Figure 3.11. Various 2000 female age-1+ blue crab maps in the Chesapeake Bay: a) map of female age-1+ blue crab density in 2000, b) selected trend map based on the best fitting multiple linear regression model in 2000, c) map of female age-1+ blue crab abundance estimates in 2000, and d) standard error map of female age-1+ blue crab abundance estimates in 2000.

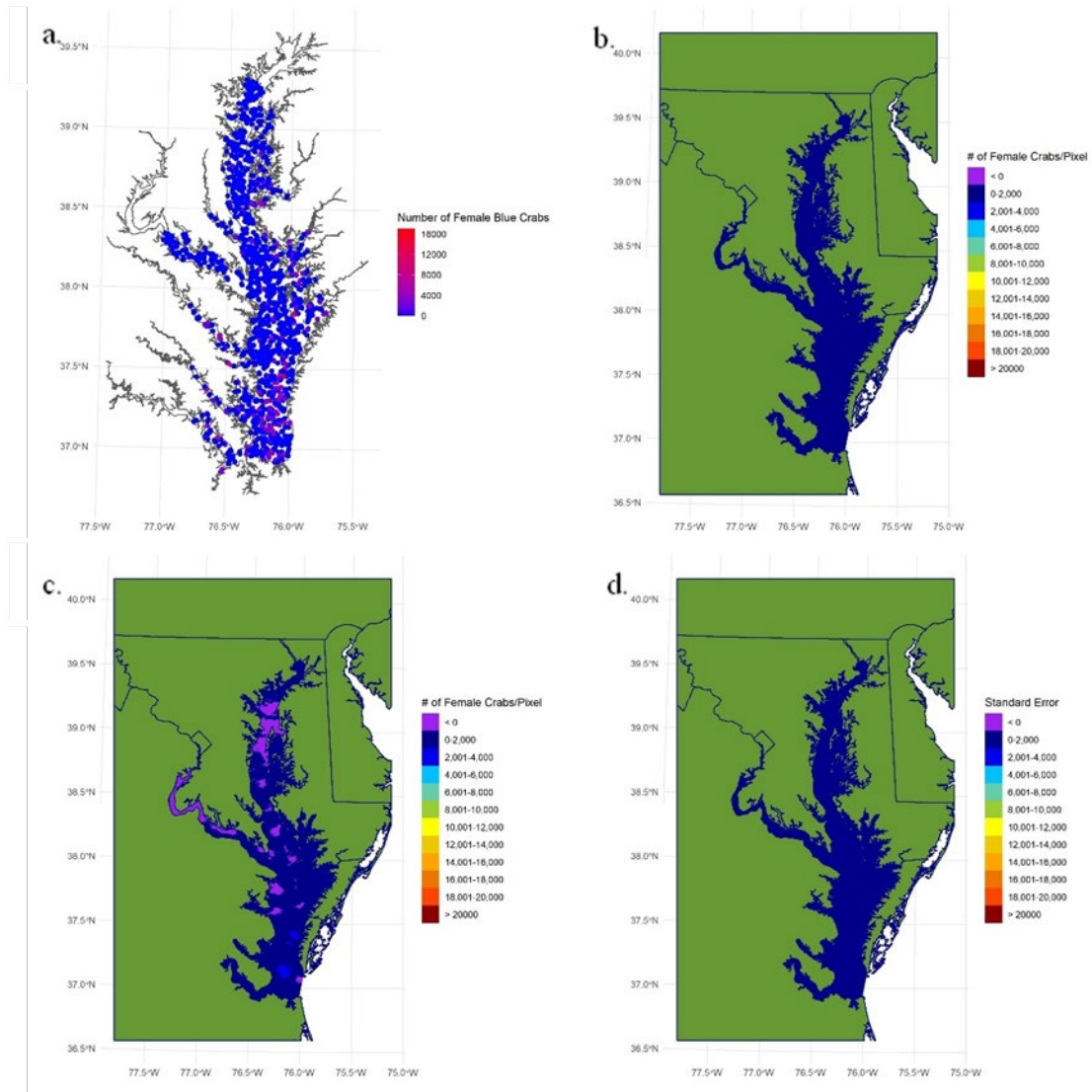


Figure 3.12. Various 2001 female age-1+ blue crab maps in the Chesapeake Bay: a) map of female age-1+ blue crab density in 2001, b) selected trend map based on the best fitting multiple linear regression model in 2001, c) map of female age-1+ blue crab abundance estimates in 2001, and d) standard error map of female age-1+ blue crab abundance estimates in 2001.

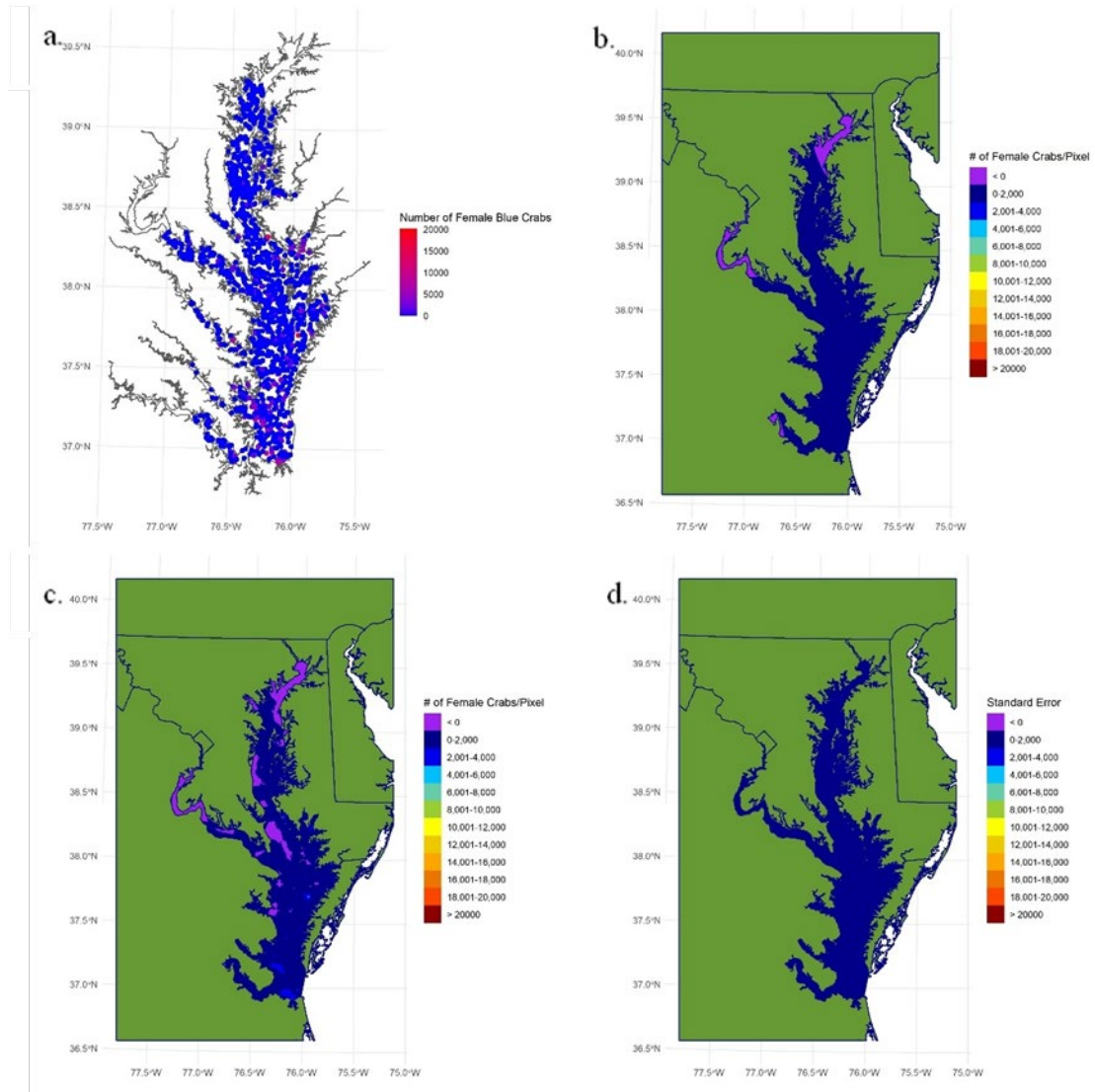


Figure 3.13. Various 2002 female age-1+ blue crab maps in the Chesapeake Bay: a) map of female age-1+ blue crab density in 2002, b) selected trend map based on the best fitting multiple linear regression model in 2002, c) map of female age-1+ blue crab abundance estimates in 2002, and d) standard error map of female age-1+ blue crab abundance estimates in 2002.

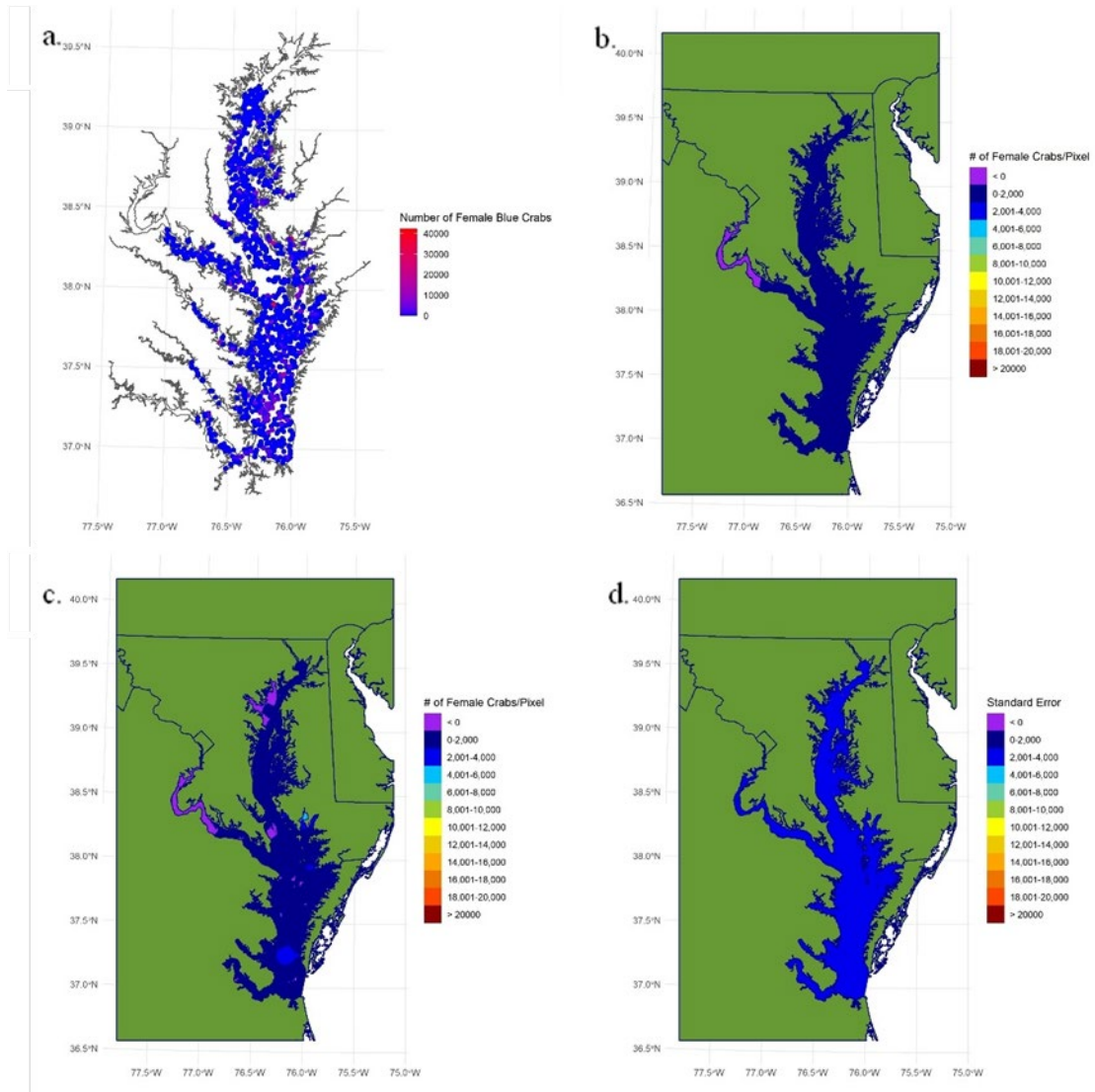


Figure 3.14. Various 2003 female age-1+ blue crab maps in the Chesapeake Bay: a) map of female age-1+ blue crab density in 2003, b) selected trend map based on the best fitting multiple linear regression model in 2003, c) map of female age-1+ blue crab abundance estimates in 2003, and d) standard error map of female age-1+ blue crab abundance estimates in 2003.

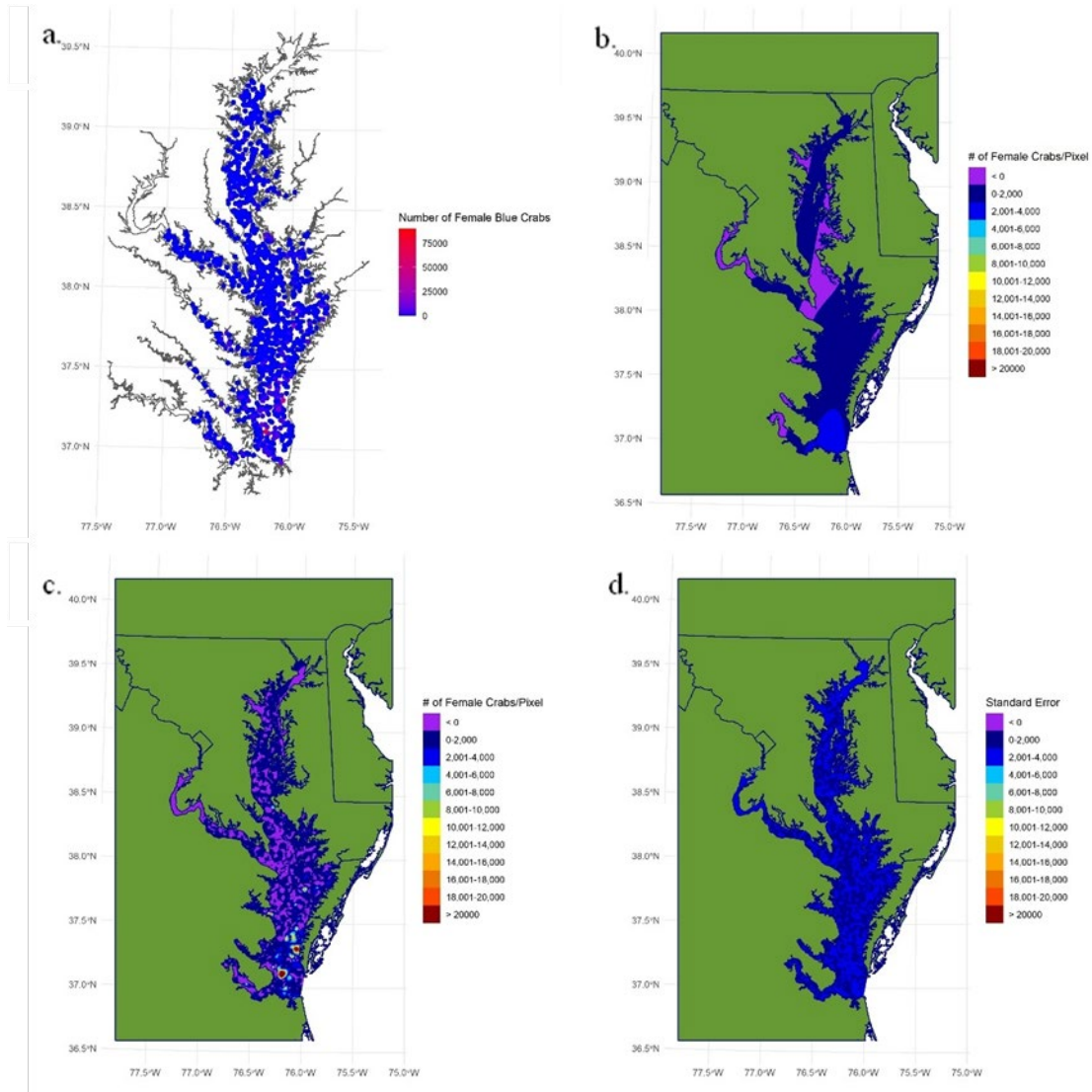


Figure 3.15. Various 2004 female age-1+ blue crab maps in the Chesapeake Bay: a) map of female age-1+ blue crab density in 2004, b) selected trend map based on the best fitting multiple linear regression model in 2004, c) map of female age-1+ blue crab abundance estimates in 2004, and d) standard error map of female age-1+ blue crab abundance estimates in 2004.

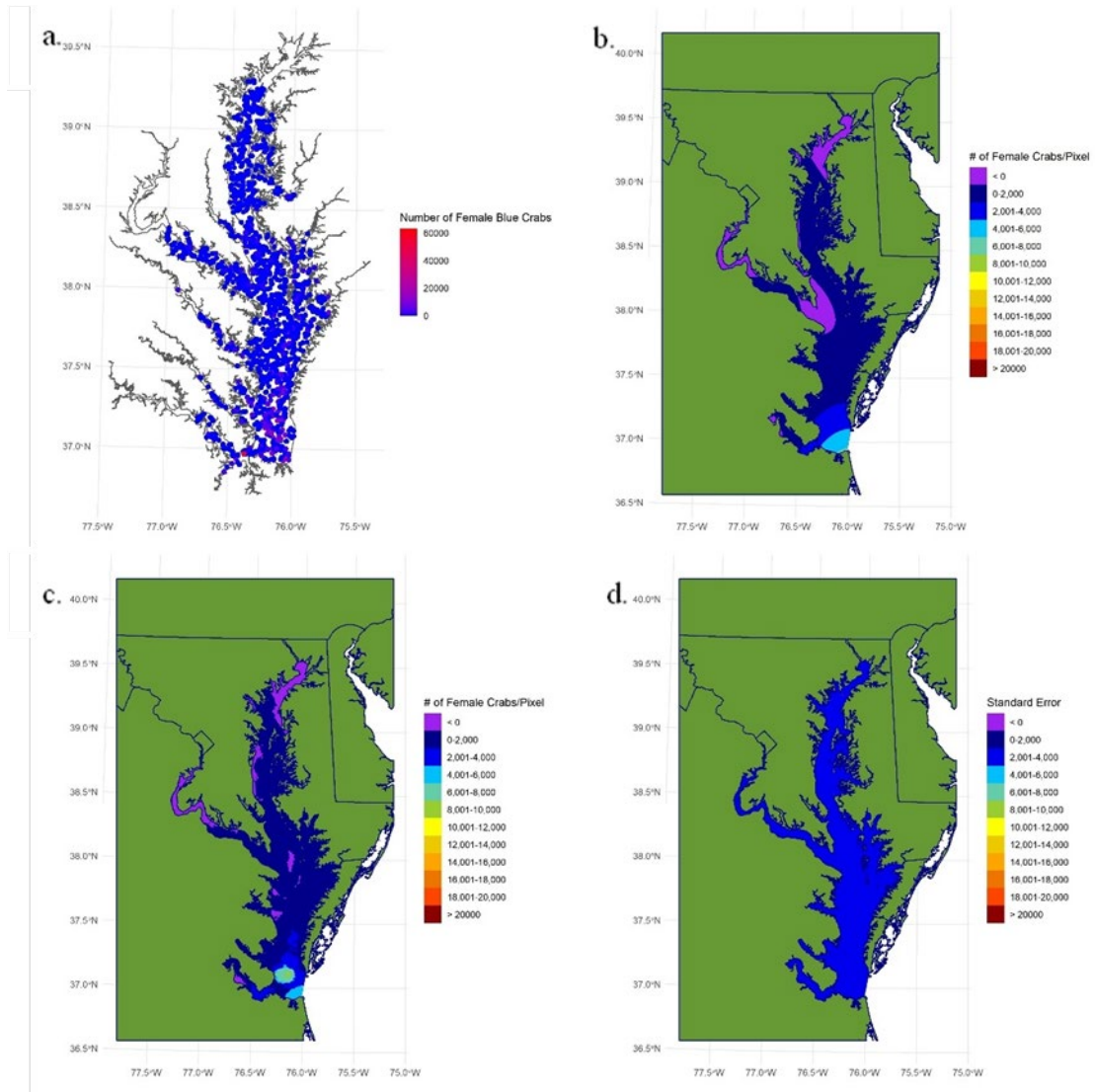


Figure 3.16. Various 2005 female age-1+ blue crab maps in the Chesapeake Bay: a) map of female age-1+ blue crab density in 2005, b) selected trend map based on the best fitting multiple linear regression model in 2005, c) map of female age-1+ blue crab abundance estimates in 2005, and d) standard error map of female age-1+ blue crab abundance estimates in 2005.

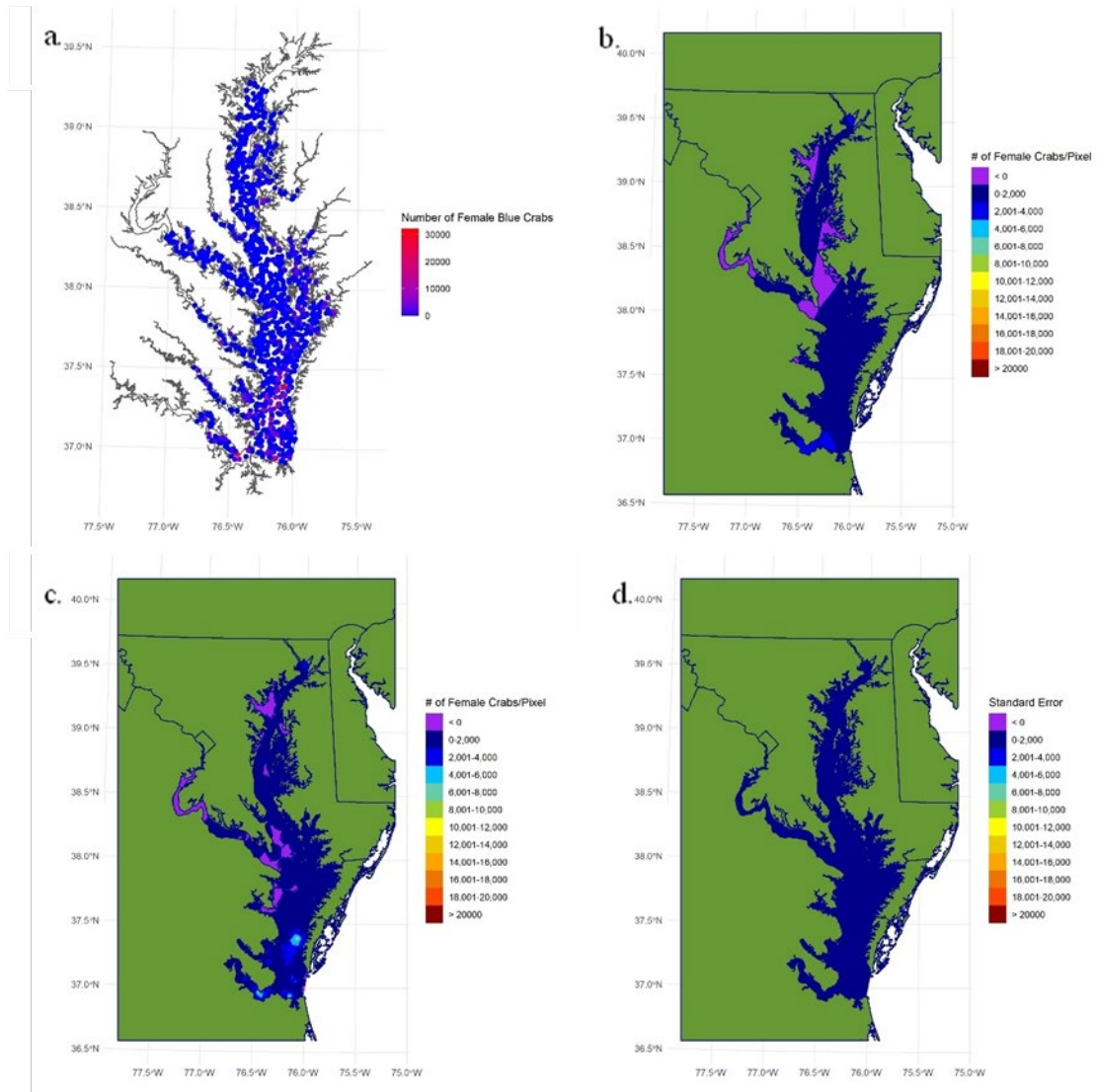


Figure 3.17. Various 2006 female age-1+ blue crab maps in the Chesapeake Bay: a) map of female age-1+ blue crab density in 2006, b) selected trend map based on the best fitting multiple linear regression model in 2006, c) map of female age-1+ blue crab abundance estimates in 2006, and d) standard error map of female age-1+ blue crab abundance estimates in 2006.

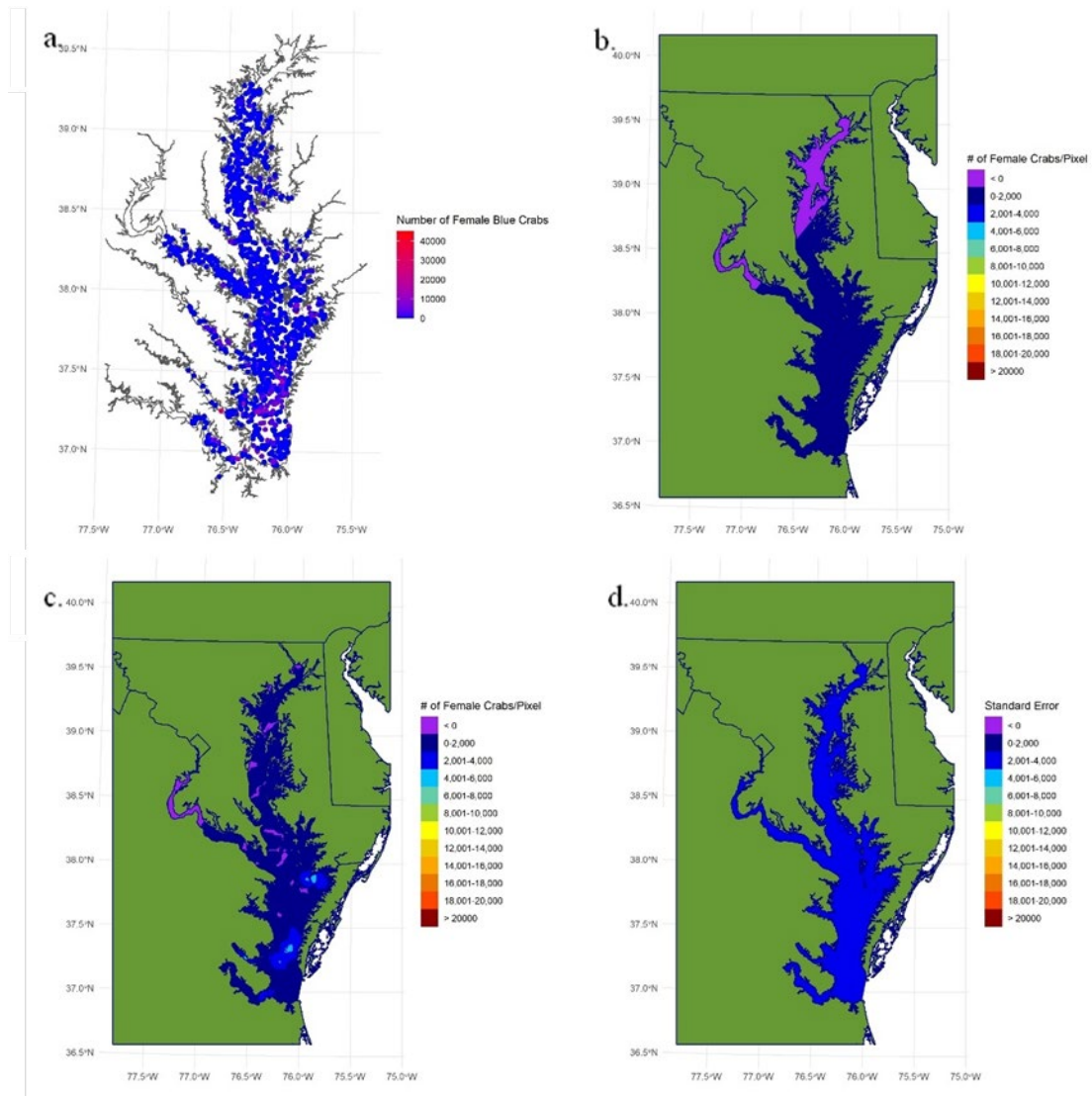


Figure 3.18. Various 2007 female age-1+ blue crab maps in the Chesapeake Bay: a) map of female age-1+ blue crab density in 2007, b) selected trend map based on the best fitting multiple linear regression model in 2007, c) map of female age-1+ blue crab abundance estimates in 2007, and d) standard error map of female age-1+ blue crab abundance estimates in 2007.

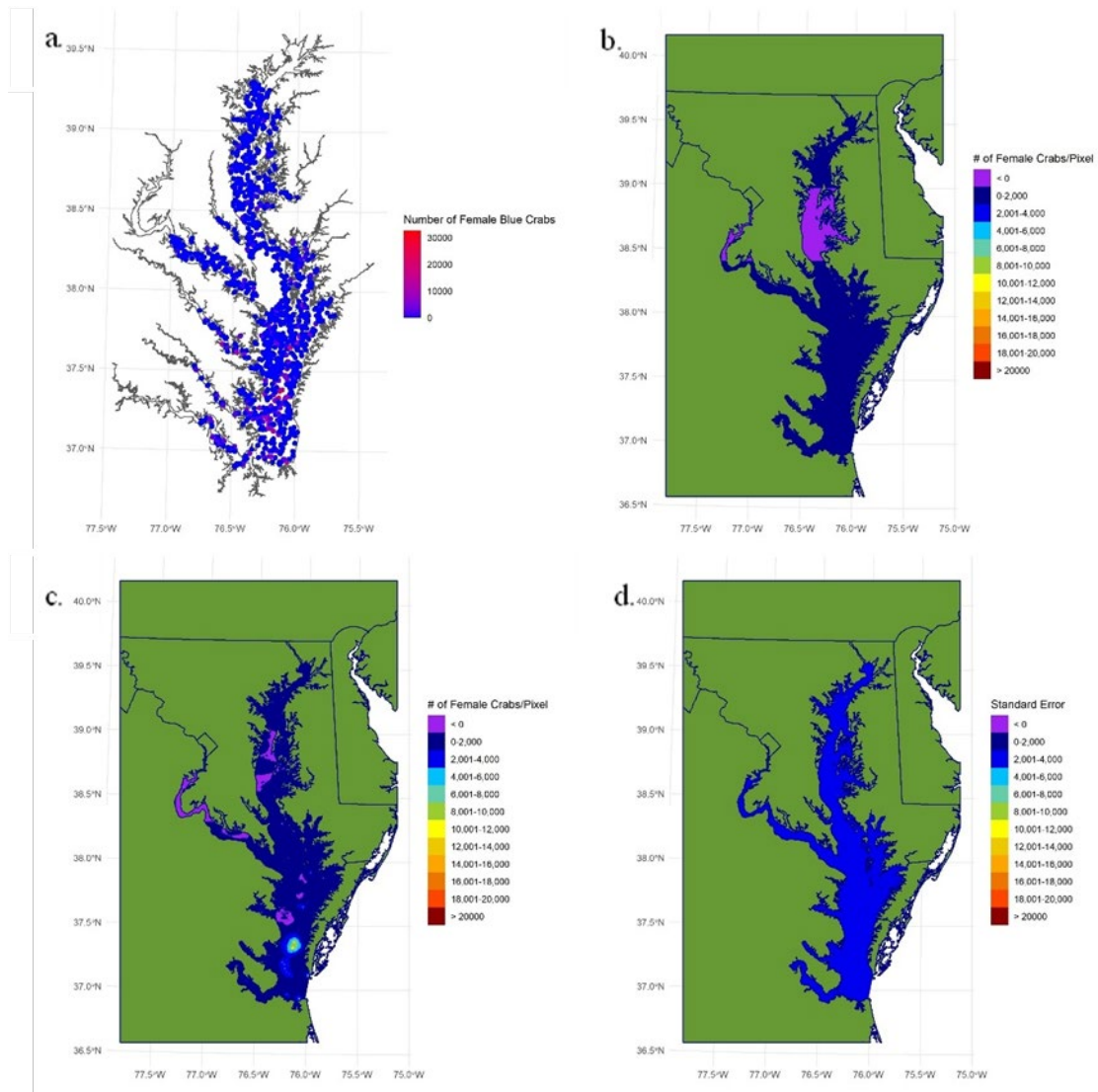


Figure 3.19. Various 2008 female age-1+ blue crab maps in the Chesapeake Bay: a) map of female age-1+ blue crab density in 2008, b) selected trend map based on the best fitting multiple linear regression model in 2008, c) map of female age-1+ blue crab abundance estimates in 2008, and d) standard error map of female age-1+ blue crab abundance estimates in 2008.

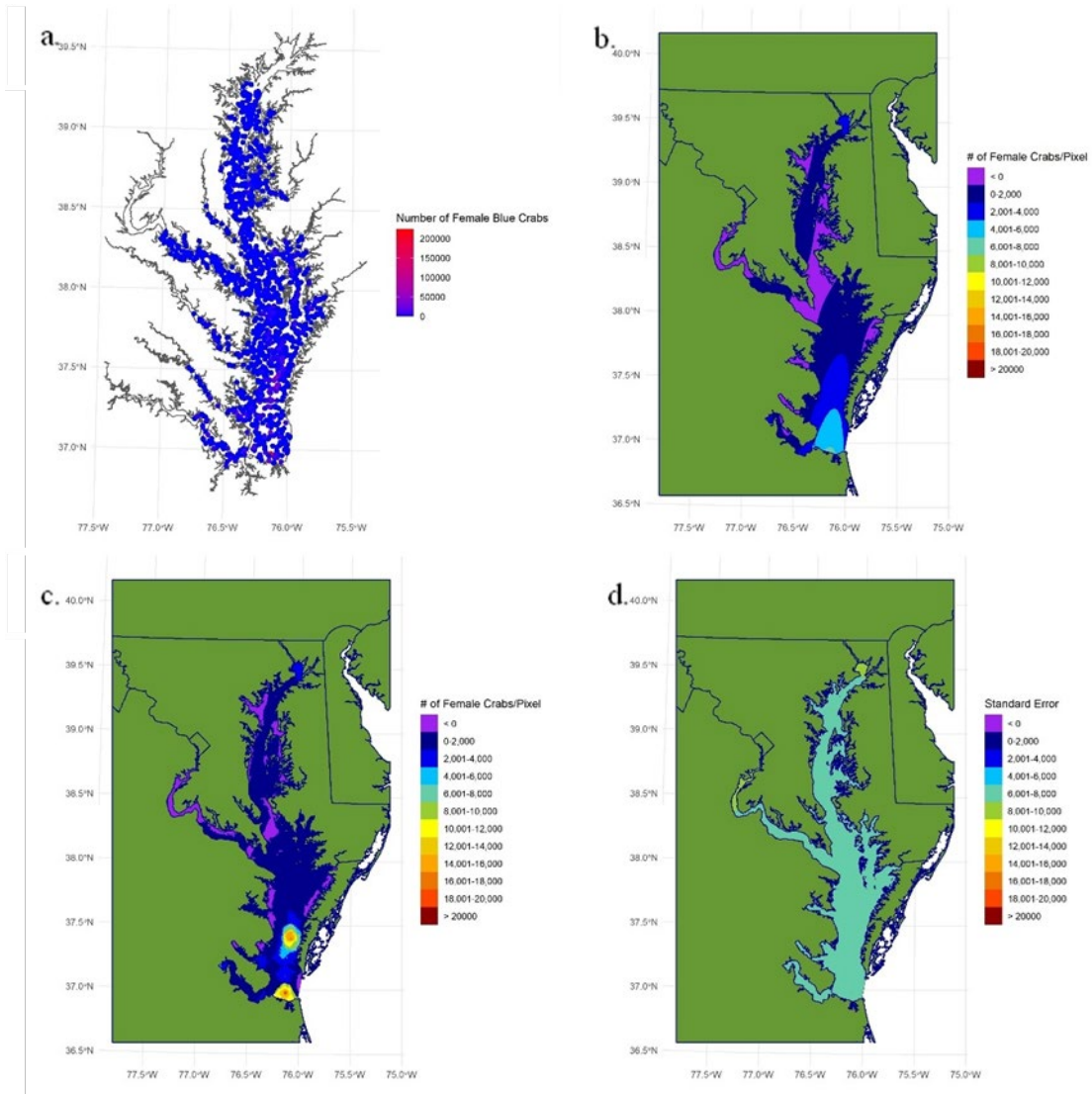


Figure 3.20. Various 2009 female age-1+ blue crab maps in the Chesapeake Bay: a) map of female age-1+ blue crab density in 2009, b) selected trend map based on the best fitting multiple linear regression model in 2009, c) map of female age-1+ blue crab abundance estimates in 2009, and d) standard error map of female age-1+ blue crab abundance estimates in 2009.

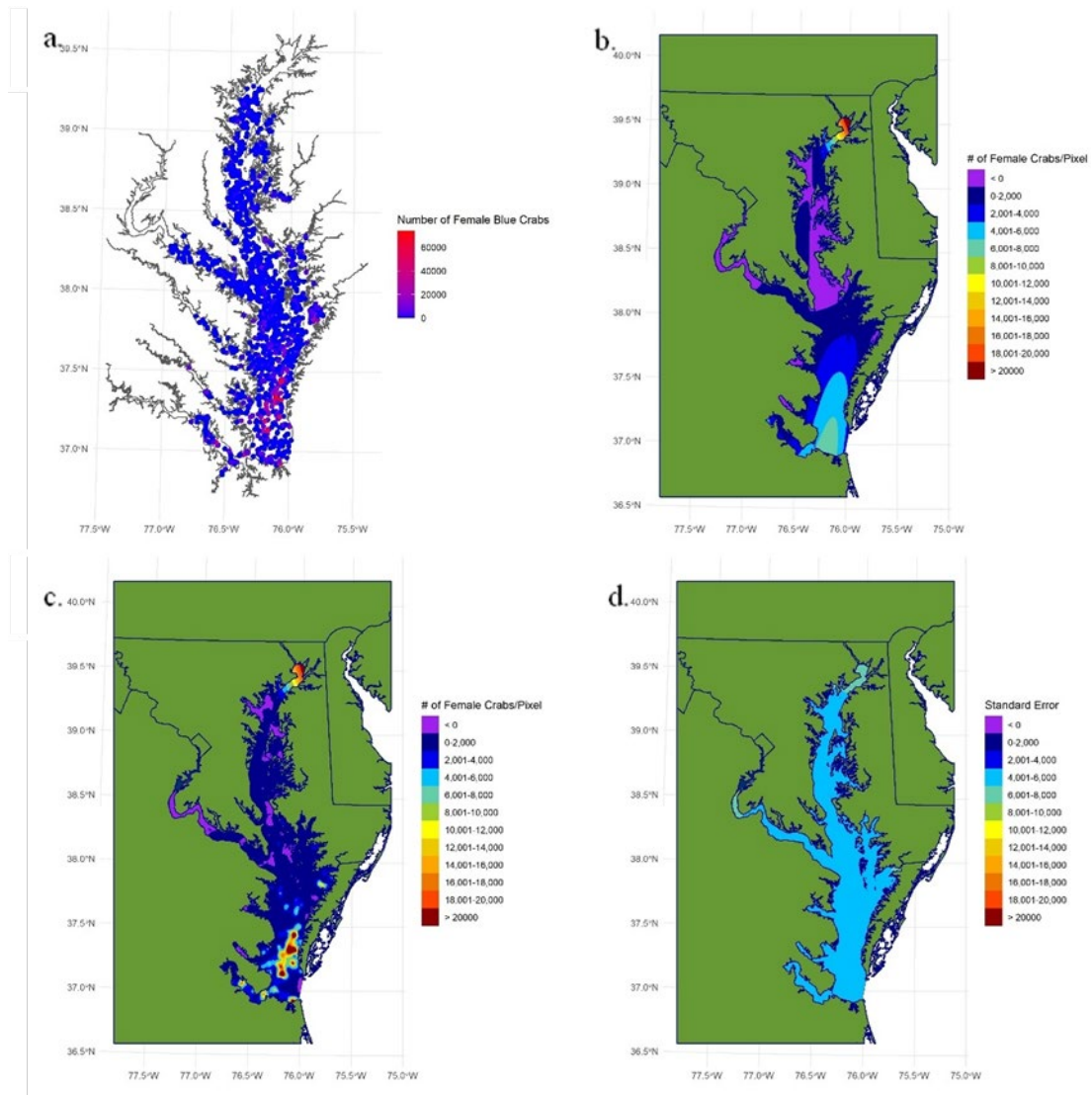


Figure 3.21. Various 2010 female age-1+ blue crab maps in the Chesapeake Bay: a) map of female age-1+ blue crab density in 2010, b) selected trend map based on the best fitting multiple linear regression model in 2010, c) map of female age-1+ blue crab abundance estimates in 2010, and d) standard error map of female age-1+ blue crab abundance estimates in 2010.

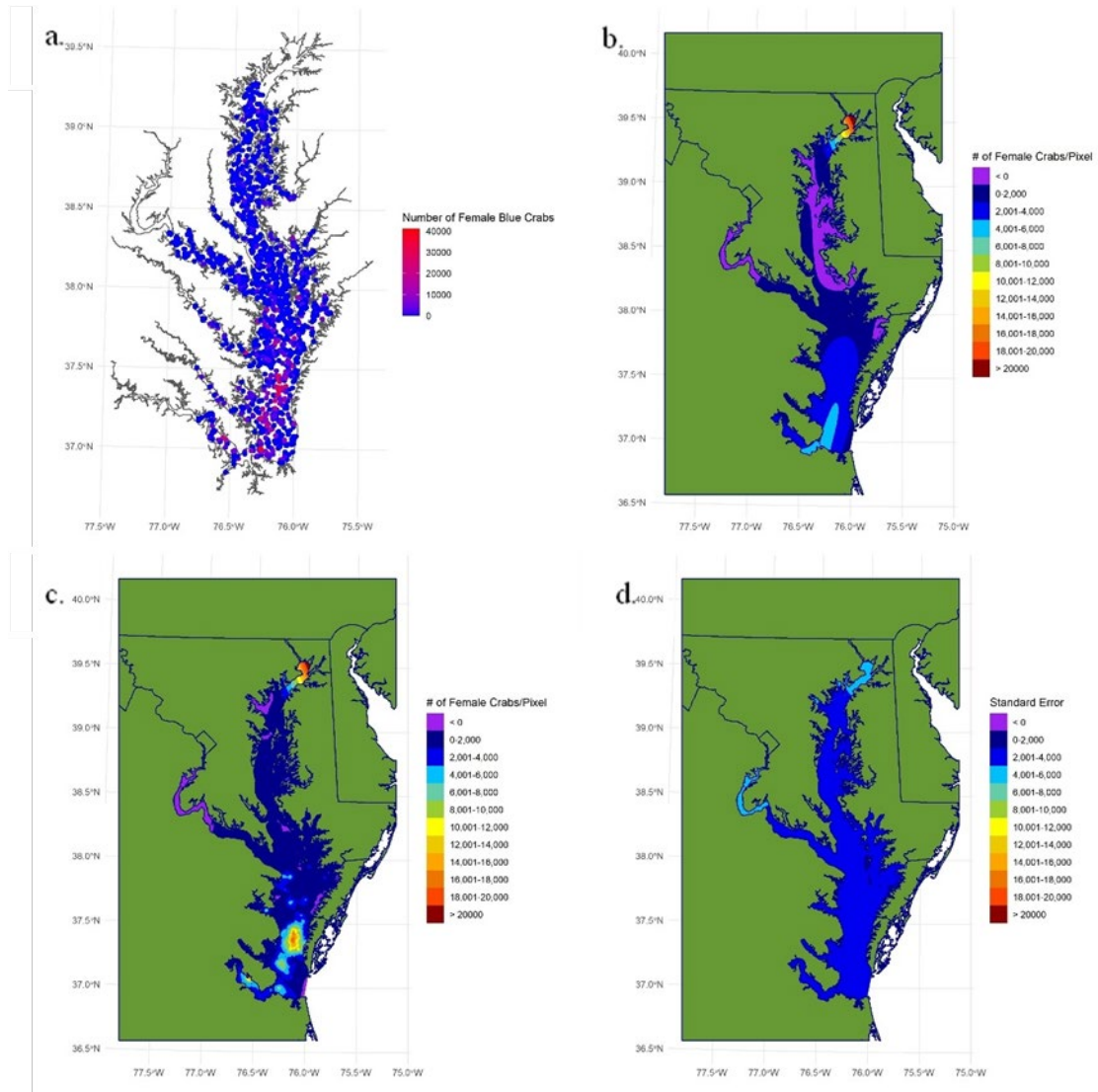


Figure 3.22. Various 2011 female age-1+ blue crab maps in the Chesapeake Bay: a) map of female age-1+ blue crab density in 2011, b) selected trend map based on the best fitting multiple linear regression model in 2011, c) map of female age-1+ blue crab abundance estimates in 2011, and d) standard error map of female age-1+ blue crab abundance estimates in 2011.

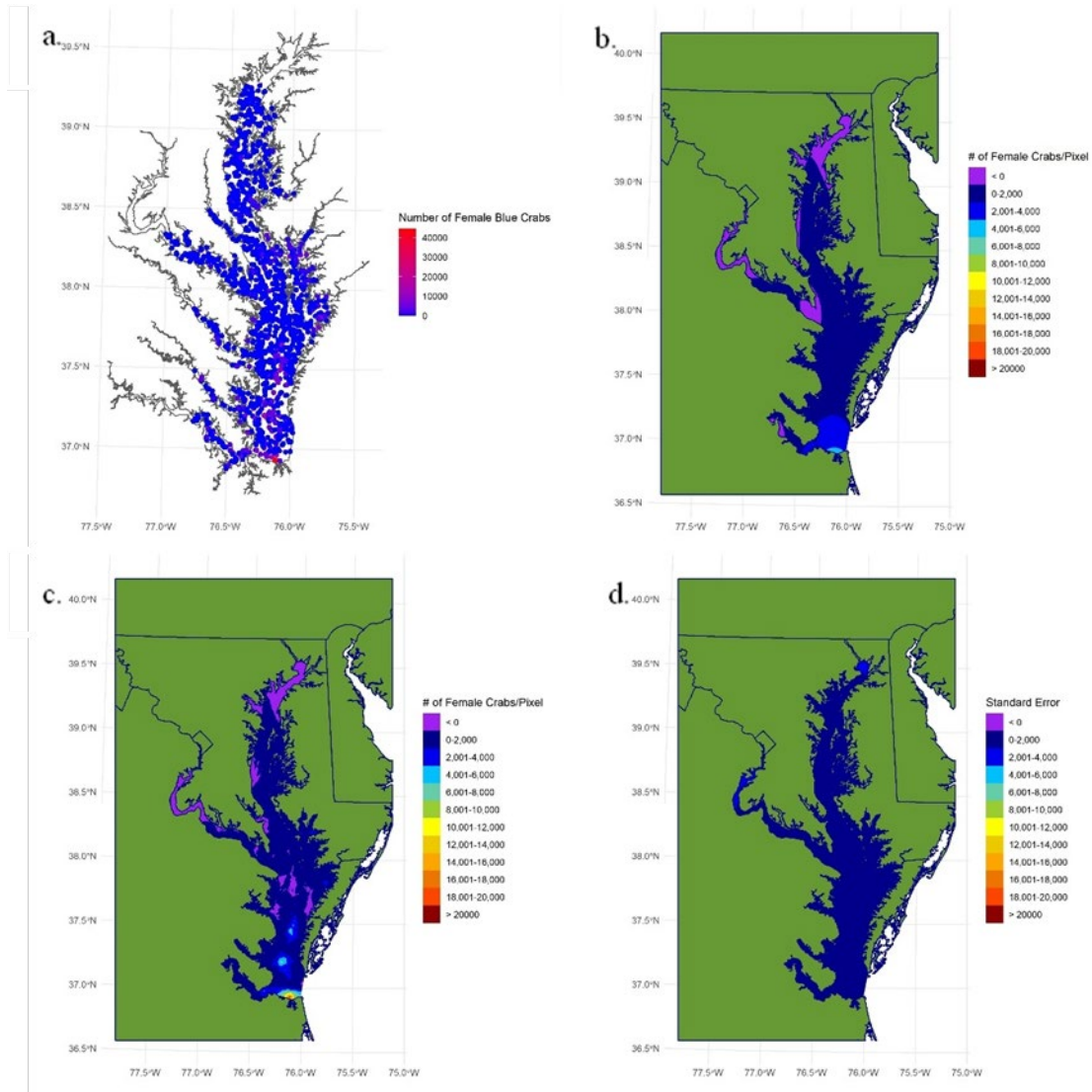


Figure 3.23. Various 2012 female age-1+ blue crab maps in the Chesapeake Bay: a) map of female age-1+ blue crab density in 2012, b) selected trend map based on the best fitting multiple linear regression model in 2012, c) map of female age-1+ blue crab abundance estimates in 2012, and d) standard error map of female age-1+ blue crab abundance estimates in 2012.

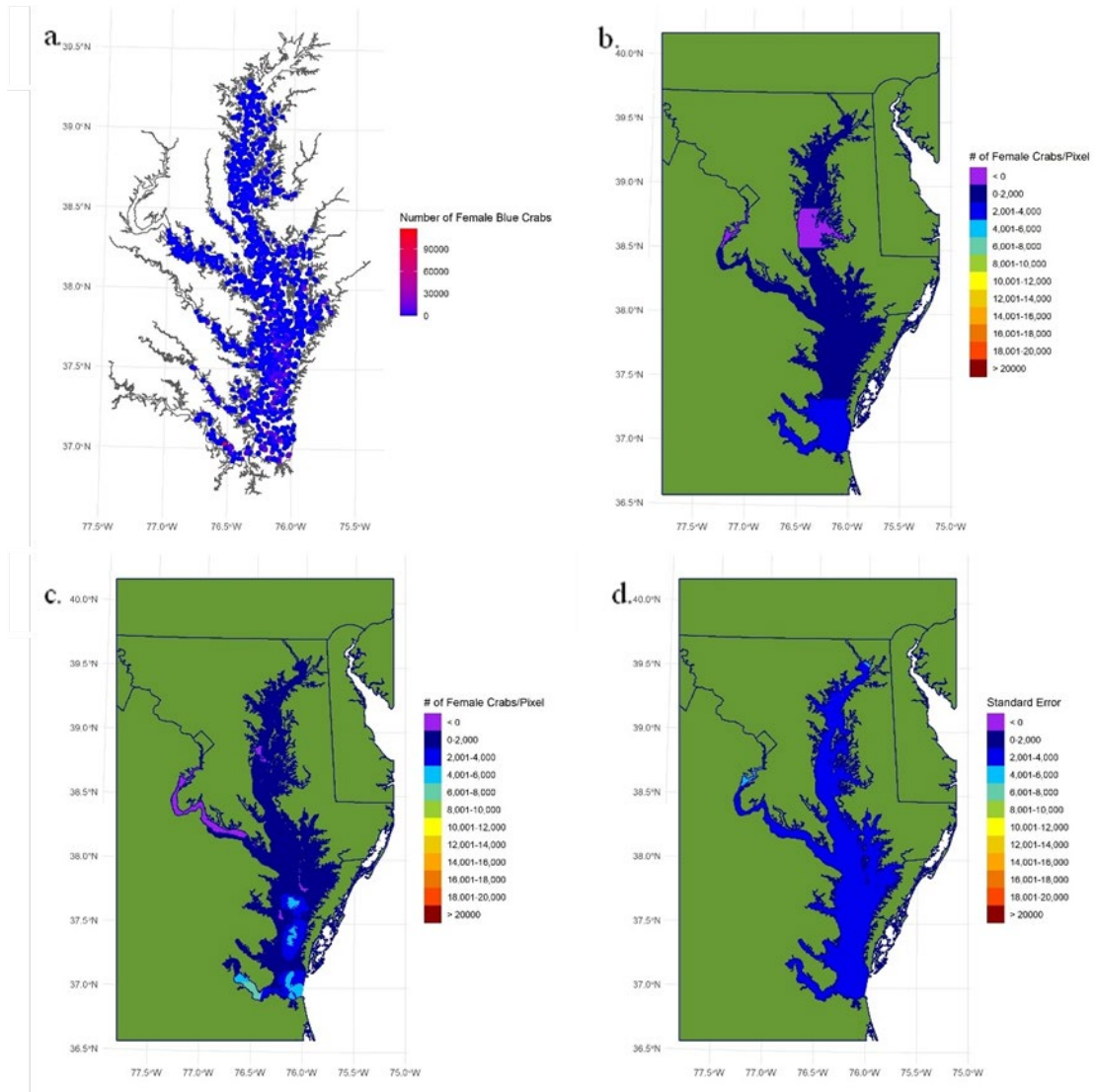


Figure 3.24. Various 2013 female age-1+ blue crab maps in the Chesapeake Bay: a) map of female age-1+ blue crab density in 2013, b) selected trend map based on the best fitting multiple linear regression model in 2013, c) map of female age-1+ blue crab abundance estimates in 2013, and d) standard error map of female age-1+ blue crab abundance estimates in 2013.

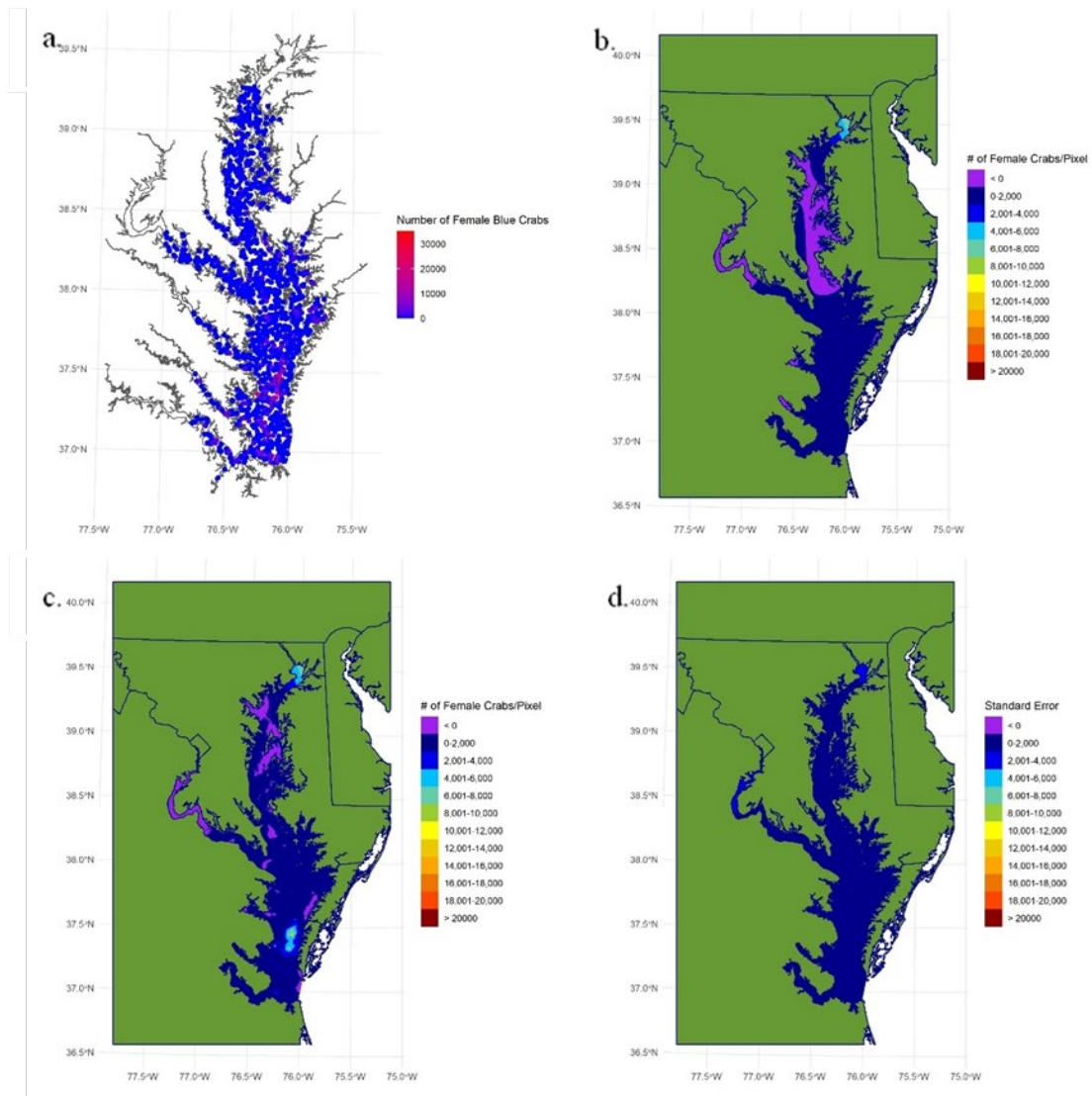


Figure 3.25. Various 2014 female age-1+ blue crab maps in the Chesapeake Bay: a) map of female age-1+ blue crab density in 2014, b) selected trend map based on the best fitting multiple linear regression model in 2014, c) map of female age-1+ blue crab abundance estimates in 2014, and d) standard error map of female age-1+ blue crab abundance estimates in 2014.

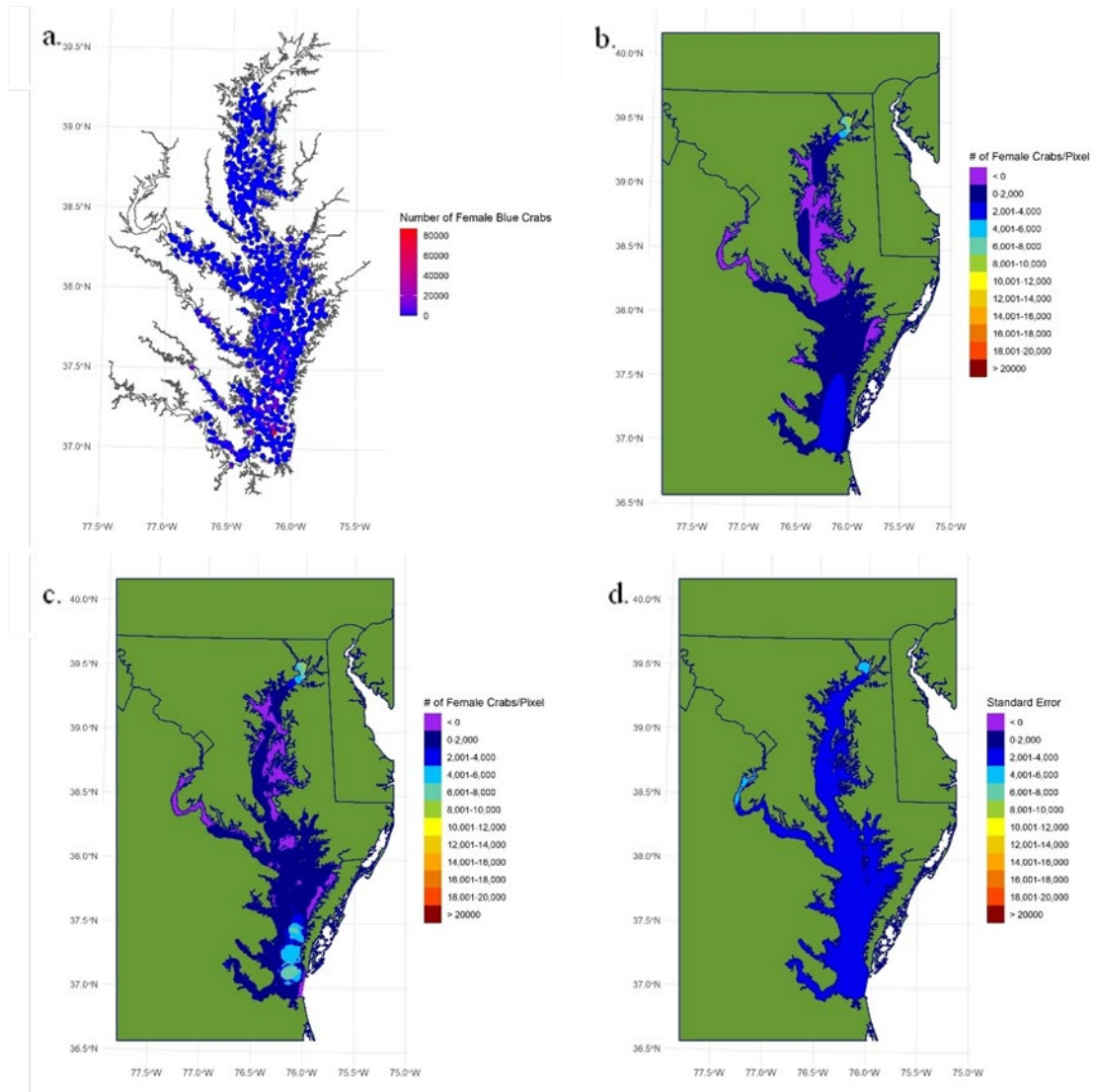


Figure 3.26. Various 2015 female age-1+ blue crab maps in the Chesapeake Bay: a) map of female age-1+ blue crab density in 2015, b) selected trend map based on the best fitting multiple linear regression model in 2015, c) map of female age-1+ blue crab abundance estimates in 2015, and d) standard error map of female age-1+ blue crab abundance estimates in 2015.

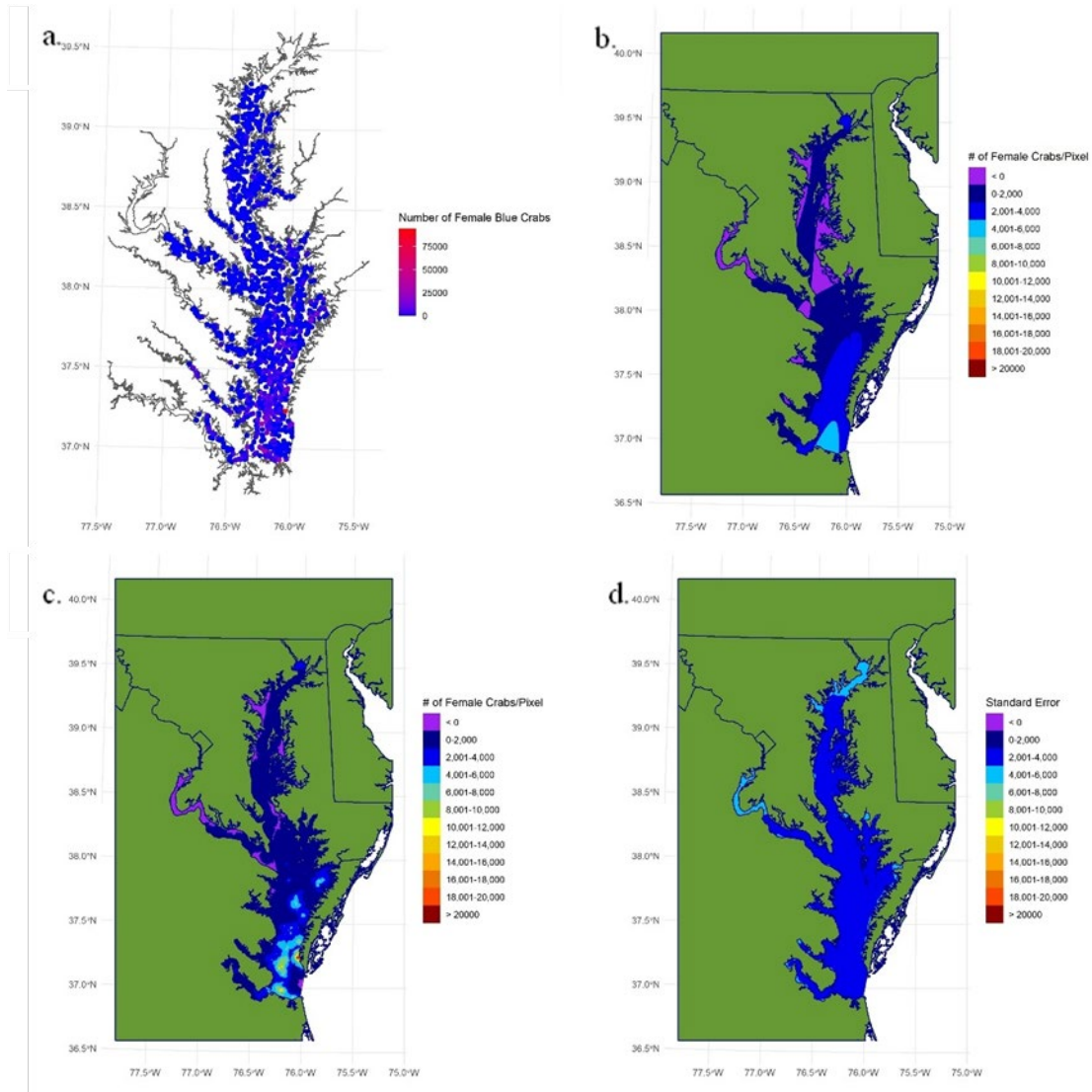


Figure 3.27. Various 2016 female age-1+ blue crab maps in the Chesapeake Bay: a) map of female age-1+ blue crab density in 2016, b) selected trend map based on the best fitting multiple linear regression model in 2016, c) map of female age-1+ blue crab abundance estimates in 2016, and d) standard error map of female age-1+ blue crab abundance estimates in 2016.

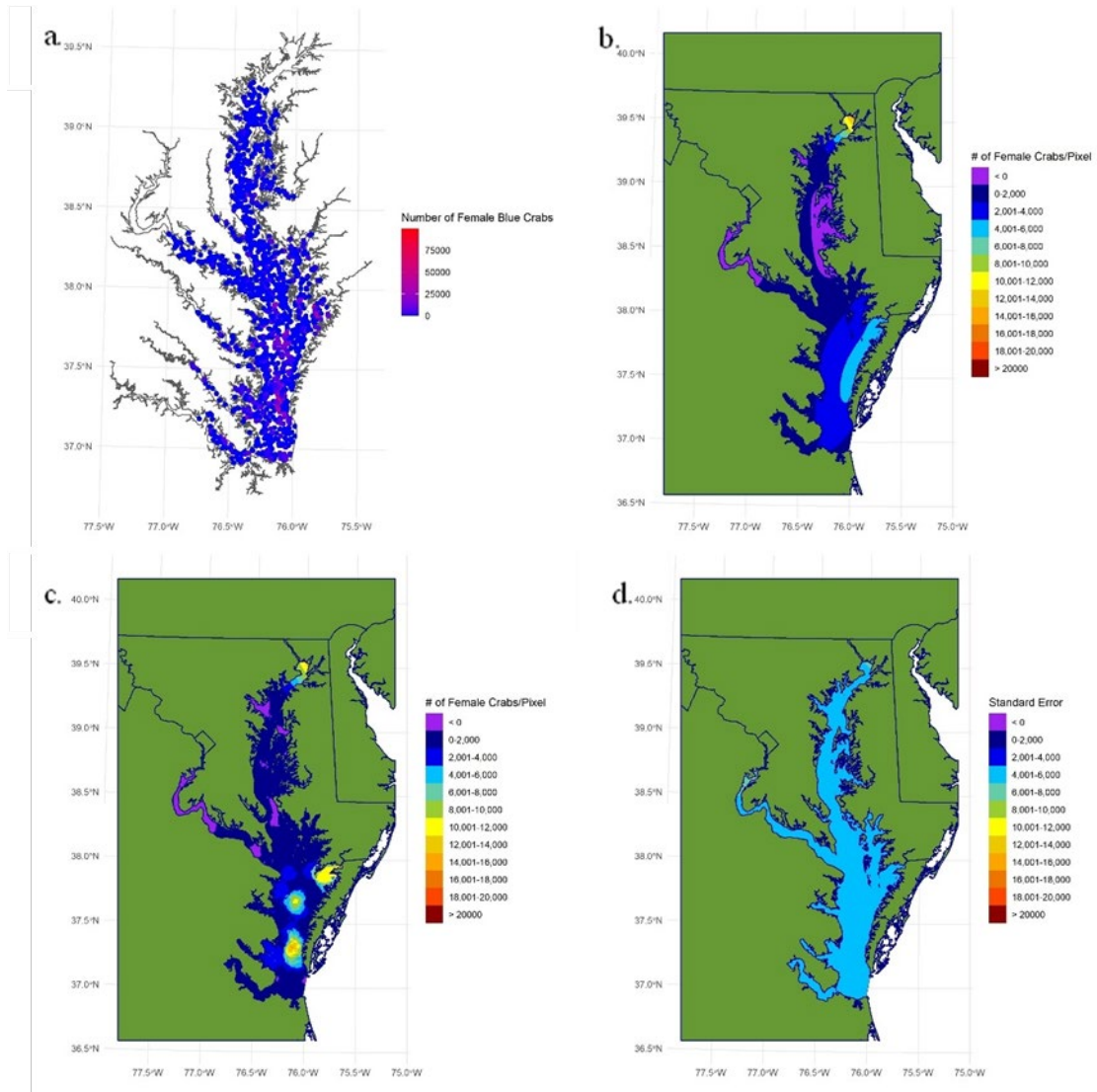


Figure 3.28. Various 2017 female age-1+ blue crab maps in the Chesapeake Bay: a) map of female age-1+ blue crab density in 2017, b) selected trend map based on the best fitting multiple linear regression model in 2017, c) map of female age-1+ blue crab abundance estimates in 2017, and d) standard error map of female age-1+ blue crab abundance estimates in 2017.

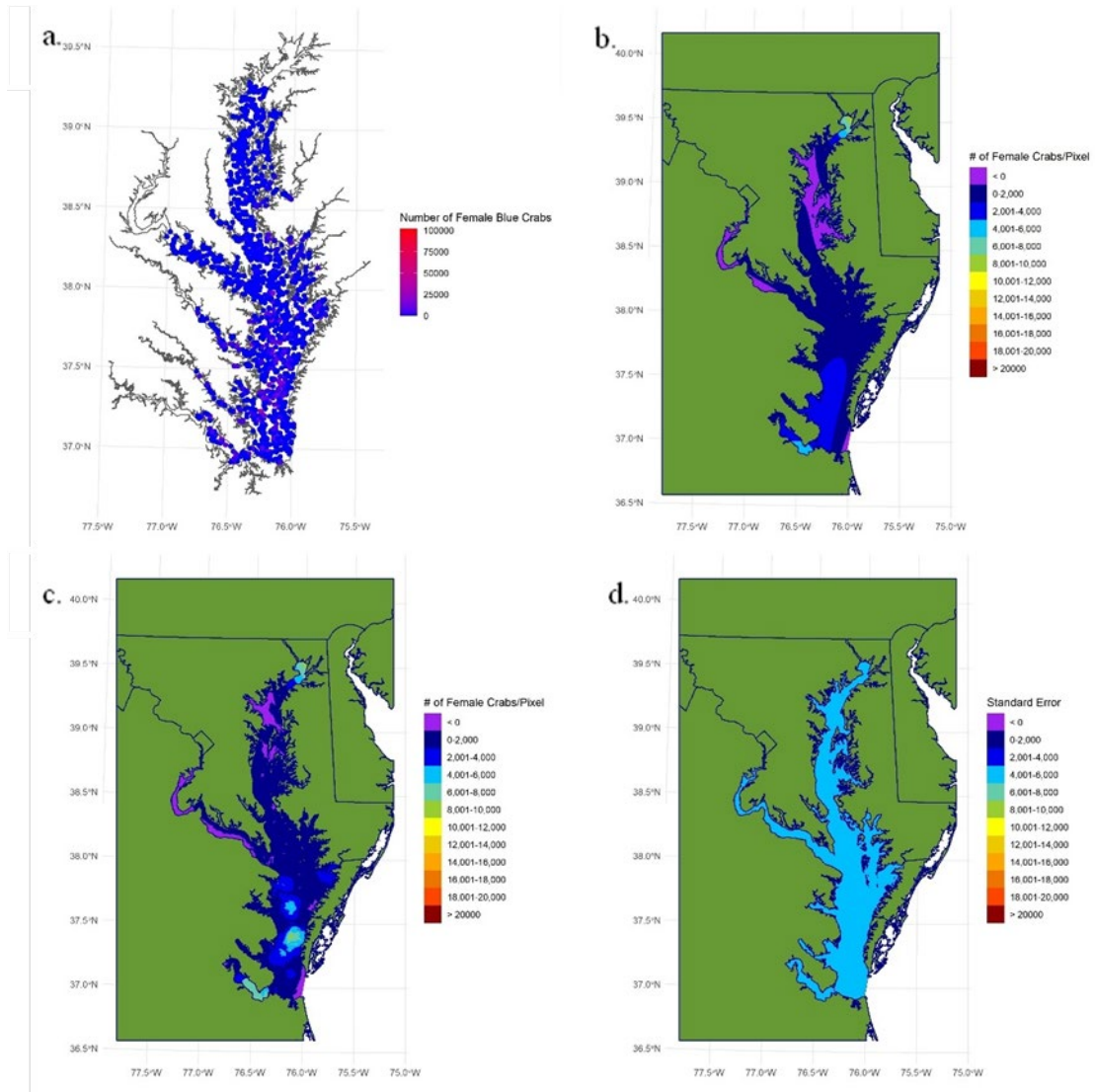


Figure 3.29. Various 2018 female age-1+ blue crab maps in the Chesapeake Bay: a) map of female age-1+ blue crab density in 2018, b) selected trend map based on the best fitting multiple linear regression model in 2018, c) map of female age-1+ blue crab abundance estimates in 2018, and d) standard error map of female age-1+ blue crab abundance estimates in 2018.

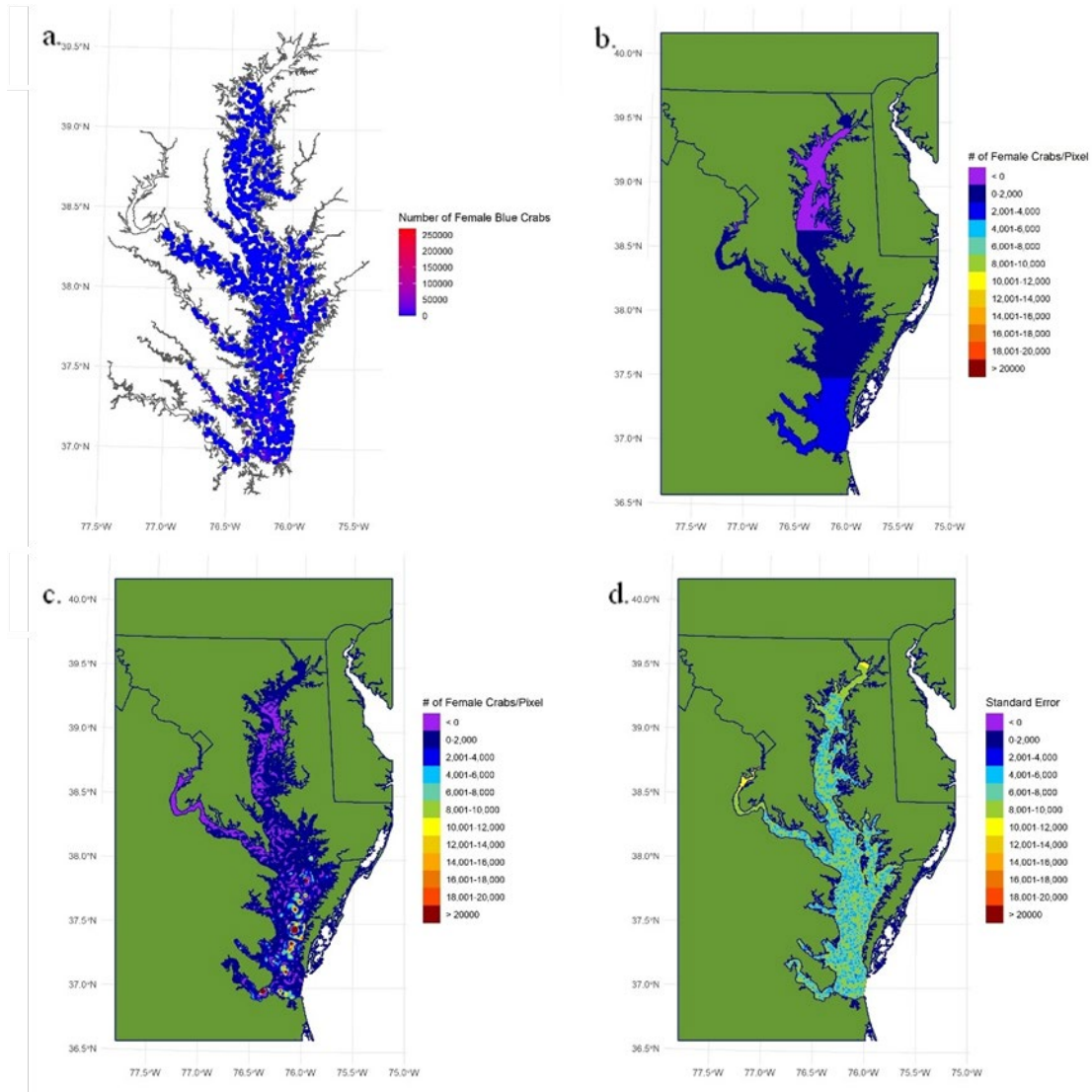


Figure 3.30. Various 2019 female age-1+ blue crab maps in the Chesapeake Bay: a) map of female age-1+ blue crab density in 2019, b) selected trend map based on the best fitting multiple linear regression model in 2019, c) map of female age-1+ blue crab abundance estimates in 2019, and d) standard error map of female age-1+ blue crab abundance estimates in 2019.

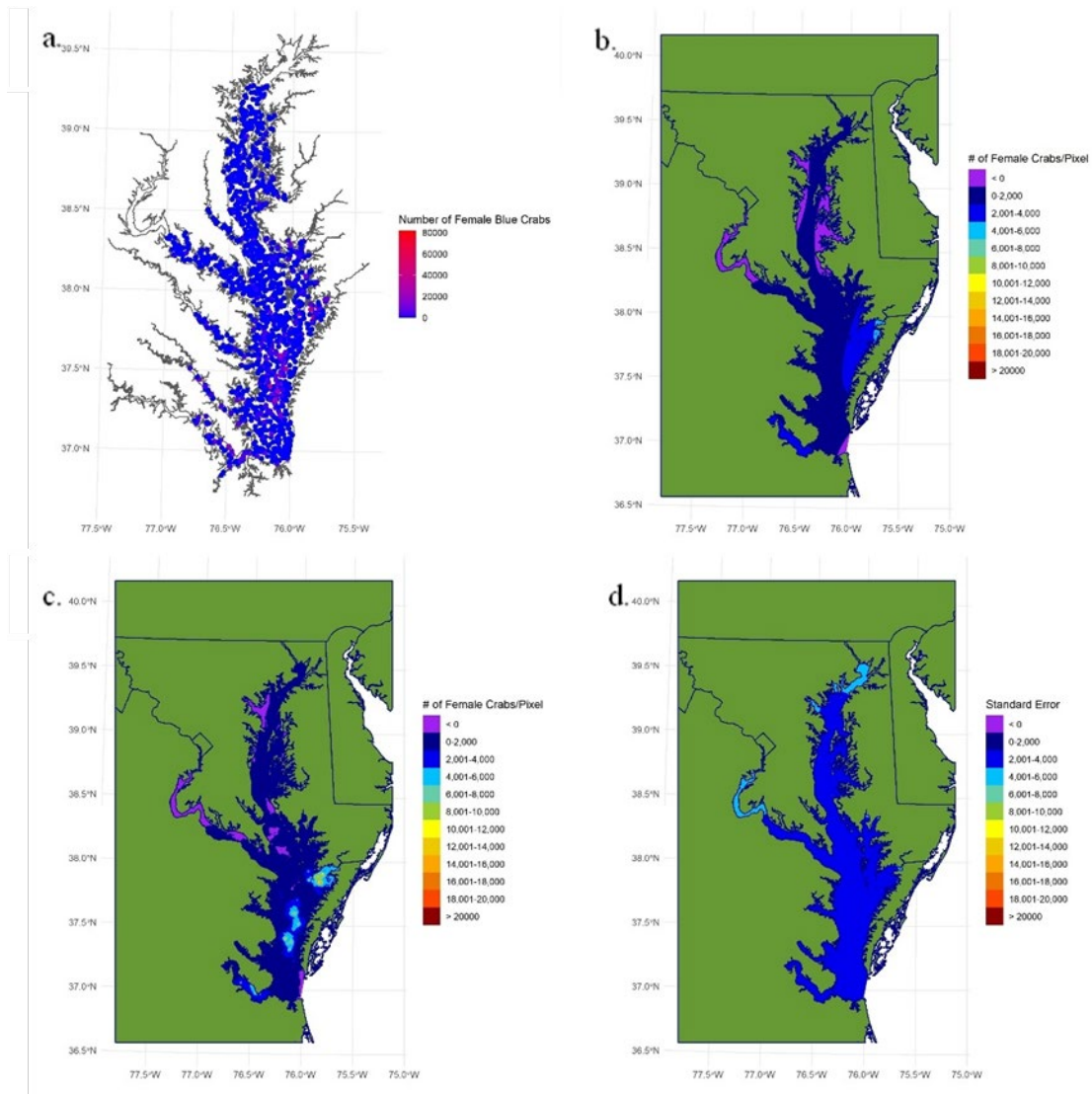


Figure 3.31. Various 2020 female age-1+ blue crab maps in the Chesapeake Bay: a) map of female age-1+ blue crab density in 2020, b) selected trend map based on the best fitting multiple linear regression model in 2020, c) map of female age-1+ blue crab abundance estimates in 2020, and d) standard error map of female age-1+ blue crab abundance estimates in 2020.

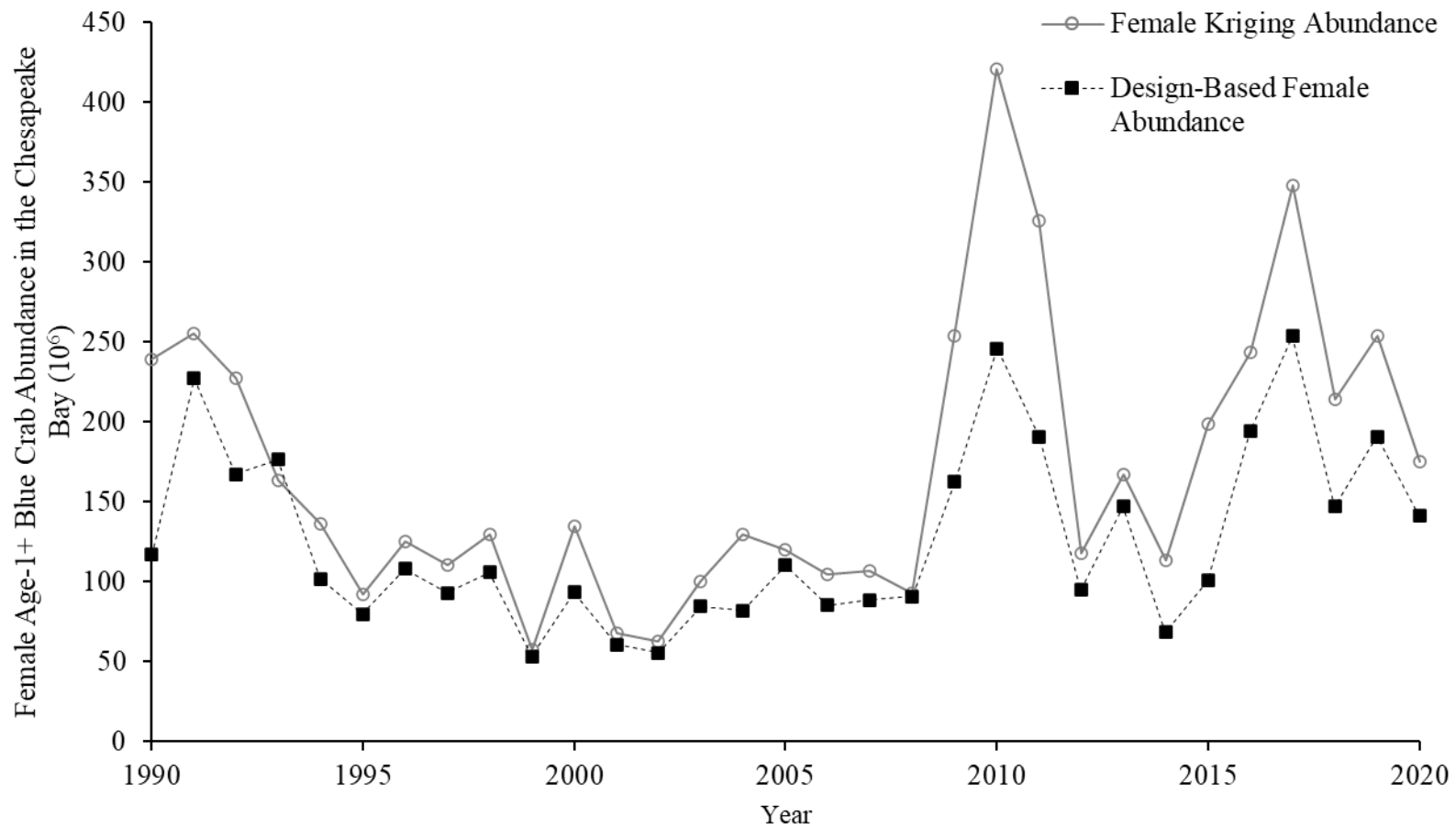


Figure 3.32. Estimates of female age-1+ blue crab abundance (millions) in Chesapeake Bay. Shown are female age-1+ kriged abundance estimates (open circles; solid, grey line) and design-based female age-1+ abundance estimates (solid squares; dashed, black line) for 1990–2020.

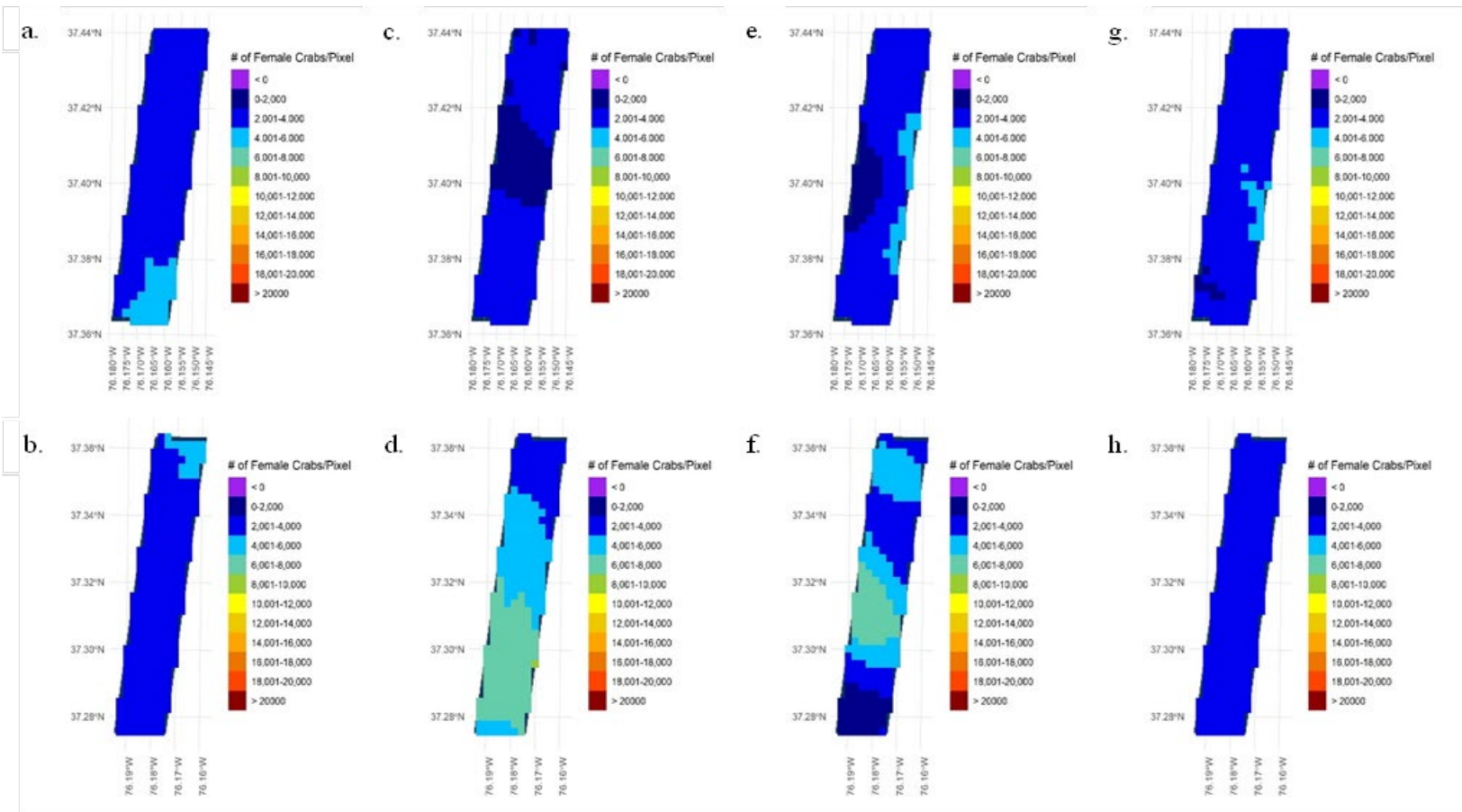


Figure 3.33. Female age 1+ blue crab abundance maps in WTAPSNE (top) and WTAPS (bottom) derived from kriging in the Chesapeake Bay for 1990–1993: a) WTAPSNE female age-1+ abundance in 1990, b) WTAPS female age-1+ abundance in 1990, c) WTAPSNE female age-1+ abundance in 1991, d) WTAPS female age-1+ abundance in 1991, e) WTAPSNE female age-1+ abundance in 1992, f) WTAPS female age-1+ abundance in 1992, g) WTAPSNE female age-1+ abundance in 1993, and h) WTAPS age-1+ abundance in 1993.

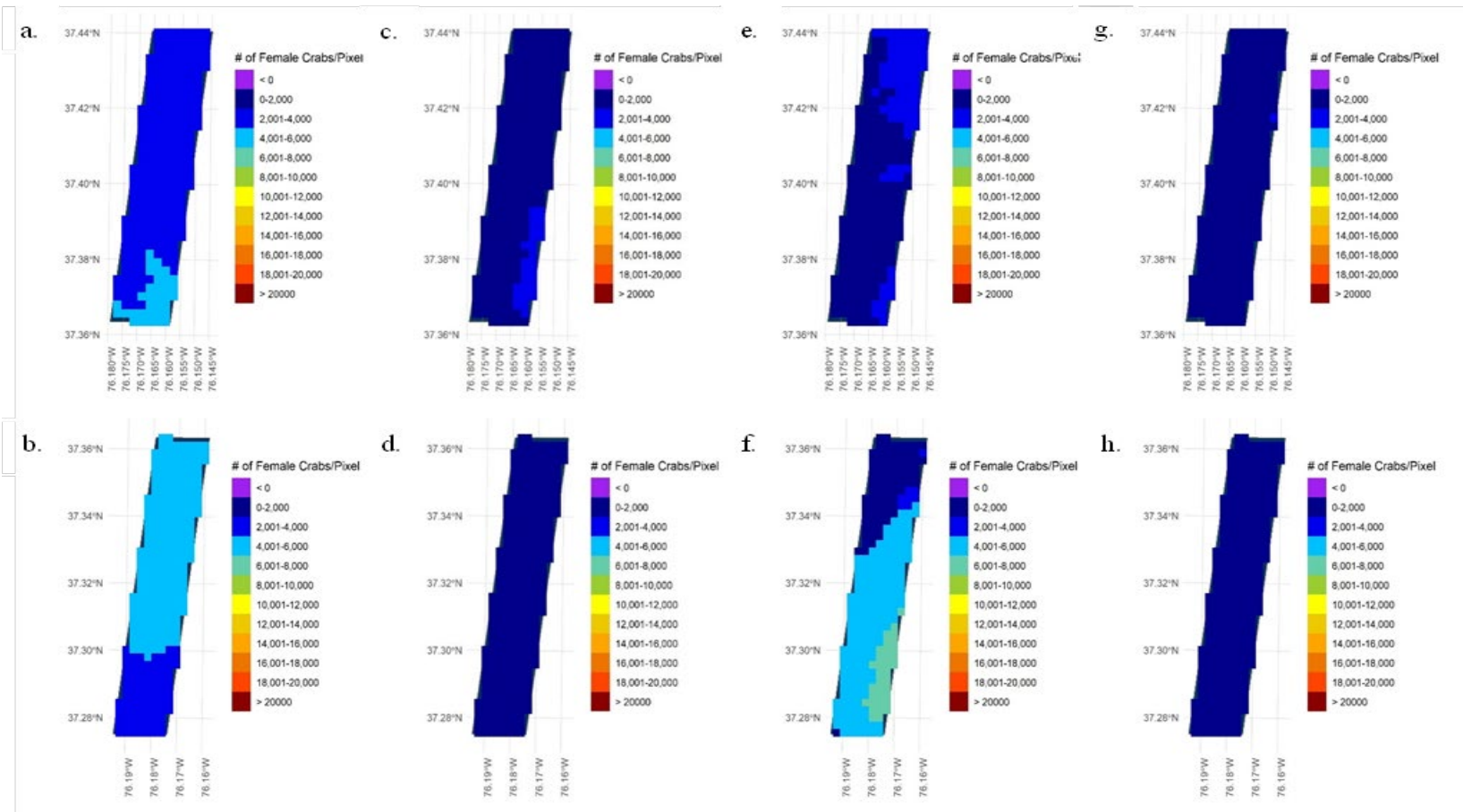


Figure 3.34. Female age 1+ blue crab abundance maps in WTAPSNE (top) and WTAPS (bottom) derived from kriging in the Chesapeake Bay for 1994–1997: a) WTAPSNE female age-1+ abundance in 1994, b) WTAPS female age-1+ abundance in 1994, c) WTAPSNE female age-1+ abundance in 1995, d) WTAPS female age-1+ abundance in 1995, e) WTAPSNE female age-1+ abundance in 1996, f) WTAPS female age-1+ abundance in 1996, g) WTAPSNE female age-1+ abundance in 1997, and h) WTAPS age-1+ abundance in 1997.

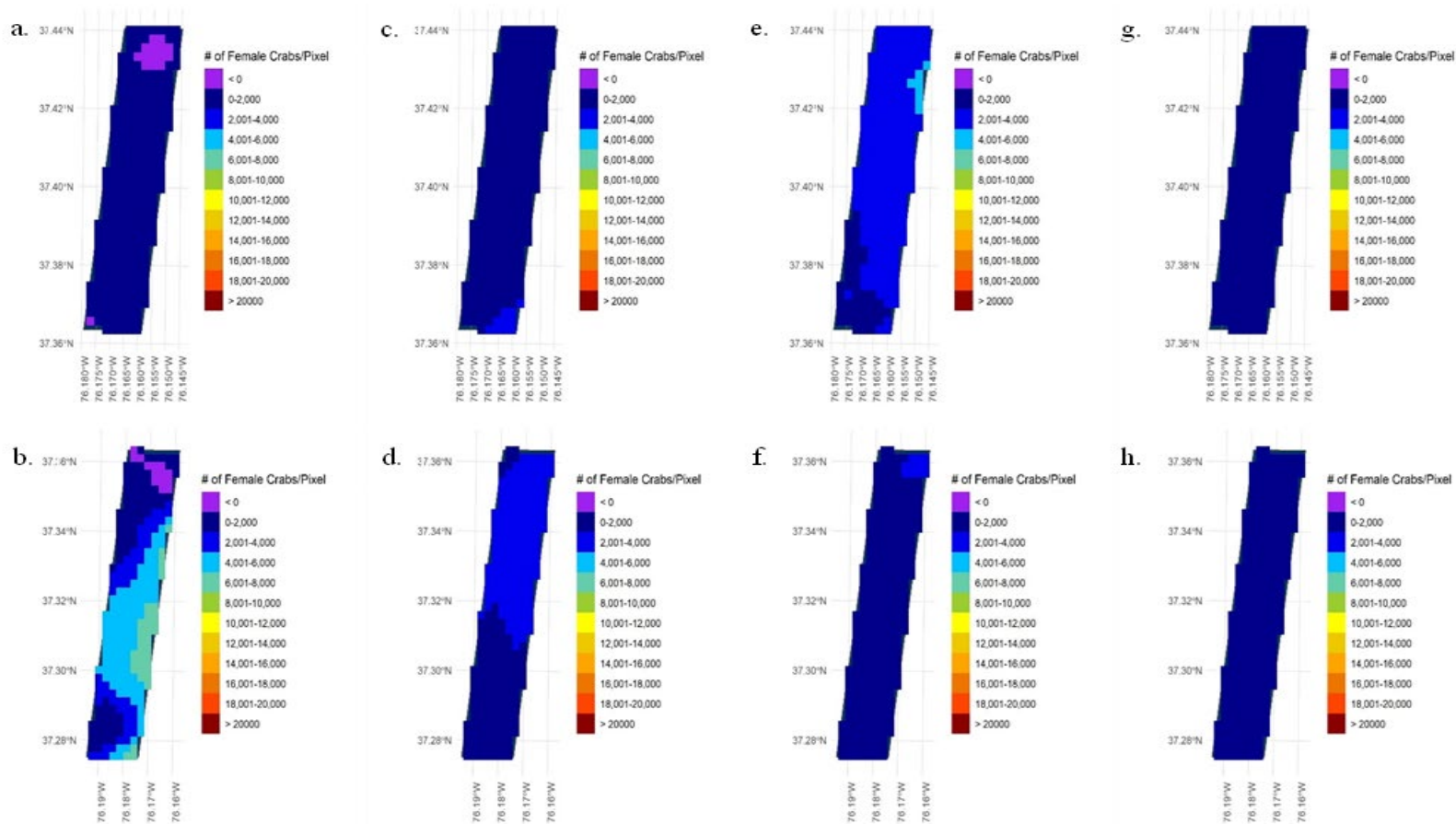


Figure 3.35. Female age 1+ blue crab abundance maps in WTAPSNE (top) and WTAPS (bottom) derived from kriging in the Chesapeake Bay for 1998–2001: a) WTAPSNE female age-1+ abundance in 1998, b) WTAPS female age-1+ abundance in 1998, c) WTAPSNE female age-1+ abundance in 1999, d) WTAPS female age-1+ abundance in 1999, e) WTAPSNE female age-1+ abundance in 2000, f) WTAPS female age-1+ abundance in 2000, g) WTAPSNE female age-1+ abundance in 2001, and h) WTAPS female age-1+ abundance in 2001.

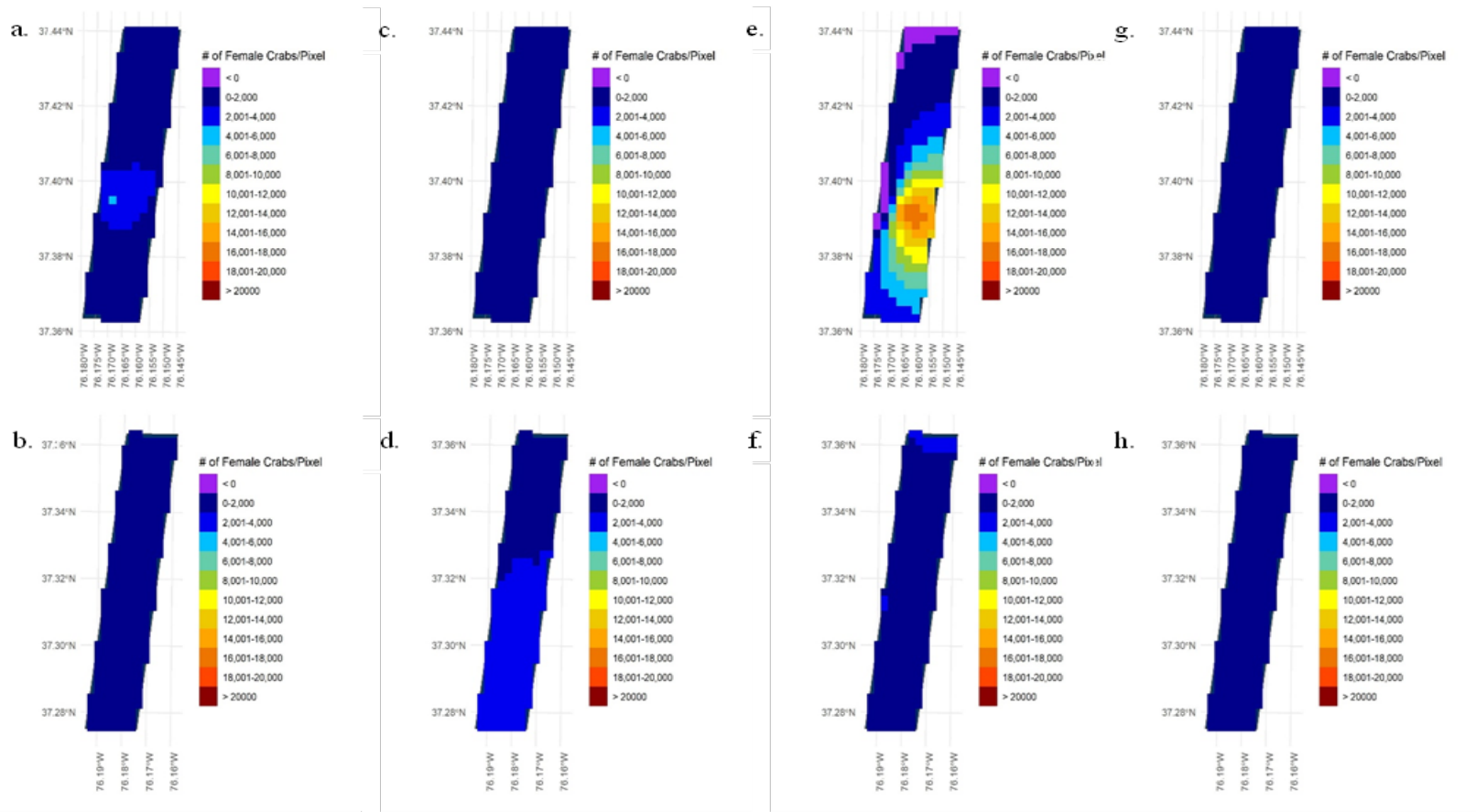


Figure 3.36. Female age 1+ blue crab abundance maps in WTAPSNE (top) and WTAPS (bottom) derived from kriging in the Chesapeake Bay for 2002–2005: a) WTAPSNE female age-1+ abundance in 2002, b) WTAPS female age-1+ abundance in 2002, c) WTAPSNE female age-1+ abundance in 2003, d) WTAPS female age-1+ abundance in 2003, e) WTAPSNE female age-1+ abundance in 2004, f) WTAPS female age-1+ abundance in 2004, g) WTAPSNE female age-1+abundance in 2005, and h) WTAPS age-1+ abundance in 2005.

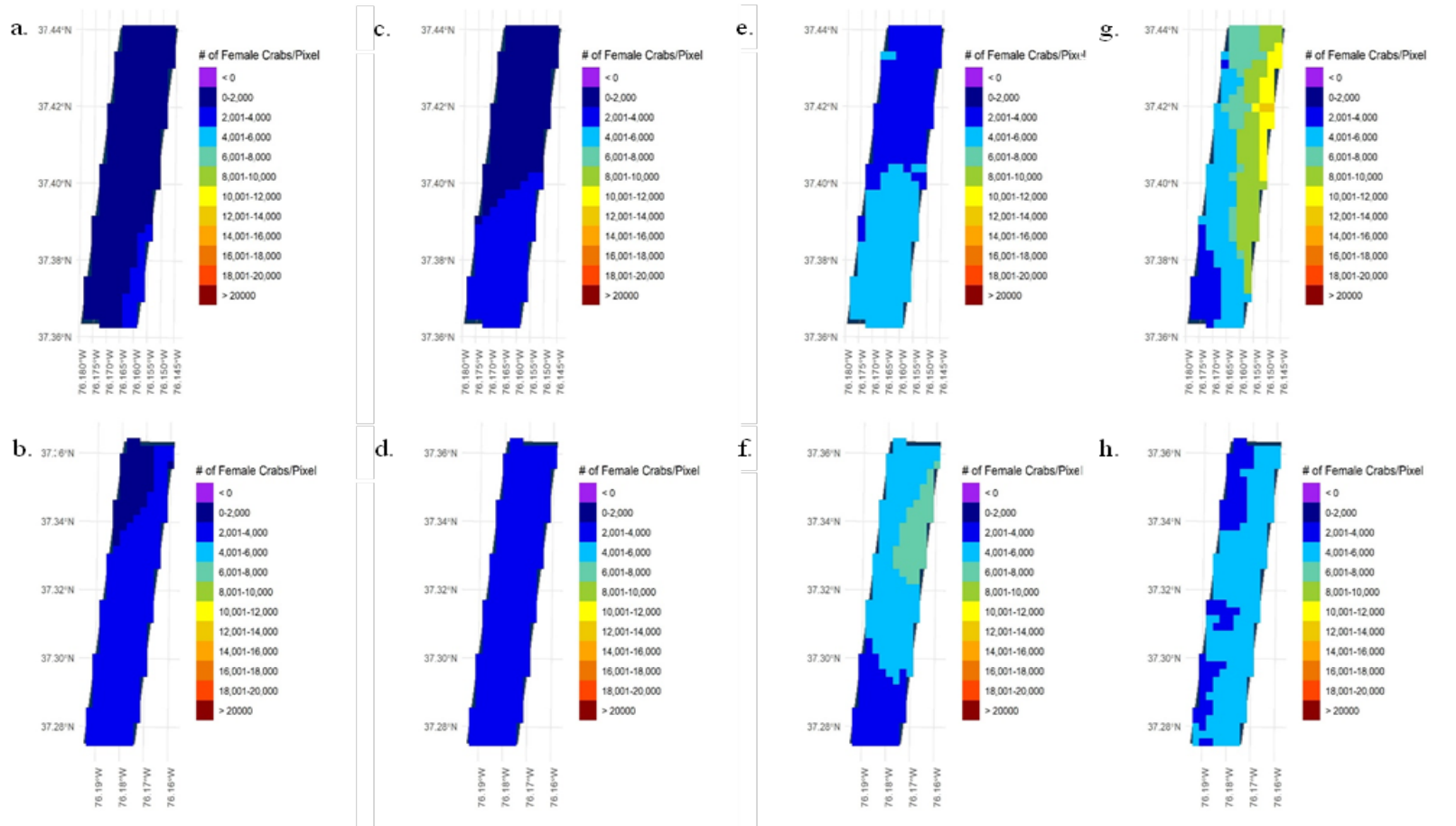


Figure 3.37. Female age 1+ blue crab abundance maps in WTAPSNE (top) and WTAPS (bottom) derived from kriging in the Chesapeake Bay for 2006–2009: a) WTAPSNE female age-1+ abundance in 2006, b) WTAPS female age-1+ abundance in 2006, c) WTAPSNE female age-1+ abundance in 2007, d) WTAPS female age-1+ abundance in 2007, e) WTAPSNE female age-1+ abundance in 2008, f) WTAPS female age-1+ abundance in 2008, g) WTAPSNE female age-1+ abundance in 2009, and h) WTAPS female age-1+ abundance in 2009.

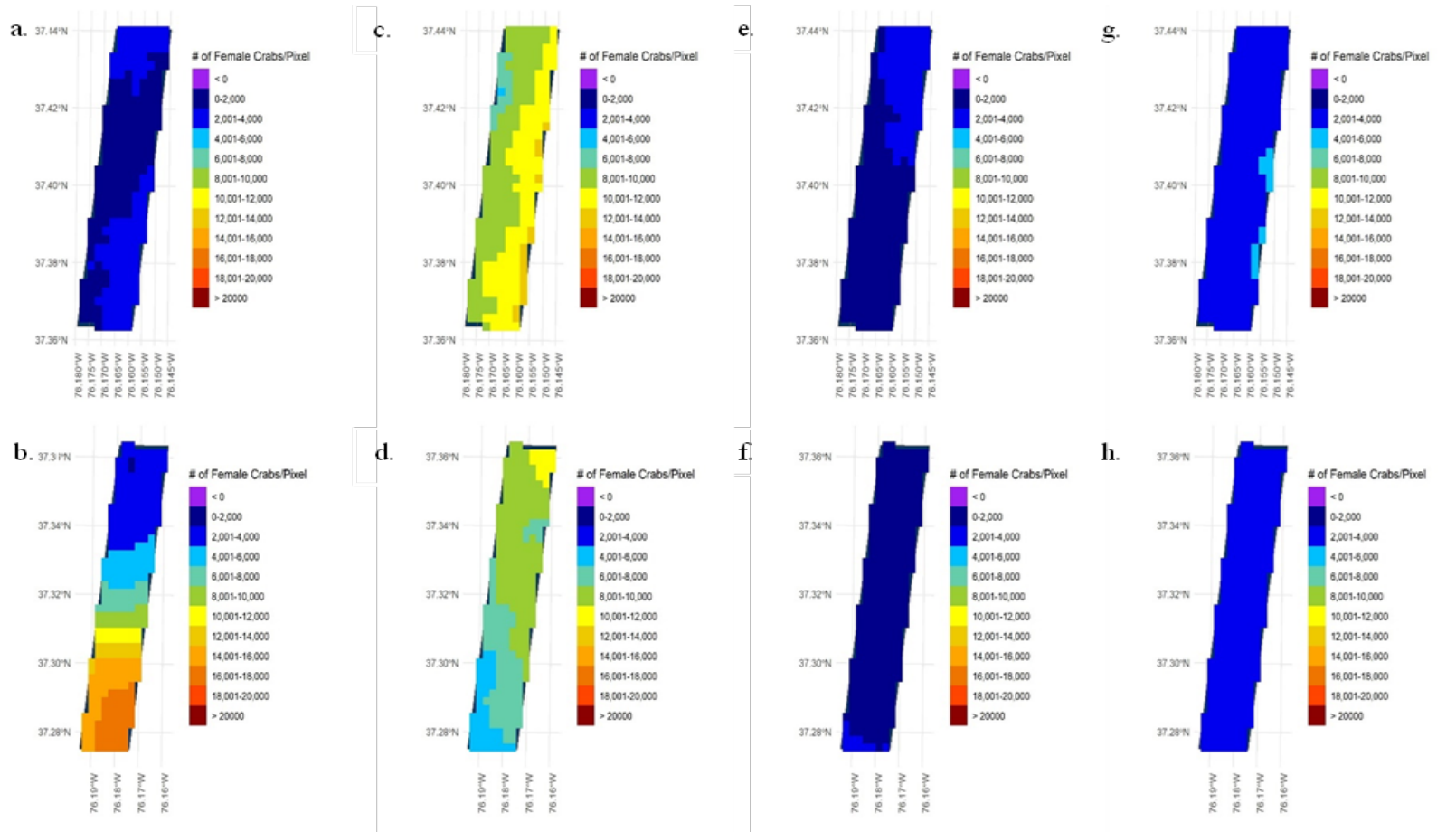


Figure 3.38. Female age 1+ blue crab abundance maps in WTAPSNE (top) and WTAPS (bottom) derived from kriging in the Chesapeake Bay for 2010–2013: a) WTAPSNE female age-1+ abundance in 2010, b) WTAPS female age-1+ abundance in 2010, c) WTAPSNE female age-1+ abundance in 2011, d) WTAPS female age-1+ abundance in 2011, e) WTAPSNE female age-1+ abundance in 2012, f) WTAPS female age-1+ abundance in 2012, g) WTAPSNE female age-1+ abundance in 2013, and h) WTAPS female age-1+ abundance in 2013.

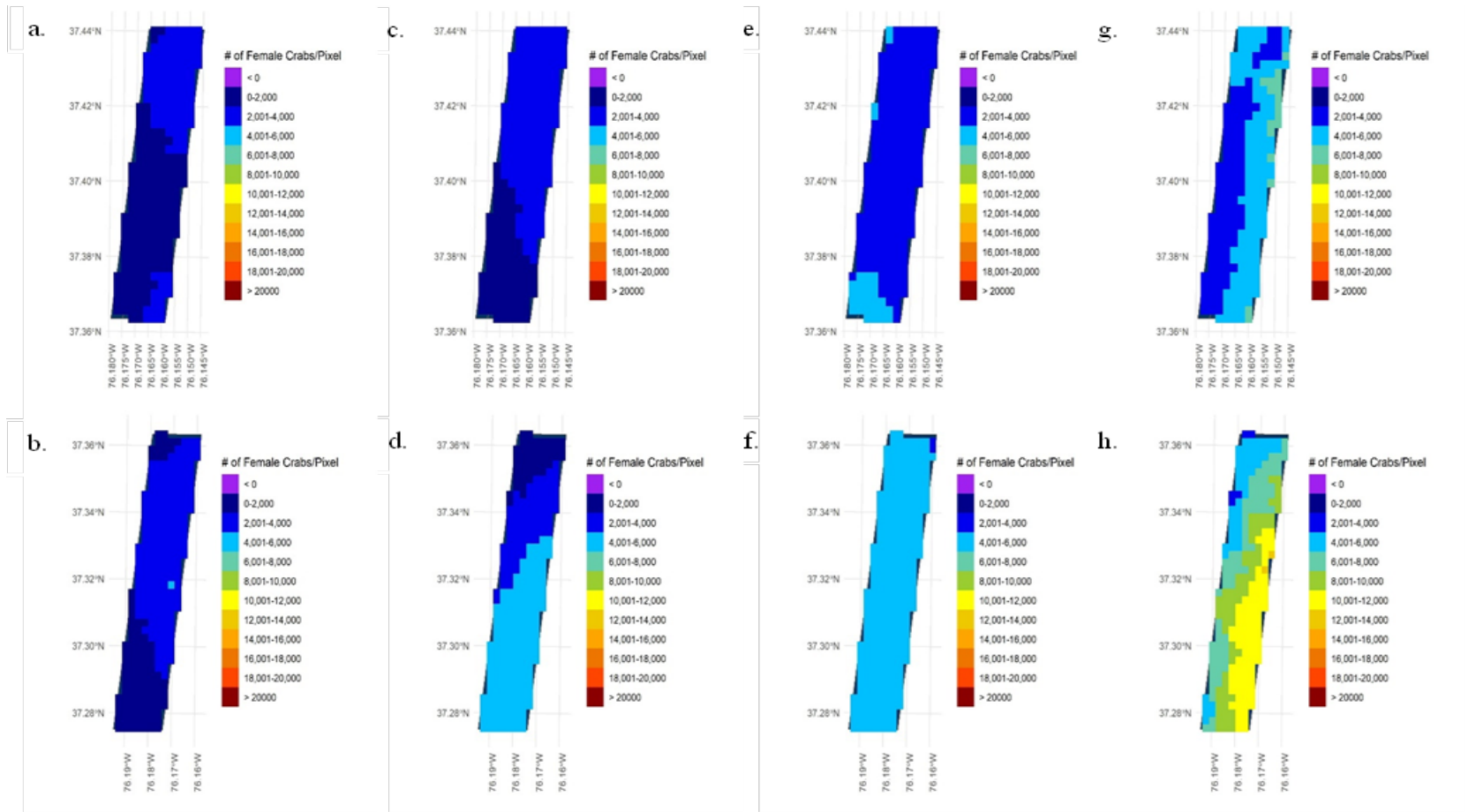


Figure 3.39. Female age 1+ blue crab abundance maps in WTAPSNE (top) and WTAPS (bottom) derived from kriging in the Chesapeake Bay for 2014–2017: a) WTAPSNE female age-1+ abundance in 2014, b) WTAPS female age-1+ abundance in 2014, c) WTAPSNE female age-1+ abundance in 2015, d) WTAPS female age-1+ abundance in 2015, e) WTAPSNE female age-1+ abundance in 2016, f) WTAPS female age-1+ abundance in 2016, g) WTAPSNE female age-1+ abundance in 2017, and h) WTAPS female age-1+ abundance in 2017.

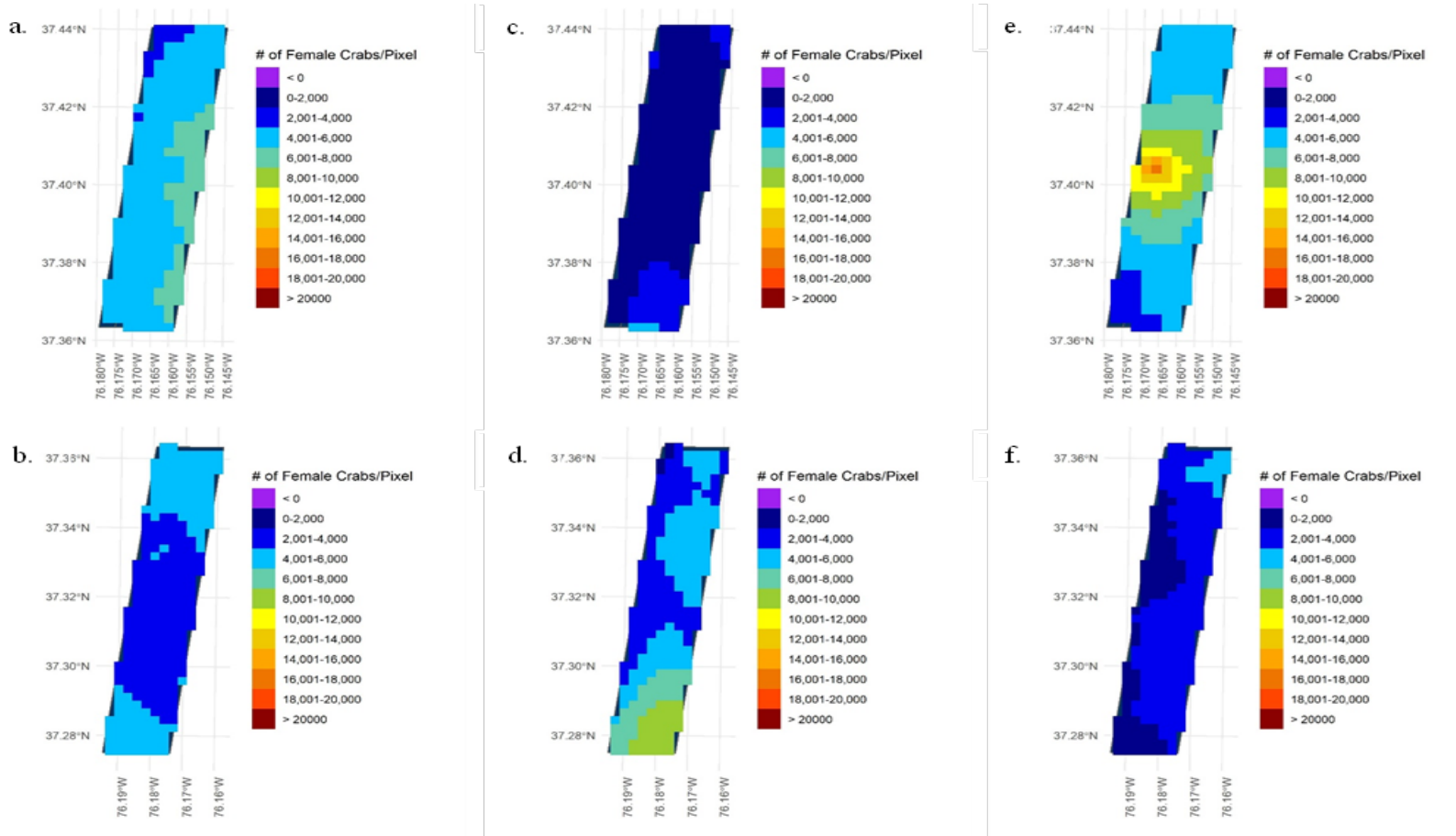


Figure 3.40. Female age 1+ blue crab abundance maps in WTAPSNE (top) and WTAPS (bottom) derived from kriging in the Chesapeake Bay for 2018–2020: a) WTAPSNE female age-1+ abundance in 2018, b) WTAPS female age-1+ abundance in 2018, c) WTAPSNE female age-1+ abundance in 2019, d) WTAPS female age-1+ abundance in 2019, e) WTAPSNE female age-1+ abundance in 2020, and f) WTAPS female age-1+ abundance in 2020.

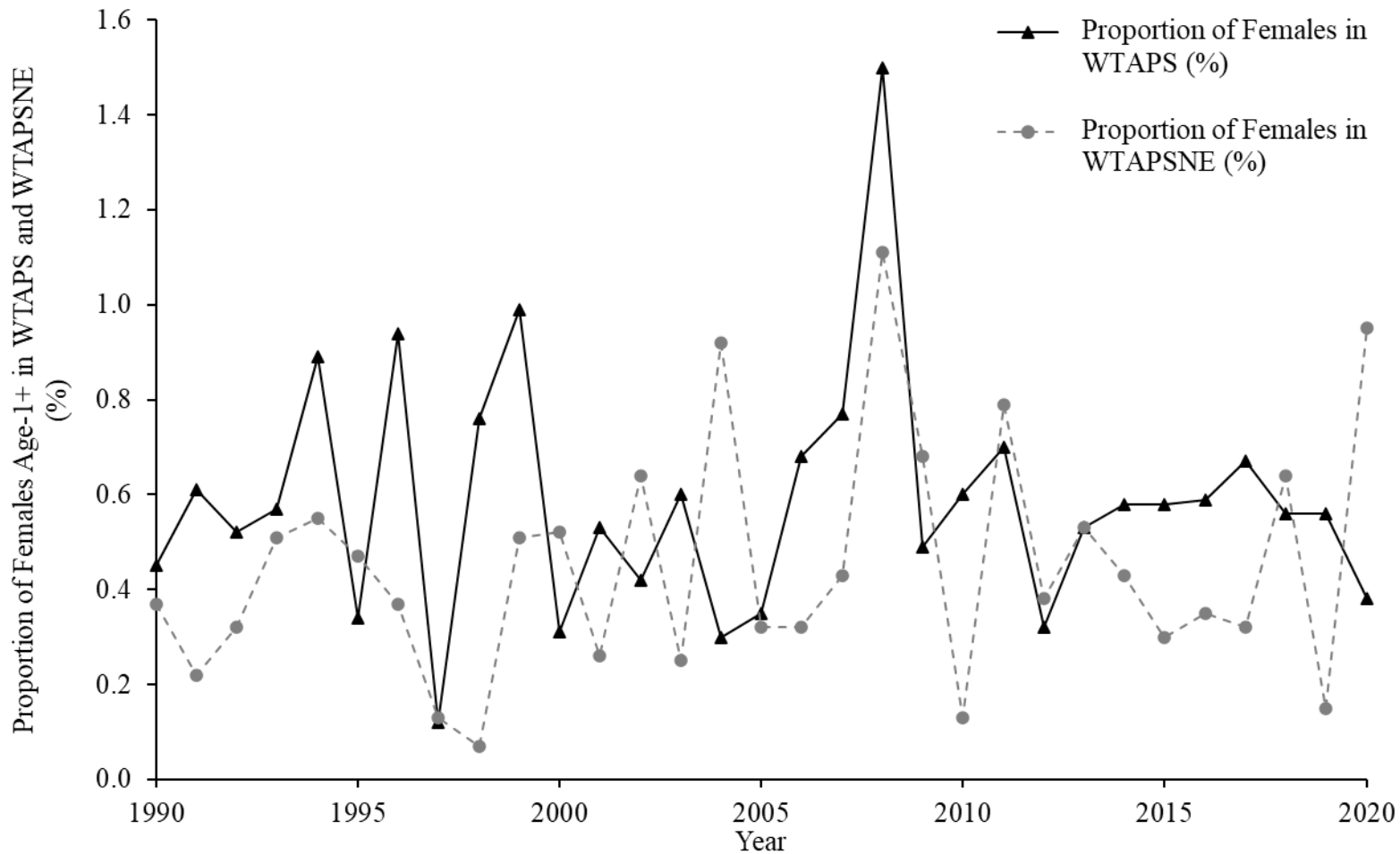


Figure 3.41. Proportion of female age-1+ blue crab abundance in WTAPS and WTAPSNE (%) out of the Bay-wide kriging abundance estimates in Chesapeake Bay. Shown are kriged estimates of the proportion of females age-1+ (%) in WTAPS (closed triangles; solid, black line) and WTAPSNE (solid circle; dashed, grey line) for 1990–2020.

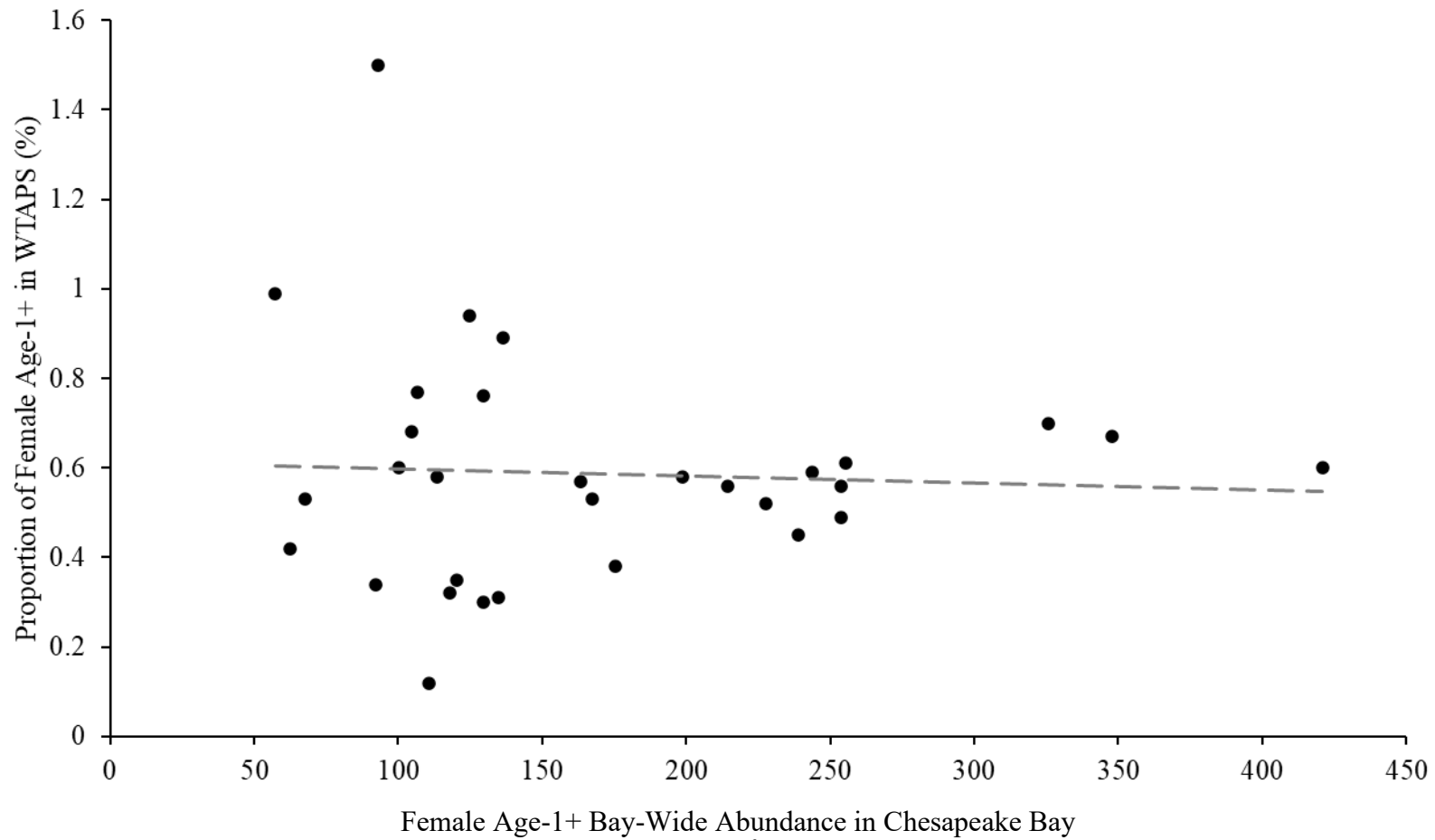


Figure 3.42. The proportion of females age-1+ in WTAPS (%) out of the Bay-wide female age-1+ kriging abundance estimate versus the Bay-wide female age-1+ abundance in Chesapeake Bay (millions) from 1990–2020. $y = -0.0002x + 0.6140$.

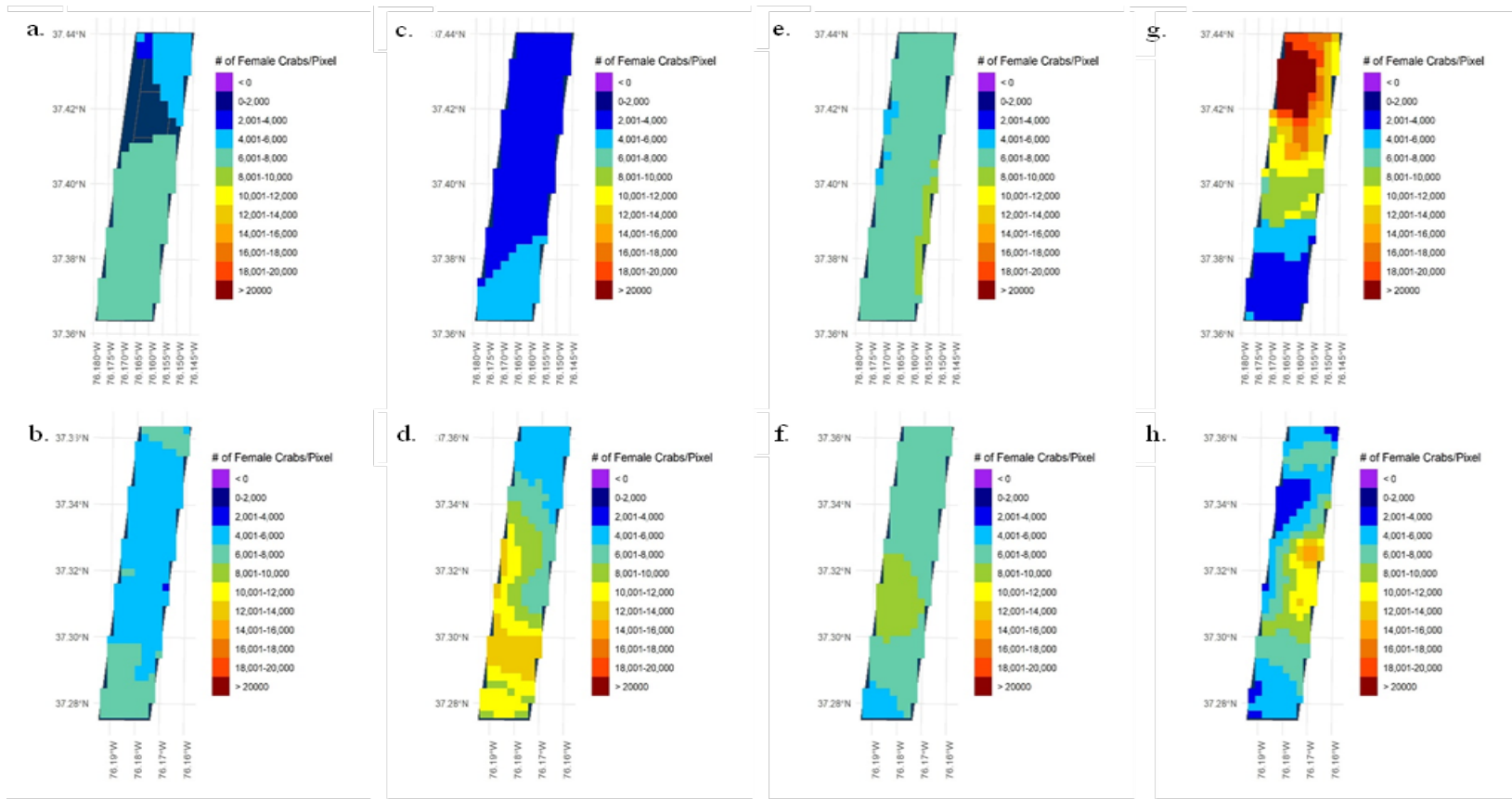


Figure 3.43. Female age-1+ blue crab abundance maps in WTAPSNE (top) and WTAPS (bottom) derived from kriging using data only from Strata 2 and 3 in the Davis WDS Strata for 1990–1993: a) WTAPSNE female age-1+ abundance in 1990, b) WTAPS female age-1+ abundance in 1990, c) WTAPSNE female age-1+ abundance in 1991, d) WTAPS female age-1+ abundance in 1991, e) WTAPSNE female age-1+ abundance in 1992, f) WTAPS female age-1+ abundance in 1992, g) WTAPSNE female age-1+ abundance in 1993, and h) WTAPS female age-1+ abundance in 1993.

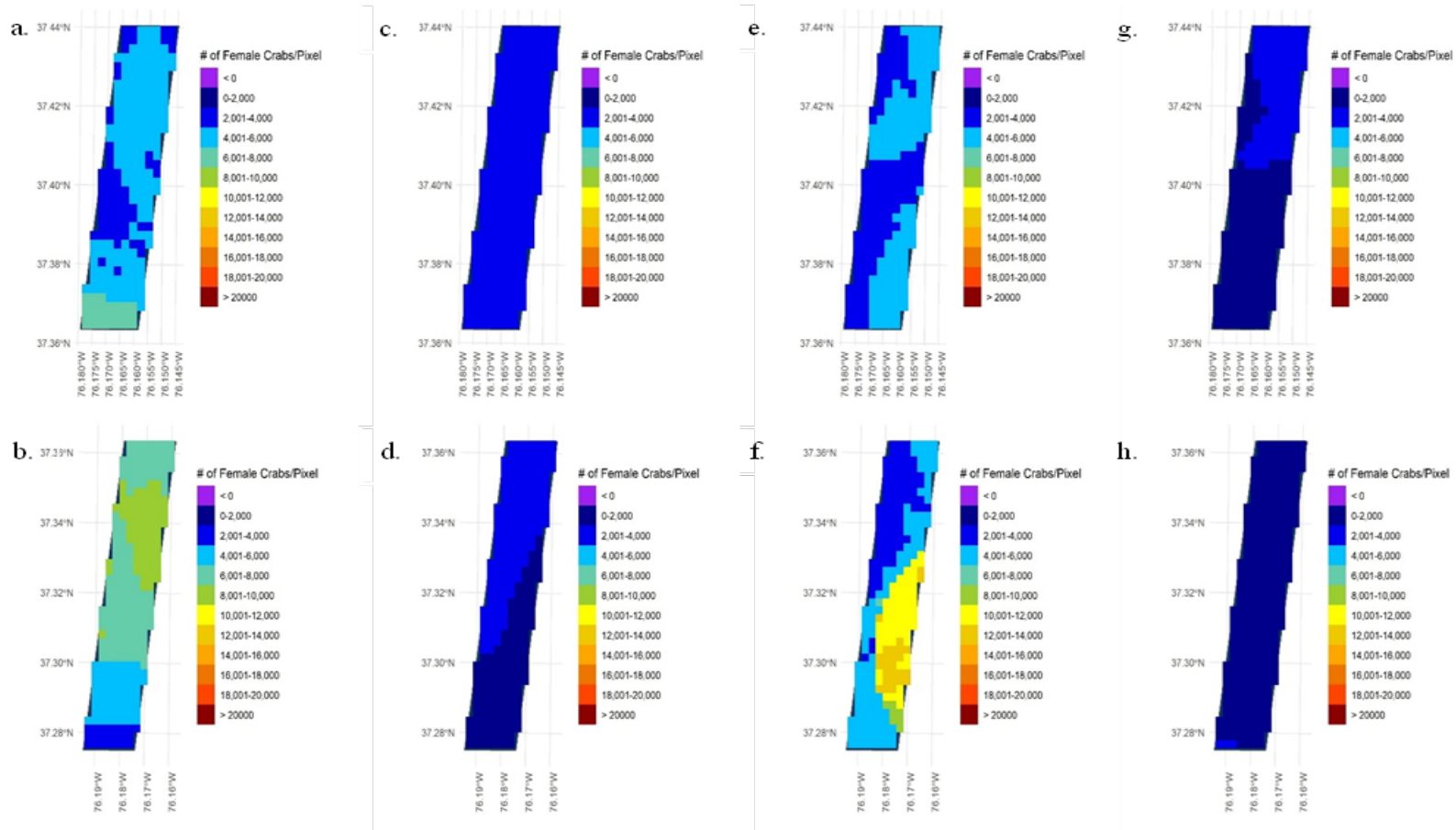


Figure 3.44. Female age-1+ blue crab abundance maps in WTAPSNE (top) and WTAPS (bottom) derived from kriging using data only from Strata 2 and 3 in the Davis WDS Strata for 1994–1997: a) WTAPSNE female age-1+ abundance in 1994, b) WTAPS female age-1+ abundance in 1994, c) WTAPSNE female age-1+ abundance in 1995, d) WTAPS female age-1+ abundance in 1995, e) WTAPSNE female age-1+ abundance in 1996, f) WTAPS female age-1+ abundance in 1996, g) WTAPSNE female age-1+ abundance in 1997, and h) WTAPS female age-1+ abundance in 1997.

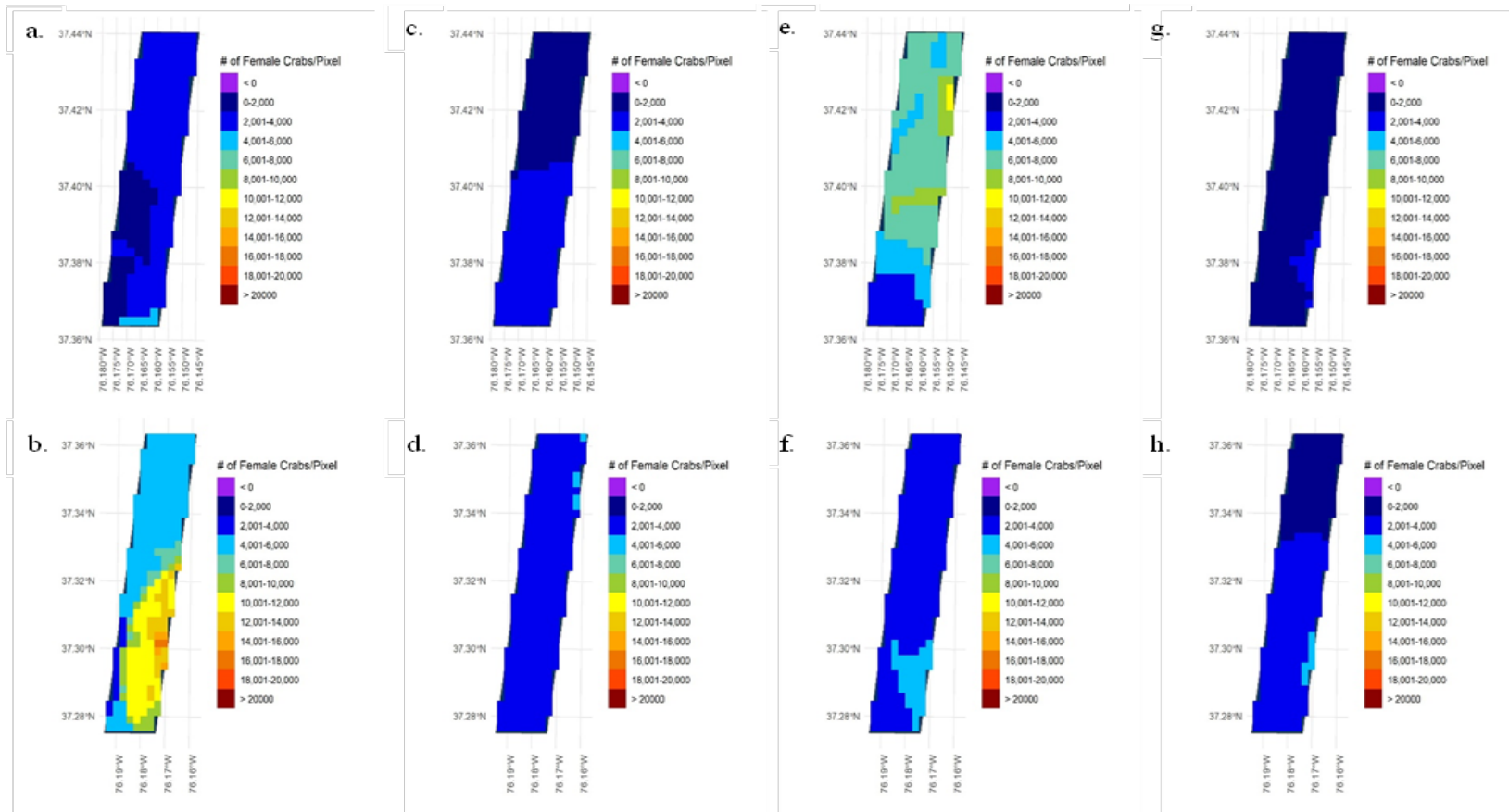


Figure 3.45. Female age-1+ blue crab abundance maps in WTAPSNE (top) and WTAPS (bottom) derived from kriging using data only from Strata 2 and 3 in the Davis Strata WDS for 1998–2001: a) WTAPSNE female age-1+ abundance in 1998, b) WTAPS female age-1+ abundance in 1998, c) WTAPSNE female age-1+ abundance in 1999, d) WTAPS female age-1+ abundance in 1999, e) WTAPSNE female age-1+ abundance in 2000, f) WTAPS female age-1+ abundance in 2000, g) WTAPSNE female age-1+ abundance in 2001, and h) WTAPS female age-1+ abundance in 2001.

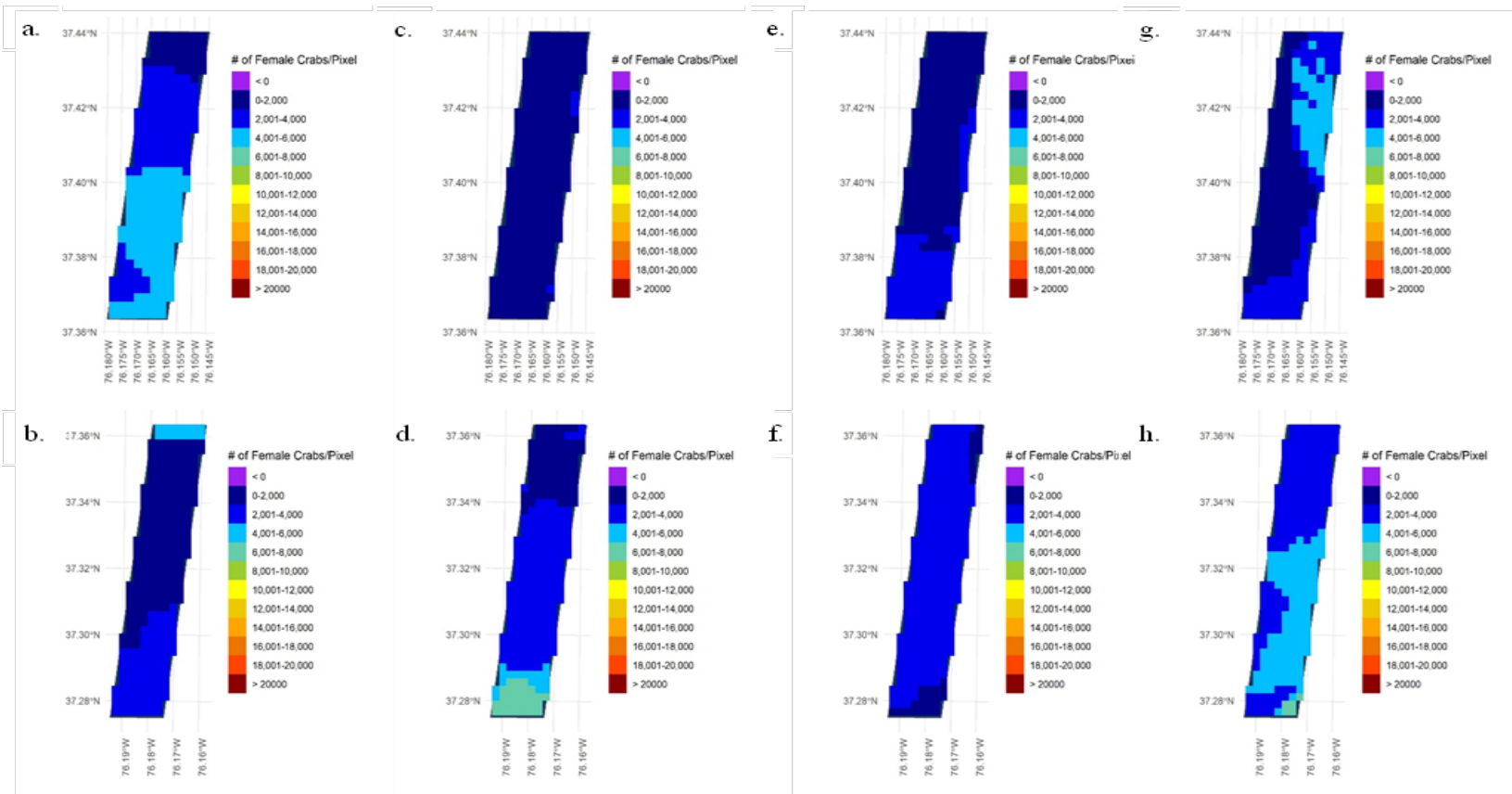


Figure 3.46. Female age-1+ blue crab abundance maps in WTAPSNE (top) and WTAPS (bottom) derived from kriging using data only from Strata 2 and 3 in the Davis WDS Strata for 2002–2005: a) WTAPSNE female age-1+ abundance in 2002, b) WTAPS female age-1+ abundance in 2002, c) WTAPSNE female age-1+ abundance in 2003, d) WTAPS female age-1+ abundance in 2003, e) WTAPSNE female age-1+ abundance in 2004, f) WTAPS female age-1+ abundance in 2004, g) WTAPSNE female age-1+ abundance in 2005, and h) WTAPS female age-1+ abundance in 2005.

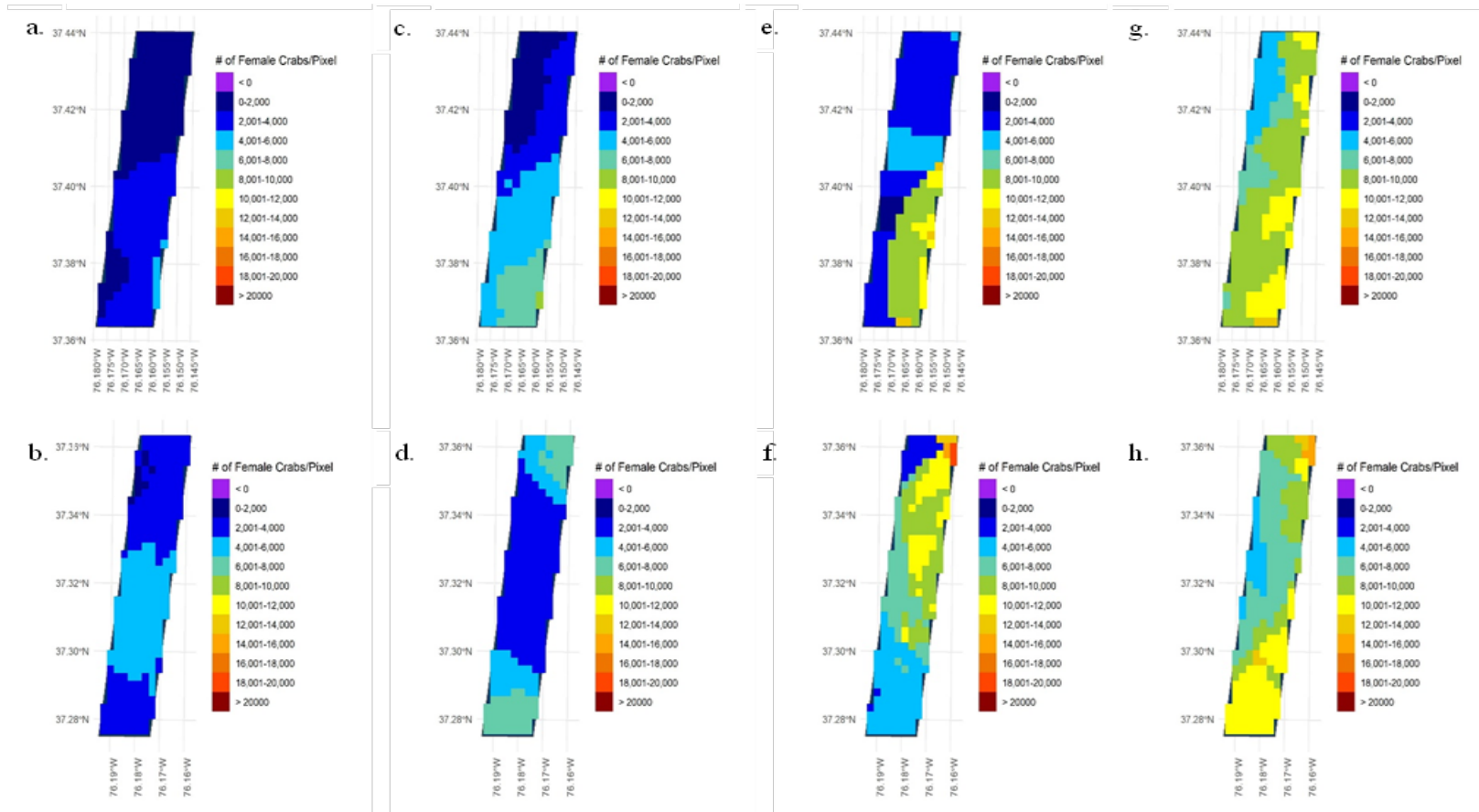


Figure 3.47. Female age-1+ blue crab abundance maps in WTAPSNE (top) and WTAPS (bottom) derived from kriging using data only from Strata 2 and 3 in the Davis WDS Strata for 2006–2009: a) WTAPSNE female age-1+ abundance in 2006, b) WTAPS female age-1+ abundance in 2006, c) WTAPSNE female age-1+ abundance in 2007, d) WTAPS female age-1+ abundance in 2007, e) WTAPSNE female age-1+ abundance in 2008, f) WTAPS female age-1+ abundance in 2008, g) WTAPSNE female age-1+ abundance in 2009, and h) WTAPS female age-1+ abundance in 2009.

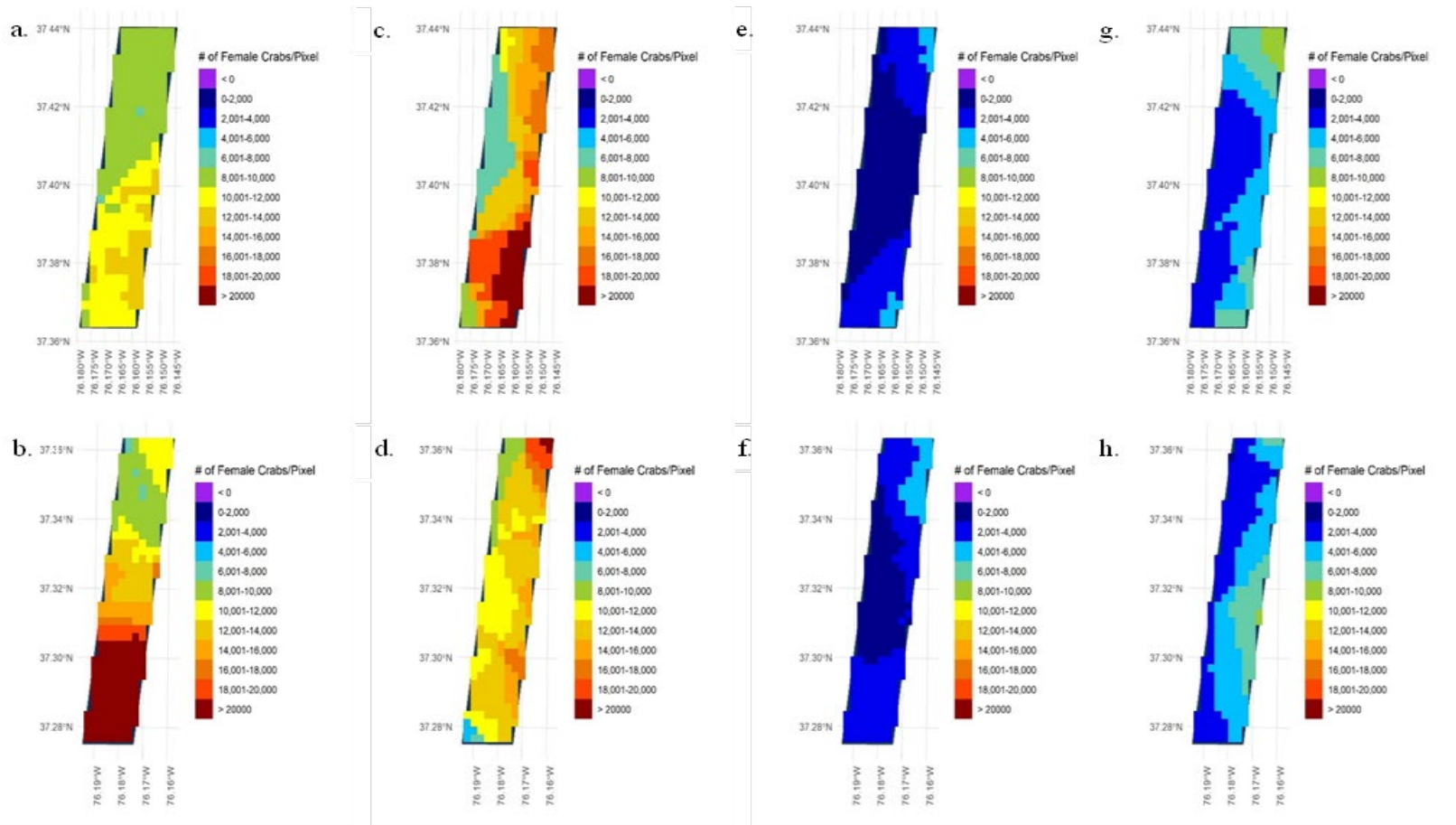


Figure 3.48. Female age-1+ blue crab abundance maps in WTAPSNE (top) and WTAPS (bottom) derived from kriging using data only from Strata 2 and 3 in the Davis WDS Strata for 2010–2013: a) WTAPSNE female age-1+ abundance in 2010, b) WTAPS female age-1+ abundance in 2010, c) WTAPSNE female age-1+ abundance in 2011, d) WTAPS female age-1+ abundance in 2011, e) WTAPSNE female age-1+ abundance in 2012, f) WTAPS female age-1+ abundance in 2012, g) WTAPSNE female age-1+ abundance in 2013, and h) WTAPS female age-1+ abundance in 2013.

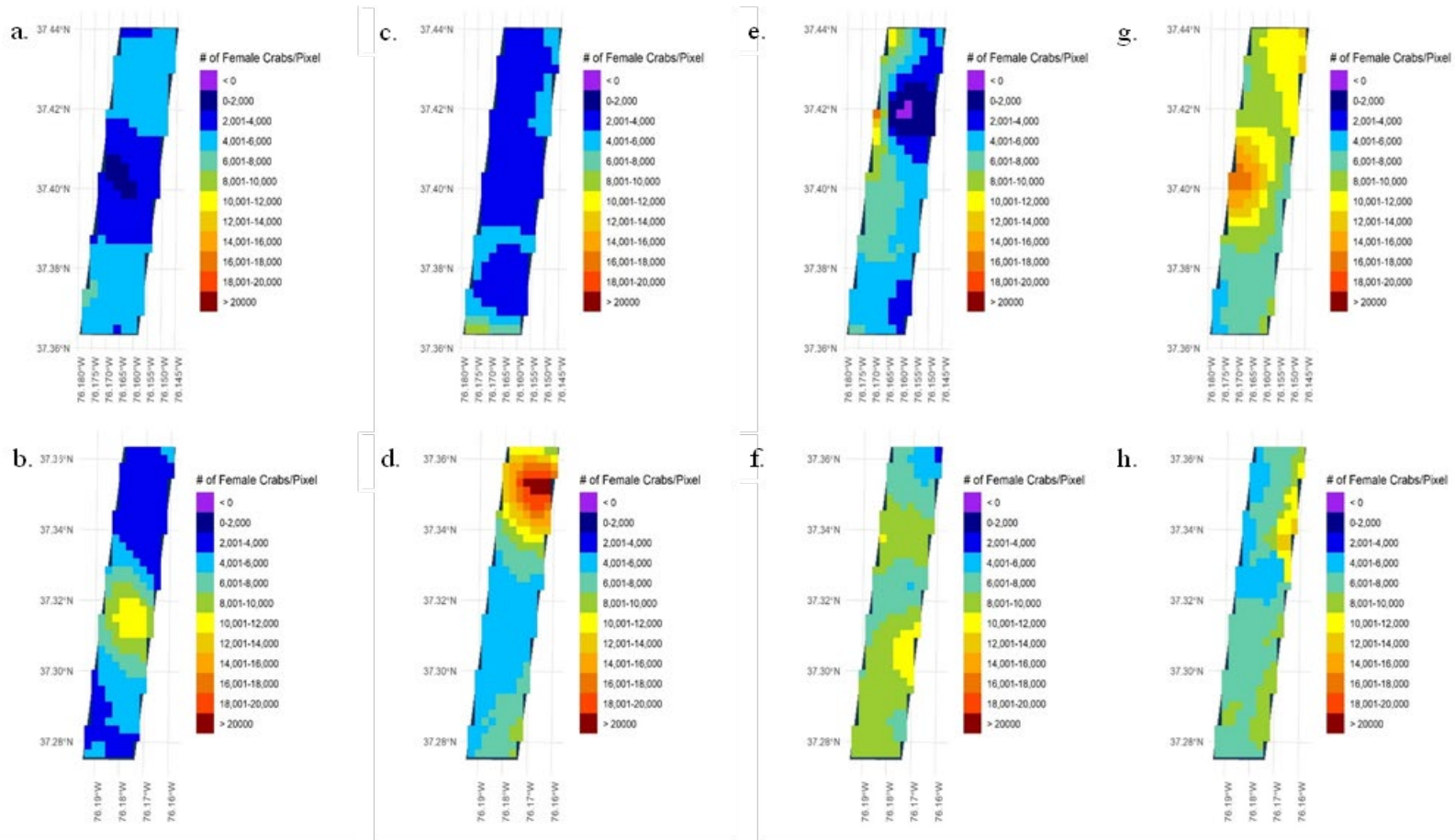


Figure 3.49. Female age-1+ blue crab abundance maps in WTAPSNE (top) and WTAPS (bottom) derived from kriging using data only from Strata 2 and 3 in the Davis WDS Strata for 2014–2017: a) WTAPSNE female age-1+ abundance in 2014, b) WTAPS female age-1+ abundance in 2014, c) WTAPSNE female age-1+ abundance in 2015, d) WTAPS female age-1+ abundance in 2015, e) WTAPSNE female age-1+ abundance in 2016, f) WTAPS female age-1+ abundance in 2016, g) WTAPSNE female age-1+ abundance in 2017, and h) WTAPS female age-1+ abundance in 2017.

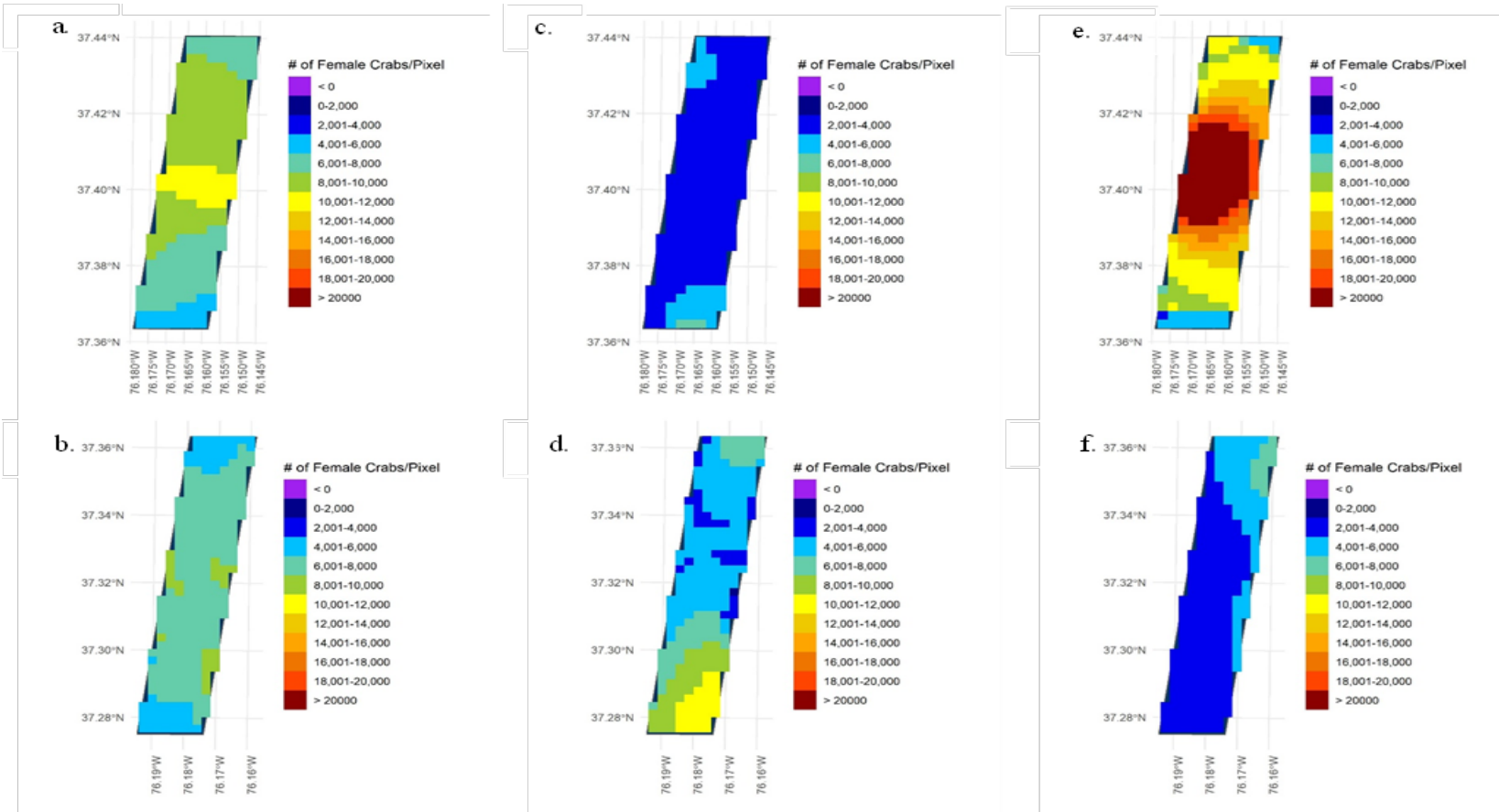


Figure 3.50. Female age-1+ blue crab abundance maps in WTAPSNE (top) and WTAPS (bottom) derived from kriging using data only from Strata 2 and 3 in the Davis WDS Strata for 2018–2020: a) WTAPSNE female age-1+ abundance in 2018, b) WTAPS female age-1+ abundance in 2018, c) WTAPSNE female age-1+ abundance in 2019, d) WTAPS female age-1+ abundance in 2019, e) WTAPSNE female age-1+ abundance in 2020, and f) WTAPS female age-1+ abundance in 2020.

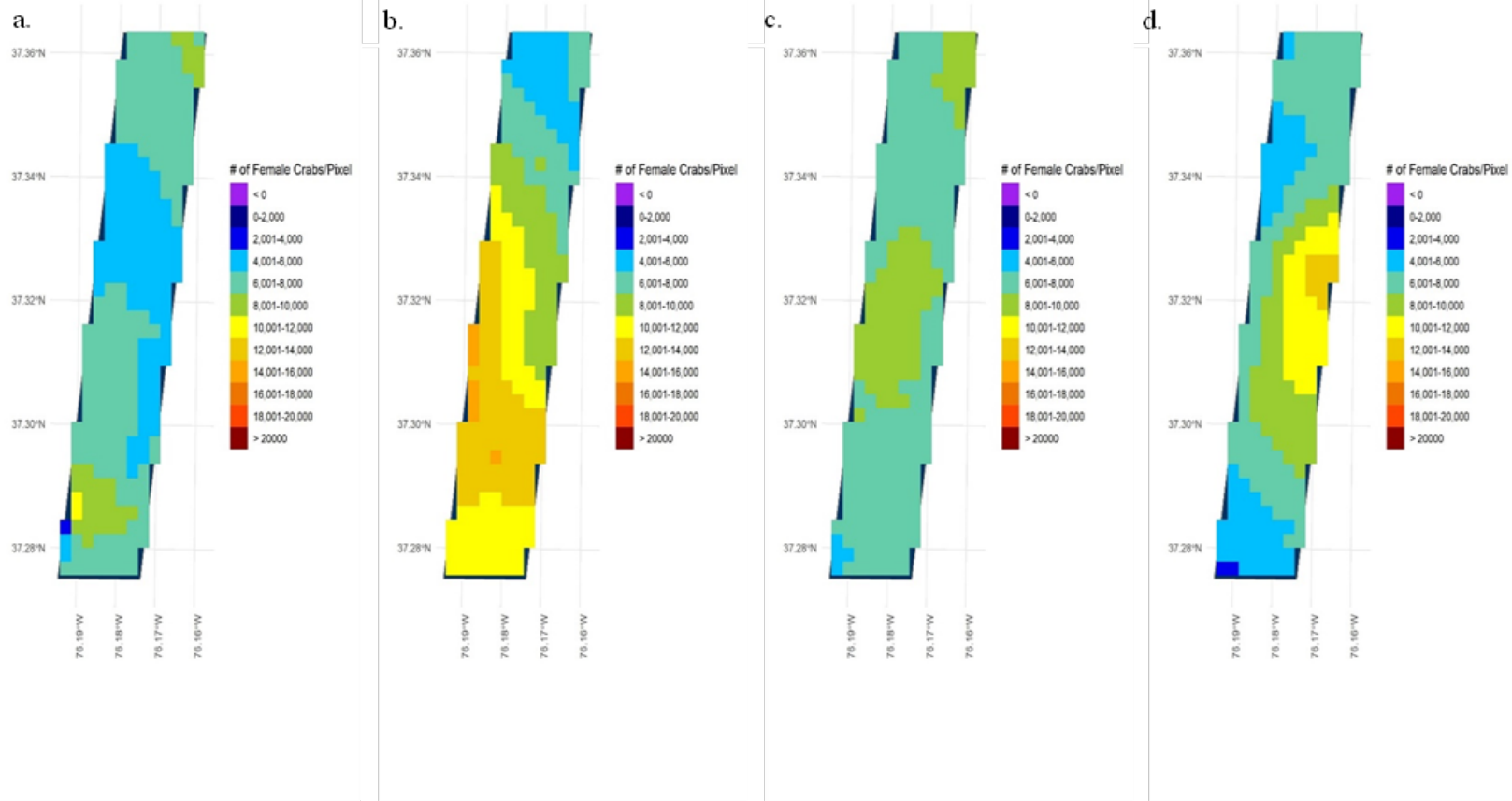


Figure 3.51. Female age-1+ blue crab abundance maps in WTAPS derived from kriging using Davis WDS Strata data only from Strata 3 for 1990–1993: a) WTAPS age-1+ abundance in 1990, b) WTAPS age-1+ abundance in 1991, c) WTAPS age-1+ abundance in 1992, and d) WTAPS age-1+ abundance in 1993.

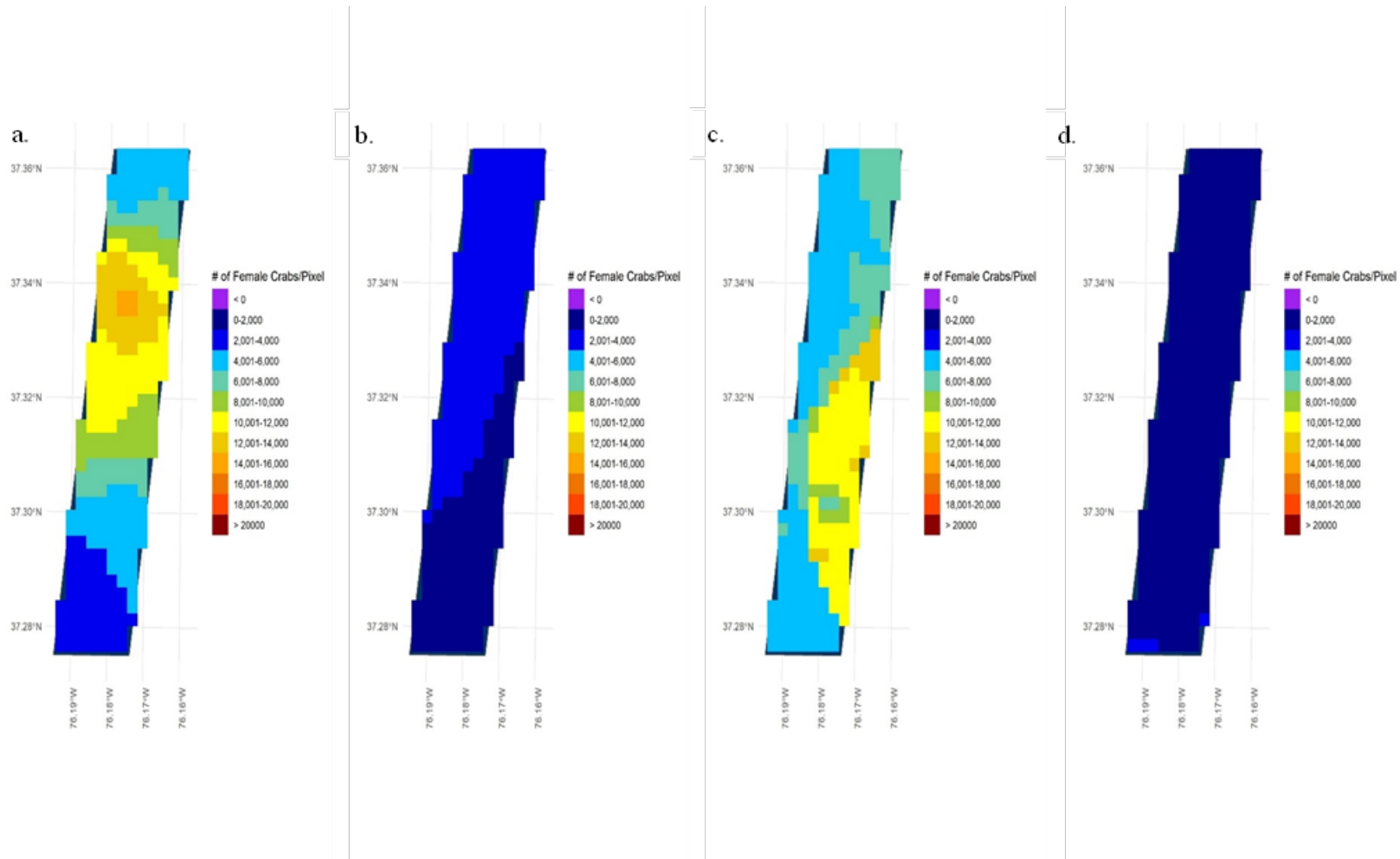


Figure 3.52. Female age-1+ blue crab abundance maps in WTAPS derived from kriging using Davis WDS Strata data only from Strata 3 for 1994–1997: a) WTAPS age-1+ abundance in 1994, b) WTAPS age-1+ abundance in 1995, c) WTAPS age-1+ abundance in 1996, and d) WTAPS age-1+ abundance in 1997.

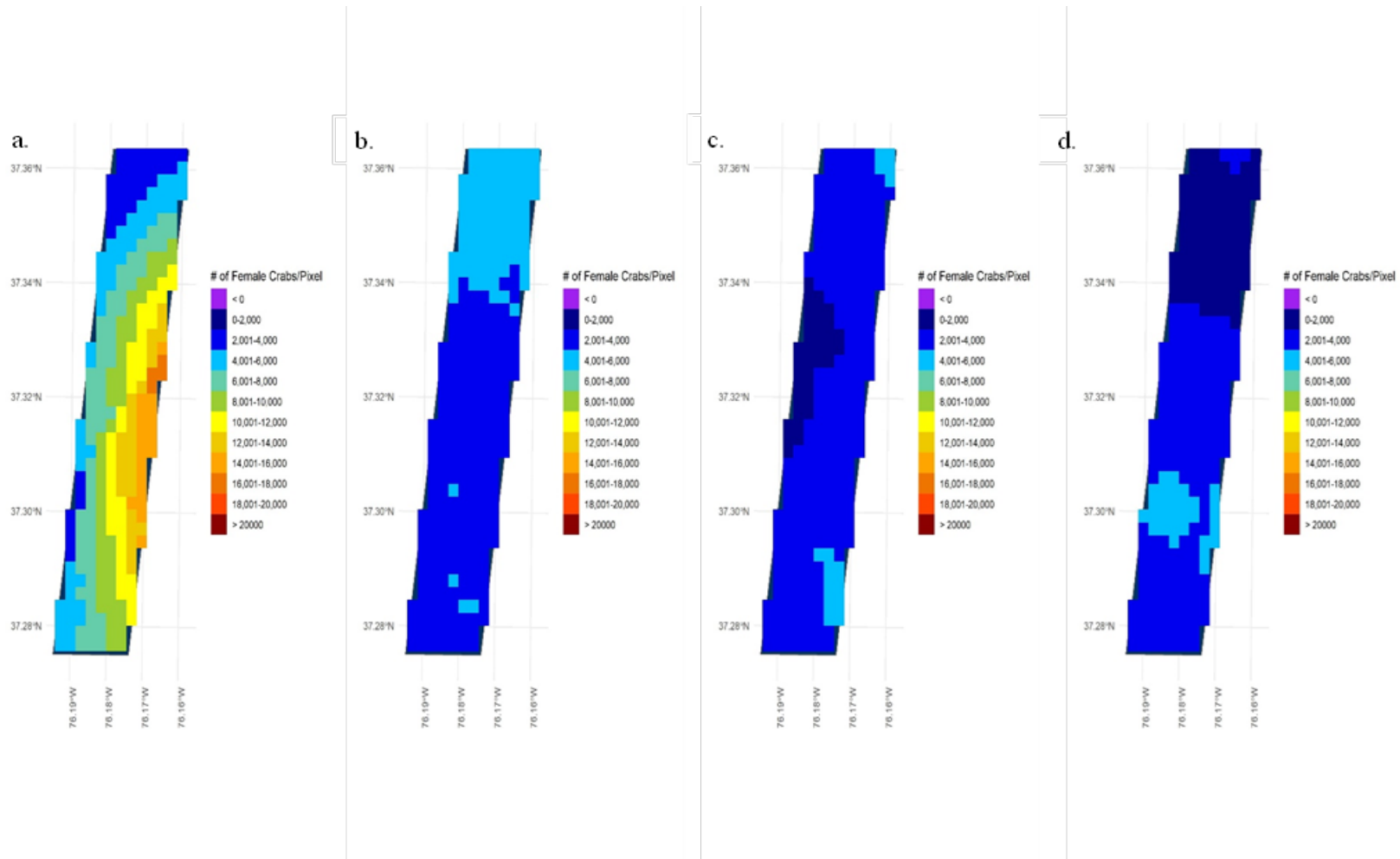


Figure 3.53. Female age-1+ blue crab abundance maps in WTAPS derived from kriging using Davis WDS Strata data only from Strata 3 for 1998–2001: a) WTAPS age-1+ abundance in 1998, b) WTAPS age-1+ abundance in 1999, c) WTAPS age-1+ abundance in 2000, and d) WTAPS age-1+ abundance in 2001.

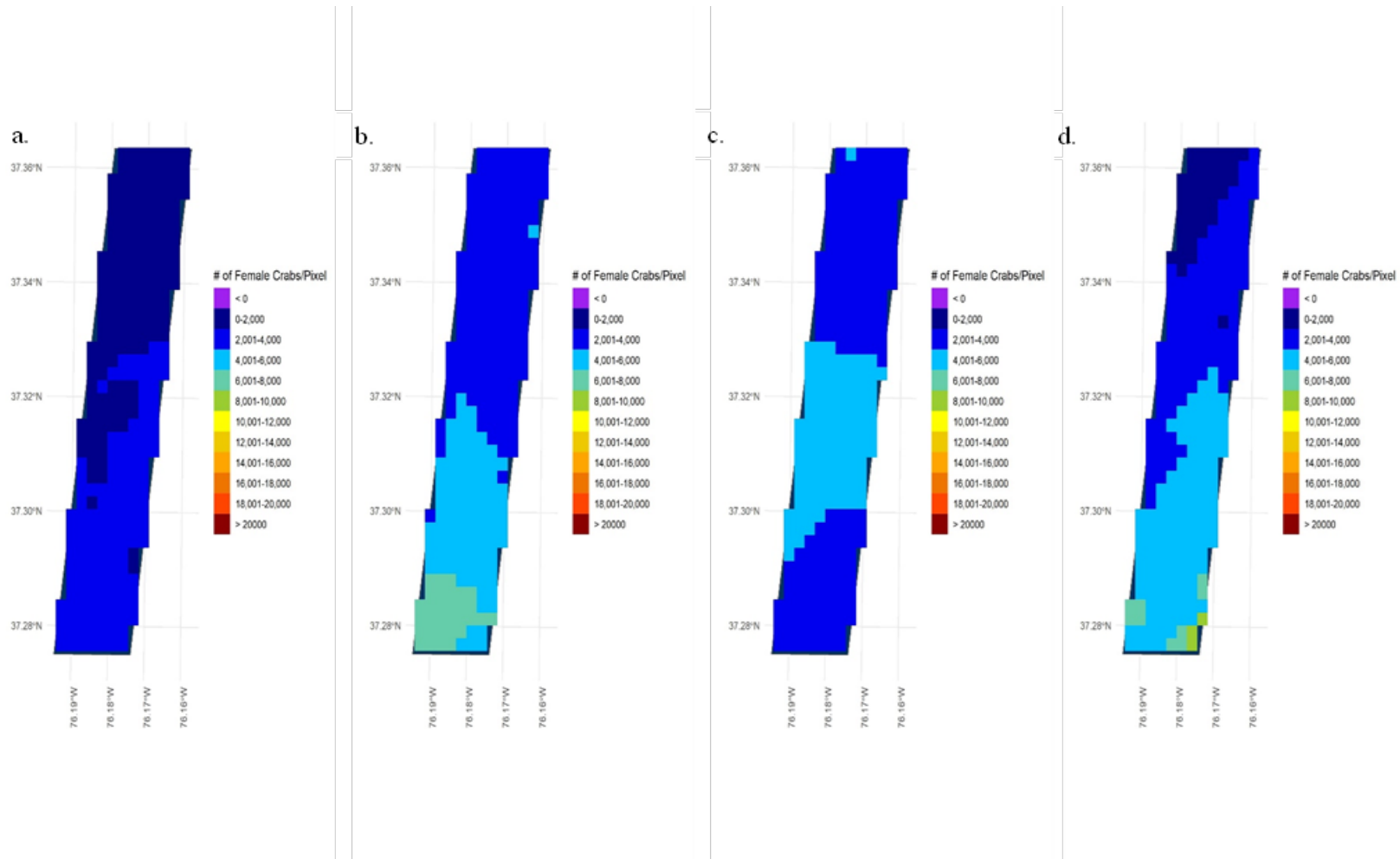


Figure 3.54. Female age-1+ blue crab abundance maps in WTAPS derived from kriging using Davis WDS Strata data only from Strata 3 for 2002–2005: a) WTAPS age-1+ abundance in 2002, b) WTAPS age-1+ abundance in 2003, c) WTAPS age-1+ abundance in 2004, and d) WTAPS age-1+ abundance in 2005.

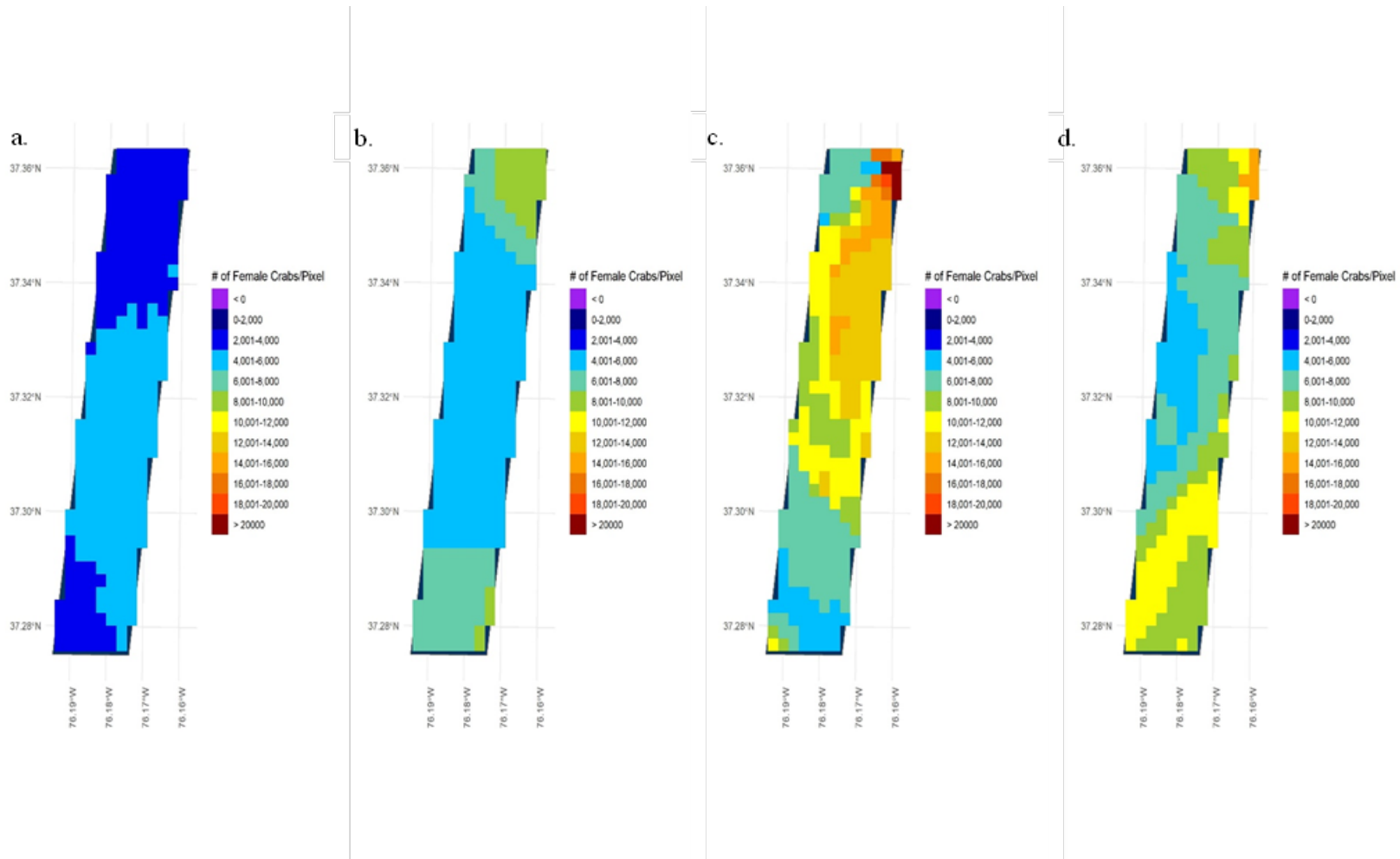


Figure 3.55. Female age-1+ blue crab abundance maps in WTAPS derived from kriging using Davis WDS Strata data only from Strata 3 for 2006–2009: a) WTAPS age-1+ abundance in 2006, b) WTAPS age-1+ abundance in 2007, c) WTAPS age-1+ abundance in 2008, and d) WTAPS age-1+ abundance in 2009.

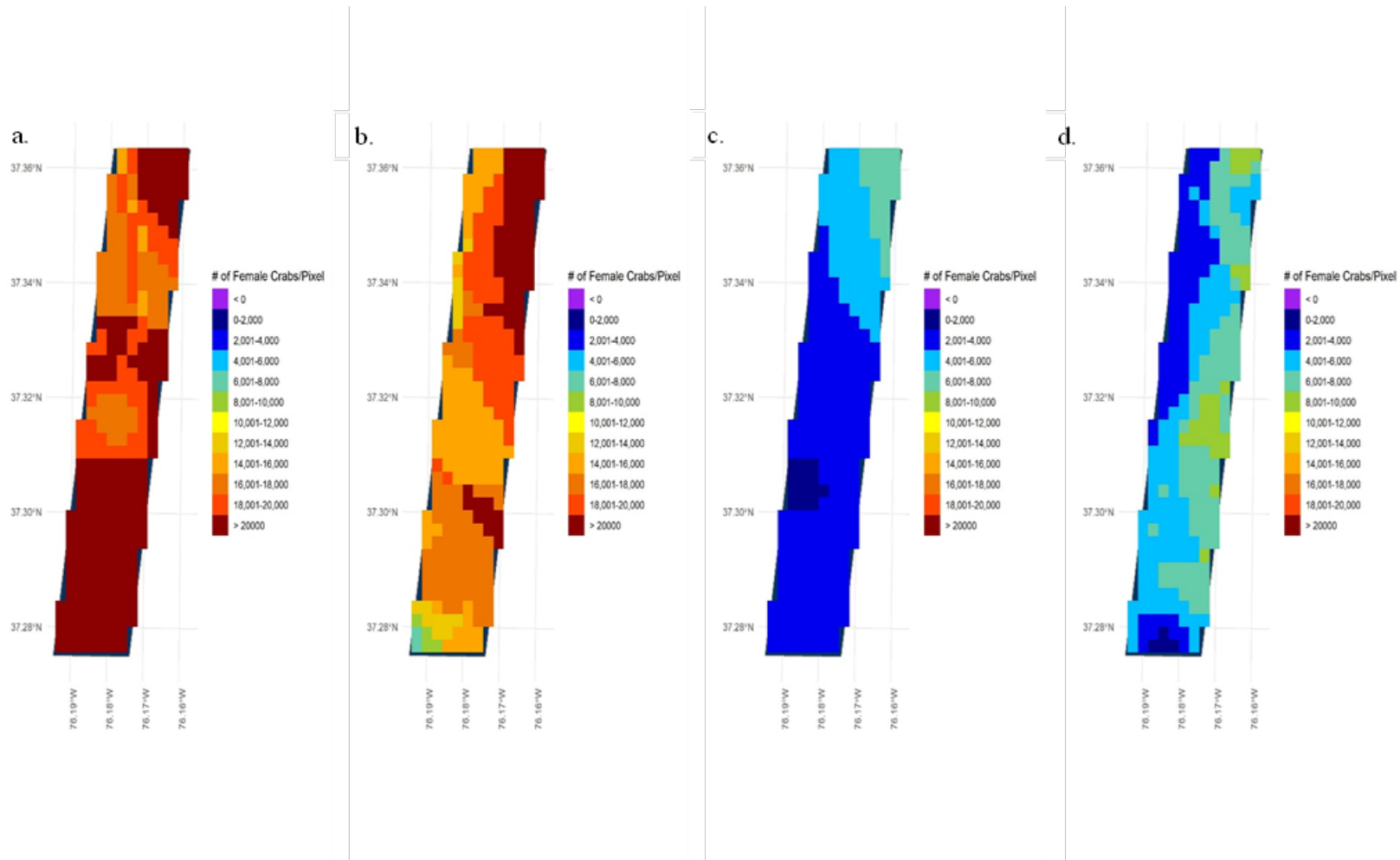


Figure 3.56. Female age-1+ blue crab abundance maps in WTAPS derived from kriging using Davis WDS Strata data only from Strata 3 for 2010–2013: a) WTAPS age-1+ abundance in 2010, b) WTAPS age-1+ abundance in 2011, c) WTAPS age-1+ abundance in 2012, and d) WTAPS age-1+ abundance in 2013.

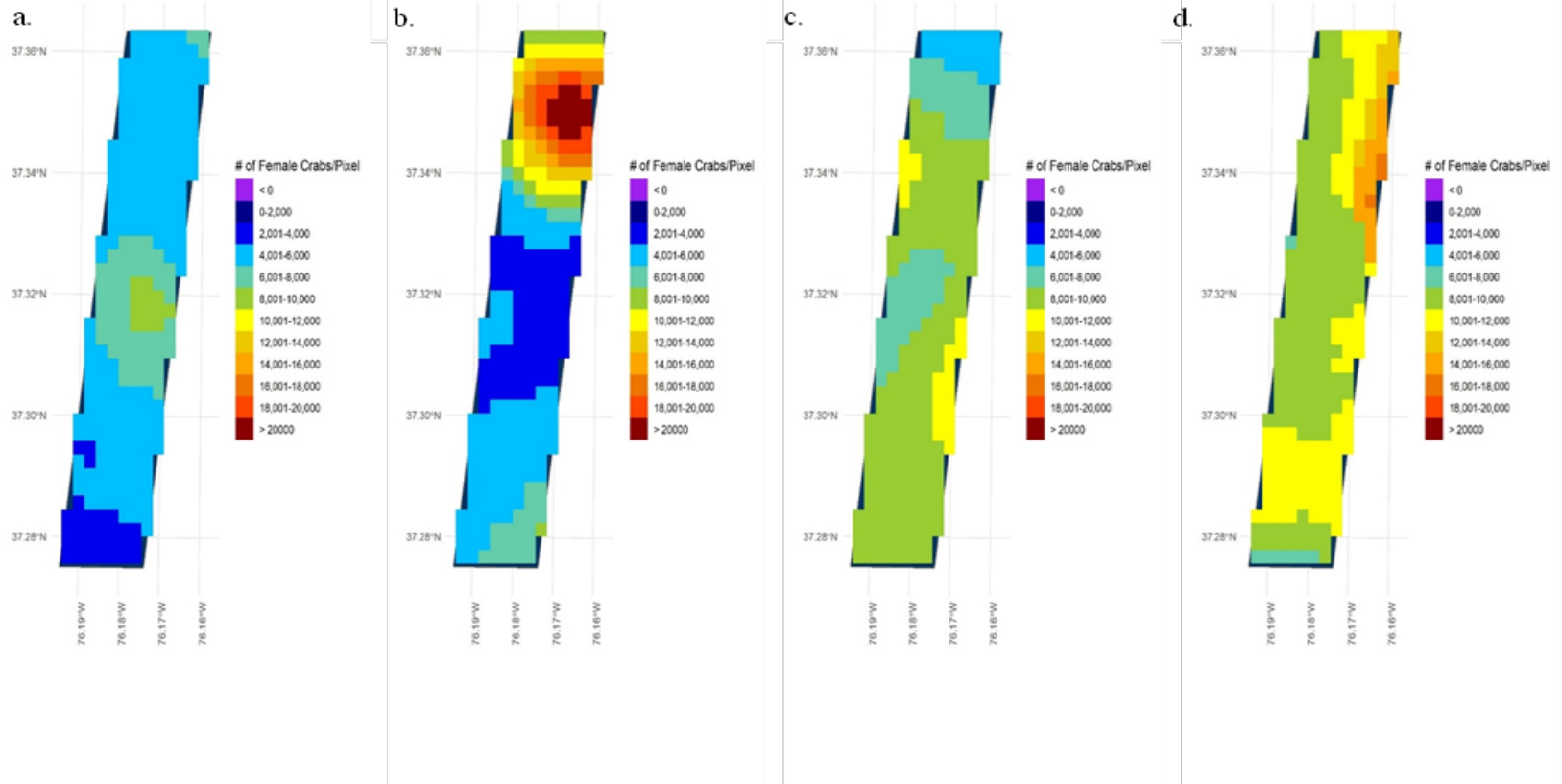


Figure 3.57. Female age-1+ blue crab abundance maps in WTAPS derived from kriging using Davis WDS data only from Strata 3 for 2014–2017: a) WTAPS age-1+ abundance in 2014, b) WTAPS age-1+ abundance in 2015, c) WTAPS age-1+ abundance in 2016, and d) WTAPS age-1+ abundance in 2017.

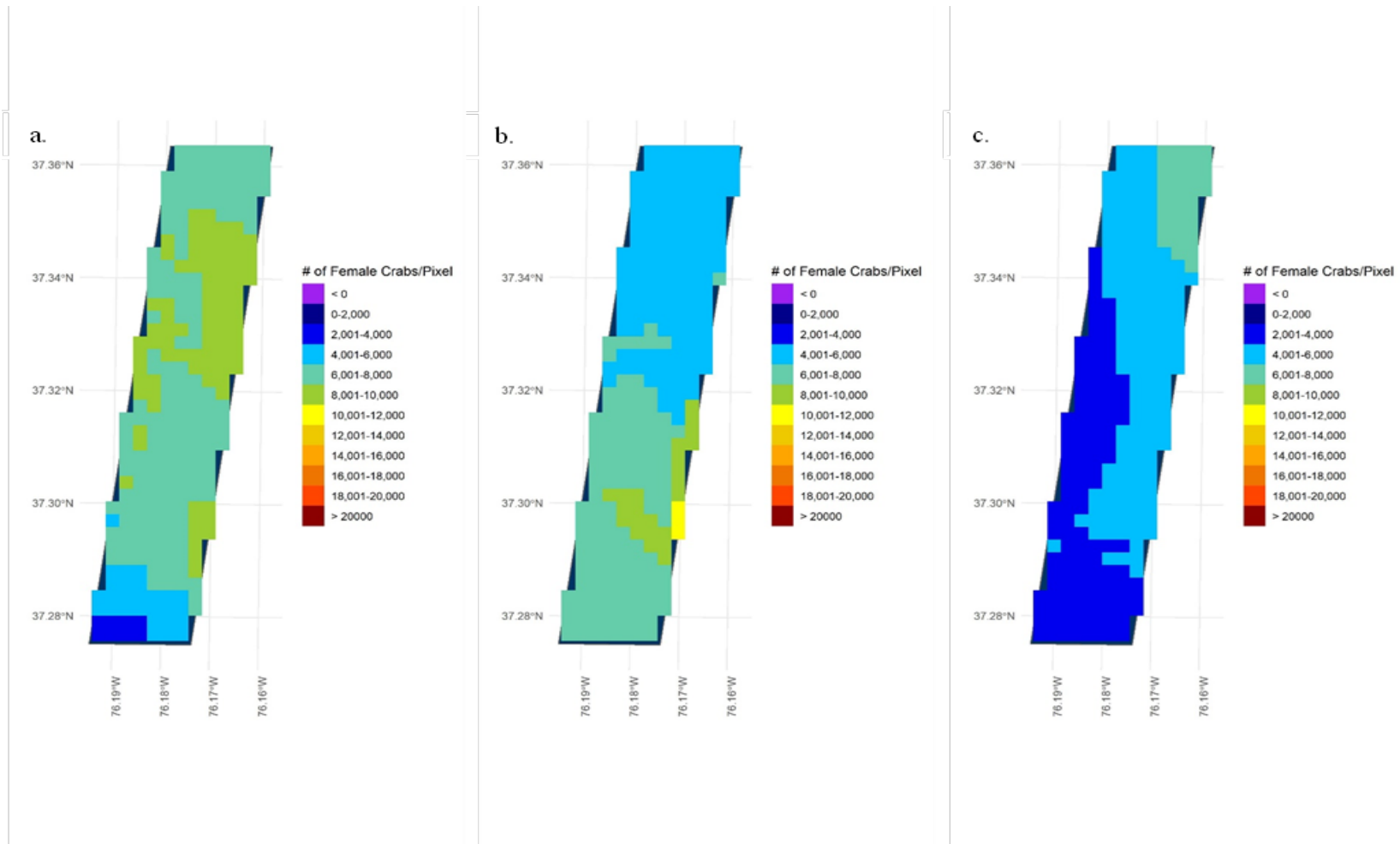


Figure 3.58. Female age-1+ blue crab abundance maps in WTAPS derived from kriging using Davis WDS Strata data only from Strata 3 for 2018–2020: a) WTAPS age-1+ abundance in 2018, b) WTAPS age-1+ abundance in 2019, and c) WTAPS age-1+ abundance in 2020.

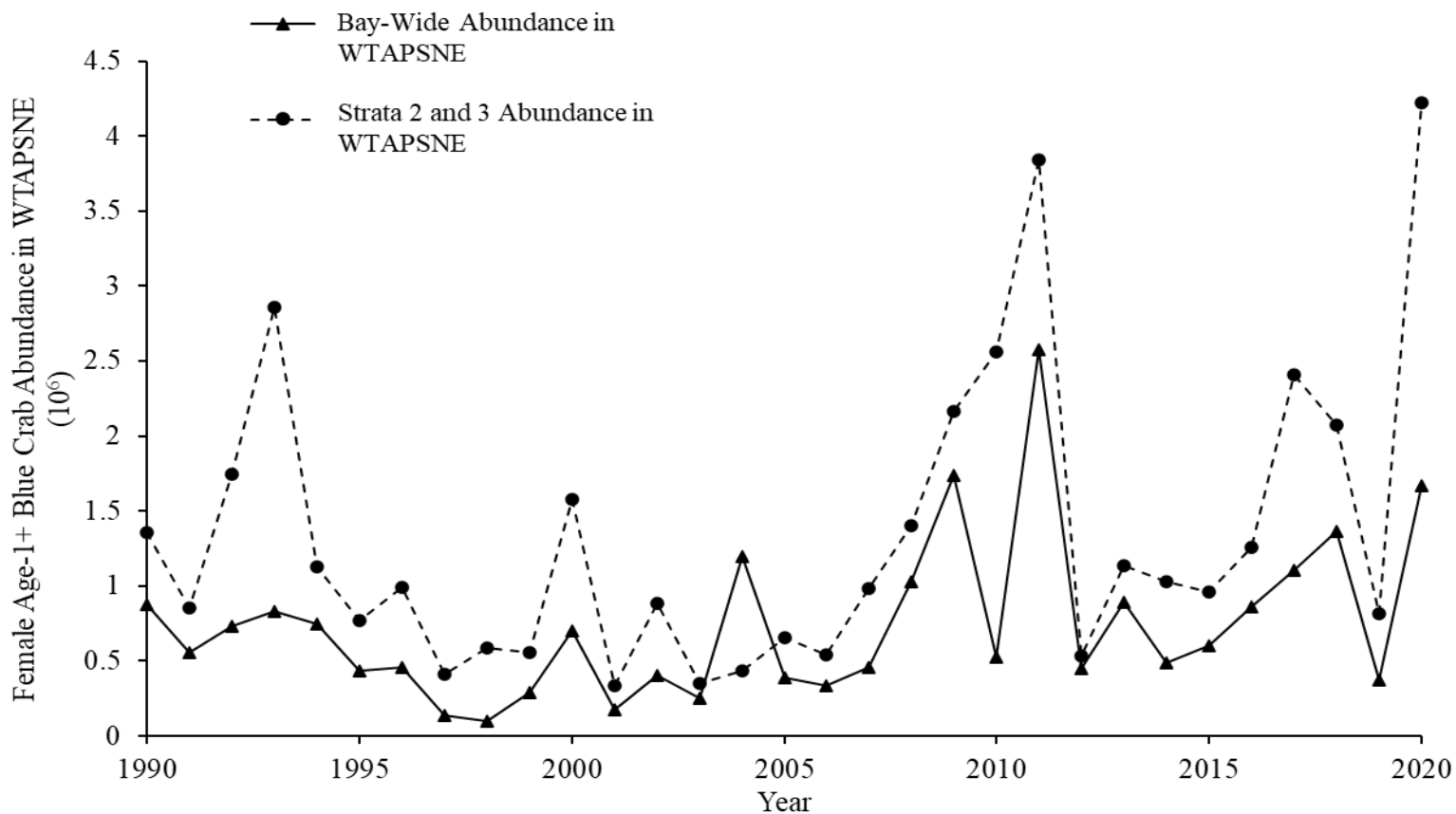


Figure 3.59. Comparison of female age-1+ blue crab abundance estimates in WTAPSNE (millions) based on Davis WDS data either for Bay-wide or Strata 2 and 3 from 1990–2020. Shown are kriged estimates of female age-1+ Bay-wide abundance estimates in WTAPSNE (closed triangles; solid, black line) and Strata 2 and 3 abundance estimates in WTAPSNE (solid circle; dashed, black line) for 1990–2020.

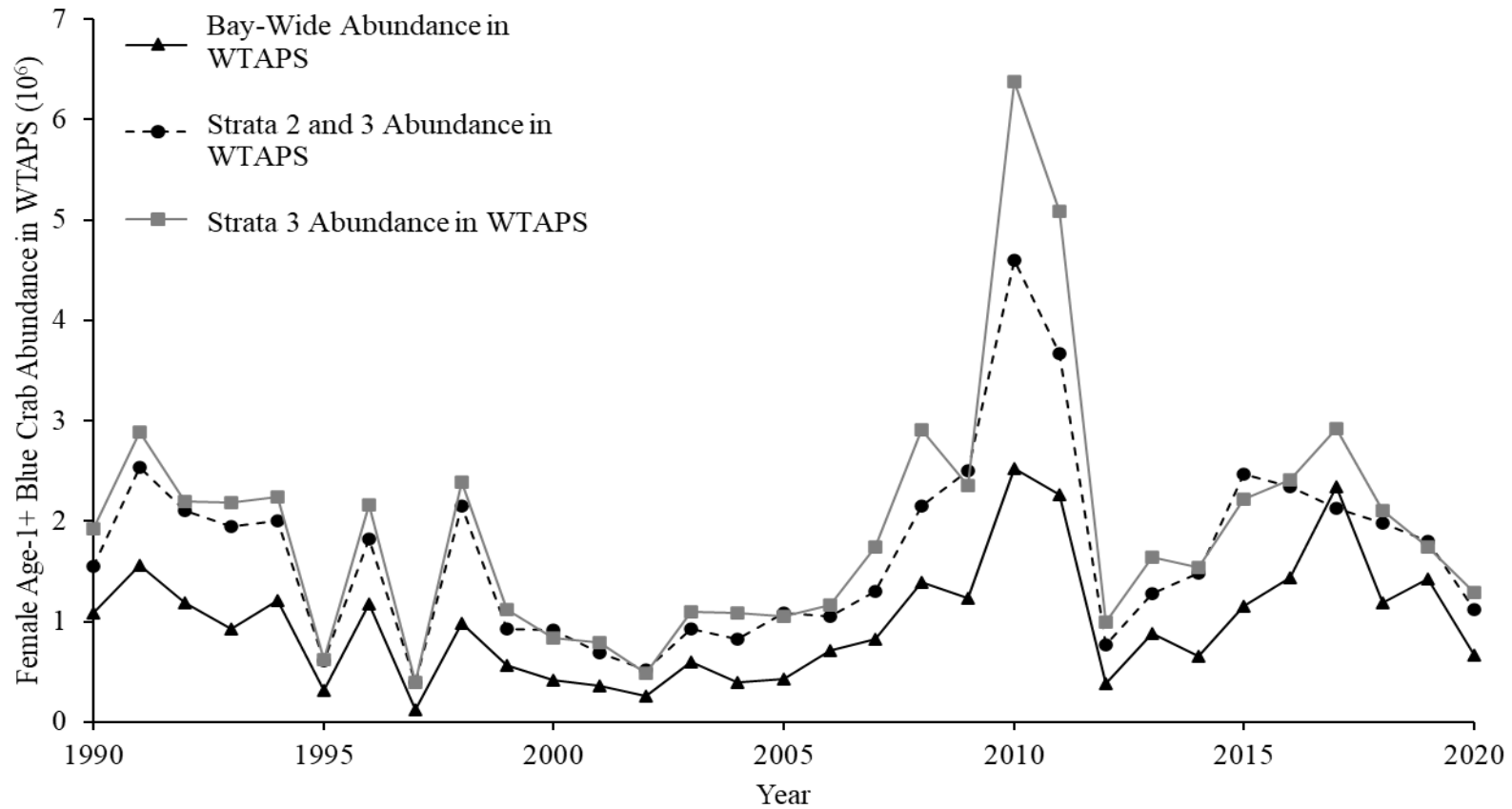


Figure 3.60. Comparison of female age-1+ blue crab abundance estimates in WTAPS (millions) based on either Davis WDS Chesapeake Bay (Bay-wide) or Davis WDS Strata data either for Bay-wide, strata 2 and 3, or strata 3 only from 1990–2020. Shown are kriged estimates of female age-1+ Bay-wide abundance estimates in WTAPS (closed triangles; solid, black line), Strata 2 and 3 abundance estimates in WTAPS (solid circle; dashed, black line), and strata 3 abundance estimates in WTAPS (solid square; solid, grey line) for 1990–2020.

Chapter 4: Summary

Because of the Panama Canal expansion, the need for dredging activities in the Chesapeake Bay has increased; however, placement of dredged material in the Bay is restricted to winter months owing to concerns for threatened and endangered species. Placement of dredged material during the winter overlaps with overwintering locations for mature female blue crab. The goal of my thesis was to determine the possible impacts of dredged material placement on mature, overwintering female blue crab in two licensed placement sites from the York Split Channel in the Chesapeake Bay: i) Wolf Trap Alternate Open Water Placement Site (WTAPS) and ii) WTAPS northern extension (WTAPSNE).

In Chapter 2, I conducted an exploratory analysis prior to the final analyses in Chapter 3. In Chapter 2, I created inverse distance weighting (IDW) maps of blue crab abundance in the Chesapeake Bay, WTAPS, and WTAPSNE, from 1990–2018 using winter dredge survey data to provide baseline estimates. I also analyzed the effects of resolution, variogram model selection, and the importance of the normality assumption of kriging. The exploratory analysis indicated that the effects of the analyzed criteria indicated minor differences in blue crab estimates. Because of results from Chapter 2, I performed ordinary kriging on the untransformed, skewed, zero-inflated WDS data in Chapter 3. In Chapter 3, I also performed kriging based on the selected fitted variogram using *autofitVariogram* with prediction grid of 250-m².

The goal of Chapter 3 was to determine the possible impacts to mature, overwintering female blue crab in two licensed placement sites for dredged material from the York Split Channel in the Chesapeake Bay: i) WTAPS and ii) WTAPSNE. Chapter 3 was accomplished by using the WDS data to visualize the distribution of

overwintering female blue crab and estimate female abundance in Chesapeake Bay through ordinary kriging each year from 1990–2020. Following Bay-wide estimation of females in the Chesapeake Bay, estimates were also derived in WTAPS and WTAPSNE by extracting estimates of females to develop worst-case scenario estimates of mature, overwintering females in the two placement areas. The effects of small-scale estimation on female blue crab in the two placement sites were also evaluated by calculating abundance in the different strata of the WDS.

Small-scale estimation effected female age-1+ abundance estimates in the Chesapeake Bay, WTAPS, and WTAPSNE. However, the results indicated that placement activities would result in the deaths of an average of 0.59% of all age-1+ female blue crab based on the Bay-wide distribution and up to 1.18% of all age-1+ females when estimates are based solely on strata 3. Compared to the exploitation rates of age-1+ female crabs in the Chesapeake Bay, placement of dredged material in WTAPS was 30-60 times lower than the threshold exploitation level. Variability of abundance estimates was high when female age-1+ abundance was less than 150 million in the Chesapeake Bay. Therefore, we suggest the Port limit placement of dredged materials in WTAPS and WTAPSNE when female age-1+ abundance is less than 150 million; we recommend the Port not undertake placement activities when the stock is declared overfished.

The geostatistical analysis of kriging was an essential tool to estimate blue crab abundance in the Chesapeake Bay and estimating blue crab at smaller scales in WTAPS and WTAPSNE. Kriging provided blue crab abundance estimates from 1990–2020 for females age-1+, males age-1+, juveniles age-0, and total blue crab

(females and males of all ages) in the Chesapeake Bay. Additionally, kriging provided visualization of blue crab abundance estimates for each life stage and sex that could be used for management of blue crab. These distributional abundance maps may be especially essential for the current management of juvenile blue crab in the Chesapeake Bay. Currently, juvenile blue crab abundance in the Chesapeake Bay has been declining since 2019 (CBSAC 2022). Juvenile blue crab abundance estimates in 2021 hit a record low since the WDS first began in 1990 (CBSAC 2022). When 2021 and 2022 WDS data are available, our kriging analysis can be used to assess the distributional patterns of juveniles in the Chesapeake Bay. If high abundance areas are identified within the abundance maps, marine protected areas can be defined to protect essential juvenile habitat.

It is important to note the complexity of kriging. Kriging has two main assumptions: i) stationarity and ii) isotropy. Stationarity of the data to be analyzed is at the hands of the researcher. To my knowledge, there is no simple test to determine if data are stationary. For my analyses, I removed underlying trends by multiple linear regression models to satisfy the assumption of kriging. Although, there is no indication whether the WDS data satisfied the stationarity assumption. There are also minor assumptions of kriging (e.g., normal distribution of data). There are also criteria during the kriging procedure that the researcher decides: i) cell resolution (Chapter 2), ii) variogram model selection (Chapter 2), and iii) maximum neighbors selection. These decisions and assumptions decided by the researcher, no matter how minor, change the abundance estimated within a given area.

The winter dredge survey data also proved to be essential for my analyses. The intensive survey of approximately 1,500 sampling locations in the Chesapeake Bay ensured that small-scale estimates could effectively be determined in WTAPS and WTAPSNE through kriging. However, obtaining WDS data with limited errors proved to be difficult. For my analyses, there were two different WDS files that differed in the points that were retained following QA/QC procedures. Glenn Davis provided WDS data for kriging analyses for which I am extremely grateful. Although, the WDS data provided by Davis contained errors associated with the location of sampling stations. Davis was able to correct most points in MD, but some MD locations and VA locations had to be removed due to incorrect strata designations. Even with the extensive sampling locations, retaining all sampling locations should be a priority to obtain precise estimates of blue crab in the Chesapeake Bay. In the future, I suggest Maryland Department of Natural Resources (MDNR) and the Virginia Institute of Marine Science (VIMS) provide the WDS as open source following QA/QC procedures to ensure that analyses for blue crab in Chesapeake Bay are conducted on a singular WDS file.

Appendix A: R-Code for Kriging Analyses

```
#####  
##           WDS analysis  
##  
## Code seeks to undertake kriging analysis and visualization  
## of winter dredge survey data for blue crab in the Chesapeake  
## Bay and in Wolf Trap, a 2,300 acre site in the lower Bay and a northern  
## extension alternative to Wolf Trap, where dredge  
## material is placed  
##  
##  
## Authors: Sarah Jones (sjones@umces.edu)  
##           Thomas J. Miller (miller@umces.edu)  
##  
## Created Date: 2020/11/16   Edited: 2022/06/28  
#####  
  
rm(list=ls(all=TRUE))  
graphics.off()  
cls <- function() cat(rep("\n",100)); cls()  
  
library(tidyverse)  
library(tidyr)  
library(dplyr)  
library(grDevices)  
library(ggplot2)  
library(foreign) # to read dbf file  
library(gstat)   # for the kriging  
library(sf)      # for spatial data  
library(automap) # for autofit of the variogram model  
library(sp)      # to produce prediction grid  
library(raster)  # mask function  
library(gridExtra) # arrange the plots in a single jpeg  
  
resol<-250 ###Resolution of grid cell in meters  
  
indirectory<-"P:/" #set where the data files are located  
outdirectory<-"P:/" #set where the outputs are placed  
  
###  
AnalVarList<-c("Tot", "Females", "Juv", "Males") ##List of the different  
##life stages of blue crab to loop through for abundance estimates
```

```

for(adx in 1:length(AnalVarList)){
  AnalVarTxt<-AnalVarList[adx] ## list of life stages to analyze in loops
  dir.create(AnalVarTxt) ##Create output folder for AnalVarList

##Categories of output. Creates folders for each category of outputs. Creating
directories for each.
densityresid<-dir.create(paste(outdirectory,AnalVarTxt,"/Density
Residuals/",sep=""), showWarnings = TRUE)
variogramplots<-
dir.create(paste(outdirectory,AnalVarTxt,"/Variogramplots/",sep=""), showWarnings
= TRUE)
backtrans<-dir.create(paste(outdirectory,AnalVarTxt,"/BackTrans/",sep=""),
showWarnings = TRUE)
krigtrend<-dir.create(paste(outdirectory,AnalVarTxt,"/krigtrendmap/",sep=""),
showWarnings = TRUE) ## 4 plot output
WTNEclip<-dir.create(paste(outdirectory,AnalVarTxt,"/WTNEclip",resol, "/",
sep=""), showWarnings = TRUE)
##Writes code that refers to the folders above
densityresid<-paste(outdirectory,AnalVarTxt,"/Density Residuals/",sep="")
variogramplots<-paste(outdirectory,AnalVarTxt,"/Variogramplots/",sep="")
backtransplots<-paste(outdirectory,AnalVarTxt,"/BackTrans/",sep="")
krigtrend<-paste(outdirectory,AnalVarTxt,"/krigtrendmap/",sep="")
WTNEclip<-paste(outdirectory,AnalVarTxt,"/WTNEclip",resol, "/", sep="")

WDSFile <- paste(indirectory, "WDS.csv",sep="")

qtable <- paste(indirectory, "Catchability Table.csv",sep="") ##Add Catchability
coefficients to the directory

WDSData <- subset(read.csv(WDSFile, as.is=FALSE))

qtable<-read.csv(qtable,as.is=FALSE) ##Catchability coefficients according to
different vessels
WDSData <- left_join(WDSData, qtable) ##Joining the data and catchability
coefficients according to the year and corresponding vessels and vessel captains

##Setting the Working Data to be analyzed for kriging
WorkingData<-data.frame(matrix(ncol=19,nrow=nrow(WDSData)))
colnames(WorkingData)<-c("Year", "Easting", "Northing", "Vessel", "q", "Tot",
"Fem", "Male", "Juv", "Area", "Tot_Area", "F_TotArea", "Juv_Area", "Male_Area",
"Tot_Q", "F_Q", "Juv_Q", "Male_Q", "ZVar")
WorkingData$Year<-WDSData$YEAR
WorkingData$Easting<-WDSData$Easting
WorkingData$Northing<-WDSData$Northing
WorkingData$Vessel<-WDSData$VESSEL

```



```

WorkingData$q<-WSDData$CATCH_q
WorkingData$Tot<-WSDData$T
WorkingData$Fem<-WSDData$Female
WorkingData$Male<-WSDData$Male
WorkingData$Juv<-WSDData$Juv
WorkingData$Area<-WSDData$AREA
##Adjusting for the tow area
WorkingData$Tot_Area<-WSDData$T/WSDData$AREA
WorkingData$F_TotArea<-WSDData$Female/WSDData$AREA
WorkingData$Juv_Area<-WSDData$Juv/WSDData$AREA
WorkingData$Male_Area<-WSDData$Male/WSDData$AREA
##Adjusting for the catchability Coefficient
WorkingData$Tot_Q<-(WorkingData$Tot_Area)/(WorkingData$q)
WorkingData$F_Q<-(WorkingData$F_TotArea)/(WorkingData$q)
WorkingData$Juv_Q<-(WorkingData$Juv_Area)/(WorkingData$q)
WorkingData$Male_Q<-(WorkingData$Male_Area)/(WorkingData$q)

##Select ZVar based on the life stage to analyze
ZVar <- case_when(
  AnalVarTxt %in% "Tot" ~ "Tot_Q",
  AnalVarTxt %in% "Females" ~ "F_Q",
  AnalVarTxt %in% "Males" ~ "Male_Q",
  AnalVarTxt %in% "Juve" ~ "Juv_Q",
)

WorkingData$ZVar<-WorkingData[[ZVar]] # Use the WSDData[] command because
ZVar is dynamic
WorkingData$ZVar<-WorkingData$ZVar*resol*resol

YearMin <-min(WorkingData$Year)
YearMax <-max(WorkingData$Year)
nYears<-YearMax-YearMin + 1 ##setting the number of years to analyze

#remove duplicate locations

WorkingData<-WorkingData %>% group_by(Year) %>% distinct(Easting, Northing,
.keep_all=TRUE)

#####
#Build the spatial domain for predictions for the Chesapeake Bay, Wolf Trap, and
Northern Extension in NAD83 Zone 18

CBshp <- st_read(paste(indirectory,'OutlineChesBayNAD83.shp',sep=''))

WTshp <- st_read(paste(indirectory,'WolfTrap.shp',sep=''))
WTshp <- st_zm(WTshp) ##remove the Z in order to do raster clip

```

```

NEshp <- st_read(paste(indirectory,'NorthernExtWT.shp',sep=""))
NEshp <- st_zm(NEshp) ##remove the Z in order to do raster clip

##National Weather Service NOAA U.S. States and Territories Map
##https://www.weather.gov/gis/USStates
USMap <- st_read(paste(indirectory,'StateBound_Zone18.shp',sep=""))
ChesBay <- st_crop(USMap, xmin = 250000, xmax = 490000, ymin = 4050000,
ymax = 4450000)
CBLand<-st_transform(ChesBay,26918) ##converts to NADS 1983 in Zone 18

##### Create the grid on which predictions will be made
Xmin<-min(WorkingData$Easting)
Ymin<-min(WorkingData$Northing)

# calculate the number of 250m cells in each direction
x_length<-max(WorkingData$Easting-Xmin)
y_length<-max(WorkingData$Northing-Ymin)

x_length<-147000
y_length<-325000
nx<-round(x_length/resol,0) ##how many cells to krig
ny<-round(y_length/resol,0)

coordinates(WorkingData)<-~Easting+Northing

grid =
GridTopology(cellcentre.offset=c(Xmin,Ymin),cellsize=c(resol,resol),cells.dim=c(nx,
ny))

pLocations<-
SpatialPixelsDataFrame(grid,data=data.frame(id=1:prod(nx,ny)),proj4string=CRS("+
proj=utm +zone=18 +ellps=GRS80 +datum=NAD83")) ## the locations to krig

#####
##
##          FUNCTIONS
## The third creates a data frame that will hold the best parameter###
## estimates from the experimental variogram.      ###
##                                     ###
#####
##

##Outputting the AIC values for the 10 models by year as a csv file

```

```

AIC<-data.frame(Year=integer(),
  Model1=double(),
  Model2=double(),
  Model3=double(),
  Model4=double(),
  Model5=double(),
  Model6=double(),
  Model7=double(),
  Model8=double(),
  Model9=double(),
  Model10=double()
)

```

```

GeoStatFits<-data.frame(Year=integer(),
  Model=character(),
  Nugget=double(),
  pSill=double(),
  Range=double(),
  kappa=double(),
  SSE=double(),
  stringsAsFactors = FALSE
)

```

```

# Define a csv file with the results of the abundance estimates, to include
# Year
# CBAbundNoZeros - the sum of the values greater than or equal to 0 in every
estimated pixel for the Chesapeake Bay
# nCells - the number of pixels for which estimates were developed for the
Chesapeake Bay
# pArea - the total area of the Bay for which estimates were developed (km2) for the
Chesapeake Bay
# WTAbundNoZeros - the sum of the values greater than or equal to 0 in every
estimated pixel in WTAPS
# Percent_Prop_in_WT - Proportion of blue crab in Wolf Trap out of the total Bay-
wide population (%)
# NEAbundNoZeros - the sum of the values greater than or equal to 0 in every
estimated pixel in Northern Extension
# Percent_Prop_in_NE - Proportion of blue crab in Northern Extension out of the
total Bay-wide population (%)

```

```

GeoEst<-data.frame(Year=integer(),
  CBAbundNoZeros=double(),
  nCells=double(),
  pArea=double(),

```

```

        WTAbundNoZeros=double(),
        Percent_Prop_in_WT=double(),
        NEAbundNoZeros=double(),
        Percent_Prop_in_NE=double()
    )

##Extracted coefficients of the best fitted regression model that residuals were
##extracted from and kriged predictions were derived from
BacktoOriginal<-data.frame(Year=integer(),
    Intercept=double(),
    Easting=double(),
    Northing=double(),
    EastingSq=double(),
    NorthingSq=double(),
    EN=double(),
    EESq = double(),
    NESq = double(),
    ENSq = double(),
    NNSq = double(),
    ESqNSq = double(),
    ENESq = double(),
    ENNSq = double(),
    EESqNSq = double(),
    NESqNSq = double(),
    ENESqNSq =double()
)

#####
##          Estimate Variograms for each WDS Year      ##
##                                     ##
## The estimation evaluates fit to matern, exponential, ##
## spherical, and, Gaussian models, and selects the best ##
## fitting model based on SSE. It reports variables for the ##
## best fitting model. The code also produces maps of the ##
## normalized variables, empirical variograms and fitted ##
## variogram plots for each year of the WDS.      ##
#####

for(idx in 1:nYears){
  iYear<-idx+YearMin-1
  WDSiYear<-as.data.frame(WorkingData[WorkingData$Year==iYear,])
  ## Table for the data and write to data
  ## This table will change according to the transformation method. As is,
  ## this results in untransformed estimates

```

```

ZVar.trn=WDSiYear$ZVar
WDSiYear[["zZVar"]]<-ZVar.trn
#####
#####
number <- iYear
##Density maps for the original data
density<- ggplot(WDSiYear) +
  geom_sf(data = CBshp,fill='White')+
  geom_point(data = WDSiYear, aes(x = Easting, y = Northing,
color=zZVar),size=2)+
  scale_color_gradient(low="blue", high="red")+
  labs(col="Number of Blue Crabs") +
  labs(x="",y="")+
  theme_minimal()

#####
#####
## New section that fits multiple linear models, calculates the best fitting model
## based on AIC criteria.
## Code also creates an object that can be used for a trend map for comparison with
krigged data

# Create model names
ModelText <- rep("Model",10)
ModelNum <- seq(1:10)
ModelIdx <- list(Model=(paste(ModelText,ModelNum,sep="")))

WDSiYear$EastingSq=WDSiYear$Easting * WDSiYear$Easting
WDSiYear$NorthingSq=WDSiYear$Northing*WDSiYear$Northing

#Build the models

Model1 <- lm(zZVar ~ 1, data=WDSiYear)
Model2 <- lm(zZVar ~ Easting, data=WDSiYear)
Model3 <- lm(zZVar ~ Northing, data=WDSiYear)
Model4 <- lm(zZVar ~ Easting + Northing, data=WDSiYear)
Model5 <- lm(zZVar ~ Easting*Northing, data=WDSiYear)
Model6 <- lm(zZVar ~ Easting + EastingSq, data=WDSiYear)
Model7 <- lm(zZVar ~ Easting*EastingSq, data=WDSiYear)
Model8 <- lm(zZVar ~ Northing + NorthingSq, data=WDSiYear)
Model9 <- lm(zZVar ~ Northing*NorthingSq, data=WDSiYear)
Model10 <- lm(zZVar ~ Easting*Northing*EastingSq*NorthingSq,
data=WDSiYear)

ModelList <- list(Model1=Model1,
  Model2=Model2,

```

```

    Model3=Model3,
    Model4=Model4,
    Model5=Model5,
    Model6=Model6,
    Model7=Model7,
    Model8=Model8,
    Model9=Model9,
    Model10=Model10
  )

#Set up the default trend equation
FullModelNames<-t(names(Model10$coefficients))
DefaultTrendParms <- as.data.frame(matrix(0, 1,length(FullModelNames)))
colnames(DefaultTrendParms)<-FullModelNames
DefaultTrendParms$idx<-"idx"

#Determine the best fitting model
BestFit <- AIC(Model1, Model2, Model3, Model4, Model5, Model6, Model7,
Model8, Model9, Model10)
BestFit <- cbind(ModelIdx,BestFit)
BestFitModel <- BestFit[which.min(BestFit$AIC),]
BestFitModelName<-as.character(BestFitModel$Model)
BestFittingModelCoefNames <-
t(names(ModelList[[BestFitModelName]]$coefficients))
BestFitModelParms <-
as.data.frame(t(as.matrix(ModelList[[BestFitModelName]]$coefficients)))
BestFitModelParms$idx <- "idx"
BestFitModelParms <- Filter(function(x)!all(is.na(x)), BestFitModelParms)

# Define the residuals for kriging
WDSiYear$E <- resid(ModelList[[BestFitModelName]])

## plot the residuals of the best fitting model
ggsave(
  paste(densityresid,"Density Residuals_",iYear,".jpg",sep=""),
  ggplot(WDSiYear) +
    geom_sf(data = CBshp,fill='White')+
    geom_point(data = WDSiYear, aes(x = Easting, y = Northing, color=E),size=2)+
    scale_color_gradient(low="blue", high="red")+
    labs(x="", y="", col="") +
    theme_minimal(),
  width=7, height=10, dpi= 300, bg="white",units="in",device='jpeg'
)

#Print results to folder through sink

```

```

sink(paste(outdirectory,AnalVarTxt,"/lmYear",iYear,".txt",sep=""))
  print(summary(ModelList[[BestFitModelName]]))
sink()

# Save results to AIC object
AIC[idx,1]<-iYear
  for (mdx in 2:11) {
    AIC[idx,mdx]<- AIC(ModelList[[paste("Model",(mdx-1),sep="")]])
  }
# Final Trend Model Parms in standard order
df1<-DefaultTrendParms %>% dplyr::select(-names(BestFitModelParms))
df1$idx <- "idx"
TrendModelParms <- merge(x=df1,y=BestFitModelParms, by="idx", all.x=TRUE)
TrendModelParms <-TrendModelParms[,names(DefaultTrendParms)]

# Write coefficients to BacktoOriginal
BacktoOriginal[idx,1]<-iYear
for (tdx in 2:17) {
  BacktoOriginal[idx,tdx]<- TrendModelParms[1,(tdx-1)]
}

#####
### Fit variogram based on the best selected model's residuals

coordinates(WDSiYear)=~Easting + Northing

emp.vg = variogram(E~1,data=WDSiYear,cutoff = 100000,width =1000) # isotropic
zTot_N
max <- max(emp.vg$gamma) ## for mapping the variogram in the loop

ggsave(
  paste(variogramplots,"Empirical Variogram_",iYear,".jpg",sep=""),
  ggplot(emp.vg, aes(x=dist,y=gamma))+
  geom_point(shape=1,color="blue",size=2)+
  scale_y_continuous(limits=c(0,1.5*max))+
  labs(x="",y="")+
  theme_minimal(),
  width=7, height=10, dpi= 300, bg="white",units="in",device='jpeg'
)

##Getting the output to a text file for all models tested within autofitVariogram
sink(paste(outdirectory,AnalVarTxt,"/FitVario",iYear,".txt",sep=""))
fit.vg<-autofitVariogram(E~1,WDSiYear,model=c("Mat", "Gau", "Exp",
"Sph"),verbose=TRUE)
print(fit.vg[iYear]) # print the stuff
sink() # close the sink!

```

```

# Inow use this to extract the variables from the model to create the fitted variogram
model
fit.vm <- vgm(psill = fit.vg$var_model[2,2], toString(fit.vg$var_model[2,1]),
fit.vg$var_model[2,3], anis = c(0, 0, 0, 1.0, 1.0), nugget=fit.vg$var_model[1,2],
kappa=fit.vg$var_model[2,4])
# check the variogram model parameters

fit.vm.line<-variogramLine(fit.vm,maxdist=max(emp.vg$dist))

ggsave(
  paste(variogramplots,"Fitted Variogram_",iYear,".jpg",sep=""),
  ggplot(emp.vg, aes(x=dist,y=gamma))+
  geom_point(shape=1,color="blue",size=2)+
  geom_line(data=fit.vm.line,color="blue")+
  scale_y_continuous(limits=c(0,1.5*max))+
  labs(x="",y="")+
  theme_minimal(),
  width=7, height=10, dpi= 300, bg="white",units="in",device='jpeg'
)

#now write the variogram model that was selected in autofitVariogram

GeoStatFits[idx,1]<-iYear
GeoStatFits[idx,2]<- toString(fit.vg$var_model[2,1])
GeoStatFits[idx,3]<- fit.vg$var_model[1,2]
GeoStatFits[idx,4]<- fit.vg$var_model[2,2]
GeoStatFits[idx,5]<- fit.vg$var_model[2,3]
GeoStatFits[idx,6]<- fit.vg$var_model[2,4]
GeoStatFits[idx,7]<- fit.vg$sser

##output all the csvs created
write.csv(GeoStatFits,paste(outdirectory,AnalVarTxt,"/GeoStatFits.csv",sep=""),row.
names=FALSE)
write.csv(AIC,paste(outdirectory,AnalVarTxt,"/AIClmFuntions.csv",sep=""),row.na
mes=FALSE)
write.csv(BacktoOriginal,paste(outdirectory,AnalVarTxt,"/Coefficients.csv",sep=""),r
ow.names=FALSE)

#####
#####
##      NOW PRODUCE THE KRIGED SURFACE      ##
##                                          ##

```



```

## This conducts kriging on the WDS having already fit variograms in the      ##
## previous step. The program reads in the GeoStatsFits file that holds the  ##
## variogram models and the specific parameter estimates. It also relies on the ##
## matrix of predicted locations (pLocations) from the first steps of the program ##
## over which kriged predictions will be made. Estimates of abundance and the  ##
## sampling variance at each location. The code also produces predication and ##
## variance maps for each year of the WDS                                  ##
#####
#####

proj4string(WDSiYear)=CRS("+proj=utm +zone=18 +ellps=GRS80
+datum=NAD83")

## run ordinary kriging
crab.kr <- krige(formula = E~1, WDSiYear, pLocations, model = fit.vm,
maxdist=40000,nmax=25,debug.level=-1) ##40 k

##backtransform based on the best fitting model's extracted coefficients
crab.kr$crab.kr.back <- crab.kr$var1.pred+
  TrendModelParms[1,1]+
  (TrendModelParms[1,2] * crab.kr$s1)+
  (TrendModelParms[1,3] * crab.kr$s2)+
  (TrendModelParms[1,4] * crab.kr$s1*crab.kr$s1)+
  (TrendModelParms[1,5] * crab.kr$s2* crab.kr$s2)+
  (TrendModelParms[1,6] * crab.kr$s1* crab.kr$s2)+
  (TrendModelParms[1,7] * crab.kr$s1* crab.kr$s1*crab.kr$s1)+
  (TrendModelParms[1,8] * crab.kr$s2* crab.kr$s1*crab.kr$s1)+
  (TrendModelParms[1,9] * crab.kr$s1* crab.kr$s2*crab.kr$s2)+
  (TrendModelParms[1,10] * crab.kr$s2*crab.kr$s2*crab.kr$s2)+
  (TrendModelParms[1,11] * crab.kr$s1*crab.kr$s1*crab.kr$s2*crab.kr$s2)+
  (TrendModelParms[1,12] * crab.kr$s1* crab.kr$s2*crab.kr$s1*crab.kr$s1)+
  (TrendModelParms[1,13] * crab.kr$s1* crab.kr$s2*crab.kr$s2*crab.kr$s2)+
  (TrendModelParms[1,14] * crab.kr$s1*
crab.kr$s1*crab.kr$s1*crab.kr$s2*crab.kr$s2)+
  (TrendModelParms[1,15] * crab.kr$s2*
crab.kr$s1*crab.kr$s1*crab.kr$s2*crab.kr$s2)+
  (TrendModelParms[1,16] * crab.kr$s1*
crab.kr$s2*crab.kr$s1*crab.kr$s1*crab.kr$s2*crab.kr$s2)

##Same units as crab abundance in meters
crab.kr$crab.back.se = sqrt(crab.kr$var1.var)

##Clip the kriged surface to the Chesapeake Bay to estimate blue crab abundance
crab.kr.back<-raster(crab.kr,layer=3,values=TRUE)
clipped_back<-mask(crab.kr.back,CBshp)
clipped_predict_back<-as(clipped_back,"SpatialGridDataFrame")

```

```

clipped_krige_back<-as.data.frame(clipped_predict_back, xy=TRUE)
colnames(clipped_krige_back)<-c("value","Easting","Northing")

##removing values that are less than zero
No_Zeros <- clipped_krige_back[which(clipped_krige_back$value > 0),]

GeoEst[idx, 1] <- iYear
GeoEst[idx,2]<-sum(No_Zeros$value)
GeoEst[idx,3]<-length(clipped_krige_back$value)
GeoEst[idx,4]<-GeoEst[idx,3]*resol*resol/10^6

##comparing the original data, residuals, predicted kriging values,
##and the back transformed kriged estimates based on the coefficients of the
##best selected model
jpeg(paste(backtransplots,"Back Transformations_",iYear,".jpg",sep=""),width=7,
height=10, res= 300, bg="white",units="in")
par(mfrow=c(4, 2))
hist(WDSiYear$zZVar,main=paste("Abundance of Total Blue Crab for
",number,sep=""),xlab="Original Abundance",nclass = 15)
plot(ecdf(WDSiYear$zZVar),main=paste("Abundance of Total Blue Crab for ",
number),xlab="Original Abundance",ylab="Cumulative")
hist(WDSiYear$E,main=paste("Residual Abundance of Total Blue Crab for
",number,sep=""),xlab="Residual Abundance",nclass = 15)
plot(ecdf(WDSiYear$E),main=paste("Residual Abundance of Total Blue Crab for
",number,sep=""),xlab="Residual Abundance",ylab="Cumulative")
hist(crab.kr$var1.pred,main=paste("Kriging Abundance of Total Blue Crab for
",number,sep=""),xlab="Kriging Abundance",nclass = 15)
plot(ecdf(crab.kr$var1.pred),main=paste("Kriging Abundance of Total Blue Crab
for ",number,sep=""),xlab="Kriging Abundance",ylab="Cumulative")
hist(crab.kr$crab.kr.back,main=paste("Backtransformed Abundance of \nTotal Blue
Crab for ",number,sep=""),xlab="BackTransformed Abundance",nclass = 15)
plot(ecdf(crab.kr$crab.kr.back),main=paste("Backtransformed Abundance of
\nTotal Blue Crab for ",number,sep=""),xlab="Backtransformed
Abundance",ylab="Cumulative")
dev.off()

# clipping the standard error estimates to the Chesapeake Bay
crab.kr.proj.se<-raster(crab.kr,layer=4,values=TRUE)
clipped_se<-mask(crab.kr.proj.se,CBshp)
clipped_predict_se<-as(clipped_se,"SpatialPixelsDataFrame")

clipped_krige_se<-as.data.frame(clipped_predict_se)

colnames(clipped_krige_se)<-c("value","x","y")

```

```

##Setting the Bins for standard error maps
clipped_krige_se <- clipped_krige_se %>%
  mutate(binned = cut(
    # the variable you want to bin
    x = clipped_krige_se$value,
    # The bins you want. Here it splits the data in 10% quantiles
    breaks = c(-200000000000000000, 0, 2000, 4000, 6000, 8000, 10000, 12000,
14000, 16000, 18000, 20000, 200000000000000000),
    labels = c("< 0", "0-2,000", "2,001-4,000", "4,001-6,000", "6,001-8,000", "8,001-
10,000",
              "10,001-12,000", "12,001-14,000", "14,001-16,000", "16,001-18,000",
"18,001-20,000", "> 20000"),
    # Include 0 with the lowest quantile
    include.lowest = TRUE,
    # ordered bins make for better plotting
    ordered_result = TRUE)
  )

```

```

##Setting the Bins for Mapping back transformed estimates
clipped_krige_back <- clipped_krige_back %>%
  mutate(binned = cut(
    # the variable you want to bin
    x = clipped_krige_back$value,
    # The bins you want. Here it splits the data in 10% quantiles
    breaks = c(-200000000000000000, 0, 2000, 4000, 6000, 8000, 10000, 12000,
14000, 16000, 18000, 20000, 200000000000000000),
    labels = c("< 0", "0-2,000", "2,001-4,000", "4,001-6,000", "6,001-8,000", "8,001-
10,000",
              "10,001-12,000", "12,001-14,000", "14,001-16,000", "16,001-18,000",
"18,001-20,000", "> 20000"),
    # Include 0 with the lowest quantile
    include.lowest = TRUE,
    # ordered bins make for better plotting
    ordered_result = TRUE)
  )

```

```

## for plotting the trend
crab.kr$trend <- TrendModelParms[1,1]+
  (TrendModelParms[1,2] * crab.kr$s1)+
  (TrendModelParms[1,3] * crab.kr$s2)+
  (TrendModelParms[1,4] * crab.kr$s1*crab.kr$s1)+
  (TrendModelParms[1,5] * crab.kr$s2* crab.kr$s2)+
  (TrendModelParms[1,6] * crab.kr$s1* crab.kr$s2)+
  (TrendModelParms[1,7] * crab.kr$s1* crab.kr$s1*crab.kr$s1)+

```

```

(TrendModelParms[1,8] * crab.kr$s2* crab.kr$s1*crab.kr$s1)+
(TrendModelParms[1,9] * crab.kr$s1* crab.kr$s2*crab.kr$s2)+
(TrendModelParms[1,10] * crab.kr$s2*crab.kr$s2*crab.kr$s2)+
(TrendModelParms[1,11] * crab.kr$s1*crab.kr$s1*crab.kr$s2*crab.kr$s2)+
(TrendModelParms[1,12] * crab.kr$s1* crab.kr$s2*crab.kr$s1*crab.kr$s1)+
(TrendModelParms[1,13] * crab.kr$s1* crab.kr$s2*crab.kr$s2*crab.kr$s2)+
(TrendModelParms[1,14] * crab.kr$s1 *
crab.kr$s1*crab.kr$s1*crab.kr$s2*crab.kr$s2)+
(TrendModelParms[1,15] * crab.kr$s2*
crab.kr$s1*crab.kr$s1*crab.kr$s2*crab.kr$s2)+
(TrendModelParms[1,16] * crab.kr$s1 *
crab.kr$s2*crab.kr$s1*crab.kr$s1*crab.kr$s2*crab.kr$s2)

```

```

##clipping the trend map to the Chesapeake Bay
crab.kr.trend<-raster(crab.kr,layer=5,values=TRUE)
clipped_trend<-mask(crab.kr.trend,CBshp)
clipped_predict_trend<-as(clipped_trend,"SpatialGridDataFrame")

```

```

clipped_krige_trend<-as.data.frame(clipped_predict_trend, xy=TRUE)
colnames(clipped_krige_trend)<-c("value","Easting","Northing")

```

```

##Setting the Bins for Mapping the trend map
clipped_krige_trend <- clipped_krige_trend %>%
mutate(binned = cut(
  # the variable you want to bin
  x = clipped_krige_trend$value,
  # The bins you want. Here it splits the data in 10% quantiles
  breaks = c(-2000000000000000000, 0, 2000, 4000, 6000, 8000, 10000, 12000,
14000, 16000, 18000, 20000, 2000000000000000000),
  labels = c("< 0", "0-2,000", "2,001-4,000", "4,001-6,000", "6,001-8,000", "8,001-
10,000",
            "10,001-12,000", "12,001-14,000", "14,001-16,000", "16,001-18,000",
"18,001-20,000", "> 20000"),
  # Include 0 with the lowest quantile
  include.lowest = TRUE,
  # ordered bins make for better plotting
  ordered_result = TRUE)
)

```

```

##plotting the trend map for the Chesapeake Bay
TrendMap <- ggplot(data = clipped_krige_trend) +
  geom_sf(data = CBshp, fill="#003366")+
  geom_raster(data=clipped_krige_trend,aes(x=Easting,y=Northing,fill=binned)) +
  scale_fill_manual(values=c('purple', 'blue4', 'blue2','deepskyblue',
'mediumaquamarine','yellowgreen', 'yellow', 'gold2', 'orange', 'darkorange2',
'orangered', 'red4'), drop=FALSE)+

```

```

labs(fill=paste("# of Crabs/Pixel",sep=""))+
geom_sf(data = CBLand, fill="#669933",color='darkblue')+
labs(x="",y="")+
theme_minimal()
##Plotting the backtransformed estimates for the Chesapeake Bay
backmap <- ggplot(data = clipped_krige_back) +
geom_sf(data = CBshp, fill="#003366")+
geom_raster(data=clipped_krige_back,aes(x=Easting,y=Northing,fill=binned)) +
scale_fill_manual(values=c('purple', 'blue4', 'blue2','deepskyblue',
'mediumaquamarine','yellowgreen', 'yellow', 'gold2', 'orange', 'darkorange2',
'orangered', 'red4'), drop=FALSE) +
labs(fill=paste("# of Crabs/Pixel",sep=""))+
geom_sf(data = CBLand, fill="#669933",color='darkblue')+
labs(x="",y="")+
theme_minimal()
##Plotting the standard error of the kriged prediction for the Chesapeake Bay
semap <- ggplot(data = clipped_krige_se) +
geom_sf(data = CBshp, fill="#003366")+
geom_raster(data=clipped_krige_se,aes(x=x,y=y,fill=binned)) +
scale_fill_manual(values=c('purple', 'blue4', 'blue2','deepskyblue',
'mediumaquamarine','yellowgreen', 'yellow', 'gold2', 'orange', 'darkorange2',
'orangered', 'red4'), drop=FALSE) +
labs(fill=paste("Standard Error",sep=""))+
geom_sf(data = CBLand, fill="#669933",color='darkblue')+
labs(x="",y="")+
theme_minimal()

##plotting the four within the same jpeg by year
allmaps <- grid.arrange(density, TrendMap, backmap, semap, nrow=2, ncol=2)
ggsave(
paste(krigtrend,"KrigeMapTrend_",resol,"_",iYear,".jpg",sep=""), allmaps,
width=15, height=15, dpi= 300, bg="white",units="in",device='jpeg'
)

#####Northern Extension
##clipping the backtransformed kriged predictions to WTAPSNE
NE_clipped_value<-mask(crab.kr.back,NEshp)
NE_clipped_predict_values<-as(NE_clipped_value,"SpatialGridDataFrame")

NE_clipped_krige<-as.data.frame(NE_clipped_predict_values)

colnames(NE_clipped_krige)<-c("value","x","y")

##Removing values less than zero
No_ZerosNE <- NE_clipped_krige[which(NE_clipped_krige$value > 0),]

```

```

GeoEst[idx,7]<-sum(No_ZerosNE$value)
GeoEst[idx,8]<-(GeoEst[idx,7]/GeoEst[idx,2])*100

##Setting the Bins for Mapping
NE_clipped_krige <- NE_clipped_krige %>%
  mutate(binned = cut(
    # the variable you want to bin
    x = NE_clipped_krige$value,
    # The bins you want.
    breaks = c(-2000000000000000000, 0, 2000, 4000, 6000, 8000, 10000, 12000,
14000, 16000, 18000, 20000, 2000000000000000000),
    labels = c("< 0", "0-2,000", "2,001-4,000", "4,001-6,000", "6,001-8,000", "8,001-
10,000",
      "10,001-12,000", "12,001-14,000", "14,001-16,000", "16,001-18,000",
"18,001-20,000", "> 20000"),
    # Include 0 with the lowest quantile
    include.lowest = TRUE,
    # ordered bins make for better plotting
    ordered_result = TRUE)
  )

#####WOLFTRAP CLIP
##clipping the kriged predicted values to WTAPS
WT_clipped_value<-mask(crab.kr.back,WTshp)
WT_clipped_predict_values<-as(WT_clipped_value,"SpatialGridDataFrame")

WT_clipped_krige<-as.data.frame(WT_clipped_predict_values)

colnames(WT_clipped_krige)<-c("value","x","y")

No_ZerosWT <- WT_clipped_krige[which(WT_clipped_krige$value > 0),]

GeoEst[idx,5]<-sum(No_ZerosWT$value)
GeoEst[idx,6]<-(GeoEst[idx,5]/GeoEst[idx,2])*100

##Setting the Bins for Mapping
WT_clipped_krige <- WT_clipped_krige %>%
  mutate(binned = cut(
    # the variable you want to bin
    x = WT_clipped_krige$value,
    # The bins you want.

```

```

    breaks = c(-2000000000000000000, 0, 2000, 4000, 6000, 8000, 10000, 12000,
14000, 16000, 18000, 20000, 2000000000000000000),
    labels = c("< 0", "0-2,000", "2,001-4,000", "4,001-6,000", "6,001-8,000", "8,001-
10,000",
        "10,001-12,000", "12,001-14,000", "14,001-16,000", "16,001-18,000",
"18,001-20,000", "> 20000"),
    # Include 0 with the lowest quantile
    include.lowest = TRUE,
    # ordered bins make for better plotting
    ordered_result = TRUE)
)

##mapping the kriged predictions in WTAPSNE
NE <- ggplot(data=NE_clipped_krige) +
  geom_sf(data = NEshp, fill="#003366")+
  geom_raster(data=NE_clipped_krige,aes(x=x,y=y,fill= binned))+
  scale_fill_manual(values=c('purple', 'blue4', 'blue2','deepskyblue',
'mediumaquamarine','yellowgreen', 'yellow', 'gold2', 'orange', 'darkorange2',
'orangered', 'red4'), drop=FALSE) +
  labs(fill=paste("# of Crabs/Pixel",sep=""))+
  labs(x="",y="")+
  theme_minimal() +
  theme(axis.text.x = element_text(angle = 90, hjust = 1))

##mapping the kriged prediction for WTAPS
WT <- ggplot(data=WT_clipped_krige) +
  geom_sf(data = WTshp, fill="#003366")+
  geom_raster(data=WT_clipped_krige,aes(x=x,y=y,fill= binned))+
  scale_fill_manual(values=c('purple', 'blue4', 'blue2','deepskyblue',
'mediumaquamarine','yellowgreen', 'yellow', 'gold2', 'orange', 'darkorange2',
'orangered', 'red4'), drop=FALSE) +
  labs(fill=paste("# of Crabs/Pixel",sep=""))+
  labs(x="",y="")+
  theme_minimal() +
  theme(axis.text.x = element_text(angle = 90, hjust = 1))

WTNE <- grid.arrange(WT, NE, nrow=2)
ggsave(
  paste(WTNEclip,"WTNEClipped_",resol,"_",iYear,".jpg",sep=""), WTNE,
  width=5, height=10, dpi= 300, bg="white",units="in",device='jpeg'
)
}

```

```
write.csv(GeoEst,paste(outdirectory,AnalVarTxt,"/GeoEst.csv",sep=""),row.names=F  
ALSE)}
```


Appendix B: Females

Tables for Appendix B

Table B.1. AIC values from multiple linear regression equations for female age-1+ abundance estimates derived from Bay-wide kriging using Davis WDS Chesapeake data. An * indicates the selected model used for fitting the variogram and kriging.

Year	Model1	Model2	Model3	Model4	Model5	Model6	Model7	Model8	Model9	Model10
1990	24,013	24,001	24,010	23,996	23,994	23,993	23,994	24,012	24,010	*23,982
1991	34,249	34,248	34,222	34,222	34,220	34,243	34,221	34,222	34,220	*34,185
1992	49,969	49,948	49,870	49,856	49,847	49,947	49,931	49,853	49,854	*49,788
1993	28,546	28,548	28,524	28,526	28,527	28,548	28,550	*28,521	28,521	28,525
1994	28,857	28,855	28,804	28,805	28,806	28,849	28,845	28,800	28,802	*28,766
1995	29,555	29,554	29,555	29,554	29,546	29,555	29,556	29,557	29,558	*29,526
1996	31,025	31,016	30,982	30,979	*30,977	31,016	31,013	30,984	30,982	30,985
1997	30,399	30,387	30,330	30,328	30,300	30,388	30,382	30,272	30,238	*30,204
1998	30,053	30,047	30,005	30,005	30,004	30,049	30,048	30,002	30,004	*30,002
1999	25,811	25,811	25,720	25,722	25,722	25,811	25,813	*25,695	25,697	25,697
2000	25,423	25,408	25,334	25,332	25,324	25,409	25,399	25,312	25,314	*25,294
2001	24,583	24,571	24,518	24,516	24,517	24,572	24,574	*24,510	24,512	24,516
2002	24,248	24,237	24,195	24,192	24,192	24,239	24,238	24,185	24,182	*24,165
2003	24,771	24,759	24,766	*24,758	24,760	24,761	24,762	24,767	24,768	24,759
2004	26,131	26,126	26,092	26,092	26,085	26,128	26,126	26,080	26,082	*26,073
2005	26,461	26,457	26,390	26,392	26,380	26,458	26,455	26,344	26,330	*26,308
2006	25,409	25,402	25,324	25,324	25,326	25,404	25,406	25,301	25,302	*25,290
2007	25,431	25,421	25,393	*25,390	25,392	25,422	25,423	25,391	25,391	25,391
2008	23,508	23,503	23,453	23,453	23,453	23,504	23,500	23,447	*23,447	23,453

Table B.1 (continued).

2009	28,576	28,572	28,548	28,548	28,543	28,574	28,570	28,543	28,545	*28,539
2010	28,680	28,664	28,594	28,590	28,579	28,666	28,660	28,574	28,574	*28,548
2011	27,081	27,075	26,982	26,983	26,983	27,073	27,068	26,968	26,960	*26,937
2012	25,401	25,391	25,325	25,323	25,316	25,392	25,392	25,290	25,276	*25,230
2013	27,495	27,491	27,446	27,446	27,447	27,493	27,493	*27,433	27,433	27,441
2014	25,887	25,868	25,828	25,821	25,819	25,870	25,867	25,828	25,817	*25,799
2015	27,115	27,113	27,083	27,084	27,083	27,115	27,112	27,080	27,080	*27,077
2016	28,148	28,119	28,045	28,035	28,022	28,121	28,115	28,032	28,032	*28,002
2017	29,251	29,208	29,209	29,181	29,178	29,205	29,207	29,210	29,189	*29,169
2018	29,303	29,298	29,247	29,248	29,247	29,299	29,300	29,246	29,245	*29,232
2019	31,554	31,551	31,533	31,533	31,535	31,553	31,553	*31,533	31,534	31,538
2020	29,067	29,047	29,040	29,028	29,028	29,035	29,033	29,041	29,032	*29,004

Table B.2. Estimated coefficients extracted from the best fitted multiple linear regression model derived from the Bay-wide female age-1+ kriging analysis. The coefficients were used to create trend maps and backtransform predicted kriged female abundance estimates.

Year	Intercept	Easting	Northing	EastingSq	NorthingSq	EN	EESq	NESq
1990	-4.66E+08	2.79E+03	2.23E+02	-3.88E-03	-3.07E-05	-1.31E-03	1.36E-09	1.49E-09
1991	-3.38E+08	2.73E+03	7.97E+01	-3.29E-03	2.91E-05	-1.33E-03	-2.98E-09	2.38E-09
1992	1.75E+09	-3.31E+03	-1.35E+03	-1.25E-03	3.59E-04	2.59E-03	-4.23E-09	1.76E-09
1993	7.33E+05	0	-3.42E-01	0	3.99E-08	0	0	0
1994	3.98E+09	-2.30E+04	-2.38E+03	4.33E-02	4.60E-04	1.25E-02	-2.71E-08	-2.02E-08
1995	-5.53E+08	1.24E+03	4.12E+02	7.94E-04	-1.00E-04	-1.03E-03	-7.17E-10	-1.91E-10
1996	-2.34E+05	6.86E-01	5.53E-02	0	0	-1.61E-07	0	0
1997	-1.91E+09	5.12E+03	1.36E+03	-3.81E-05	-3.23E-04	-3.63E-03	2.25E-10	-4.27E-11
1998	5.98E+08	-1.23E+03	-4.58E+02	-6.66E-05	1.22E-04	9.03E-04	-1.87E-09	5.40E-10
1999	6.41E+05	0	-3.00E-01	0	3.50E-08	0	0	0
2000	1.45E+09	-3.44E+03	-1.06E+03	5.82E-05	2.66E-04	2.45E-03	-2.00E-09	5.20E-10
2001	4.02E+05	0	-1.87E-01	0	2.17E-08	0	0	0
2002	-3.71E+08	7.38E+02	2.33E+02	9.24E-04	-4.65E-05	-3.96E-04	-4.55E-10	-6.99E-10
2003	3.78E+03	9.85E-03	-1.67E-03	0	0	0	0	0
2004	2.89E+08	4.73E+01	-2.74E+02	-1.01E-03	8.81E-05	1.63E-04	-2.12E-09	1.06E-09
2005	-9.35E+08	1.17E+03	6.15E+02	4.09E-03	-1.32E-04	-6.18E-04	-5.72E-10	-3.02E-09
2006	1.04E+09	-2.11E+03	-7.83E+02	-8.89E-04	2.00E-04	1.67E-03	-1.04E-09	7.02E-10
2007	2.34E+04	7.52E-03	-6.12E-03	0	0	0	0	0
2008	-1.95E+07	0	1.40E+01	0	-3.37E-06	0	00	0
2009	1.48E+09	-3.29E+03	-1.09E+03	1.54E-03	2.90E-04	2.08E-03	-6.49E-09	1.05E-09
2010	5.36E+09	-1.47E+04	-3.77E+03	5.33E-03	9.11E-04	9.52E-03	-8.83E-09	-1.28E-10
2011	4.89E+09	-1.38E+04	-3.41E+03	4.08E-03	8.06E-04	9.08E-03	-4.52E-09	-7.18E-10
2012	-1.52E+09	5.19E+03	9.87E+02	-2.21E-03	-2.07E-04	-3.29E-03	-1.27E-09	1.40E-09
2013	1.69E+06	0	-7.89E-01	0	9.21E-08	0	0	0
2014	1.61E+09	-4.66E+03	-1.12E+03	1.81E-03	2.64E-04	3.00E-03	-2.03E-09	-3.11E-10

Table B.2 (continued).

2015	2.07E+09	-5.73E+03	-1.45E+03	2.72E-03	3.55E-04	3.61E-03	-4.91E-09	5.31E-11
2016	1.94E+09	-3.71E+03	-1.50E+03	-1.63E-03	3.96E-04	2.95E-03	-4.12E-09	1.92E-09
2017	1.54E+09	4.24E+02	-1.09E+03	-1.08E-02	2.70E-04	-5.69E-04	-3.53E-09	9.04E-09
2018	2.82E+09	-7.30E+03	-2.02E+03	6.77E-05	4.82E-04	5.19E-03	-7.78E-10	1.66E-10
2019	1.35E+06	0	-6.26E-01	0	7.24E-08	0	0	0
2020	1.69E+09	-3.28E+03	-1.30E+03	-2.45E-03	3.37E-04	2.77E-03	-1.35E-09	1.55E-09

Table B.2 (continued).

Year	ENSq	NNSq	ESqNSq	ENESq	ENNSq	EESqNSq	NESqNSq	ENESqNSq
1990	1.80E-10	9.80E-13	-1.34E-16	-3.26E-16	-6.40E-18	0	0	0
1991	9.48E-11	-6.86E-12	-3.80E-16	7.02E-16	1.59E-17	0	0	0
1992	-7.76E-10	-3.25E-11	-3.47E-16	9.98E-16	8.25E-17	0	0	0
1993	0	0	0	0	0	0	0	0
1994	-2.10E-09	-2.85E-11	2.35E-15	9.48E-15	9.90E-17	0	0	-1.72E-28
1995	2.61E-10	7.97E-12	7.66E-19	1.69E-16	-2.08E-17	0	0	0
1996	0	0	0	0	0	0	0	0
1997	8.63E-10	2.56E-11	1.21E-17	-5.25E-17	-6.88E-17	0	0	0
1998	-2.66E-10	-1.12E-11	-1.25E-16	4.45E-16	2.88E-17	0	0	0
1999	0	0	0	0	0	0	0	0
2000	-6.32E-10	-2.26E-11	-1.26E-16	4.73E-16	5.78E-17	0	0	0
2001	0	0	0	0	0	0	0	0
2002	5.25E-11	2.88E-12	2.05E-16	1.08E-16	0	0	-2.16E-23	0
2003	0	0	0	0	0	0	0	0
2004	-1.39E-10	-9.32E-12	-1.95E-16	5.03E-16	2.30E-17	0	0	0
2005	8.06E-11	9.17E-12	7.81E-16	1.35E-16	0	0	-6.97E-23	0
2006	-4.61E-10	-1.72E-11	-1.17E-16	2.46E-16	4.35E-17	0	0	0
2007	0	0	0	0	0	0	0	0
2008	0	2.69E-13	0	0	0	0	0	0
2009	-5.96E-10	-2.70E-11	-3.35E-16	1.53E-15	6.80E-17	0	0	0
2010	-2.26E-09	-7.55E-11	-2.70E-16	2.10E-15	1.96E-16	0	0	0
2011	-2.10E-09	-6.45E-11	-5.89E-17	1.07E-15	1.70E-16	0	0	0
2012	6.52E-10	1.39E-11	-2.08E-16	3.01E-16	-3.88E-17	0	0	0
2013	0	0	0	0	0	0	0	0

Table B.2 (continued).

2014	-6.86E-10	-2.12E-11	-2.80E-17	4.81E-16	5.61E-17	0	0	0
2015	-8.67E-10	-3.01E-11	-1.65E-16	1.16E-15	7.90E-17	0	0	0
2016	-8.77E-10	-3.57E-11	-3.62E-16	9.76E-16	9.17E-17	0	0	0
2017	1.11E-10	-2.31E-11	-2.23E-15	8.39E-16	0	0	1.65E-22	0
2018	-1.25E-09	-3.86E-11	-4.33E-17	1.84E-16	1.01E-16	0	0	0
2019	0	0	0	0	0	0	0	0
2020	-7.96E-10	-2.93E-11	-2.29E-16	3.22E-16	7.67E-17	0	0	0

Table B.3. Selected fitted variogram models by year for female age-1+blue crab abundance estimates derived from Bay-wide kriging on the Davis WDS Chesapeake Bay data.

Year	Model	Nugget (10^6)	pSill (10^6)	Range (10^6)	kappa	SSE (10^6)
1990	Mat	83.33	2.19	7,514.53	1.70	634.57
1991	Mat	0.00	16.47	39,732.68	0.05	27,246.75
1992	Mat	24.75	8.34	1,048.52	1.60	3,815.88
1993	Exp	121.83	0.00	31,024.18	0.00	7,885.21
1994	Exp	76.48	0.00	31,504.19	0.00	6,154.33
1995	Sph	21.35	0.61	11,284.41	0.00	17.70
1996	Exp	102.51	0.00	28,556.51	0.00	22,875.30
1997	Mat	91.90	5.61	203,347.04	1.80	14,059.35
1998	Mat	0.00	10.30	585.59	1.20	9,183.11
1999	Mat	15.20	0.00	29,205.54	1.10	11.20
2000	Mat	50.53	0.00	29,348.35	0.90	182.56
2001	Exp	16.79	0.00	29,495.35	0.00	89.26
2002	Mat	0.00	1.62	43,019.33	0.05	103.09
2003	Mat	45.95	1.61	13,771.48	1.90	1,508.39
2004	Mat	0.00	9.60	1,676.98	0.90	3,916.80
2005	Mat	79.31	0.00	29,424.74	0.40	894.97
2006	Mat	0.00	3.11	10,562.28	0.05	203.96
2007	Mat	51.31	1.62	6,011.17	1.60	196.55
2008	Mat	0.00	5.64	29,845.69	0.05	736.10
2009	Mat	433.82	25.67	3,146,026.80	0.05	1,068,648.10
2010	Mat	157.27	16.57	1,831.31	1.30	3,844.47
2011	Mat	0.00	17.04	60,092.13	0.05	3,457.91
2012	Mat	0.00	3.81	90,239.56	0.05	400.04
2013	Mat	142.52	0.00	28,671.59	0.60	41,743.78
2014	Mat	0.00	3.65	7,280.38	0.05	652.15
2015	Exp	150.24	0.00	28,545.09	0.00	38,932.46
2016	Mat	0.00	18.22	28,980.61	0.05	29,934.83
2017	Mat	318.94	0.00	28,647.38	5.00	22,954.06
2018	Mat	158.36	21.69	176,664.49	1.90	16,741.59
2019	Sph	13.32	85.75	3,874.71	0.00	209,119.54
2020	Mat	0.00	15.66	8,659.22	0.05	18,431.61

Figures for Appendix B

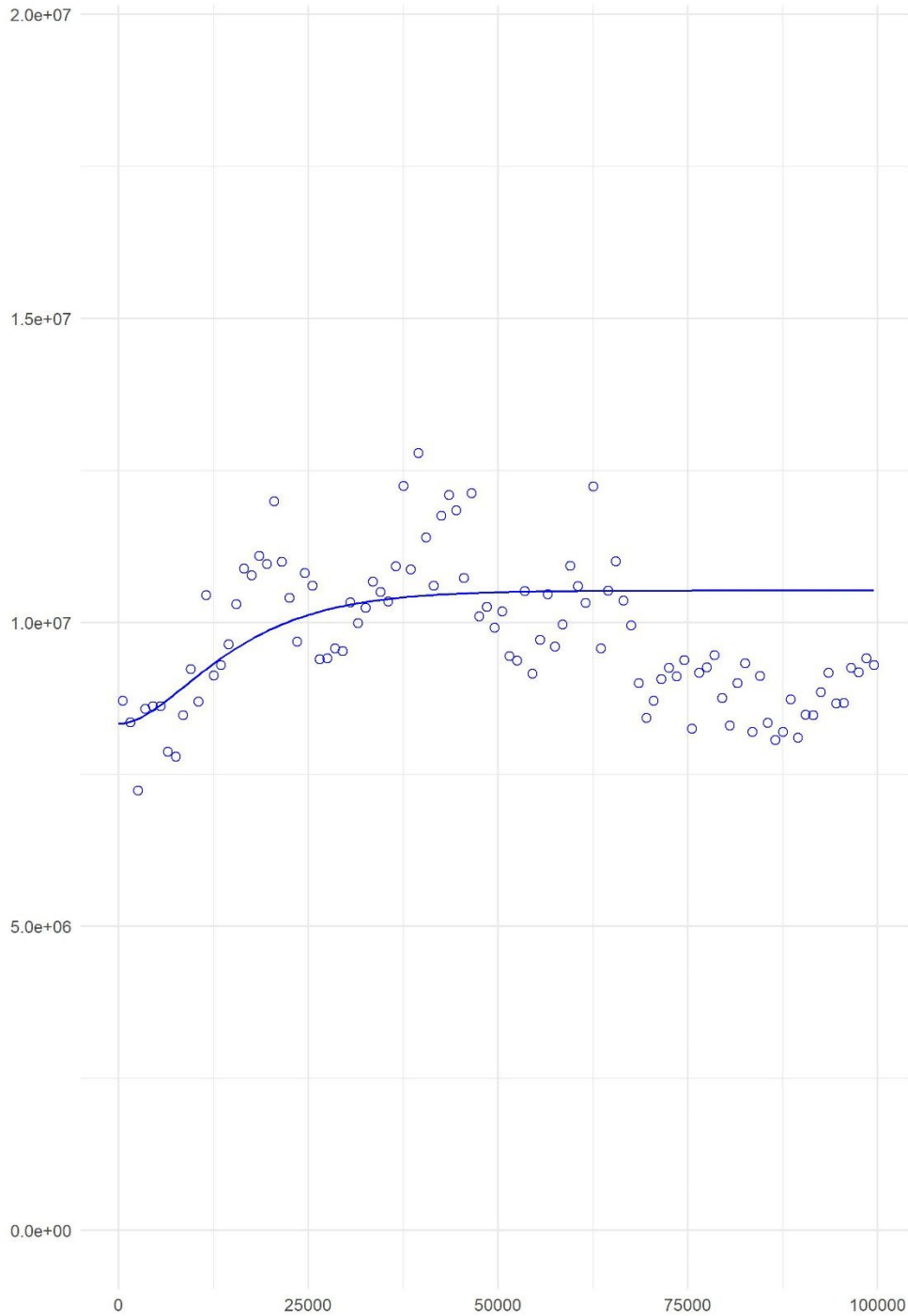


Figure B.1. 1990 female age-1+ blue crab fitted variogram derived from Bay-wide kriging using Davis WDS Chesapeake Bay data. Model parameters are provided in Table B.3.

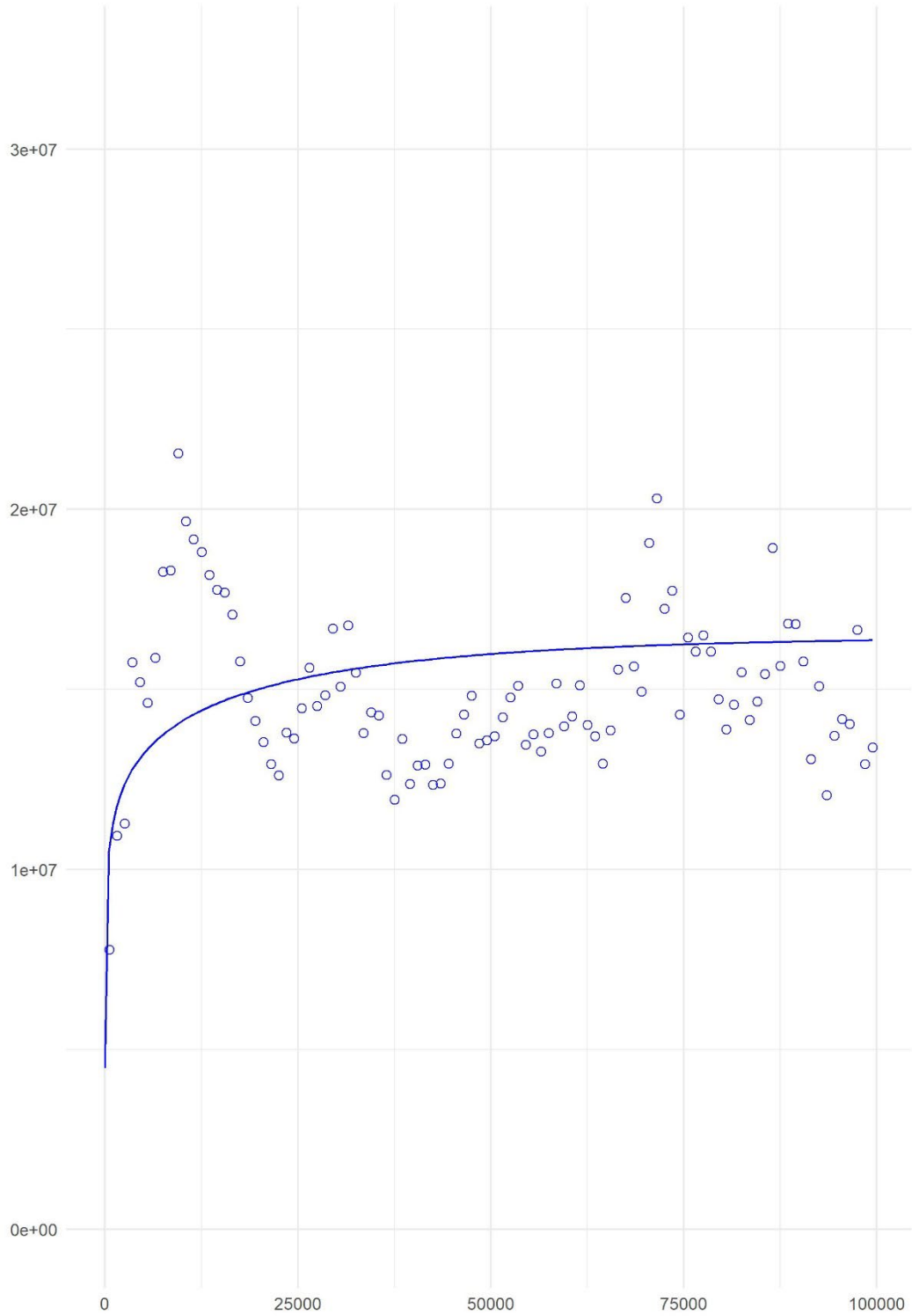


Figure B.2. 1991 female age-1+ blue crab fitted variogram derived from Bay-wide kriging using Davis WDS Chesapeake Bay data. Model parameters are provided in Table B.3.

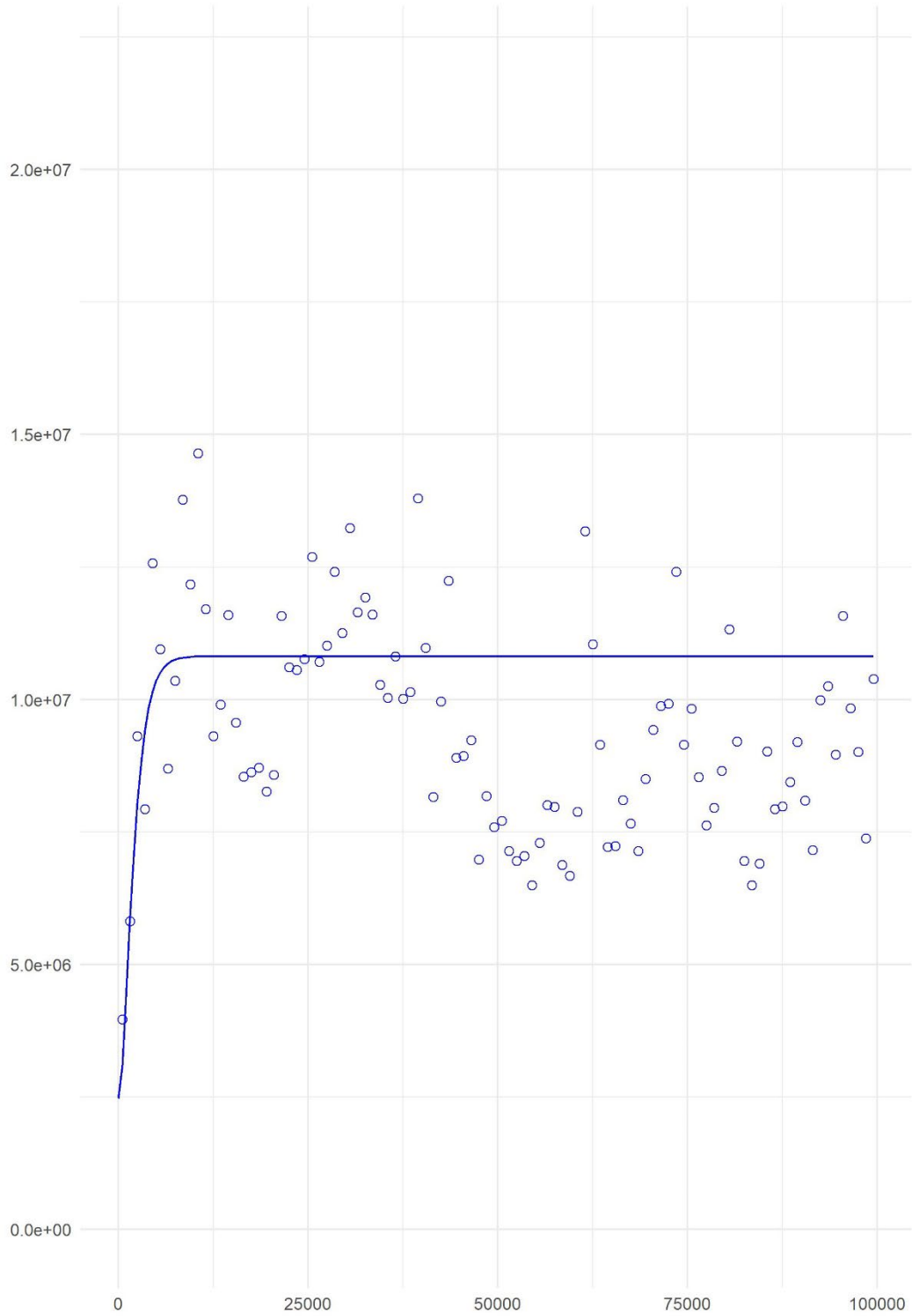


Figure B.3. 1992 female age-1+ blue crab fitted variogram derived from Bay-wide kriging using Davis WDS Chesapeake Bay data. Model parameters are provided in Table B.3.

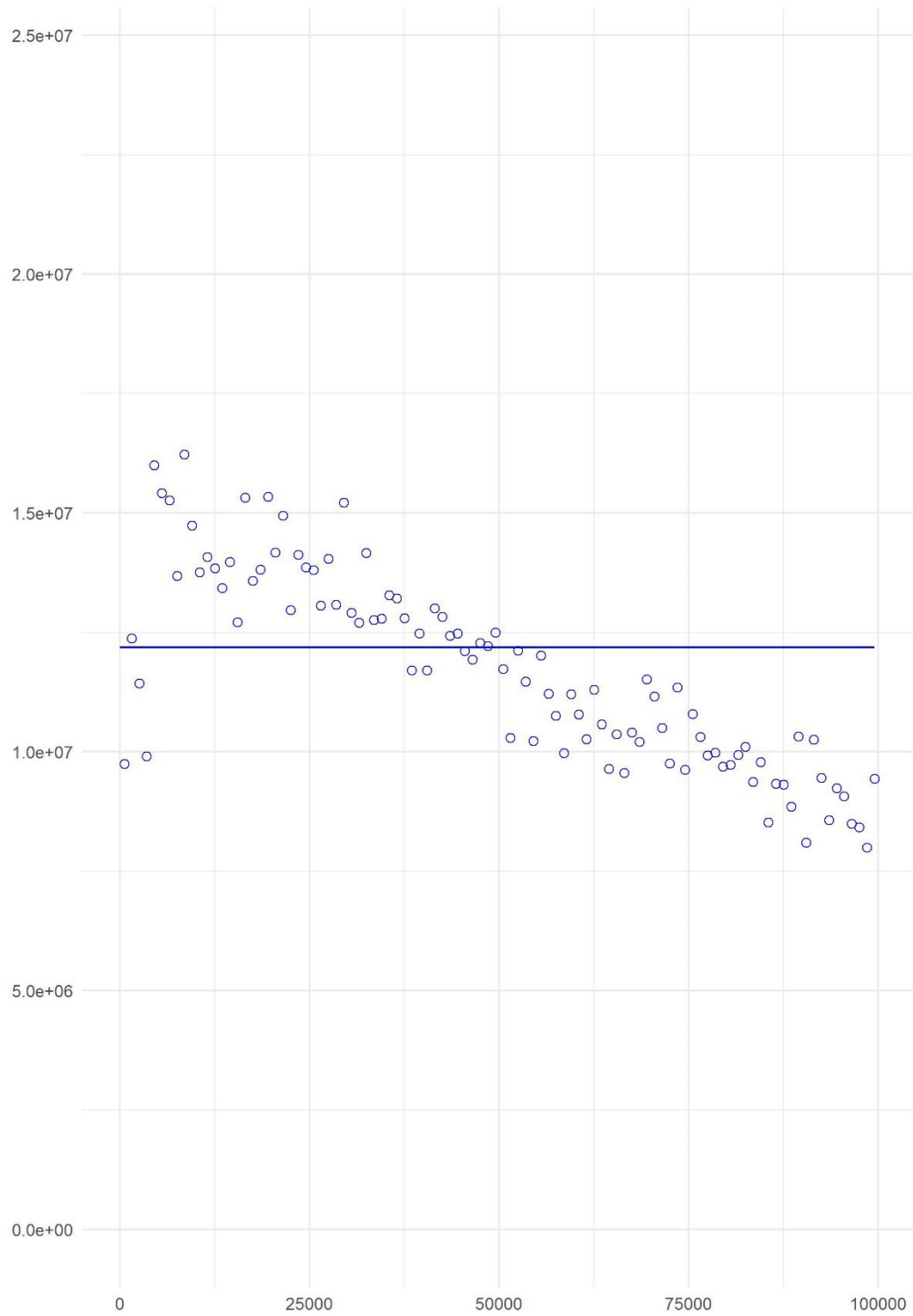


Figure B.4. 1993 female age-1+ blue crab fitted variogram derived from Bay-wide kriging using Davis WDS Chesapeake Bay data. Model parameters are provided in Table B.3.

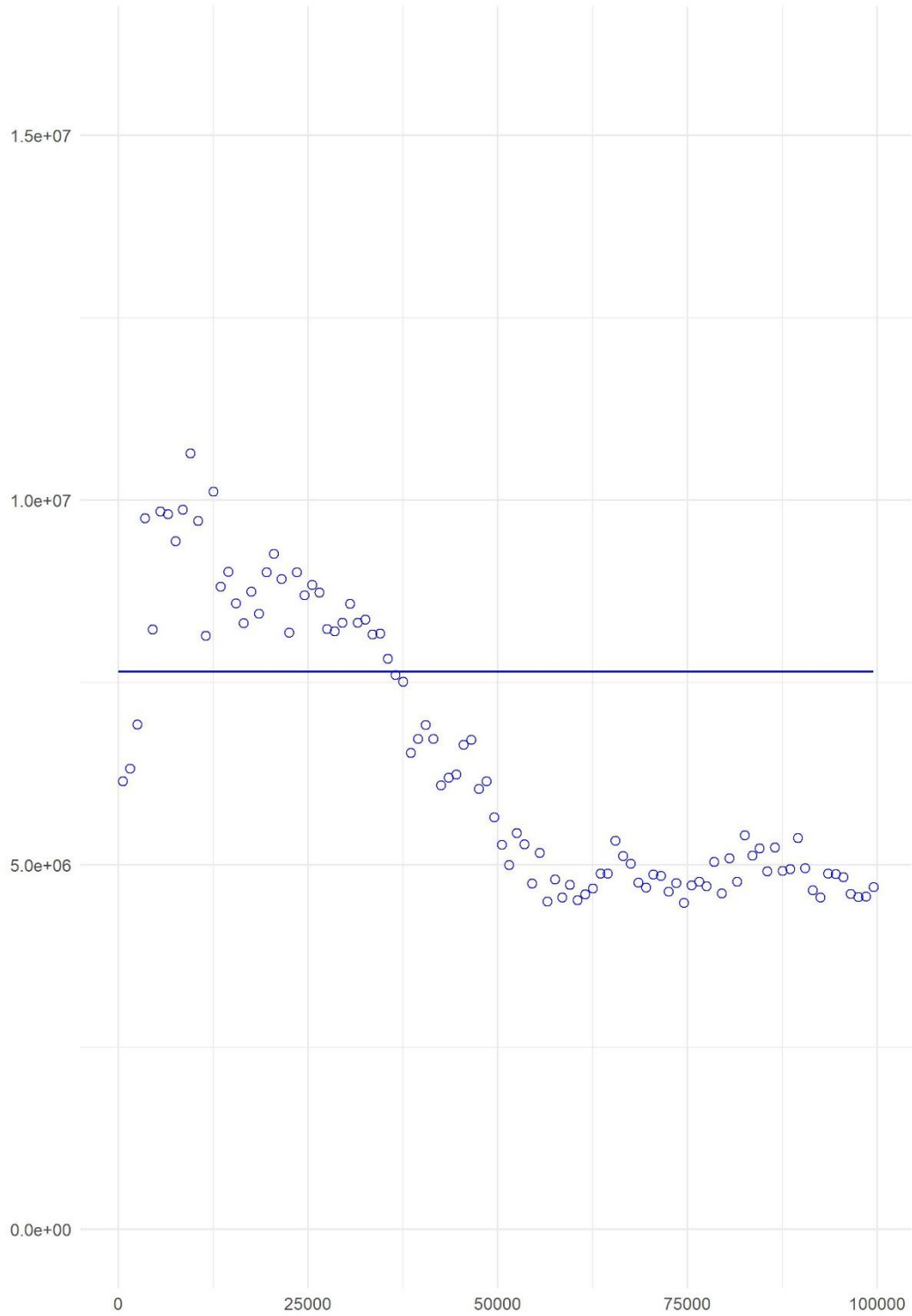


Figure B.5. 1994 female age-1+ blue crab fitted variogram derived from Bay-wide kriging using Davis WDS Chesapeake Bay data. Model parameters are provided in Table B.3.

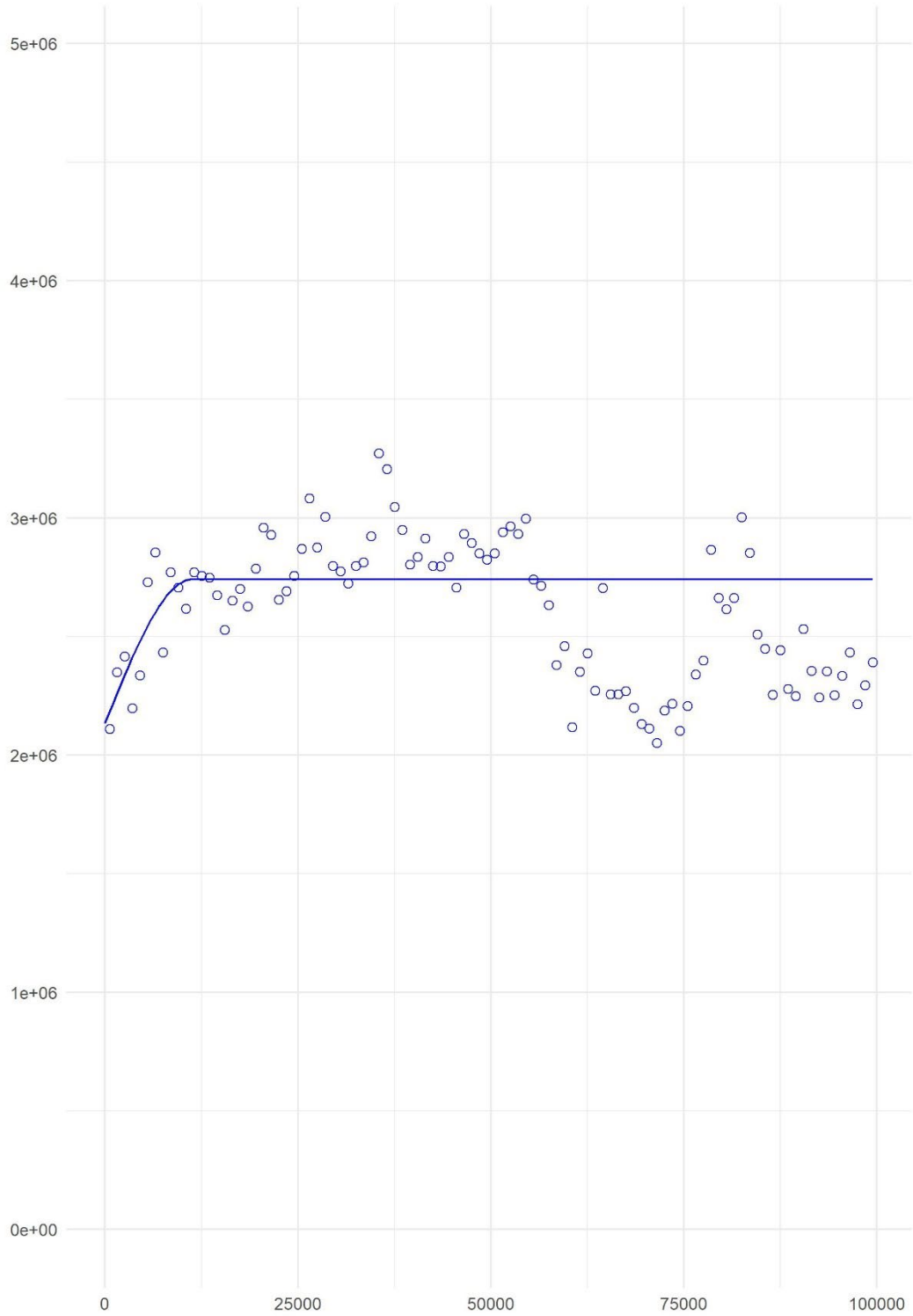


Figure B.6. 1995 female age-1+ blue crab fitted variogram derived from Bay-wide kriging using Davis WDS Chesapeake Bay data. Model parameters are provided in Table B.3.

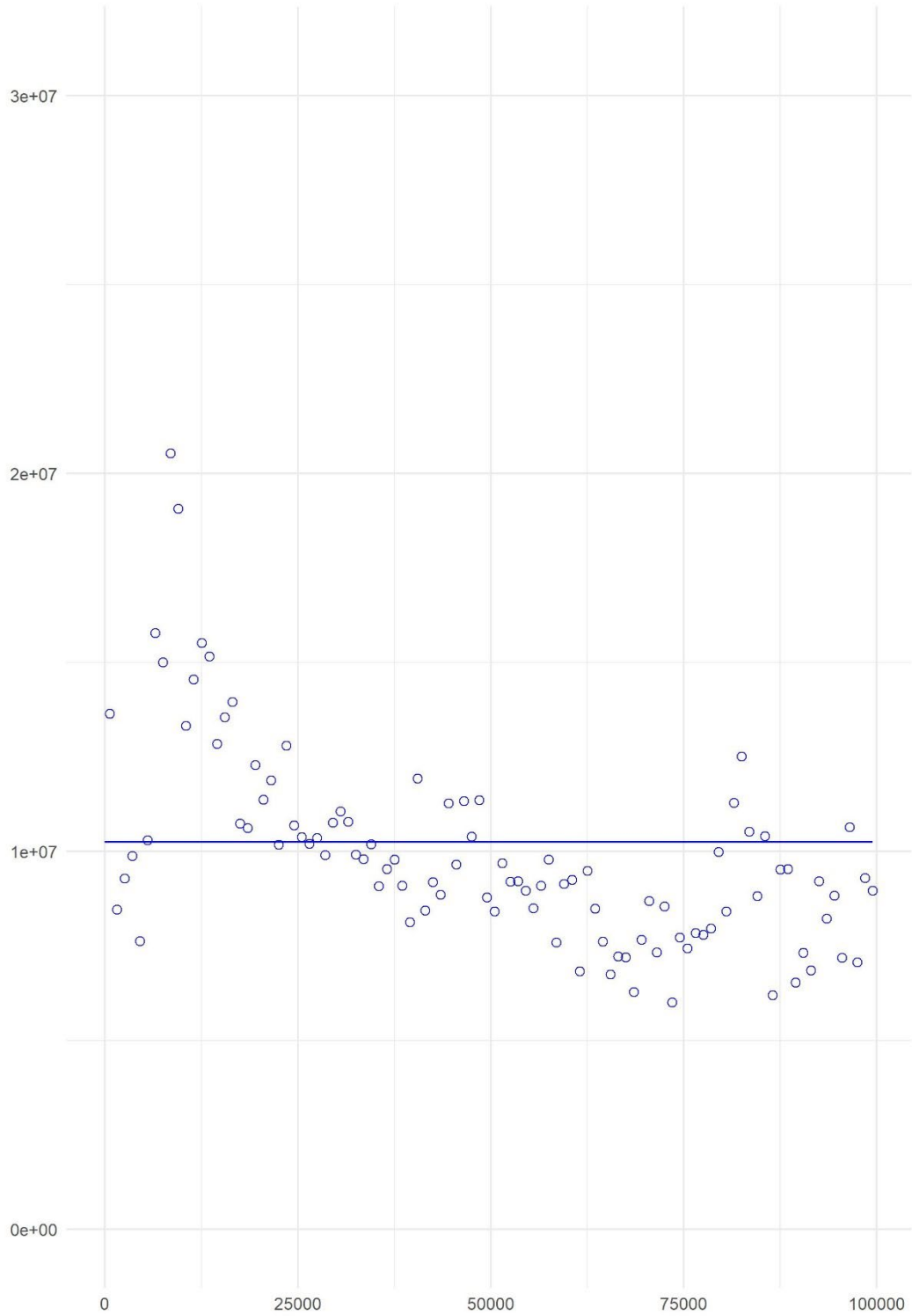


Figure B.7. 1996 female age-1+ blue crab fitted variogram derived from Bay-wide kriging using Davis WDS Chesapeake Bay data. Model parameters are provided in Table B.3.

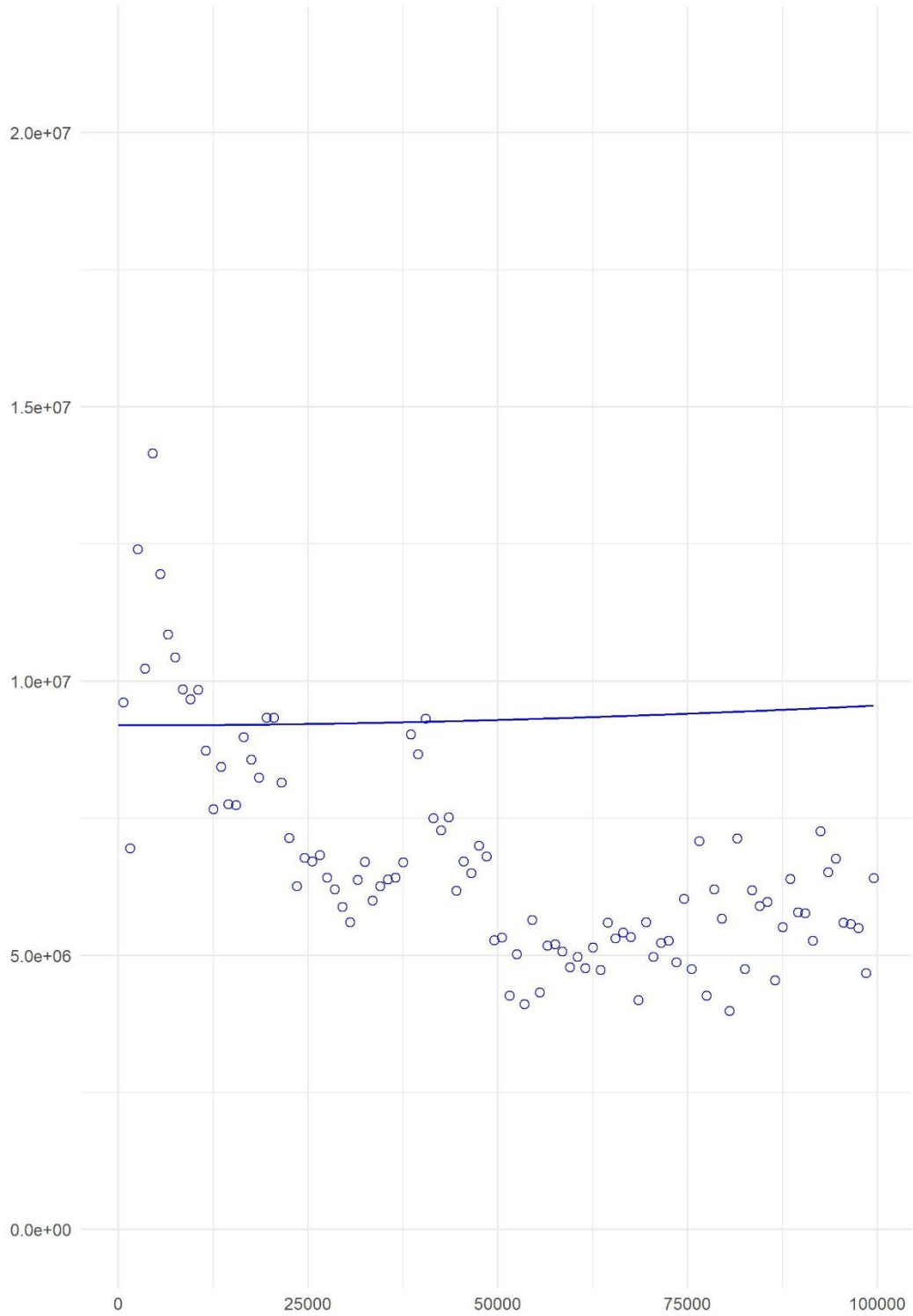


Figure B.8. 1997 female age-1+ blue crab fitted variogram derived from Bay-wide kriging using Davis WDS Chesapeake Bay data. Model parameters are provided in Table B.3.

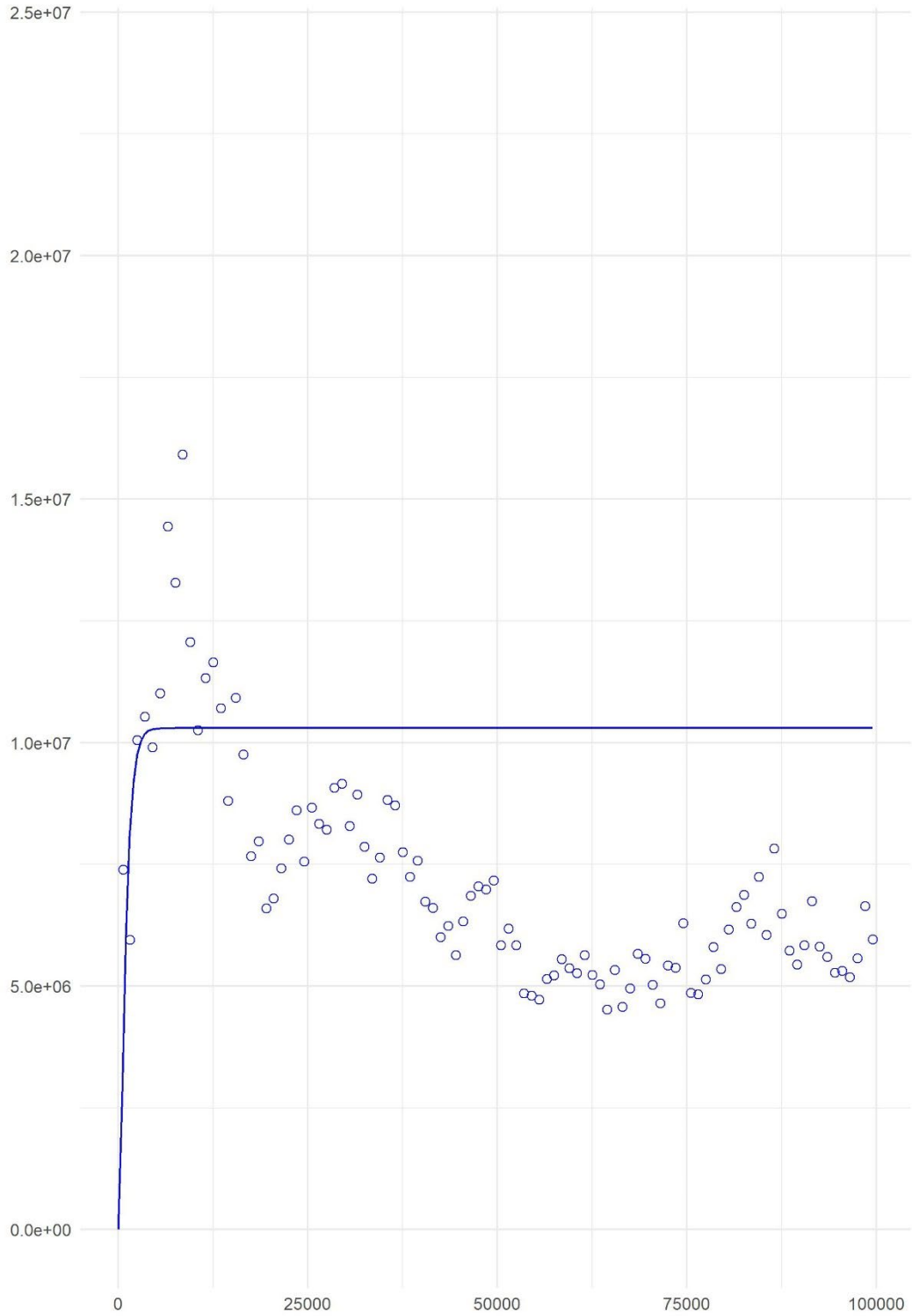


Figure B.9. 1998 female age-1+ blue crab fitted variogram derived from Bay-wide kriging using Davis WDS Chesapeake Bay data. Model parameters are provided in Table B.3.

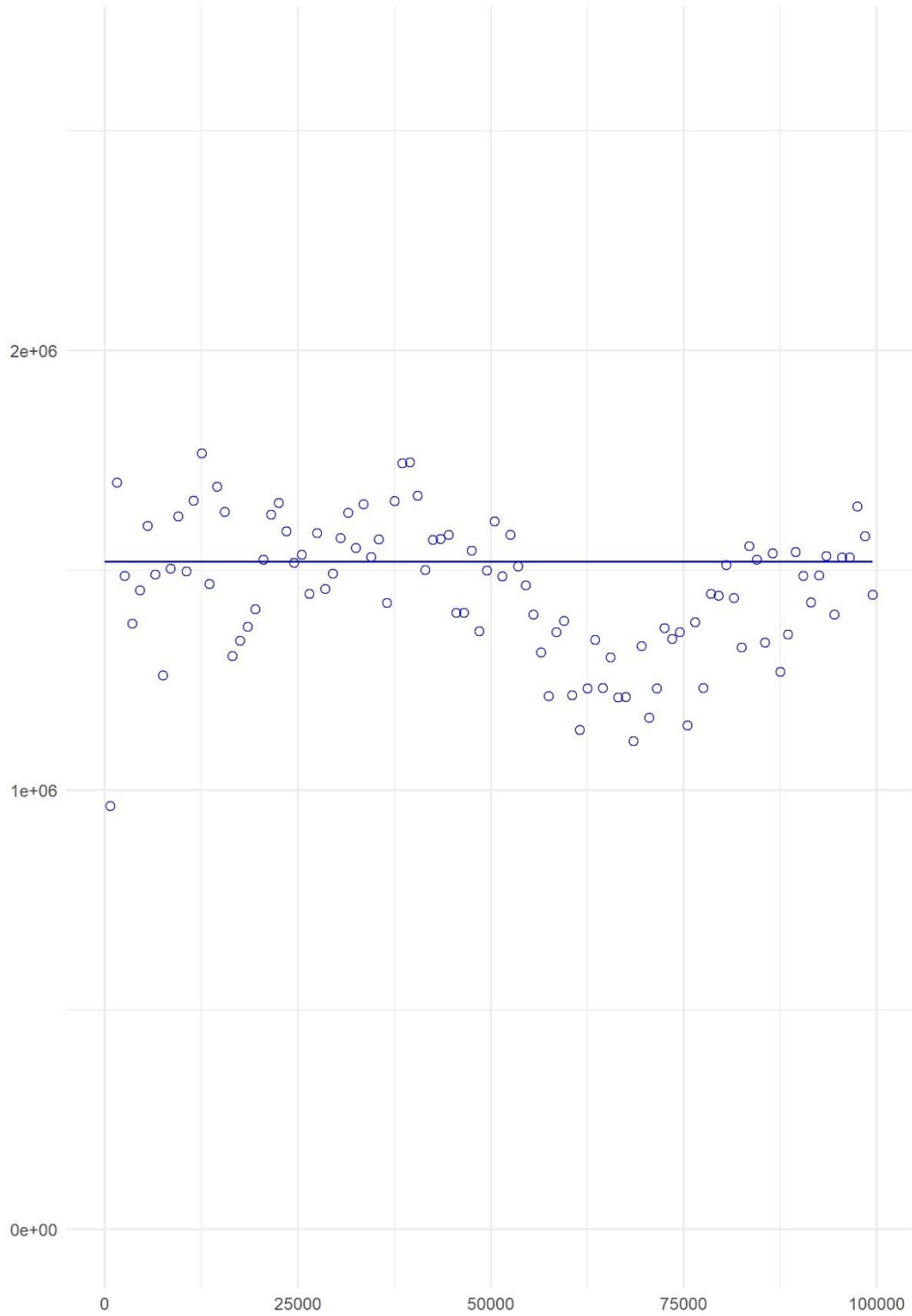


Figure B.10. 1999 female age-1+ blue crab fitted variogram derived from Bay-wide kriging using Davis WDS Chesapeake Bay data. Model parameters are provided in Table B.3.

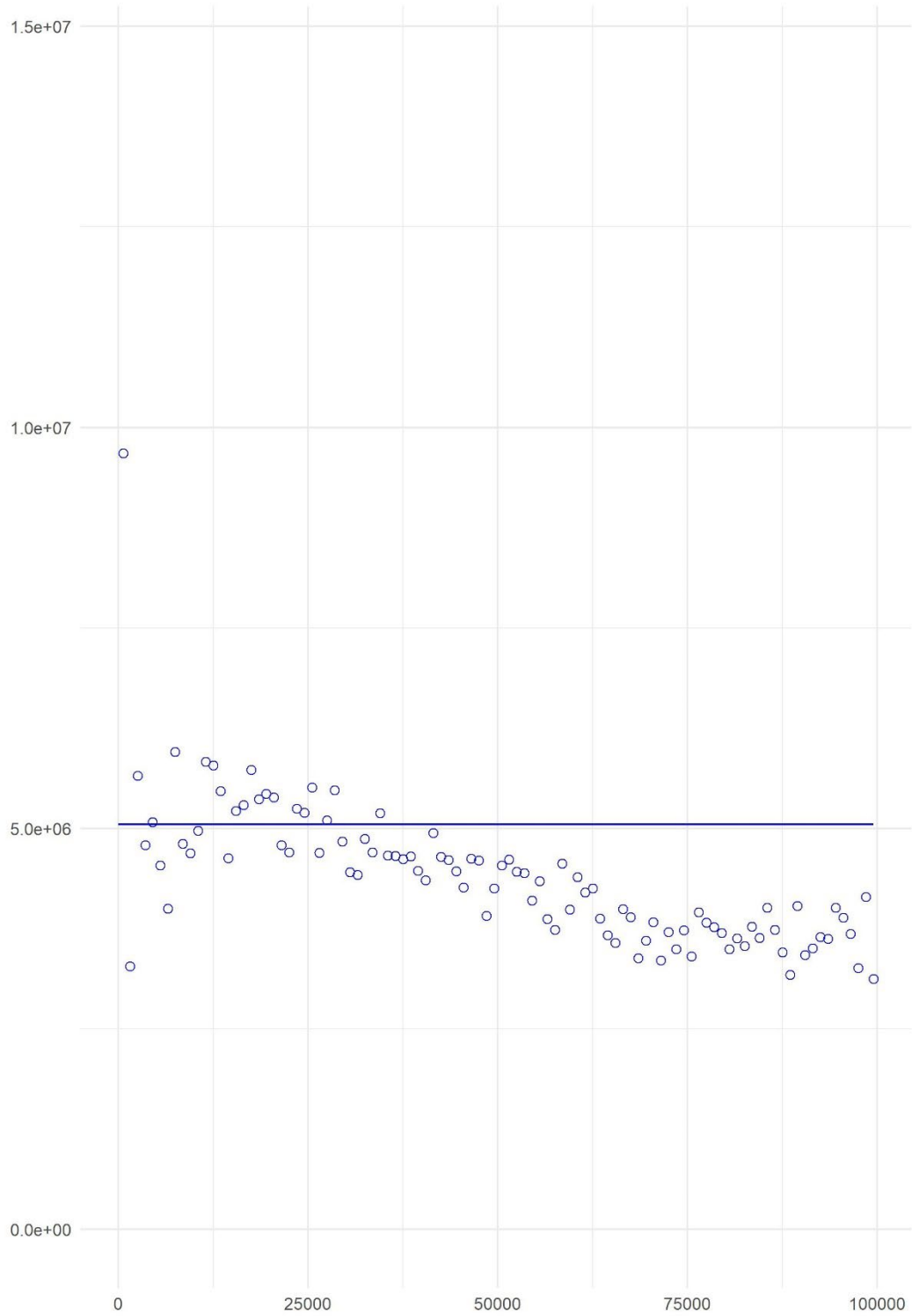


Figure B.11. 2000 female age-1+ blue crab fitted variogram derived from Bay-wide kriging using Davis WDS Chesapeake Bay data. Model parameters are provided in Table B.3.

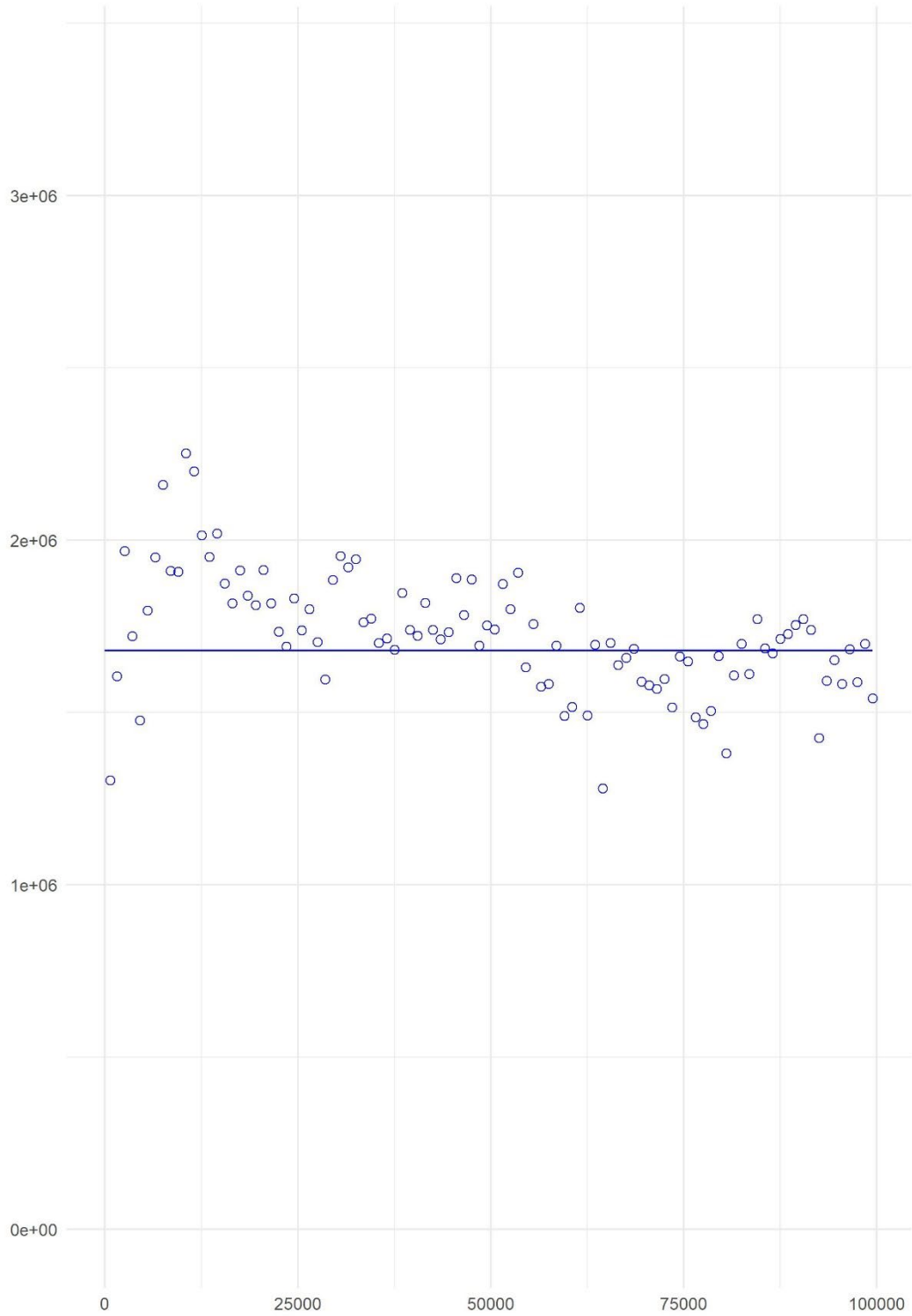


Figure B.12. 2001 female age-1+ blue crab fitted variogram derived from Bay-wide kriging using Davis WDS Chesapeake Bay data. Model parameters are provided in Table B.3.

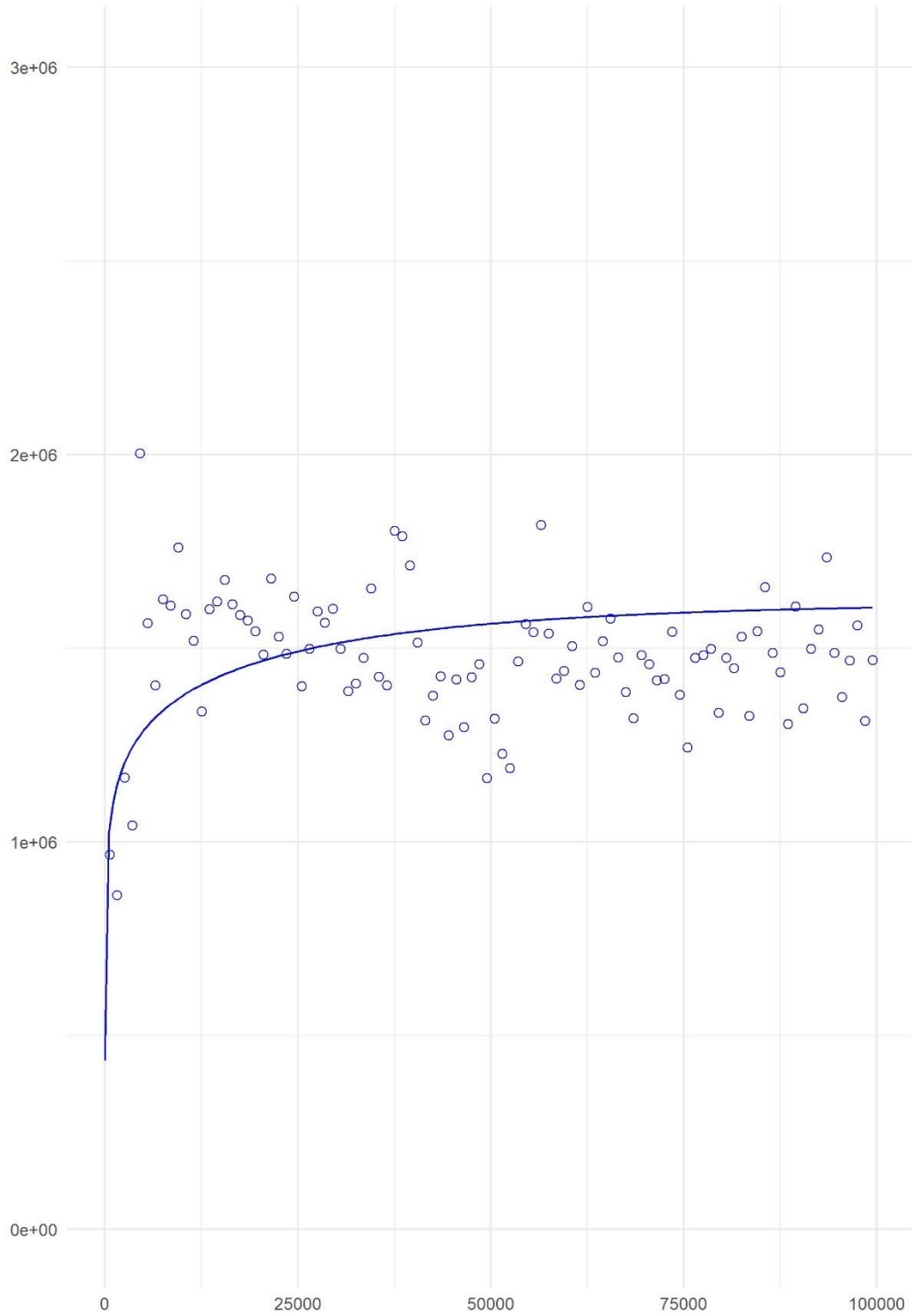


Figure B.13. 2002 female age-1+ blue crab fitted variogram derived from Bay-wide kriging using Davis WDS Chesapeake Bay data. Model parameters are provided in Table B.3.

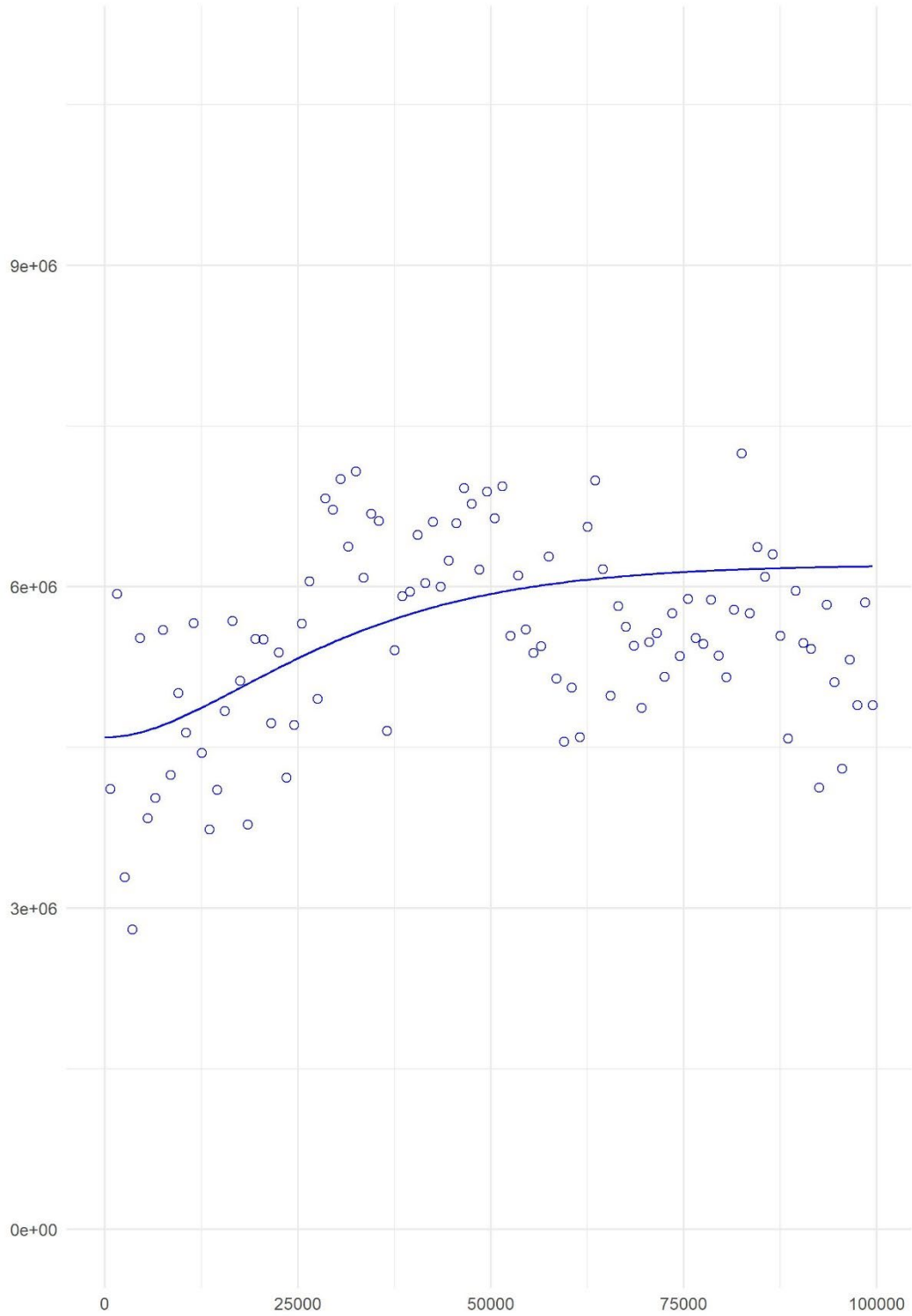


Figure B.14. 2003 female age-1+ blue crab fitted variogram derived from Bay-wide kriging using Davis WDS Chesapeake Bay data. Model parameters are provided in Table B.3.

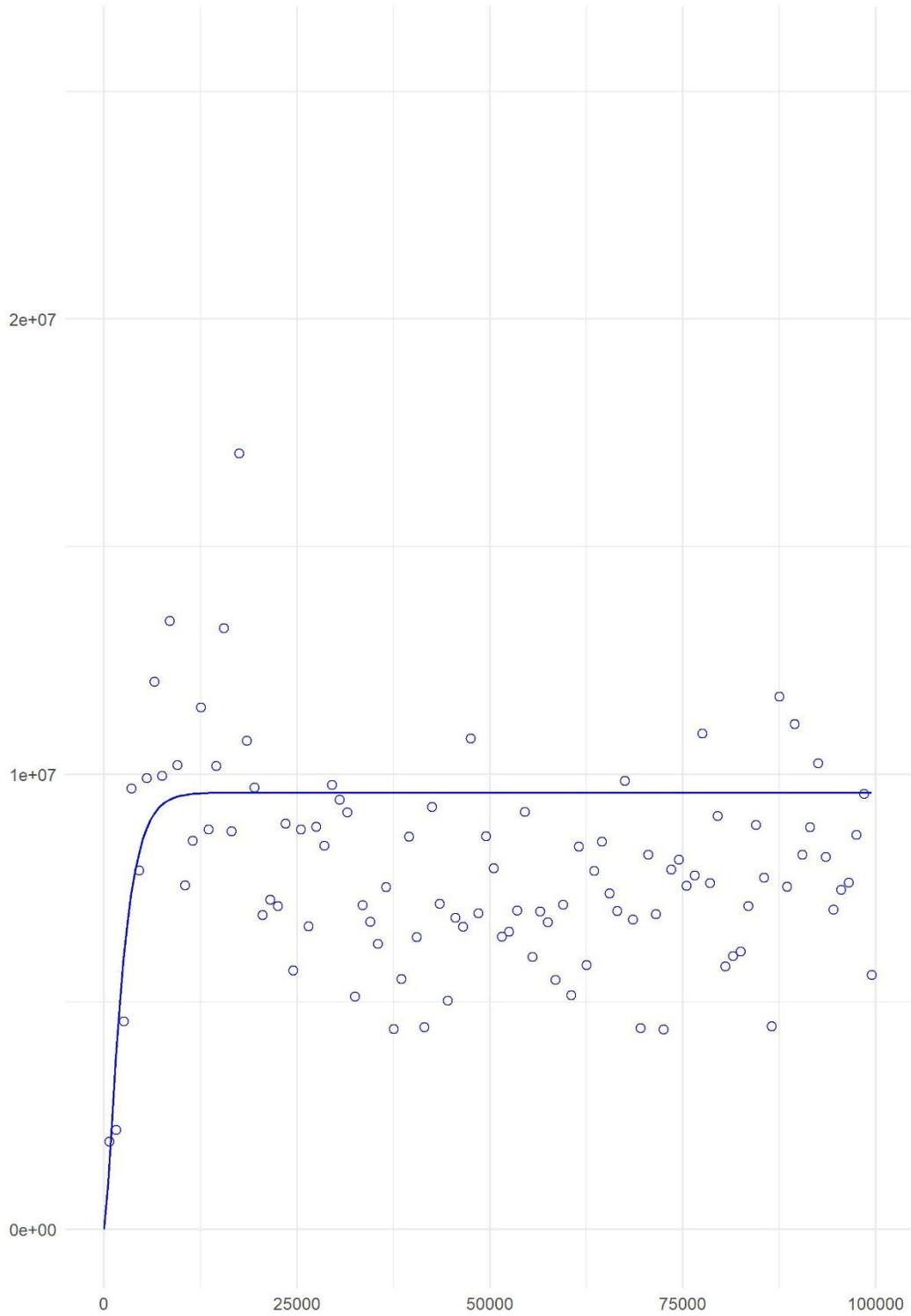


Figure B.15. 2004 female age-1+ blue crab fitted variogram derived from Bay-wide kriging using Davis WDS Chesapeake Bay data. Model parameters are provided in Table B.3.

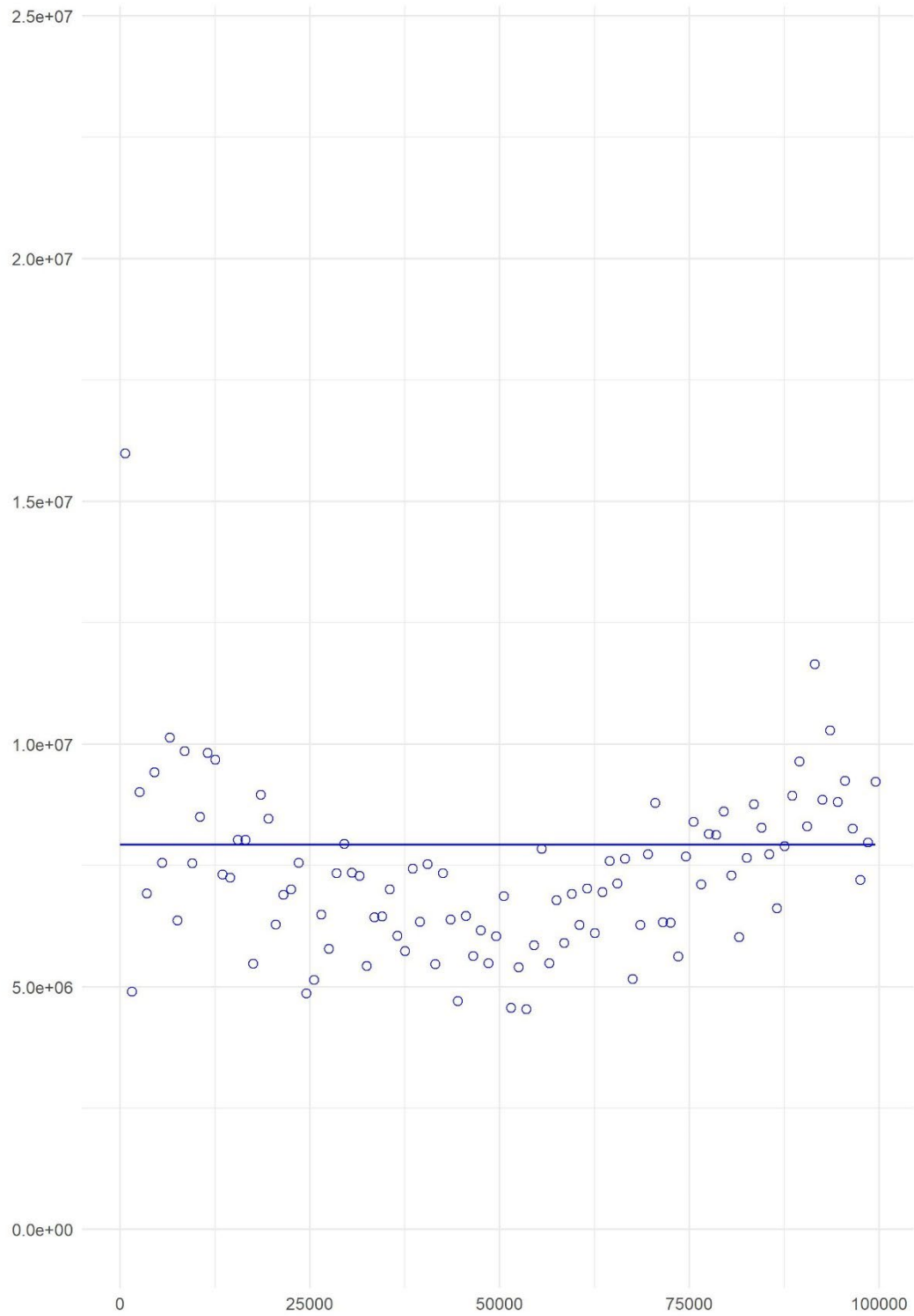


Figure B.16. 2005 female age-1+ blue crab fitted variogram derived from Bay-wide kriging using Davis WDS Chesapeake Bay data. Model parameters are provided in Table B.3.

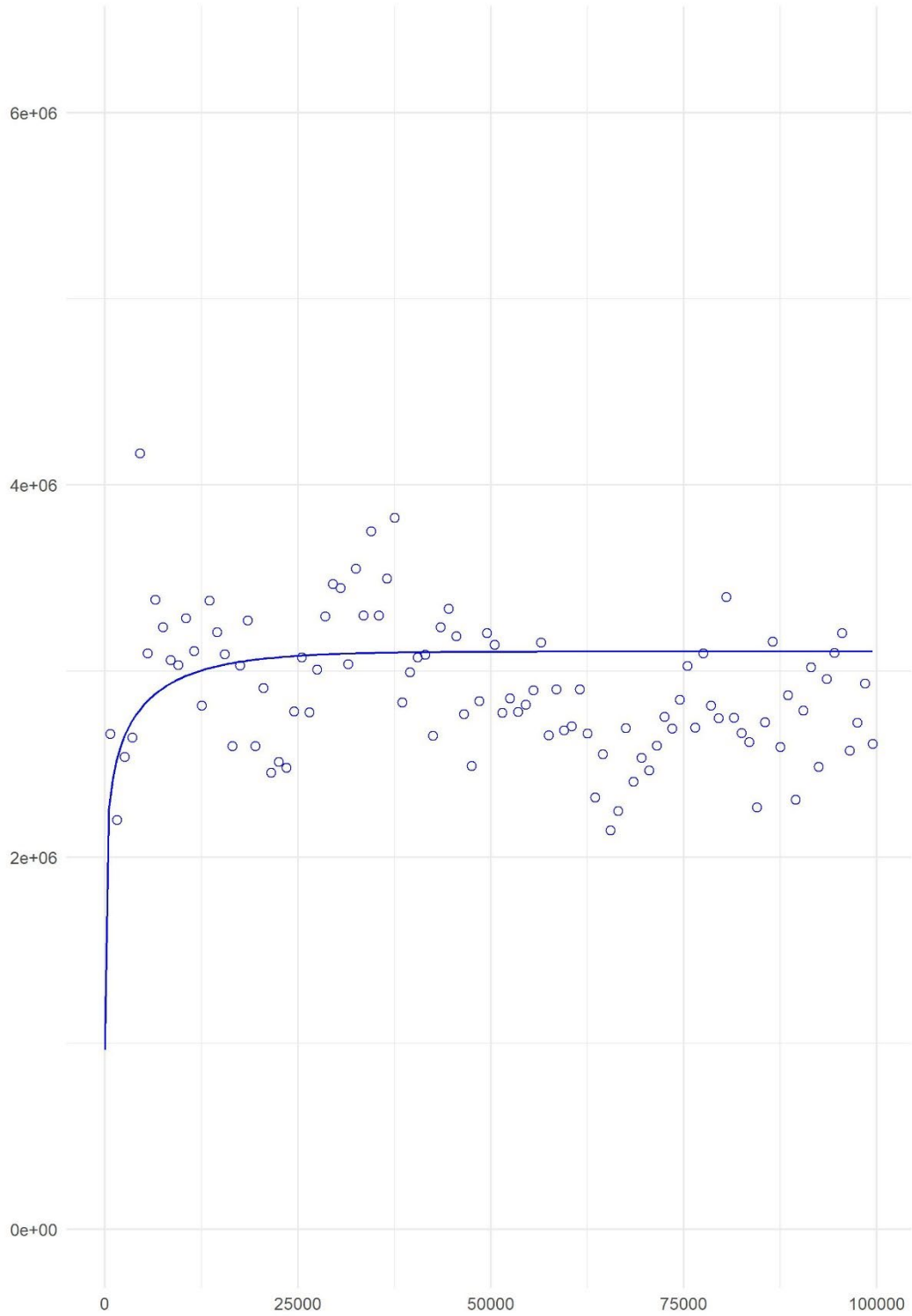


Figure B.17. 2006 female age-1+ blue crab fitted variogram derived from Bay-wide kriging using Davis WDS Chesapeake Bay data. Model parameters are provided in Table B.3.

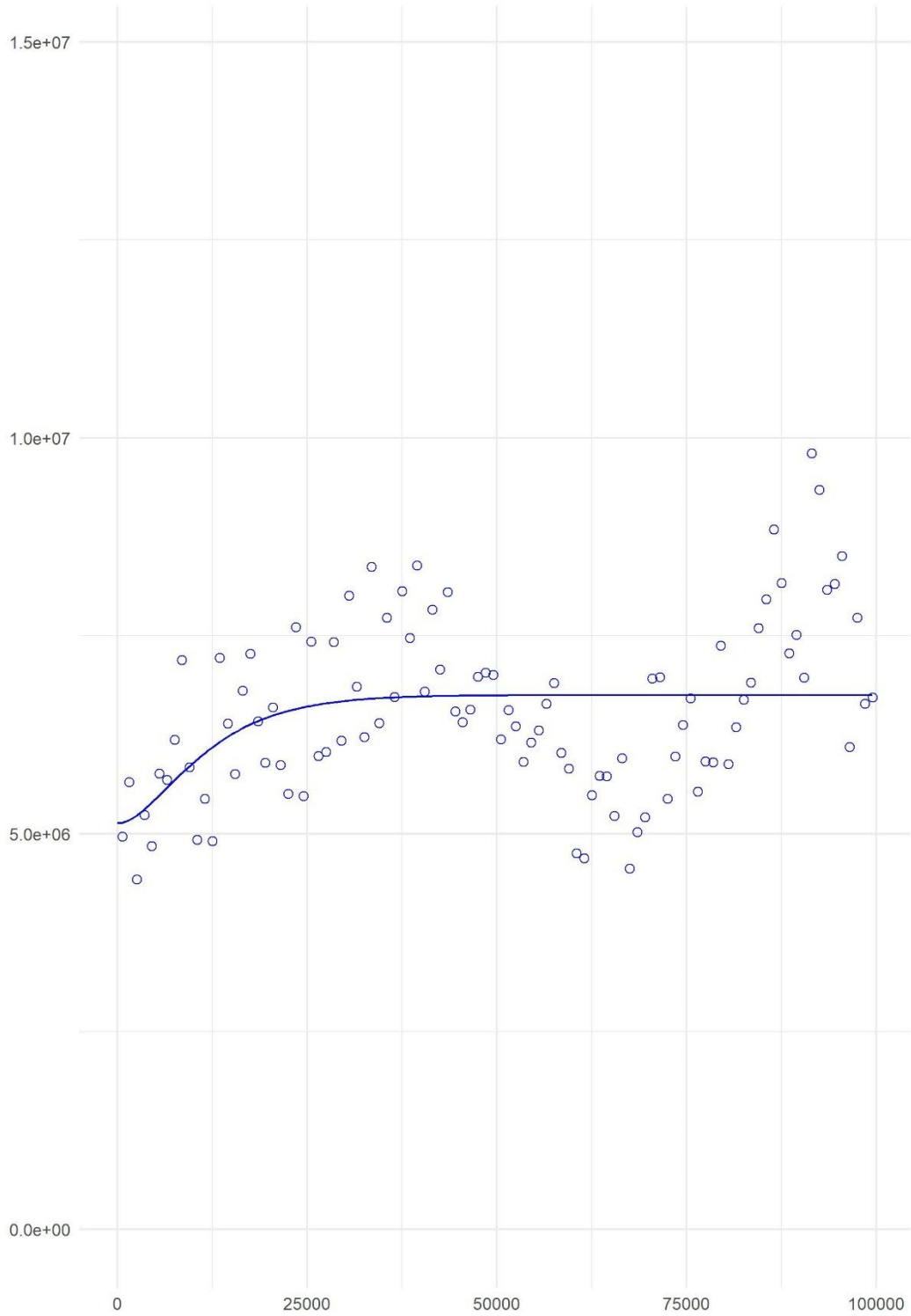


Figure B.18. 2007 female age-1+ blue crab fitted variogram derived from Bay-wide kriging using Davis WDS Chesapeake Bay data. Model parameters are provided in Table B.3.

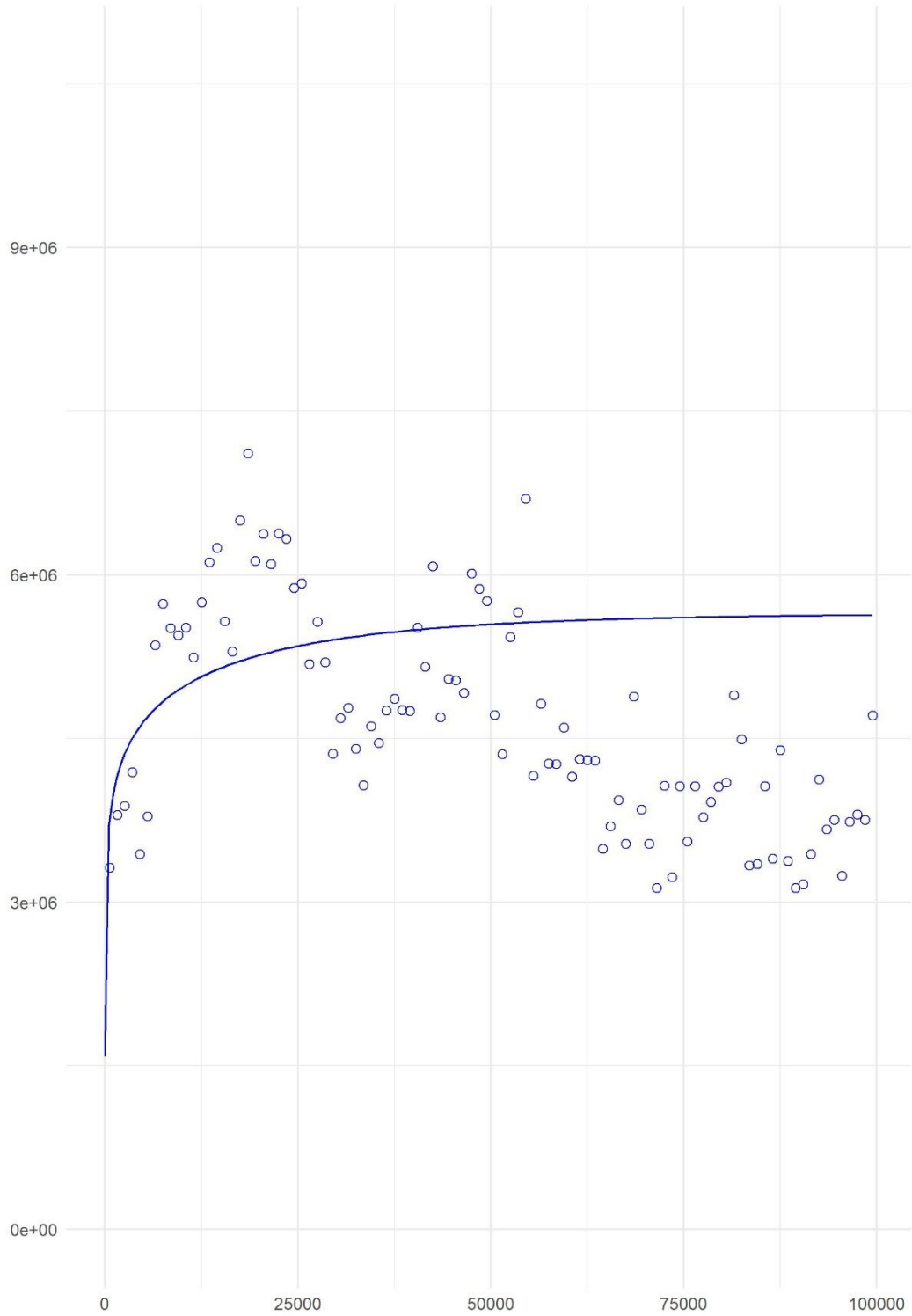


Figure B.19. 2008 female age-1+ blue crab fitted variogram derived from Bay-wide kriging using Davis WDS Chesapeake Bay data. Model parameters are provided in Table B.3.

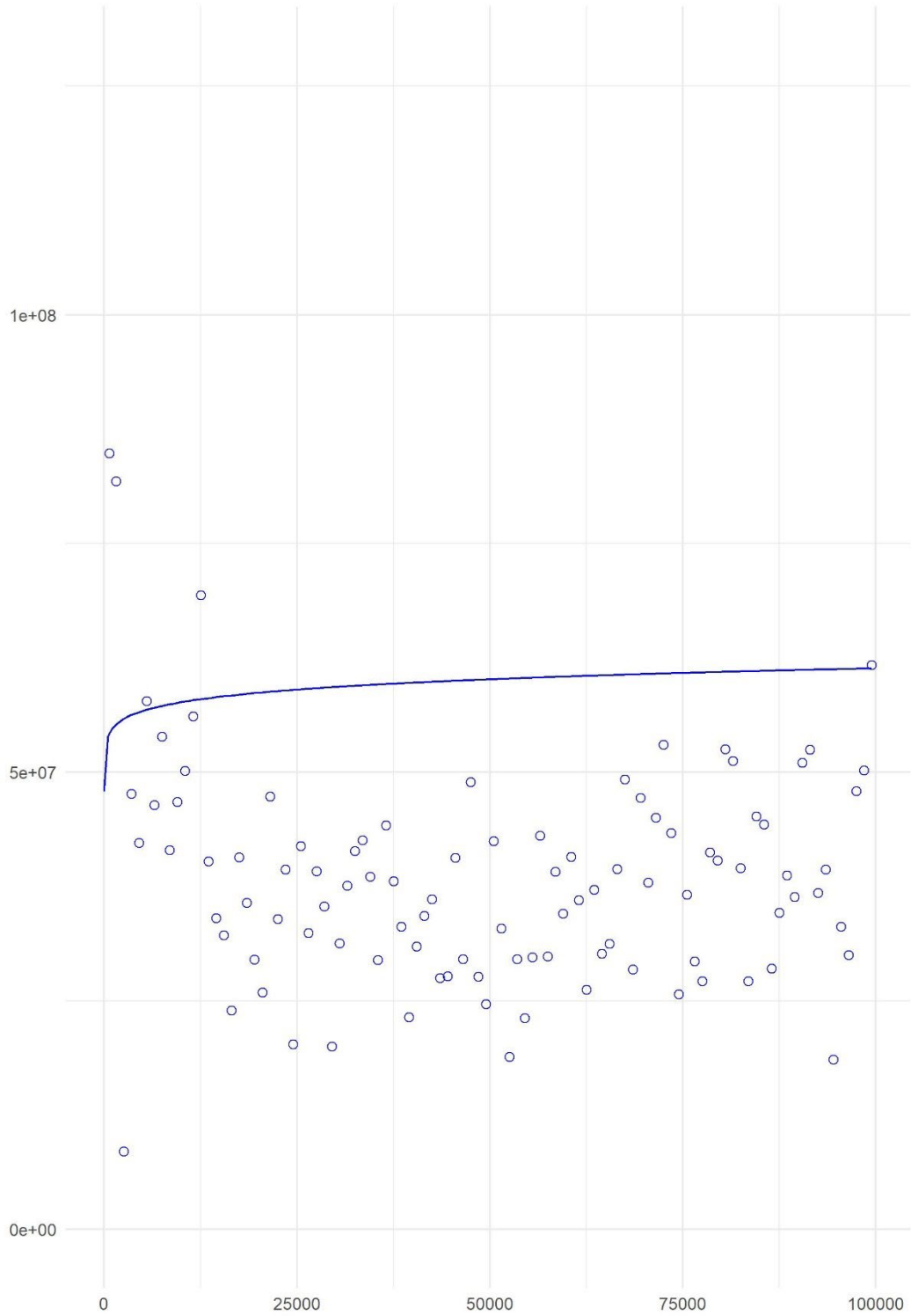


Figure B.20. 2009 female age-1+ blue crab fitted variogram derived from Bay-wide kriging using Davis WDS Chesapeake Bay data. Model parameters are provided in Table B.3.

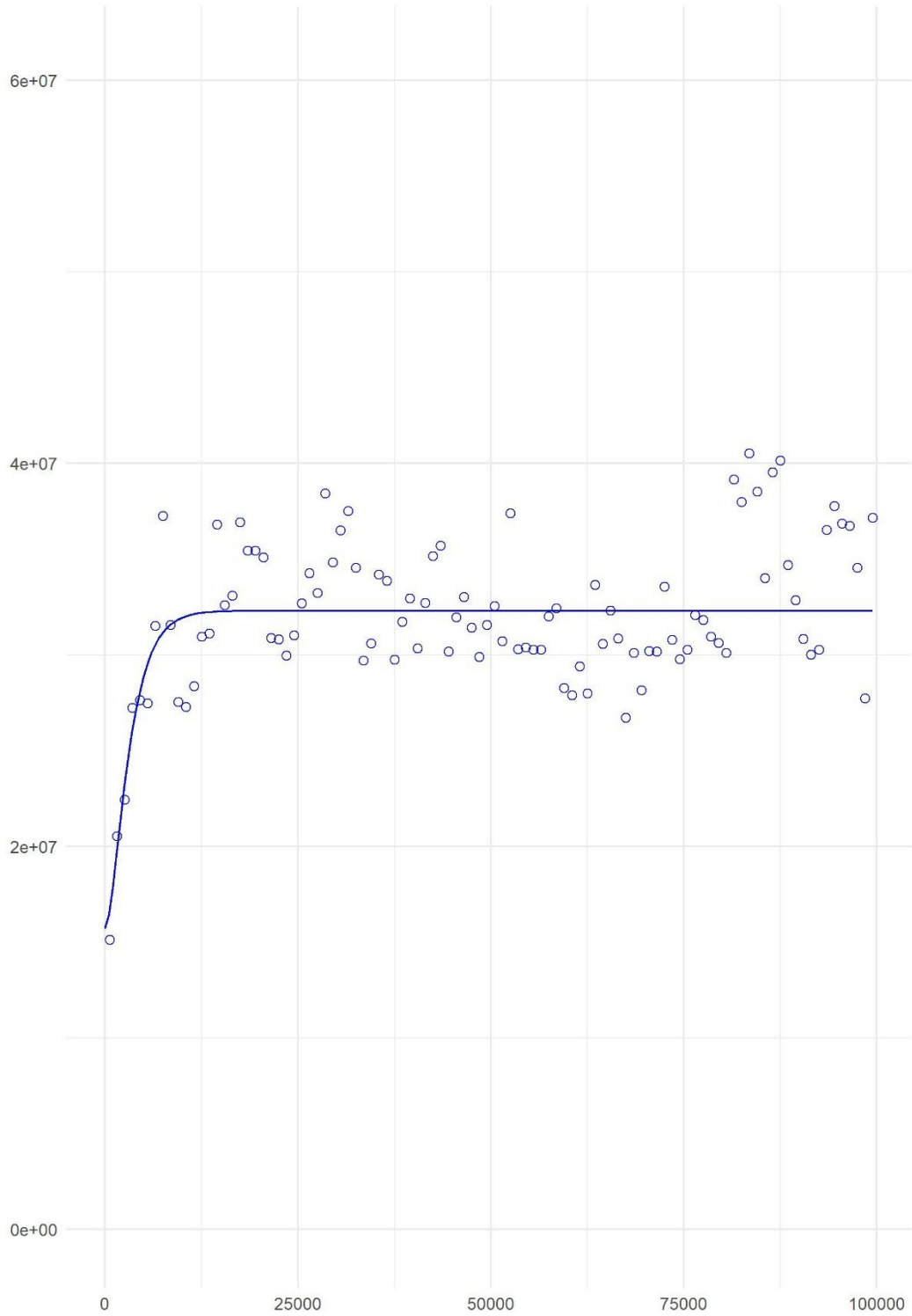


Figure B.21. 2010 female age-1+ blue crab fitted variogram derived from Bay-wide kriging using Davis WDS Chesapeake Bay data. Model parameters are provided in Table B.3.

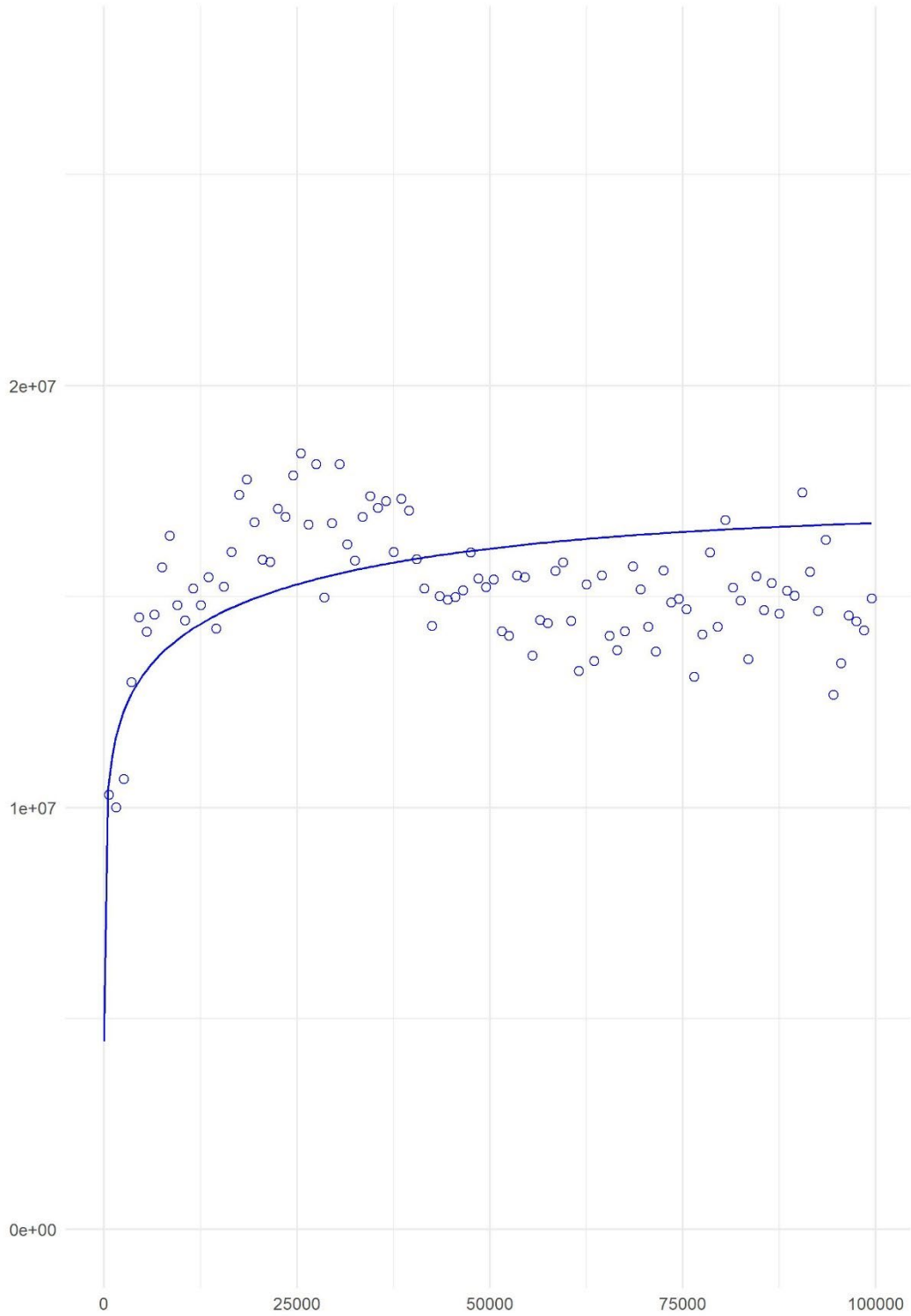


Figure B.22. 2011 female age-1+ blue crab fitted variogram derived from Bay-wide kriging using Davis WDS Chesapeake Bay data. Model parameters are provided in Table B.3..

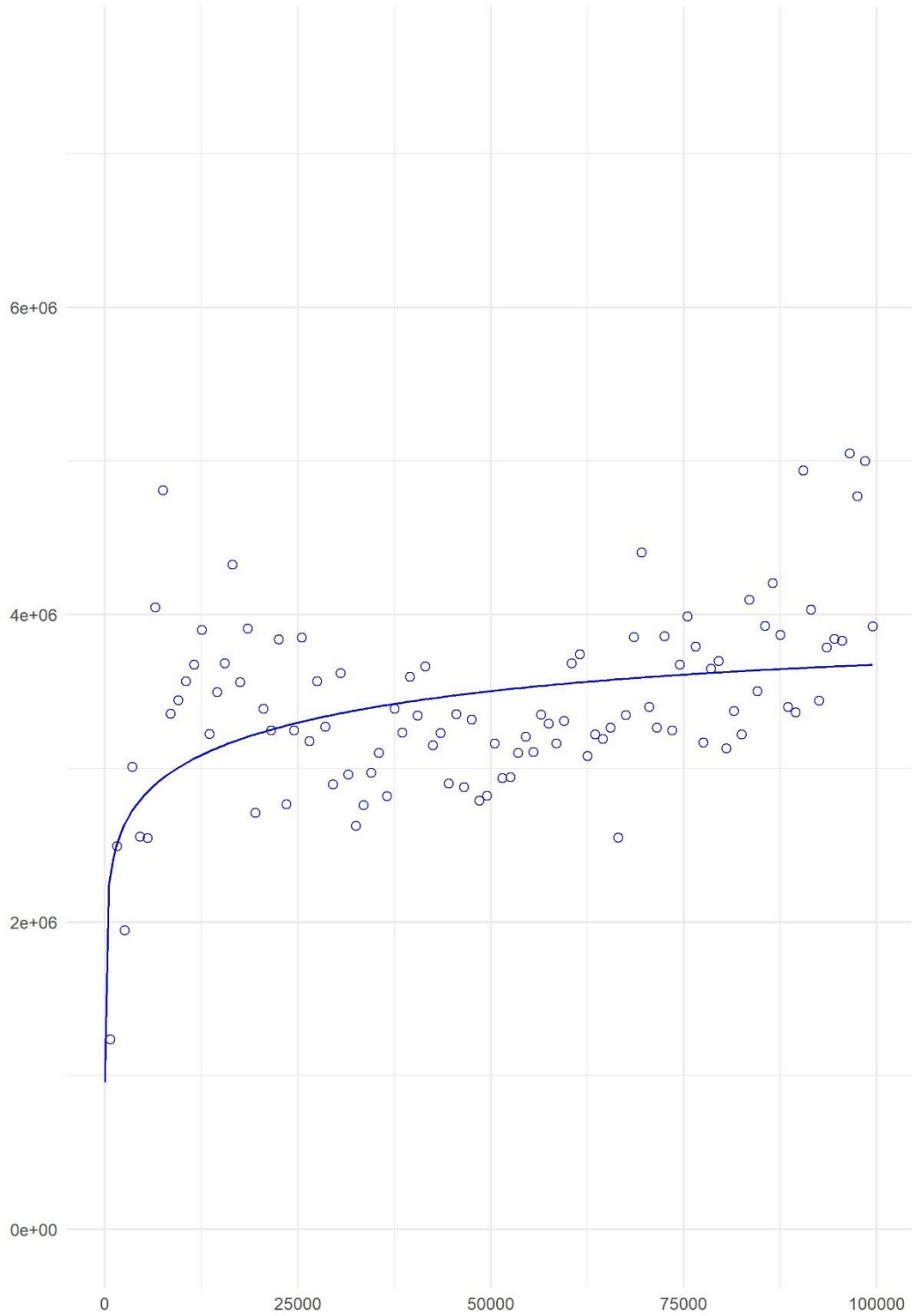


Figure B.23. 2012 female age-1+ blue crab fitted variogram derived from Bay-wide kriging using Davis WDS Chesapeake Bay data. Model parameters are provided in Table B.3.

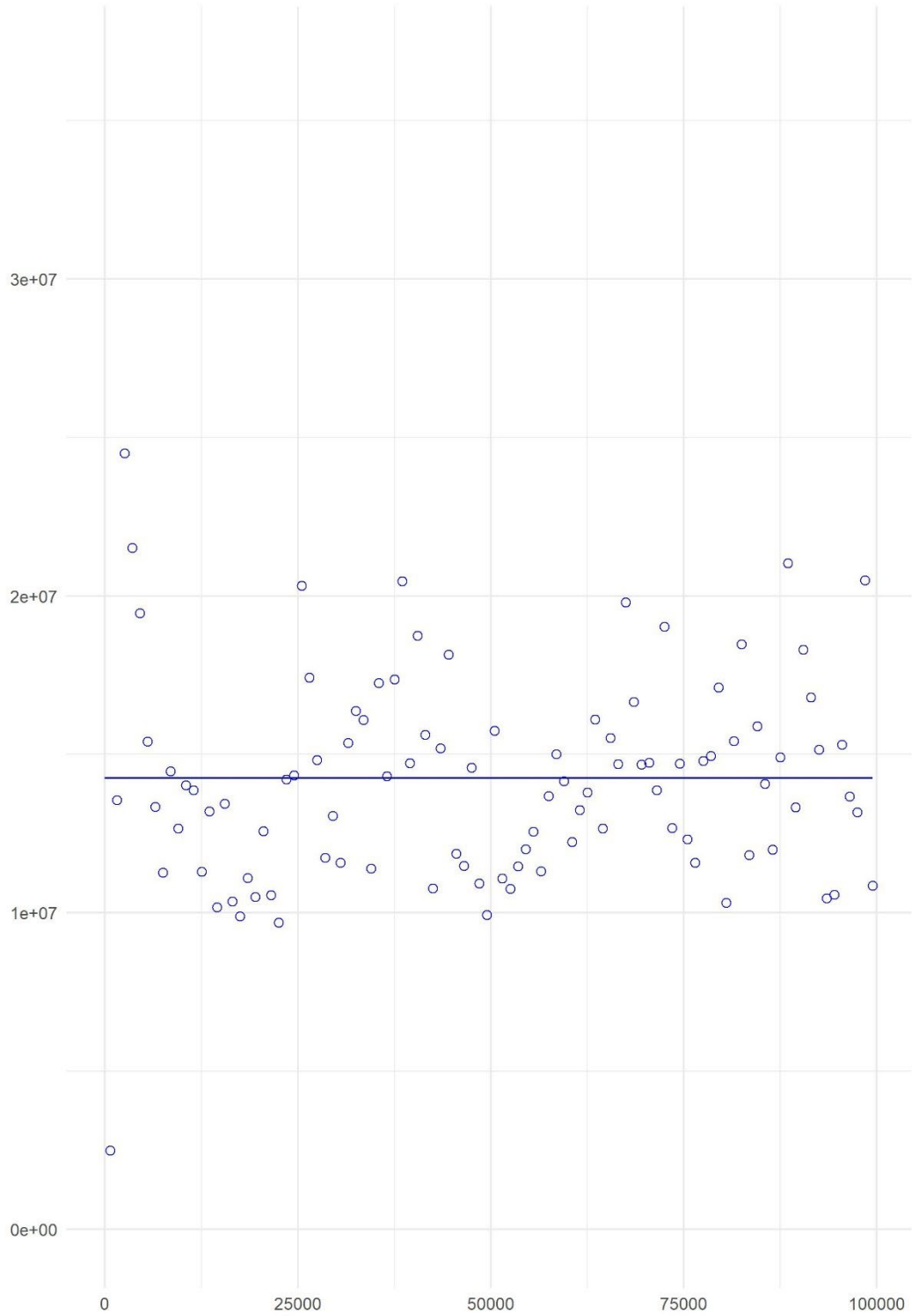


Figure B.24. 2013 female age-1+ blue crab fitted variogram derived from Bay-wide kriging using Davis WDS Chesapeake Bay data. Model parameters are provided in Table B.3.

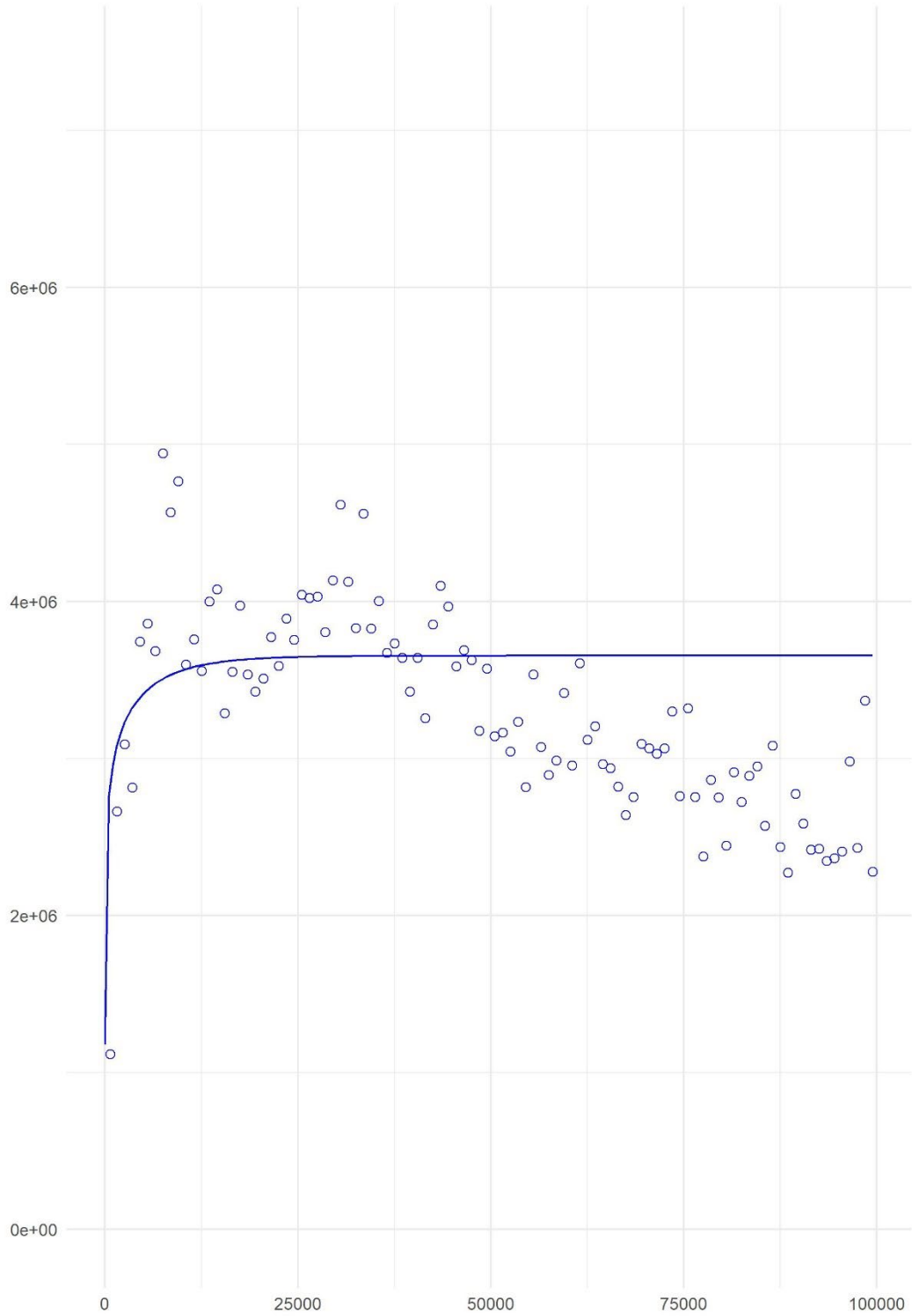


Figure B.25. 2014 female age-1+ blue crab fitted variogram derived from Bay-wide kriging using Davis WDS Chesapeake Bay data. Model parameters are provided in Table B.3.

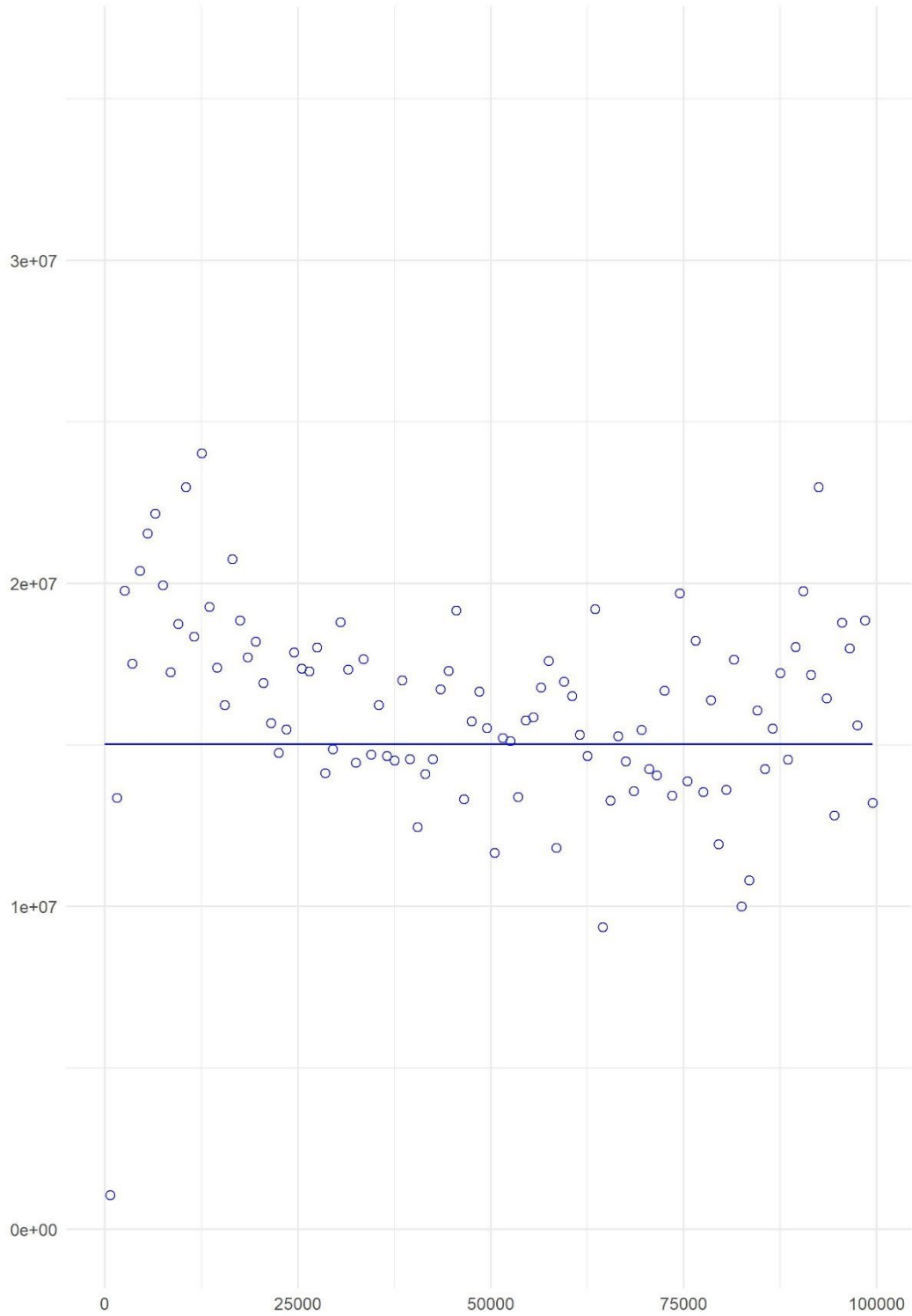


Figure B.26. 2015 female age-1+ blue crab fitted variogram derived from Bay-wide kriging using Davis WDS Chesapeake Bay data. Model parameters are provided in Table B.3.

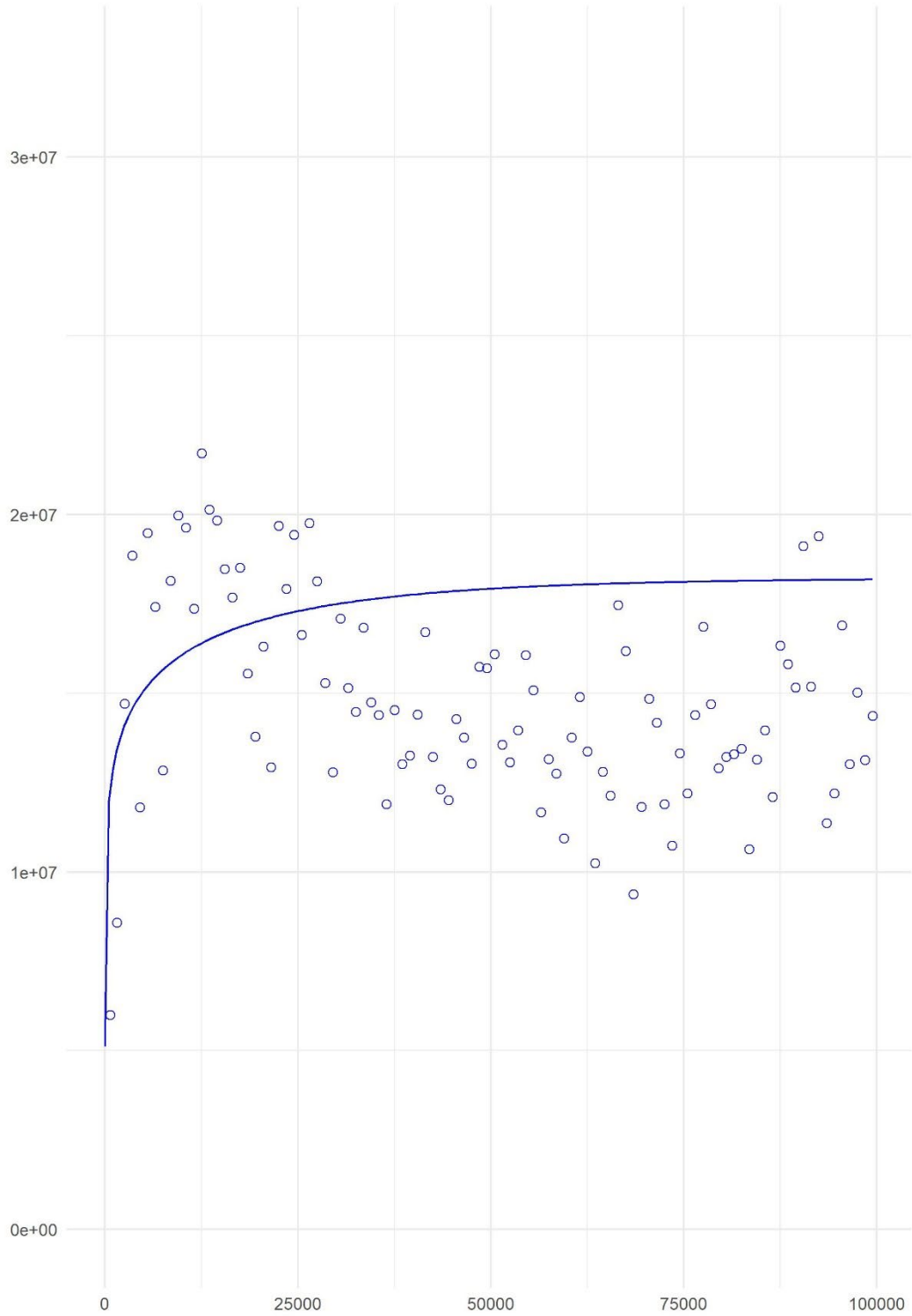


Figure B.27. 2016 female age-1+ blue crab fitted variogram derived from Bay-wide kriging using Davis WDS Chesapeake Bay data. Model parameters are provided in Table B.3.

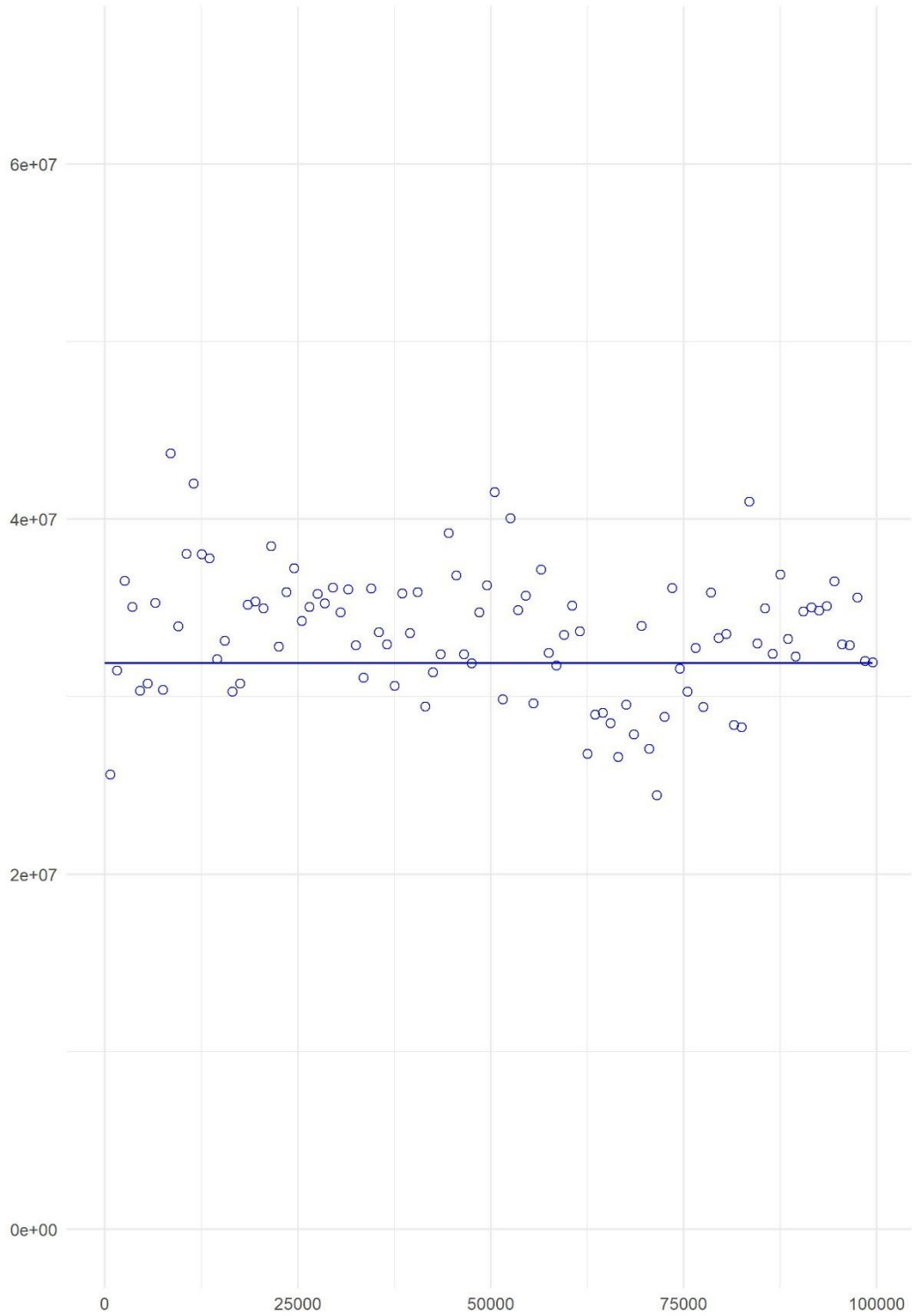


Figure B.28. 2017 female age-1+ blue crab fitted variogram derived from Bay-wide kriging using Davis WDS Chesapeake Bay data. Model parameters are provided in Table B.3.

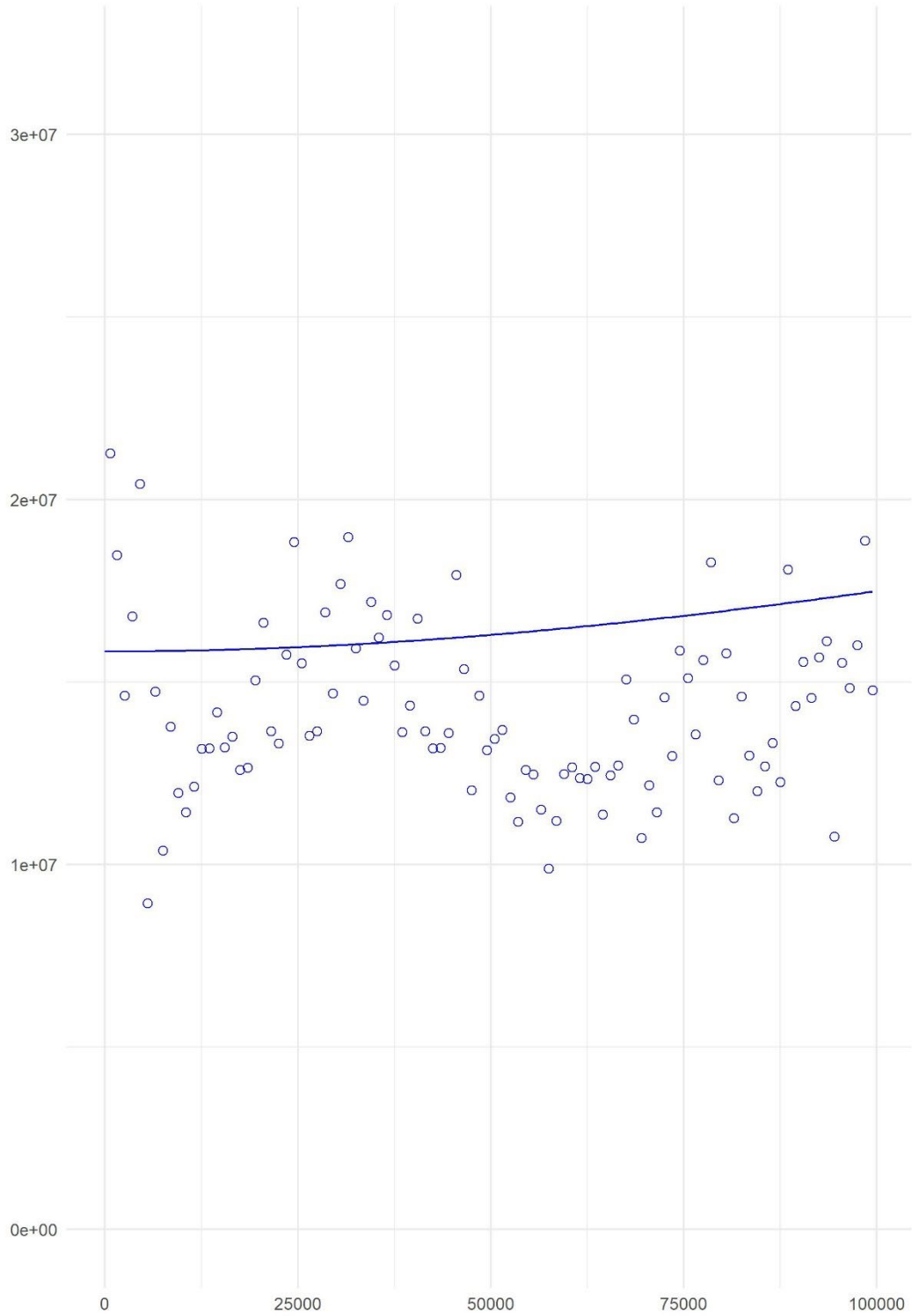


Figure B.29. 2018 female age-1+ blue crab fitted variogram derived from Bay-wide kriging using Davis WDS Chesapeake Bay data. Model parameters are provided in Table B.3.

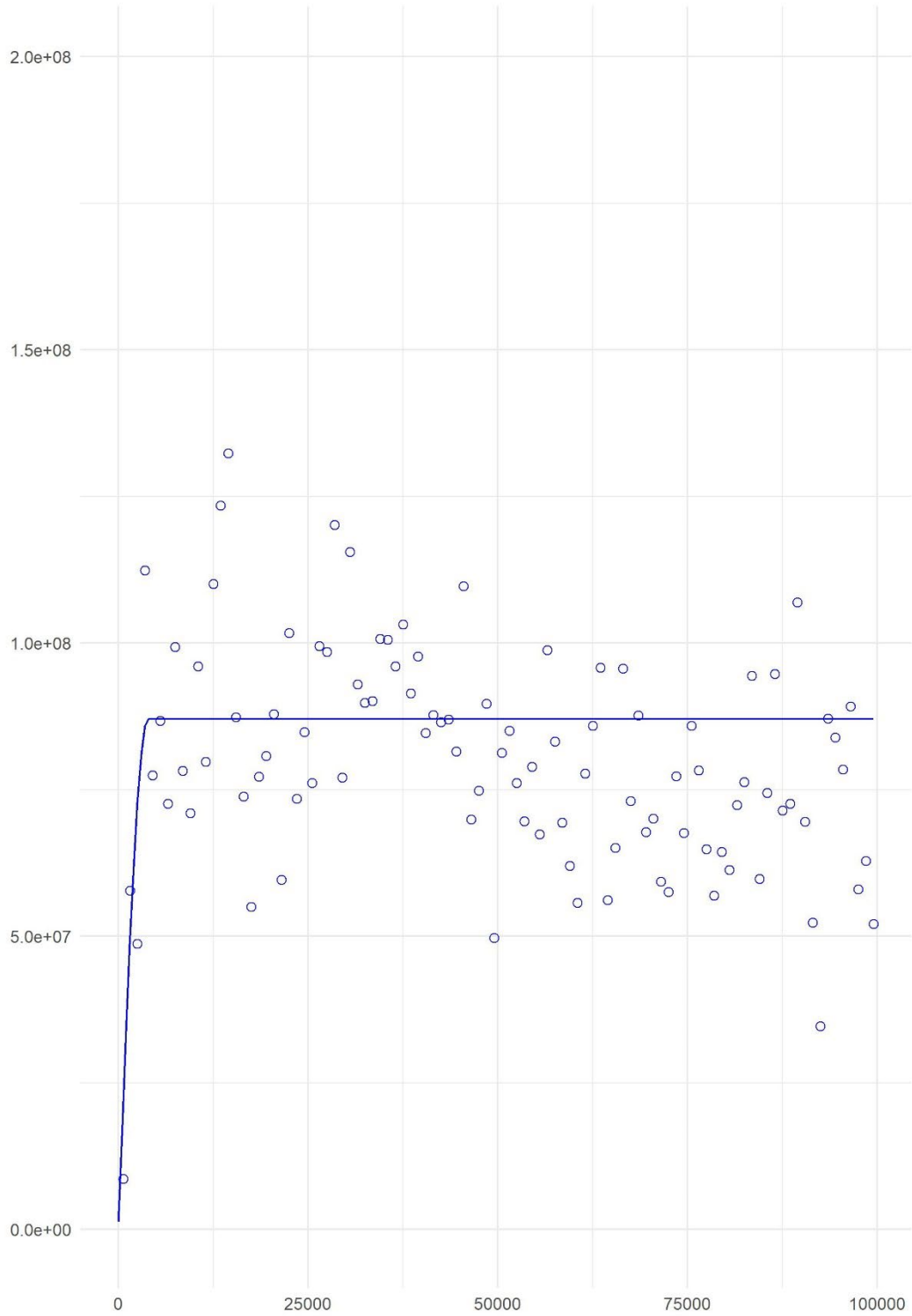


Figure B.30. 2019 female age-1+ blue crab fitted variogram derived from Bay-wide kriging using Davis WDS Chesapeake Bay data. Model parameters are provided in Table B.3.

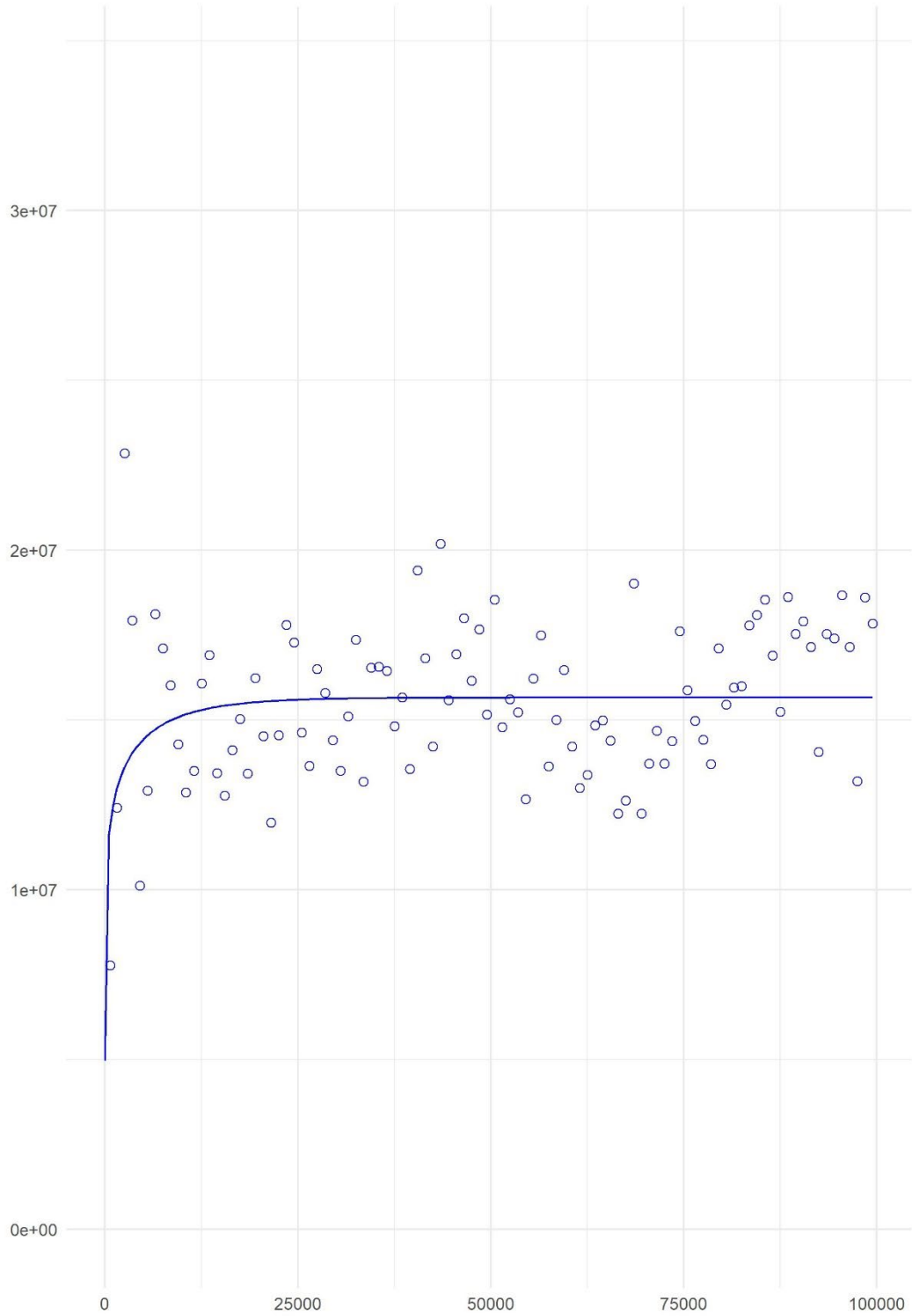


Figure B.31. 2020 female age-1+ blue crab fitted variogram derived from Bay-wide kriging using Davis WDS Chesapeake Bay data. Model parameters are provided in Table B.3.

Appendix C: Total

Tables for Appendix C

Table C.1. Estimates of total blue crab (females and males of all ages) abundance (millions) in Chesapeake Bay, WTAPS, and WTAPSNE, derived from Bay-wide kriging using Davis WDS Chesapeake Bay data.

Year	Blue Crab Abundance Estimates (*10 ⁶)	# of 250 m ² Cells	Area (m ²)	WTAPS Abundance Estimates (*10 ⁶)	Proportion of Crabs in WTAPS (%)	WTAPSNE Abundance Estimates (*10 ⁶)	Proportion of Crabs in WTAPSNE (%)
1990	1,643.65	182,218	11,389	1.56	0.10	1.53	0.09
1991	1,327.57	178,956	11,185	1.81	0.14	0.90	0.07
1992	494.46	182,971	11,436	1.18	0.24	0.95	0.19
1993	753.42	184,205	11,513	1.03	0.14	0.96	0.13
1994	782.09	184,174	11,511	1.27	0.16	0.88	0.11
1995	518.29	182,962	11,435	0.34	0.07	0.52	0.10
1996	1,100.06	183,167	11,448	1.19	0.11	0.50	0.05
1997	931.90	182,896	11,431	0.31	0.03	0.35	0.04
1998	431.55	182,142	11,384	2.03	0.47	0.09	0.02
1999	494.73	183,303	11,456	0.61	0.12	0.28	0.06
2000	394.61	182,990	11,437	0.44	0.11	0.75	0.19
2001	349.82	182,702	11,419	0.38	0.11	0.18	0.05
2002	379.55	182,879	11,430	0.29	0.08	0.37	0.10
2003	549.74	182,855	11,428	0.64	0.12	0.28	0.05
2004	406.98	183,087	11,443	0.66	0.16	0.59	0.15
2005	492.77	182,909	11,432	0.65	0.13	0.57	0.11
2006	478.60	182,519	11,407	0.79	0.17	0.43	0.09

Table C.1 (continued).

2007	311.43	182,669	11,417	0.87	0.28	0.50	0.16
2008	409.78	182,692	11,418	1.43	0.35	1.22	0.30
2009	633.39	182,637	11,415	1.21	0.19	1.93	0.31
2010	902.43	181,500	11,344	2.93	0.32	1.12	0.12
2011	705.45	182,564	11,410	2.61	0.37	2.89	0.41
2012	882.11	182,680	11,418	0.52	0.06	0.70	0.08
2013	405.24	182,600	11,413	0.89	0.22	0.93	0.23
2014	446.37	182,775	11,423	0.70	0.16	0.51	0.11
2015	600.60	182,377	11,399	1.57	0.26	0.41	0.07
2016	765.22	182,748	11,422	1.64	0.21	0.97	0.13
2017	609.98	182,661	11,416	2.14	0.35	1.17	0.19
2018	609.97	182,893	11,431	1.22	0.20	1.42	0.23
2019	740.54	182,779	11,424	1.20	0.16	0.47	0.06
2020	679.98	183,032	11,440	0.71	0.10	1.44	0.21

Figures for Appendix C

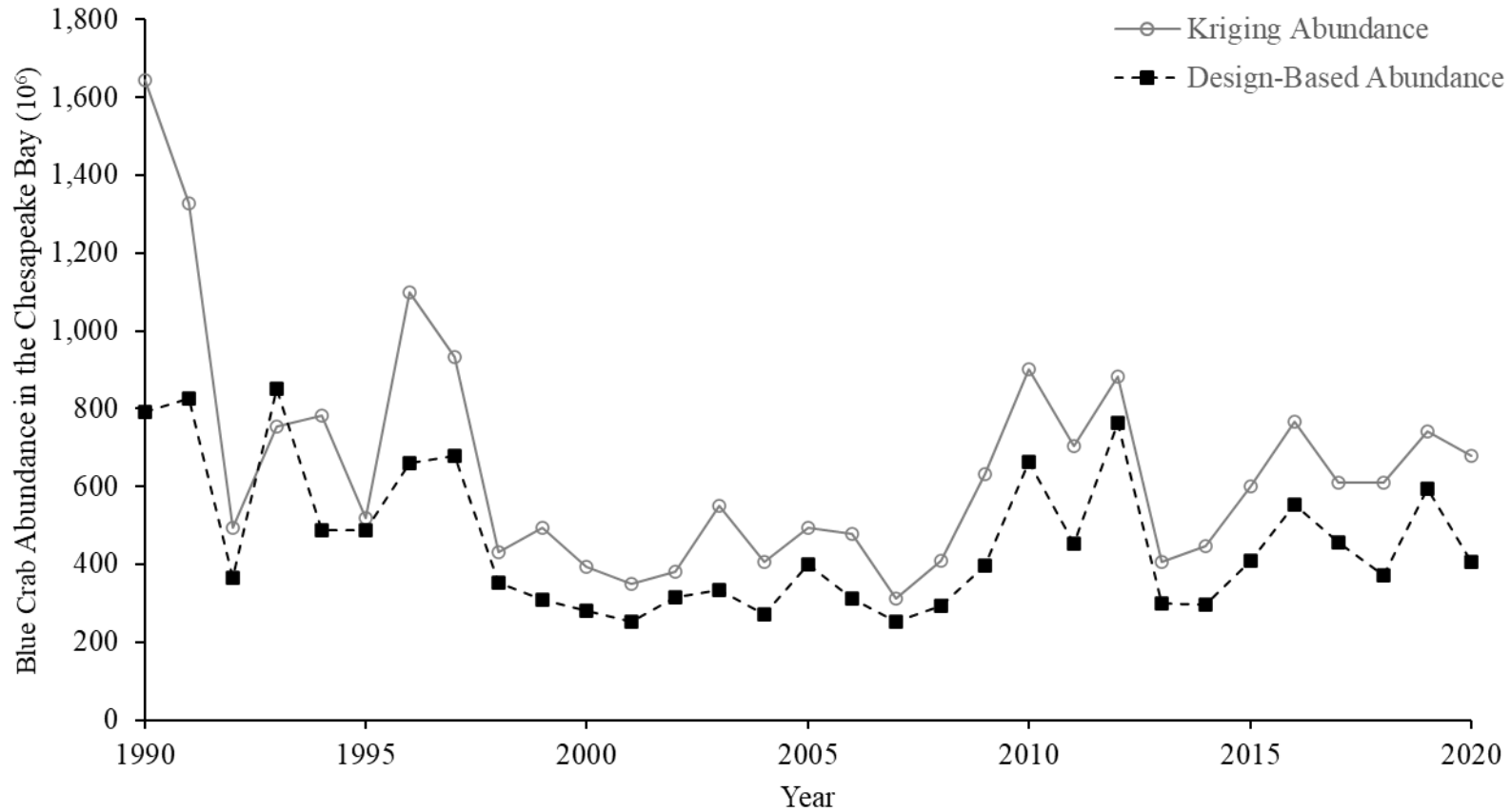


Figure C.1. Estimates of total blue crab (females and males of all ages) abundance (millions) in Chesapeake Bay. Shown are total blue crab kriged abundance estimates (open circles; solid, grey line) and design-based blue crab abundance estimates (solid squares; dashed, black line) for 1990–2020.

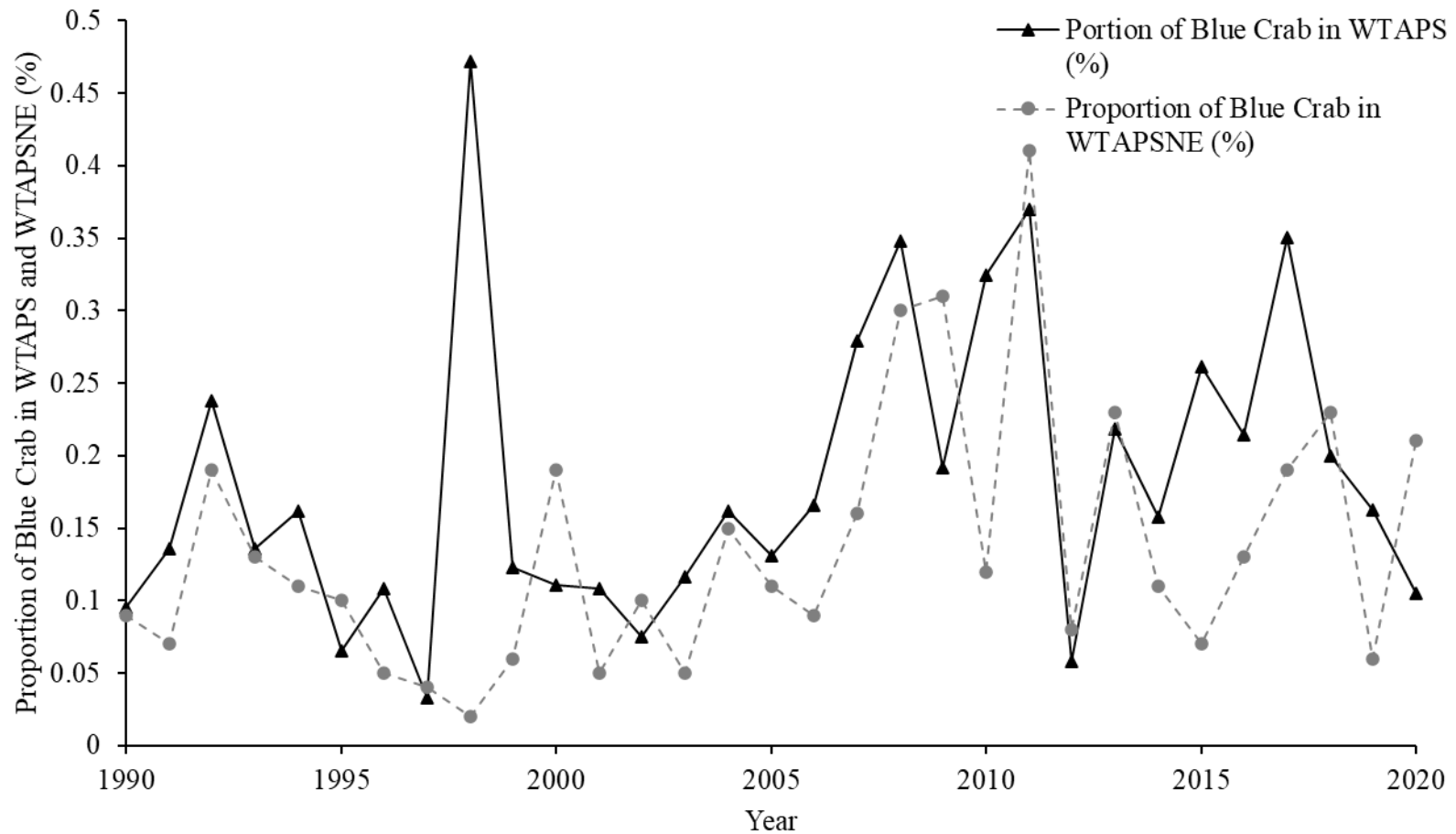


Figure C.2. Proportion of total blue crab (females and males of all ages) abundance in WTAPS and WTAPSNE (%) out of the Bay-wide kriging abundance in Chesapeake Bay. Shown are kriged estimates of the proportion of blue crab (%) in WTAPS (closed triangles; solid, black line) and WTAPSNE (solid circle; dashed, grey line) for 1990–2020.

Appendix D: Males

Tables for Appendix D

Table D.1. Estimates of male age-1+ abundance (millions) estimates in Chesapeake Bay, WTAPS, and WTAPSNE, derived from Bay-wide kriging in Chesapeake Bay using Davis WDS Chesapeake Bay data.

Year	Male Bay-wide Abundance Estimates (*10 ⁶)	# of 250 m ² Cells	Area (m ²)	WTAPS Male Abundance Estimates (*10 ⁶)	Proportion of Males in WTAPS (%)	WTAPSNE Male Abundance Estimates (*10 ⁶)	Proportion of Males in WTAPSNE (%)
1990	461.69	182,218	11,389	0.15	0.03	0.17	0.04
1991	431.03	178,956	11,185	0.22	0.05	0.20	0.05
1992	156.68	182,971	11,436	0.05	0.03	0.05	0.03
1993	213.69	184,205	11,513	0.08	0.04	0.11	0.05
1994	242.90	184,174	11,511	0.05	0.02	0.06	0.03
1995	135.44	182,962	11,435	0.00	0.00	0.05	0.04
1996	168.45	183,167	11,448	0.04	0.02	0.04	0.03
1997	144.75	182,896	11,431	0.04	0.03	0.00	0.00
1998	116.10	182,142	11,384	0.12	0.11	0.01	0.01
1999	45.36	183,303	11,456	0.02	0.04	0.01	0.02
2000	71.54	182,990	11,437	0.03	0.04	0.03	0.04
2001	73.90	182,702	11,419	0.01	0.02	0.01	0.01
2002	105.40	182,879	11,430	0.03	0.03	0.04	0.04
2003	186.02	182,855	11,428	0.05	0.03	0.03	0.01
2004	65.59	183,087	11,443	0.06	0.09	0.04	0.06
2005	69.56	182,909	11,432	0.10	0.14	0.10	0.15
2006	72.26	182,519	11,407	0.09	0.12	0.04	0.06

Table D.1 (continued).

2007	81.12	182,669	11,417	0.06	0.07	0.04	0.06
2008	58.02	182,692	11,418	0.06	0.11	0.05	0.09
2009	118.06	182,637	11,415	0.06	0.05	0.04	0.04
2010	136.11	181,500	11,344	0.07	0.05	0.08	0.06
2011	130.09	182,564	11,410	0.18	0.14	0.20	0.15
2012	102.71	182,680	11,418	0.05	0.05	0.16	0.16
2013	71.14	182,600	11,413	0.00	0.00	0.03	0.04
2014	58.52	182,775	11,423	0.07	0.12	0.01	0.01
2015	86.77	182,377	11,399	0.07	0.08	0.12	0.13
2016	156.93	182,748	11,422	0.17	0.11	0.12	0.07
2017	144.32	182,661	11,416	0.09	0.06	0.06	0.04
2018	126.22	182,893	11,431	0.06	0.05	0.08	0.06
2019	129.37	182,779	11,424	0.09	0.07	0.06	0.05
2020	200.53	183,032	11,440	0.05	0.02	0.06	0.03

Figures for Appendix D

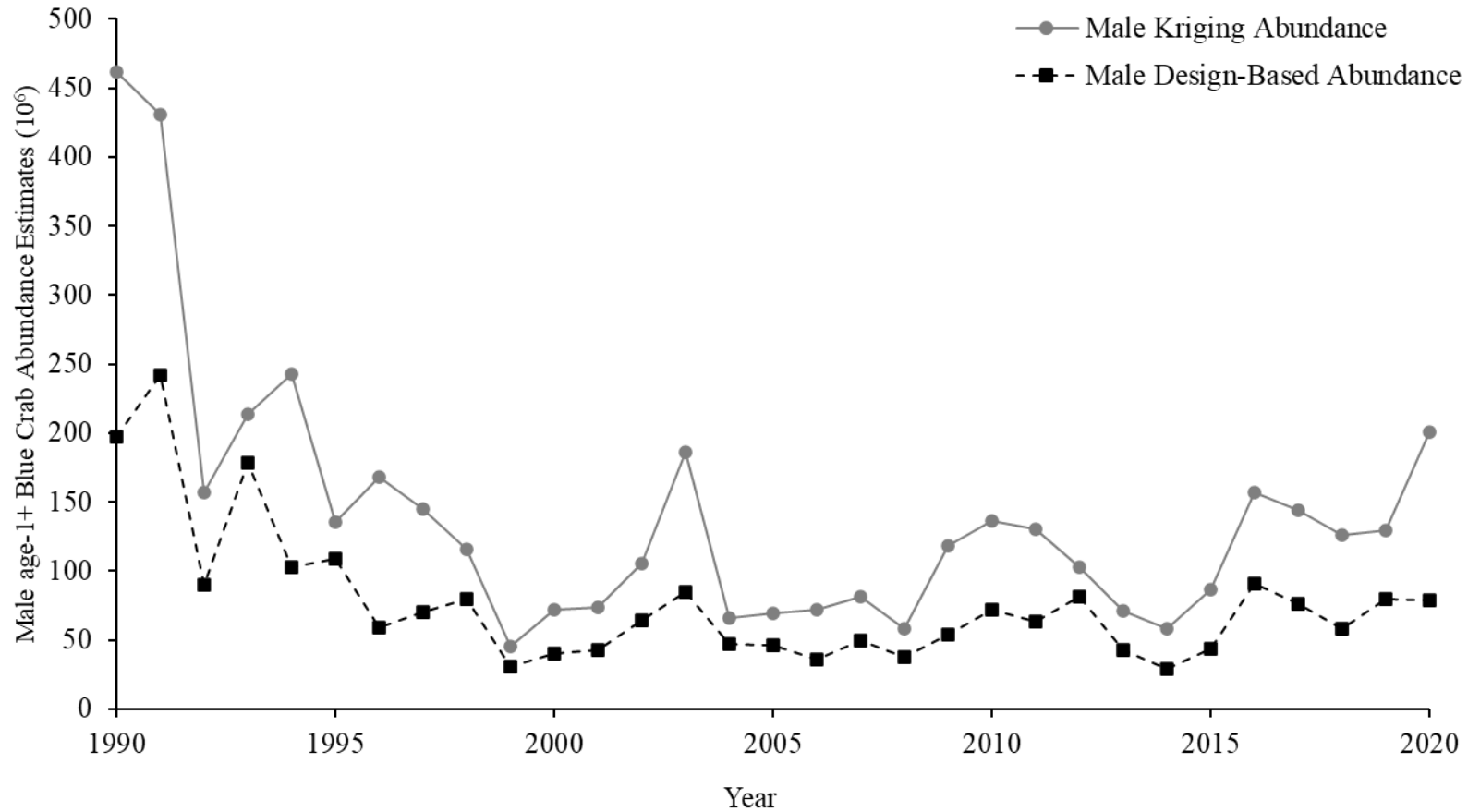


Figure D.1. Estimates of male age-1+ blue crab abundance (millions) in Chesapeake Bay. Shown are male age-1+ blue crab kriged estimates (open circles; solid, grey line) and design-based male age-1+ abundance estimates (solid squares; dashed, black line) for 1990–2020.

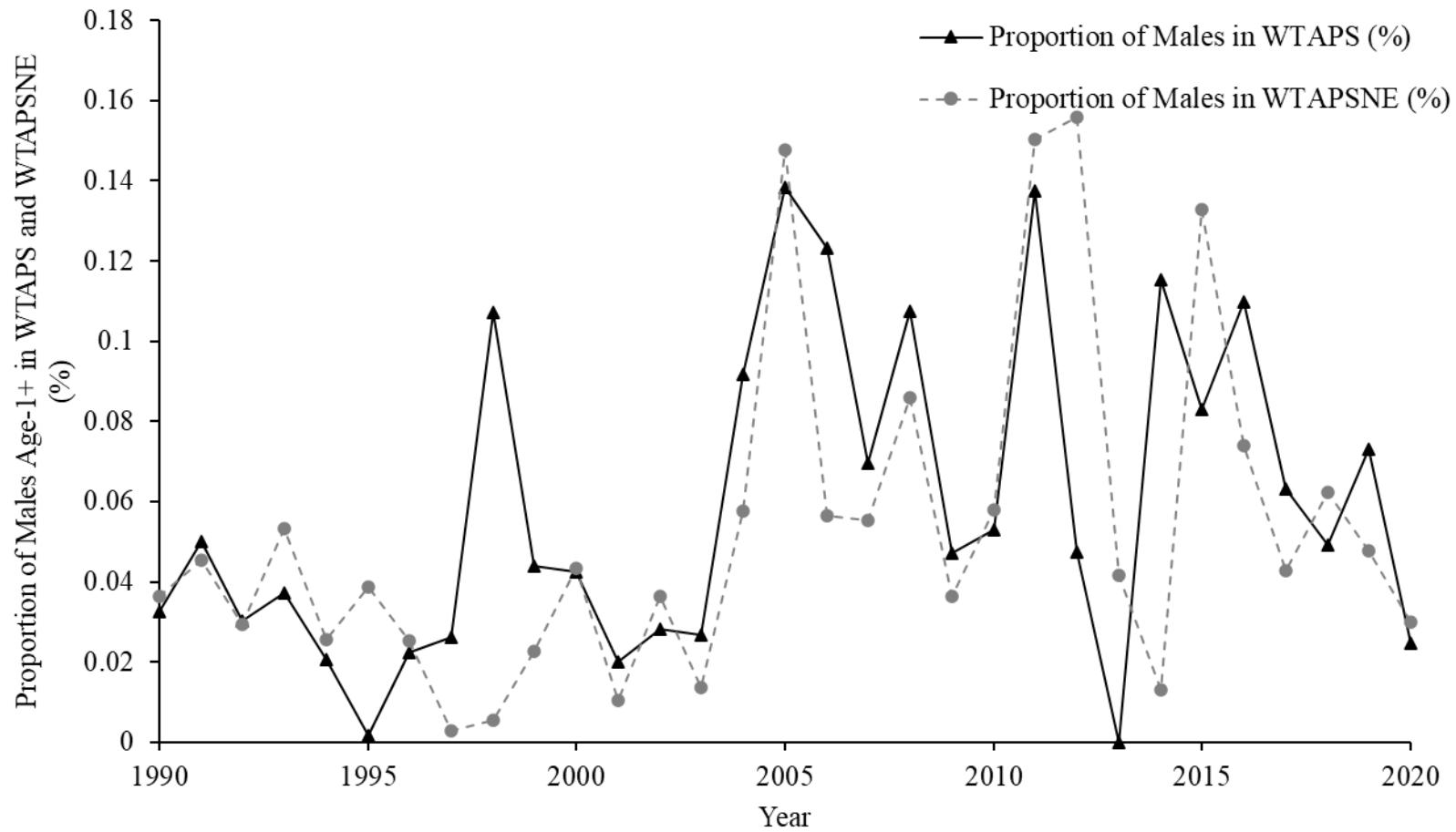


Figure D.2. Proportion of male age-1+ blue crab abundance in WTAPS and WTAPSNE (%) out of the Bay-wide abundance. Shown are kriged estimates of the proportion of males age-1+ (%) in WTAPS (closed triangles; solid, black line) and WTAPSNE (solid circle; dashed, grey line) for 1990–2020.

Appendix E: Juveniles

Tables for Appendix E

Table E.1. Estimates of juvenile age-0 abundance (millions) in Chesapeake Bay, WTAPS, and WTAPSNE, derived from Bay-wide kriging using Davis WDS data.

Year	Juvenile Bay-wide Abundance Estimates (*10 ⁶)	# of 250 m ² Cells	Area (m ²)	WTAPS Juvenile Abundance Estimates (*10 ⁶)	Proportion of Juveniles in WTAPS (%)	WTAPSNE Juvenile Abundance Estimates (*10 ⁶)	Proportion of Juveniles in WTAPSNE (%)
1990	912.06	182,218	11,389	0.388	0.043	0.387	0.042
1991	689.83	178,956	11,185	0.091	0.013	0.002	0.000
1992	158.44	182,971	11,436	0.021	0.013	0.013	0.008
1993	416.23	184,205	11,513	0.017	0.004	0.012	0.003
1994	439.74	184,174	11,511	0.017	0.004	0.063	0.014
1995	310.49	182,962	11,435	0.030	0.010	0.019	0.006
1996	792.43	183,167	11,448	0.020	0.003	0.038	0.005
1997	712.82	182,896	11,431	0.145	0.020	0.194	0.027
1998	233.42	182,142	11,384	0.002	0.001	0.018	0.008
1999	404.31	183,303	11,456	0.021	0.005	0.000	0.000
2000	264.18	182,990	11,437	0.001	0.001	0.002	0.001
2001	229.51	182,702	11,419	0.005	0.002	0.003	0.001
2002	223.37	182,879	11,430	0.000	0.000	0.002	0.001
2003	260.76	182,855	11,428	0.000	0.000	0.002	0.001
2004	272.31	183,087	11,443	0.011	0.004	0.026	0.010
2005	328.67	182,909	11,432	0.084	0.026	0.105	0.032
2006	326.79	182,519	11,407	0.000	0.000	0.005	0.002

Table E.1 (continued).

2007	149.39	182,669	11,417	0.000	0.000	0.000	0.000
2008	267.23	182,692	11,418	0.033	0.012	0.002	0.001
2009	278.58	182,637	11,415	0.000	0.000	0.007	0.002
2010	494.41	181,500	11,344	0.019	0.004	0.114	0.023
2011	298.65	182,564	11,410	0.052	0.017	0.029	0.010
2012	685.28	182,680	11,418	0.063	0.009	0.094	0.014
2013	183.64	182,600	11,413	0.004	0.002	0.008	0.004
2014	348.45	182,775	11,423	0.019	0.006	0.016	0.005
2015	452.98	182,377	11,399	0.010	0.002	0.021	0.005
2016	420.89	182,748	11,422	0.023	0.005	0.046	0.011
2017	174.57	182,661	11,416	0.028	0.016	0.016	0.009
2018	284.79	182,893	11,431	0.000	0.000	0.004	0.001
2019	428.88	182,779	11,424	0.082	0.019	0.075	0.017
2020	355.69	183,032	11,440	0.001	0.000	0.015	0.004

Figures for Appendix E

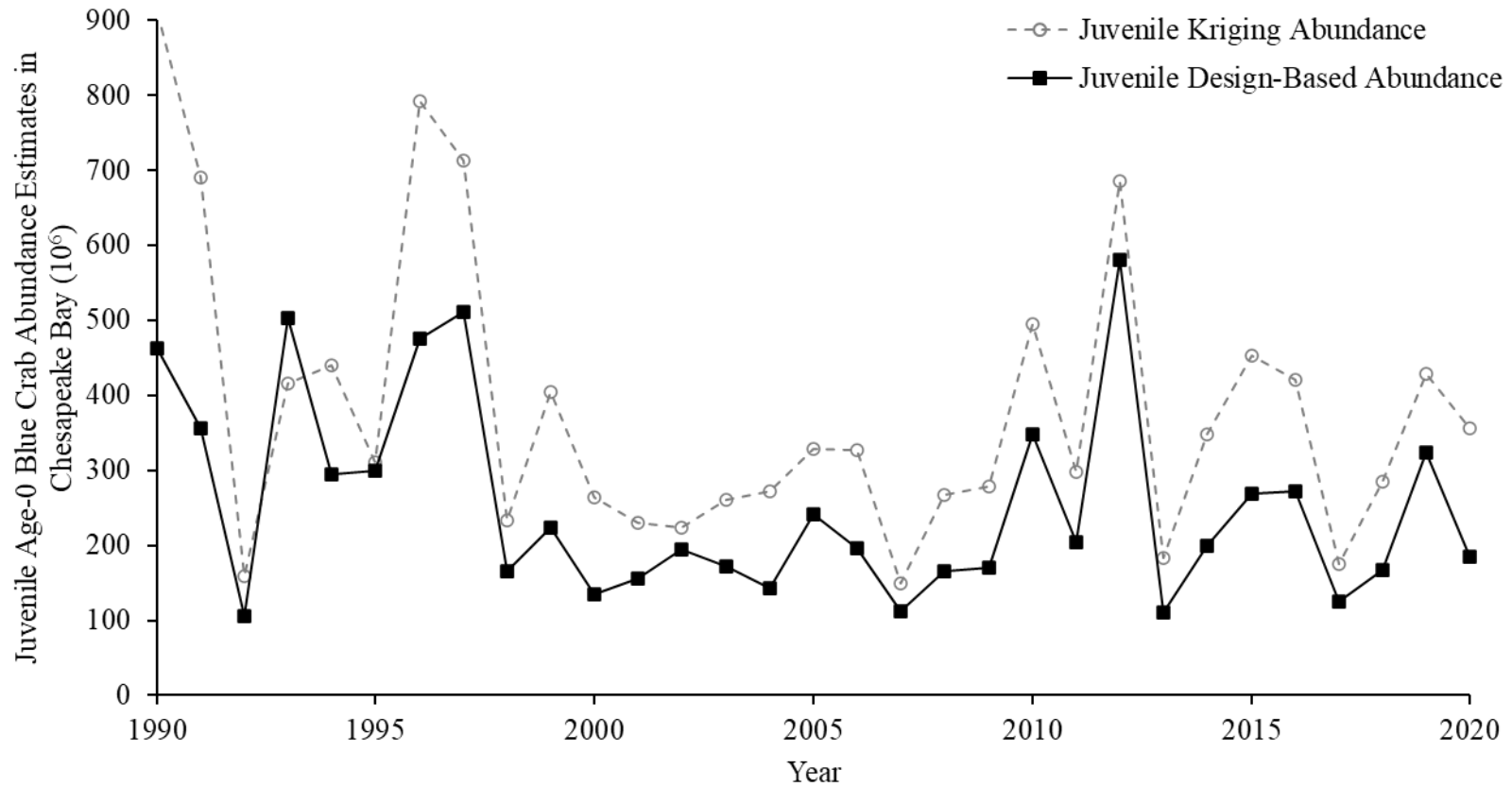


Figure E.1. Estimates of juvenile age-0 blue crab abundance (millions) in Chesapeake Bay. Shown are juvenile age-0 blue crab kriged estimates (open circles; solid, grey line) and design-based juvenile age-0 abundance estimates (solid squares; dashed, black line) for 1990–2020.

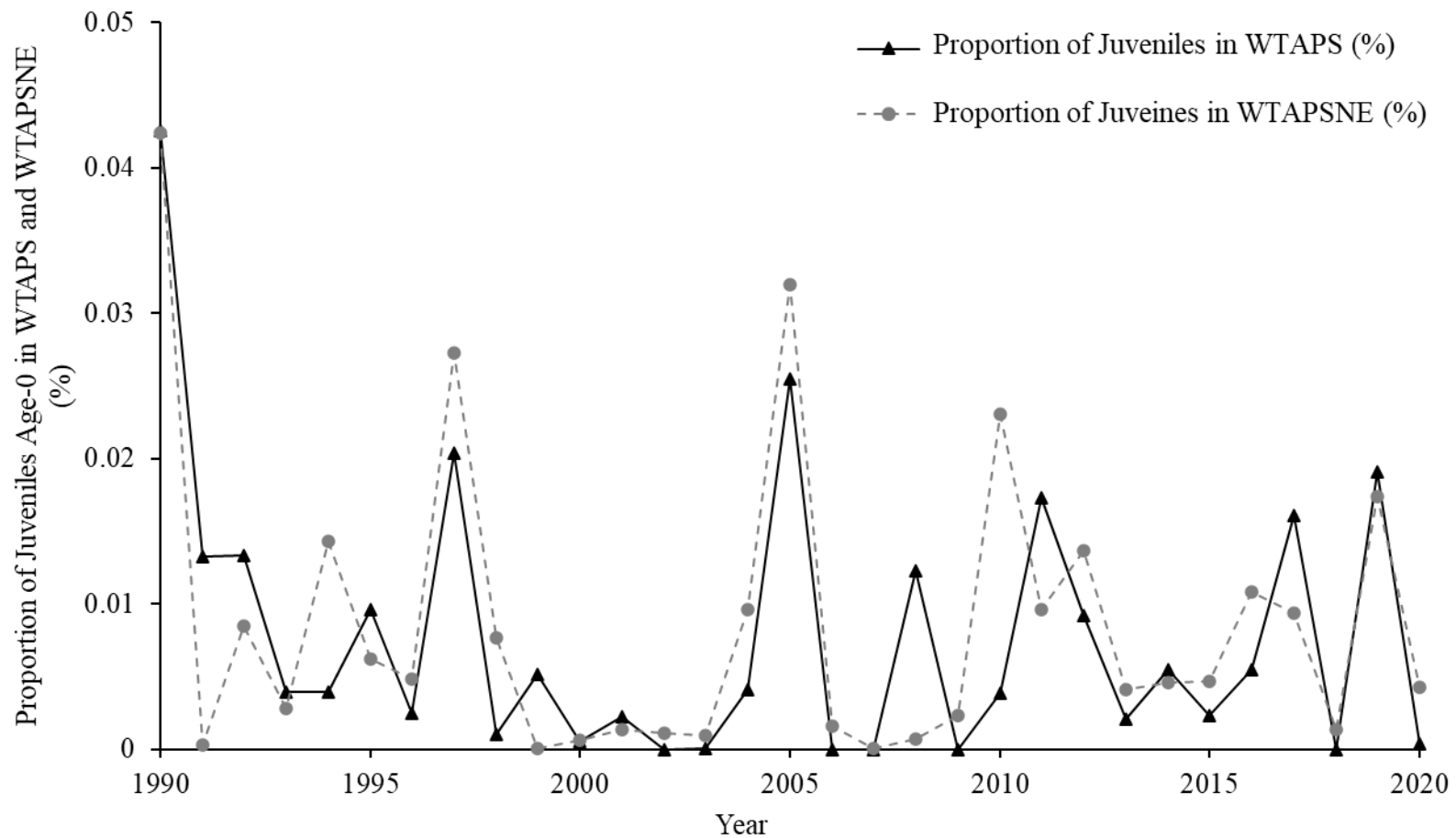


Figure E.2. Proportion of juvenile age-0 blue crab abundance in WTAPS and WTAPSNE (%) out of the Bay-wide kriging abundance in Chesapeake Bay. Shown are kriged estimates of the proportion of juveniles age-0 (%) in WTAPS (closed triangles; solid, black line) and WTAPSNE (solid circle; dashed, grey line) for 1990–2020.

Bibliography

- Bailey, H., K.L. Brookes, and P.M. Thompson. 2014. Assessing environmental impacts of offshore wind farms: lessons learned and recommendations for the future. *Aquatic Biosystems*. doi: 10.1186/2046-9063-10-8
- Balazik, M. 2017. First verified occurrence of the shortnose sturgeon (*Acipenser brevirostrum*) in the James River, Virginia. *Fishery Bulletin*. doi: 10.7755/FB.115.2.6
- Bauer, L.J. and T.J. Miller. 2010a. Spatial and interannual variability in winter mortality of the blue crab (*Callinectes sapidus*) in the Chesapeake Bay. *Estuaries and Coasts*. doi: 10.1007/s12237-009-9237-x
- Bauer, L.J. and T.J. Miller. 2010b. Temperature-, salinity-, and size-dependent winter mortality of juvenile blue crabs (*Callinectes sapidus*). *Estuaries and Coasts*. doi: 10.1007/s12237-010-9277-2
- Brylawski, B.J. and T.J. Miller. 2006. Temperature-dependent growth of the blue crab (*Callinectes sapidus*): a molt process approach. *Canadian Journal of Fisheries and Aquatic Sciences*. doi: 10.1139/F06-011
- Chen, F.W. and C.W. Liu. 2012. Estimation of the spatial rainfall distribution using inverse distance weighting (IDW) in the middle of Taiwan. *Paddy and Water Environment*. doi: 10.1007/s10333-012-0319-1
- Chesapeake Bay Stock Assessment Committee (CBSAC). 2022. 2022 Chesapeake Bay blue crab advisory report. Chesapeake Bay Program. https://www.chesapeakebay.net/who/publications-archive/sustainable_fisheries. Accessed 7 August 2022.
- Derrick, P., J. McKee, S. Johnson, and M. Mendelsohn. 2007. Poplar Island environmental restoration project: project successes, lessons learned, and future plans. *Proceedings of the World Dredging Congress* 1: 487–500.
- Doyle, B. and J.F. Ports. 2022. Maryland Department of Transportation Maryland Port Administration (MPA) fiscal year 2023 budget overview MPA operating and capital programs presentation to budget committees 2022 session. Maryland Department of Budget and Management. <https://dbm.maryland.gov/budget/FY2023Testimony/J00D00.pdf>. Accessed 8 June 2022.
- Epifanio, C.E. 2007. Biology of larvae. In *The blue crab Callinectes sapidus*, eds. V.S. Kennedy and L.E. Cronin, 513-533. College Park: Maryland Sea Grant College.
- Fischer-Huettner, S.E., T. Baden Jr., E. Cunningham, M. Kelly, T. Bumba, R. Roberts, D. Dixon, N. Foster, B. Morman, M. Franz, M. Cook, and C.M. Sheehan. 2015. Port of Baltimore report, ed. T. Baden Jr. The Daily Record. <https://gbc.org/wp-content/uploads/2015/03/The-Daily-Record-2015-Port-of-Baltimore-special-section.pdf>. Accessed 6 June 2022.
- Fischer, M.M. and A. Getis. 2010. Introduction. In *Handbook of applied spatial analysis*, 1-24. Heidelberg Dordrecht London New York: Springer.

- Hiemstra, P. 2022. automap: Automatic interpolation package. *R package version 1.0-16*.
- Hijmans, R.J., J. van Etten, M. Sumner, J. Cheng, D. Baston, A. Bevan, R. Bivand et al. 2022. raster: geographic data analysis and modeling. *R package version 3.5-21*.
- Hilton, E.J., B. Kynard, M.T. Balazik, A.Z. Horodysky, and C.B. Dillman. 2016. Review of the biology, fisheries, and conservation status of the Atlantic sturgeon, (*Acipenser oxyrinchus oxyrinchus* Mitchell, 1815). *Journal of Applied Ichthyology*. doi: 10.1111/jai.13242
- Hirzel, A.H., G.L. Lay, V. Helfer, C. Randin, and A. Guisan. 2006. Evaluating the ability of habitat suitability models to predict species presences. *Ecological Modelling* 199: 142–152.
- The Independent Technical Review Team. 2009. Sediment in Baltimore Harbor: quality and suitability for innovative reuse: an independent technical review. Maryland Sea Grant College. https://www.mdsg.umd.edu/sites/default/files/files/_Dredge_Report_and_Appendices_Web.pdf. Accessed 9 June 2022.
- Jensen, O.P. and T.J. Miller. 2005. Geostatistical analysis of the abundance and winter distribution patterns of the blue crab *Callinectes sapidus* in Chesapeake Bay. *Transactions of the American Fisheries Society*. doi: 10.1577/t04-218.1
- Jensen, O.P., M.C. Christman, and T.J. Miller. 2006. Landscape-based geostatistics: a case study of the distribution of blue crab in Chesapeake Bay. *Environmetrics*. doi: 10.1002/env.767
- Jivoff, P., A.H. Hines, and L.S. Quackenbush. 2007. Reproduction biology and embryonic development. In *The blue crab Callinectes sapidus*, eds. V.S. Kennedy and L.E. Cronin, 255-298. College Park: Maryland Sea Grant College.
- Krivoruchko, K. 2012. Empirical bayesian kriging: implemented in ArcGIS Geostatistical Analyst. *Esri*. <https://www.esri.com/news/arcuser/1012/files/ebk.pdf>. Accessed 27 June 2022.
- Liang, D., G. Nessler, M. Wilberg, and T. Miller. 2017. Bayesian calibration of blue crab (*Callinectes sapidus*) abundance indices based on probability surveys. *Journal of Agricultural, Biological, and Environmental Statistics*. doi: 0.1007/s13253-017-0295-4
- Lipcius, R.N and K.E. Knick. 2016. Dredge disposal effects on blue crab: report to USACE, Baltimore District. United States Army Corps of Engineers, Baltimore District. https://www.nab.usace.army.mil/Portals/63/docs/Civil%20Works/DMMP/WTA_PS_EA/Appendix%20F_Lipcius_and_Knick2016.pdf?ver=2020-01-29-115617-310. Accessed 6 June 2022.
- Lipcius, R.N., D.B. Eggleston, K.L. Heck Jr., R.D. Seitz, and J.V. Montfrans. 2007. Post-settlement abundance, survival, and growth of postlarvae and young juvenile blue crabs in nursery habitats. In *The blue crab Callinectes sapidus*, eds. V.S. Kennedy and L.E. Cronin, 535-564. College Park: Maryland Sea Grant College.

- Liu, Z., Z. Zhang, C. Zhou, W. Ming, and Z. Du. 2021. An adaptive inverse-distance weighting interpolation method considering spatial differentiation in 3D geological modeling. *Geosciences*. doi: 10.3390/geosciences11020051
- Lynch, G.C. 2001. Port of Baltimore navigation simulation study. Defense Technical Information Center. <https://apps.dtic.mil/sti/citations/ADA391922>. Accessed 8 June 2022.
- Maryland Department of the Environment. 2019. Innovative reuse and beneficial use of dredged material guidance document. Maryland Department of the Environment. https://mde.maryland.gov/programs/Marylander/Documents/Dredging/FINAL_IBR_GUIDANCE_12.05.2019_MDE.pdf. Accessed 6 June 2022.
- Maryland Department of Transportation Maryland Port Administration (MDOT MPA). 2021. MDOT MPA dredged material management program: annual report 2021. Maryland Dredged Material Management Program. <https://maryland-dmmp.com/wp-content/uploads/2021/12/DMMP-Annual-Report-2021-12.3.21.pdf>. Accessed 6 June 2022.
- Miller, T.J. 2003. Incorporating space into models of the Chesapeake Bay blue crab population. *Bulletin of Marine Science* 72: 567–588.
- Miller, T.J., M.J. Wilberg, A.R. Colton, G. Davis, A.F. Sharov, R.N. Lipcius, G.M. Ralph, E.G. Johnson, and A.G. Kaufman. 2011. Stock assessment of blue crab in Chesapeake Bay: 2011 Final assessment report. Chesapeake Bay Program. https://www.chesapeakebay.net/documents/CBSAC_2016_Report_6-30-16_FINAL.pdf. Accessed 8 August 2022.
- Millikin, M.R. and A.B. Williams. 1984. Synopsis of biological data on the blue crab, *Callinectes sapidus* Rathbun. National Oceanic and Atmospheric Administration, National Marine Fisheries Service. <https://www.fao.org/3/ap942e/ap942e.pdf>. Accessed 10 June 2022.
- Morris, L. and D. Ball. 2006. Habitat suitability modelling of economically important fish species with commercial fisheries data. *ICES Journal of Marine Science*. doi: 10.1016/j.icesjms.2006.06.008
- Nichols, M., R.J. Diaz, and L.C. Schaffner. 1990. Effects of hopper dredging and sediment dispersion, Chesapeake Bay. *Environmental Geology and Water Sciences*. doi: 10.1007/BF01704879
- Oliver, M.A. 2010. The variogram and kriging. In *Handbook of applied spatial analysis*, 319-352. Heidelberg Dordrecht London New York: Springer.
- Pebesma, E. and B. Graeler. 2022. gstat: spatial and spatio-temporal geostatistical modelling, prediction, and simulation. *R package version 2.0-9*.
- R Core Team. 2013. R: A language and environment for statistical computing. Vienna, Austria: R Foundation for Statistical Computing.
- Roberts, E.A., R.L. Sheley, and R.L. Lawrence. 2004. Using sampling and inverse distance weighted modeling for mapping invasive plants. *Western North American Naturalist* 64: 312-323.
- Rodrigue, J.P., and T. Notteboom. 2015. Impacts of the Panama Canal expansion on U.S. infrastructure. *TR News* 296: 3–11.

- Roman, M.R. and W.C. Boicourt. 1999. Dispersion and recruitment of crab larvae in the Chesapeake Bay plume: physical and biological controls. *Estuaries*. doi: 10.2307/1353044
- Sabonge, R. 2014. The Panama Canal expansion: a driver of change for global trade flows. The Economic Commission for Latin America. https://www.cepal.org/sites/default/files/publication/files/37039/S1420341_en.pdf. Accessed 9 June 2022.
- Salvelieva, E. 2005. Using ordinary kriging to model radioactive contamination data. *Applied GIS*. doi: 10.2104/ag050010
- Secor, D.H., H.P. O'Brien, N. Coleman, A. Horne, I. Park, D.C. Kazyak, D.G. Bruce, and C. Stence. 2022. Atlantic sturgeon status and movement ecology in an extremely small spawning habitat: the Nanticoke River-Marshyhope Creek, Chesapeake Bay. *Reviews in Fisheries Science & Aquaculture* 30: 195–214.
- Sharov, A.F., J.H. Vølstad, G.R. Davis, B.K. Davis, R. Lipcius, and M.M. Montane. 2003. Abundance and exploitation rate of blue crab (*Callinectes sapidus*) in Chesapeake Bay. *Bulletin of Marine Science* 72: 543–565.
- State of Maryland. 2022. Maryland manual on-line: Port of Baltimore. Maryland State Archives. <https://msa.maryland.gov/msa/mdmanual/01glance/html/port.html>. Accessed 6 June 2022.
- United States Army Corps of Engineers, Baltimore District. 2019. Final environmental assessment: Wolf Trap alternate open water placement site northern extension, Virginia waters of the Chesapeake Bay. Engineer Research and Development Center Knowledge Core. <https://hdl.handle.net/11681/37475>. Accessed 3 July 2022.
- United States Army Corps of Engineers (USACE). 2012. Summary of law: Rivers and Harbors Act of 1899, Section 10. United States Army Corps of Engineers. <https://coast.noaa.gov/data/Documents/OceanLawSearch/Summary%20of%20Law%20-%20Rivers%20Harbors%20Act%20of%201899,%20Section%2010.pdf>. Accessed 6 June 2022.
- United States Environmental Protection Agency. 2021. Overview of the Clean Water Act Section 404. United States Environmental Protection Agency. <https://www.epa.gov/cwa-404/overview-clean-water-act-section-404>. Accessed 6 June 2022.
- van Engel, W.A. 1958. The blue crab and its fishery in Chesapeake Bay: part 1: reproduction, early development, growth and migration. *Commercial Fisheries Review* 20: 6–17.
- Vølstad, J.H., A.F. Sharov, G. Davis, and B. Davis. 2000. A method for estimating dredge catching efficiency for blue crabs, *Callinectes sapidus*, in Chesapeake Bay. *Fishery Bulletin* 98: 410–420.
- Vølstad, J. Rothschild, and T. Maurer. 1994. Abundance estimation and population dynamics of the blue crab in the Chesapeake Bay. *University of Maryland Center for Environmental & Estuarine Studies Chesapeake Biological Laboratory*. Ref. No. UMCEES[CBL] 94-014

- Wang, G.W.Y., W. Talley, and M.R. Brooks. 2016. Maritime economics in a post-expansion Panama Canal era. *Maritime Policy and Management*. doi: 10.1080/03088839.2016.1133160
- Welsh, S.A., M.F. Mangold, J.E. Skjeveland, and A.J. Spells. 2002. Distribution and movement of shortnose sturgeon (*Acipenser brevirostrum*) in the Chesapeake Bay. *Estuaries* 25: 101–104.
- Wickham, H., W. Chang, L. Henry, T.L. Pederson, K. Takahashi, C. Wilke, K. Woo, H. Yutani, and D. Dunnington. 2022. ggplot2: create elegant data visualizations using the grammar of graphics. *R package version 3.3.6*.
- Williams, A.B. 1974. The swimming crabs of the genus *Callinectes* (Decapods: Portunidae). *Fishery Bulletin* 72: 685–798.